Title
Advancements in the Nuclear Data of Fission Yields

Author
Matthews, Eric Francis

Publication Date
2021

Peer reviewed|Thesis/dissertation

Advancements in the Nuclear Data of Fission Yields

by

Eric Francis Matthews

A dissertation submitted in partial satisfaction of the

requirements for the degree of

Doctor of Philosophy

in

Engineering - Nuclear Engineering

in the

Graduate Division

of the

University of California, Berkeley

Committee in charge:

Professor Lee A. Bernstein, Chair
Professor Jasmina L. Vujic
Dr. Bethany L. Goldblum
Professor John Arnold

Summer 2021

Advancements in the Nuclear Data of Fission Yields

Abstract

Advancements in the Nuclear Data of Fission Yields

by

Eric Francis Matthews

Doctor of Philosophy in Engineering - Nuclear Engineering

University of California, Berkeley

Professor Lee A. Bernstein, Chair

Fission yields are an important set of nuclear data observables. They are used in a number of important applications including reactor design, nuclear forensics and safeguards, nuclear medicine, and stockpile stewardship. While great advancements have been made in the understanding of fission since its discovery just over 80 years ago, there are still significant gaps and uncertainties in this knowledge. Fission yields are a prime example of an area of understanding with such gaps and uncertainties. There is significant disagreement in measured, evaluated, and theoretically predicted fission yields; a lack of standardization and regularity in fission yield evaluation; and measured fission yields often exhibit large uncertainties. To enable new developments in research and applications, improvements in the nuclear data of fission yields are required. The work presented in this dissertation seeks to improve the current understanding of the nuclear data related to fission yields.

Introductory material on nuclear data is offered, with a particular focus on the current state of fission yield nuclear data. Then, a description of the fission process is provided to establish a background on fission yield phenomenology. Finally, three chapters about three projects on fission yields and their uncertainties/covariances are presented. These chapters form the basis of this dissertation. First, an extensive review of fission yield measurements and their associated sources of uncertainty is presented. Using this review, a series of templates for expected uncertainties in fission yield measurements is established, forming a guide for experimentalists and evaluators. Second, a stochastic method for the estimation of fission yield covariances is developed. The results of this method provide a basis towards closing a crucial gap in fission yield nuclear data: a complete set of fission yield covariance information was previously absent. Finally, a new measurement of short-lived fission product yields using cyclical neutron activation analysis is discussed. The analysis of the resulting experimental data offers a novel method for fission yield determination. Together, these results advance the current understanding of fission yield nuclear data.

Contents

List of Figures

List of Tables

Acknowledgments

As I reflect on the conclusion of my studies, I am honored by the community that has enabled my accomplishments. The adage, "it takes a village," holds true. It is impossible to imagine being here today without the support of my colleagues, friends, and family. I am so grateful for that support, and I hope that I will be able to pay it back to the community. Some specific acknowledgements are due:

To Bethany: Thank you for giving me my start in this field! Your early support enabled my success and brought me to where I am today. Your mentorship has improved my critical thinking and scientific ability; I am a better scientist because of you. I hope there are many years of collaboration and friendship ahead of us!

To Lee: You changed my life the moment that I stepped into NE101 some seven years ago. Your passion for nuclear physics and nuclear data was infectious. Not only have I been blessed by your abilities as a teacher and mentor, but I have been touched by your friendship and personal generosity. Your deep concern for the happiness and well-being of your students is extraordinary. Magnus and I cannot thank you enough for all your support!

To My Committee: Dr. Bernstein, Dr. Goldblum, Dr. Vujic, Dr. Arnold: Thank you very much for taking the time to review my work. Your feedback significantly improved the quality of this dissertation.

To Josh: I greatly appreciate the mentorship and help you have provided me throughout my studies. I have always been in awe of how much I can learn from you and I hope that I can continue to do so.

To Jon: You are an incredible scientist and I am very glad I was able to benefit from your technical expertise! I know that you are destined for great things and I wish you all the best at Los Alamos!

To Dan: You were the best fellowship supervisor that I could have asked for! The space and flexibility that you gave me during my NNSA Fellowship allowed me to explore new topics while continuing research that was essential to my degree.

To Denise: Thank you for giving me the honor of writing a chapter in the templates paper! It was an incredibly enriching project that allowed me to delve deeper into nuclear data evaluation. I am inspired by your dedication to improving nuclear data and I hope we will continue to collaborate in the future!

To Amanda: I am very glad our paths crossed; no peer has had such a profound impact on my career, interests, and studies! I contracted your passion for evaluation and statistics.

You are an amazing friend, colleague, and housemate. Trips to plant nurseries, movie nights, sickeningly sweet Chablis at La Val's, and that poor pulverized chiclet are all special memories that I will cherish for the rest of my life.

To Mitch: You are truly one of the kindest people that I have ever met. Being around you has always brightened my day and I have been so glad to have had you as a friend throughout my studies!

To Franziska: The laughter and friendship we shared always made me very happy! I wish we had had more time together over the last two years. I know you are doing great things in Los Alamos and I miss you!

To Ian: Your friendship has meant so much to me! It has been very important to have another queer friend in nuclear science. From obsessing about plants together to going out to the Castro, you have helped keep me sane throughout my studies and the pandemic. I am very impressed by your accomplishments and wish you all the best as you start your graduate studies!

To Sunniva: My academics and research were both deeply enriched by the international collaboration that you have given me. My exchange at the University of Oslo not only grew my network but also my family. Your support made it possible for me to be with Magnus when it would have otherwise been impossible because of the pandemic. I cannot thank you enough for that support; it is difficult to imagine what my life would have been like without it. I hope for many more years of friendship and collaboration!

To Dorthea: Thank you for being my twin fission fragment! You are a great friend and I have greatly enjoyed our academic exchanges. I am always impressed by your work and look forward to continuing our shared love of fission!

To Vala: Thank you for being a trusted confidant and source of advice! I appreciate all the help and advice you have given me with career decisions; your independent viewpoints have been invaluable. You are an amazing friend and I am so happy that you were my best man!

To Masha: I have always been amazed by both your academic brilliance and complexity as a person. I am so happy to have you as a friend!

To Magnus: Thank you for bringing so much happiness to my life! You have taught me so much and have expanded my mind. You help me enjoy more of life and save me from living it too monotonously. I am very content that we are now family and I look forward to the many journeys that lie ahead in our new life together!

To Dad, Mom, Stephen, Michael, and Mommom: Thank you for fostering my interests and offering guidance over the years. I love you all very much and I hope that when the pandemic ends that we will be able to see each other more often!

To Baba and Grandma: You both were incredible influences in my early life. You taught me the value of an education and gave me the confidence to always aspire for something better. I miss you both dearly and wish you could be here.

Special thanks to the entities that have funded my research:

This material is based upon work supported by the Department of Energy National Nuclear Security Administration through the Nuclear Science and Security Consortium under Award Numbers DE-NA0003180 and DE-NA000097, Lawrence Berkeley National Laboratory under Contract Number DE-AC02-05CH11231 for the United States Nuclear Data Program, the Office of Counter-Proliferation Research and Development through the Nuclear Data Interagency Working Group managed by the Department of Energy - Nuclear Physics, and the National Nuclear Security Administration Graduate Fellowship Program.

Chapter 1

Introduction

This dissertation will present original research that is focused on the improvement of the nuclear data related to fission yields. This section provides an introduction to nuclear data as a field of research, an overview of the state of nuclear data related to fission yields, and a review of the motivation for the research that will be presented in this dissertation.

1.1 Nuclear Data

As a field of research, nuclear data is broadly defined as the study, compilation, and production of a recommended set of values and uncertainties for the properties of atomic nuclei. Nuclear data research is driven by both basic scientific curiosity and the needs of applications. This research is particularly important for certain applications that play a critical role in society, such as nuclear energy and stockpile stewardship.

Because of critical application needs, research in nuclear data has evolved into a coordinated, international effort. National and international organizations, such as the International Atomic Energy Agency (IAEA), the United States Nuclear Data Program (USNDP), the Japan Atomic Energy Agency (JAEA), and the Nuclear Energy Agency (NEA) continuously review application needs and coordinate research efforts to maximize efficiency and output. Coordinated research together with steady feedback from applications has led to the development of a scheme for the production of nuclear data called the "nuclear data pipeline" [1, 2].

1.1.1 Nuclear Properties

Understanding these properties furthers the basic understanding of nuclear physics and enables applications, which provide the societal benefits listed above. Some nuclear properties can be observed directly, while some can only be observed or inferred indirectly. Nuclear properties are generally placed into two categories: structure and reactions. Nuclear struc-

ture properties are those that describe the intrinsic properties of an atomic nucleus and its excited states. Some examples of nuclear structure properties are:

- mass,
- half-lives,
- decay modes and branching ratios,
- excited state energies, spins, parities, and magnetic moments,
- relative γ ray intensities, types, and multipolarities, and
- average quantities for ensembles of excited states where individual properties are not known, such as level densities and gamma-emission probabilities.

Nuclear reaction properties are those that describe how atomic nuclei interact with subatomic particles and other atomic nuclei. Some examples of nuclear reaction properties are:

- reaction cross sections,
- energy and angular momenta of outgoing particles,
- angular distributions of outgoing particles, and
- fission yields.

1.1.2 Uncertainties and Covariances in Nuclear Data

The vast majority of nuclear properties generally cannot be accurately calculated *ab initio*. Therefore, experimental measurement is the primary means by which nuclear properties are determined. Each experimental measurement of a nuclear property will have some degree of uncertainty associated with it, and therefore nuclear data will always carry uncertainty.

There are two types of uncertainties that users of nuclear data are likely to encounter: experimental uncertainties and evaluated uncertainties. Experimental uncertainties are those that result from the process of the nuclear property measurement itself. Evaluated uncertainties are those that result from the process of evaluation (further detailed in Sec. 1.1.3.3). Evaluated uncertainties are related to experimental uncertainties as they are derived using data from multiple measurements together with a theoretical model to produce a recommended value. The vast majority of nuclear applications use evaluated nuclear data and their associated uncertainties.

Covariance arises when there is a correlation between two measured or deduced nuclear properties. These properties can be two points in a differential measurement (e.g., a cross section at two different energies) or two distinct properties (e.g., beta decay level feeding and decay γ intensities). Numerous correlations exist between nuclear properties, making covariance information an important part of complete uncertainty estimation.

Accurate and fully-characterized uncertainties and covariances in nuclear data are as important as the values themselves. Users require uncertainties and covariances to determine what level of confidence they can have in their calculations and simulations. This information enables decision-making and planning for applications requiring nuclear data as input.

1.1.3 The Nuclear Data Pipeline

The process of producing evaluated nuclear data from experimental measurements is often referred to as the "nuclear data pipeline." The pipeline takes the form of a feedback loop between applications and measurement/evaluation [1, 2, 3]. The needs of applications are determined through sensitivity studies. Information from these sensitivity studies informs experimental activities and the development of nuclear theory. Differential and integral measurements together with nuclear theory and modeling are combined to produce consensus values for nuclear properties in a process called "evaluation." The results of an evaluation are entered into specially formatted libraries. Before these libraries are released to the public, they are checked against the results of integral benchmarks in a process called "validation," if such benchmarks are available. Finally, the evaluated libraries are published and go into use in applications, closing the loop. Figure 1.1 shows an illustration of the nuclear data pipeline.

1.1.3.1 Experiments

Experimental measurement of nuclear properties is the first step in the nuclear data pipeline. As there exists no complete theory of nuclear physics, nuclear theory cannot accurately predict most nuclear properties. Therefore, experimentation is required to determine nuclear properties. Experimentation is also important in guiding theoretical developments. Most theoretical capabilities in nuclear physics have been informed by previously-made experimental observations. An example of this is the Shell Model of Nuclei, which was developed to describe the observed enhancement in binding in nuclei with "magic" numbers of protons and/or neutrons [11, p. 117]. Theorists may need specific nuclear properties to be measured in order to benchmark or further develop their theories. As such, a feedback loop between experimental measurements and nuclear theory forms, as shown in Fig. 1.1.

There exist two categories of nuclear experiments: differential and integral. Differential experiments measure a nuclear property as a function of one or more variables. For example, the measurement of the fission cross section of ^{235}U as a function of incident neutron energy

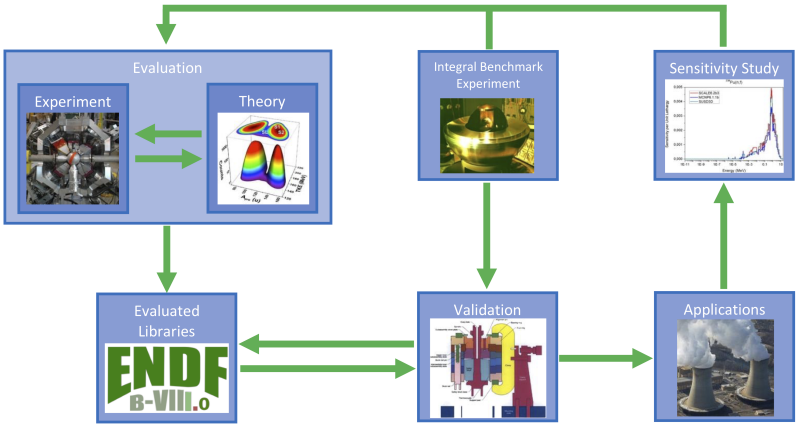

Figure 1.1: An illustration of the feedback loop that forms the nuclear data pipeline. Applications inform experimental and theoretical development needs. New evaluations are produced and validated. These new evaluations go into use in applications and new needs are found. The stages of this pipeline and their interaction with other stages are discussed in Secs. 1.1.3.1-1.1.3.8. The images used in this figure are sourced from References [4, 5, 6, 7, 8, 9, 10]. This figure is modified from Fig. 1 of Reference [1].

is a differential experiment. Integral experiments measure a nuclear observable that depends simultaneously on several different nuclear properties. For example, the measurement of the effective neutron multiplication factor in critical assemblies (which will be further discussed in Sec. 1.1.3.5) is an integral measurement. Many measurements are differential with respect to one nuclear quantity and integral with respect to others, playing different roles in different evaluation processes.

Experimentalists publish their results in peer-reviewed journals, conference proceedings, academic theses, and laboratory reports. These publications are indexed in the Nuclear Science References (NSR) database [12]. The results from these publications are compiled into two unevaluated, formatted databases: the Exchange Format (EXFOR) database [13] for nuclear reaction data and the Experimental Unevaluated Nuclear Data List (XUNDL) database [14] for nuclear structure data. The process of entering published experimental results into NSR, EXFOR, and XUNDL is referred to as "compilation." Evaluators use the information compiled in these databases to produce an evaluation.

1.1.3.2 Theory

Nuclear theory is the physics-based modeling of nuclei, their properties, and their interactions. As previously mentioned, nuclear properties predicted from pure nuclear theory are generally not sufficiently accurate for use in applications. Instead, several theoretical models and tools have been developed to help explain observed phenomena. These models and

tools are tuned on experimental measurements, providing a semi-empirical understanding of nuclear properties.

Among these theoretical tools are "reaction codes," which provide theoretical predictions of properties of nuclear reactions (e.g., reaction cross sections). Examples of reaction codes include TALYS [15] and CoH_3 [16]. The EMPIRE code [17] incorporates several different models and codes to provide a broad suite of theoretical tools. These codes are based on the optical and statistical Hauser-Feshbach theories of nuclear cross sections [18].

A number of theoretical tools exist for predicting and describing nuclear structure and decay properties. The Gamma to Level (GTOL) code uses a least-squares method to determine nuclear level energies from observed γ-ray energies [19]. The RULER code is used to calculate reduced transition probabilities for nuclear level schema [20]. The GABS code calculates the absolute intensities and normalization constants of γ rays [21]. The BrIcc database tabulates internal conversion and electron-positron pair conversion coefficients for decaying nuclear levels [22]. The LogFT code is used to calculate properties of β and electron-capture decays, such as log(ft) values, average β energies, and capture fractions [23]. The ALPHAD, ALPHAD-RadD, and RadD codes are used to calculate the properties of α decay and nuclear radii [24]. Together with experimental measurements, these codes form a standard basis for nuclear structure evaluation.

1.1.3.3 Evaluation

Nuclear data evaluation is the process of combining experimentally measured nuclear properties and nuclear theory to produce consensus values that can be used in applications. Experimental approaches do not currently exist to measure every differential nuclear property; its domain falls short of the needs of many applications. Theory cannot currently predict most properties without strong guidance from experimental data. Thus, evaluation expands the domain of knowledge about nuclear properties far beyond the sum of the individual domains of experiment and theory.

Evaluation is a complex process that must be conducted by an expert with good knowledge of both experiment and theory. This expert is called an "evaluator" and an international network of evaluators work continuously to incorporate new experimental data and theoretical capabilities into updated evaluations. The evaluator combines information from differential experiments and theoretical tools to produce an evaluation. An evaluation is validated against integral benchmark experimental data (as will be discussed in Secs. 1.1.3.5 and 1.1.3.6). Evaluations usually undergo peer review and are published in journals. The primary journal for the publication of evaluations is Nuclear Data Sheets (NDS), which is managed by the United States National Nuclear Data Center (NNDC).

1.1.3.4 Evaluated Libraries

Once an evaluation has been published, it is compiled into specially formatted libraries for distribution to users. Two numerical database formats are used: the Evaluated Nuclear Data File (ENDF) for nuclear reaction data [25] and the Evaluated Nuclear Structure Data File (ENSDF) for nuclear structure data [26]. ENDF and ENSDF are based on the 80-column format that was required for use in punch-card computers. The Generalized Nuclear Database Structure (GNDS) is a newer Extensible Markup Language (XML) based format that is more appropriate for modern computing needs [27]. These three formats and their structure are regulated by committees of users and experts to ensure consistent implementation.

These formats are used in the general-purpose nuclear data libraries that are published by nuclear data centers around the world. As of early 2021, the major nuclear reactions libraries are ENDF/B-VIII.0 from the USNDP [28], the Joint Evaluated Fission and Fusion Nuclear Data Library (JEFF-3.3) coordinated by the NEA [29], the Japanese Evaluated Nuclear Data Library (JENDL-4.0) from the Japanese Nuclear Data Committee [30], the Chinese Evaluated Nuclear Data Library (CENDL-3.2) from the Chinese Nuclear Data Center [31, 32], and the Russian Evaluated Nuclear Data Library (BROND-3.1) from the Institute of Physics and Power Engineering in Russia [33]. In addition to these, the TALYS Evaluated Nuclear Data Library (TENDL) is based on evaluator-reviewed predictions from the TALYS reaction code [34]. The USNDP maintains and continuously updates the primary ENSDF-formatted nuclear structure library.

Additional nuclear data libraries with specific uses also exist. The Reference Input Parameter Library (RIPL) contains input parameters to reaction codes that are used in evaluations [35]. The Evaluated Gamma-ray Activation File (EGAF) contains thermal production cross sections for prompt and delayed γ rays [36]. There are processed libraries for use in neutronics codes such as the Monte Carlo N-Particle transport (MCNP) code [37] and the Standardized Computer Analyses for Licensing Evaluation (SCALE) code [38].

1.1.3.5 Integral Benchmark Experiments

Integral measurements are conducted to provide benchmark data. These integral benchmark data are used to validate evaluated nuclear data libraries. In these experiments, a bulk quantity that is dependent on many differential nuclear properties is measured. In general, these experiments measure the effective multiplication factor (k_{eff}) [39, p. 74] with high precision for a critical assembly with a carefully calibrated and documented geometry and composition.

Conducting, detailing, and reporting these measurements is an internationally coordinated effort. The International Criticality Safety Benchmark Evaluation Project (ICSBEP) and International Reactor Physics Experiment Evaluation Project (IRPhEP) work to com-

pile databases of critical and subcritical integral benchmark experiments that can be used to validate nuclear data libraries for the purposes of criticality safety and reactor physics [40]. In addition to their compilation efforts, these projects also seek to identify gaps in the databases and guide future experiments to fill these gaps. These review efforts form an important part of the feedback loop in the nuclear data pipeline.

1.1.3.6 Validation

When a new evaluated library is compiled, it is first compared against data from integral benchmark experiments before release. This is done by inputting the new evaluated library into neutronics codes (namely MCNP [37]). Geometries and compositions of integral benchmark experiments (such as those in the ICSBEP and IRPhEP databases) are input to the neutronics code and the effective multiplication factor is calculated from the simulation results. If simulations using the new evaluated library do not match the integral benchmark data with sufficient precision, then the evaluation needs adjustment before release.

1.1.3.7 Applications

Once an evaluated nuclear data library is validated, it is published and enters into use in applications. The applications that rely on nuclear data are broad. Some applications may only use a handful of nuclear data properties (e.g., production of a specific medical isotope), while others use many (e.g., reactor design). The applications that use evaluated nuclear data include, but are not limited to:

- advanced reactor design,
- medical isotope production,
- nuclear forensics,
- nuclear safeguards,
- stockpile stewardship,
- detector response modeling,
- fusion reactor design,
- criticality safety,
- nuclear waste management,
- medical physics and radiation therapy,
- radiation shielding,

- dosimetry,
- radiological dating, and
- electronics hardening.

1.1.3.8 Sensitivity Studies

The process of validation reveals issues with evaluated libraries that are then corrected prior to their release. However, the process of validation cannot reveal every problem with an evaluated library, as integral benchmarks are only sensitive to certain properties of certain nuclei (e.g., materials that are present in the critical assemblies in sufficient quantities). Moreover, as applications evolve, new nuclear data needs emerge. Sensitivity studies are an important method for identifying and prioritizing nuclear data needs.

The results of sensitivity studies primarily inform experimentalists of what differential measurements need to be conducted or repeated. These results may also inform the development of new integral benchmark experiments; sensitivity to specific nuclear properties can be incorporated so that issues do not pass validation in the future. Finally, the results of sensitivity studies can influence the development of theory. Sensitivity studies close the feedback loop that forms the nuclear data pipeline.

1.2 Fission Yield Nuclear Data

This dissertation is focused on nuclear data related to fission yields. Below is a review of the current state of fission yield nuclear data and needs for improvements. Together, these pieces of information motivate the work presented in this dissertation; this work seeks to address fission yield nuclear data needs by expanding the current state of knowledge on fission yields.

1.2.1 The Current State of Fission Yield Data

1.2.1.1 Experimental Data

A review of the neutron-induced fission yield data stored in EXFOR was conducted to assist the development of the template of expected measurement uncertainties in fission yield nuclear data that is presented in Chapter 3. The review covered the three major actinides: ^{235}U, ^{238}U, and ^{239}Pu. A total of 812 EXFOR entries were reviewed, and these entries contained a total of 18214 individual fission yield values and uncertainties. The entries spanned the years 1943 to 2019 and thus the review provides a suitable overview of the current state of experimental fission yield data. Some norms and trends in the experimentally measured fission yields covered by this review are discussed below and some trends are further discussed in Sec. 3.2.3.1.

The information compiled in this review is useful in assessing the current state of fission yield nuclear data and the representative uncertainties in that data. Figure 1.2 displays the distribution of the quoted fission yield uncertainty values for each of the three target nuclei reviewed. A number of values in the dataset quoted uncertainties in excess of 100%. This is because some reports quoted constant experimental uncertainties that exceeded the value of some of the lower fission yields that were claimed to be observed. These values have been removed from the dataset as a measured value with uncertainty greater than the value itself does not provide much useful information. In the process of the EXFOR review, uncertainty values that were listed as being only statistical were excluded as these values under-represent the measurement uncertainty. It should be kept in mind only 6.8% of the subentries found in this review self-reported their uncertainties as statistical. The majority of entries/subentries list no information about what sources contribute to the quoted uncertainty. Therefore, it is very likely that more than 6.8% of the measurements quote only their statistical uncertainties.

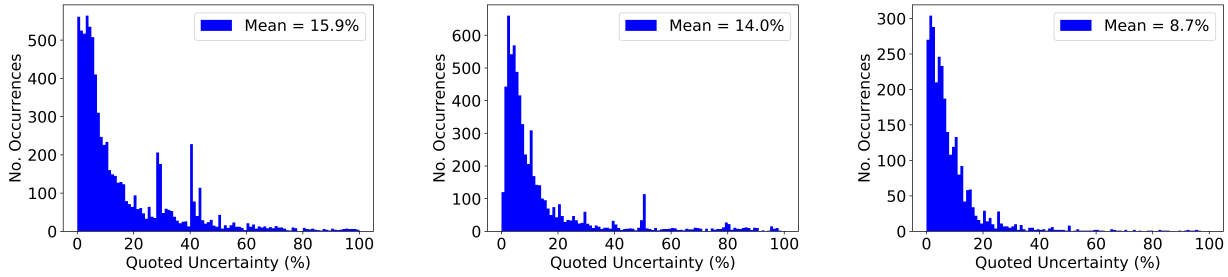

(a) ^{235}U (b) ^{238}U (c) ^{239}Pu

Figure 1.2: Histograms of the quoted relative uncertainty values for EXFOR-compiled fission yields for ^{235}U, ^{238}U, and ^{239}Pu. Uncertainty values that were listed as being only statistical or exceeded 100% were removed from the dataset.

Figure 1.3 displays the average quoted uncertainty for each target nucleus as a function of publication date. For each year on these plots, the quoted uncertainty values used to calculate the mean are cumulative (i.e., all values prior to and including that year are used). The error envelope on these plots is taken as the standard deviation of the cumulative values. Two notable trends can be observed: the average quoted uncertainty tends to decrease until approximately 1960 and thereafter the average quoted uncertainty slowly increases. This may be due to enhanced contemporary focus on the characterization of various systematic sources of uncertainty.

A large variety of experimental methods are used in the measurement of fission yields. Table 1.1 tabulates all of the experimental methods found in the review and their corresponding EXFOR codes. The description of each of these codes was taken from Dictionary 21 in the EXFOR manual [41]. Of these methods, those that were cited particularly frequently

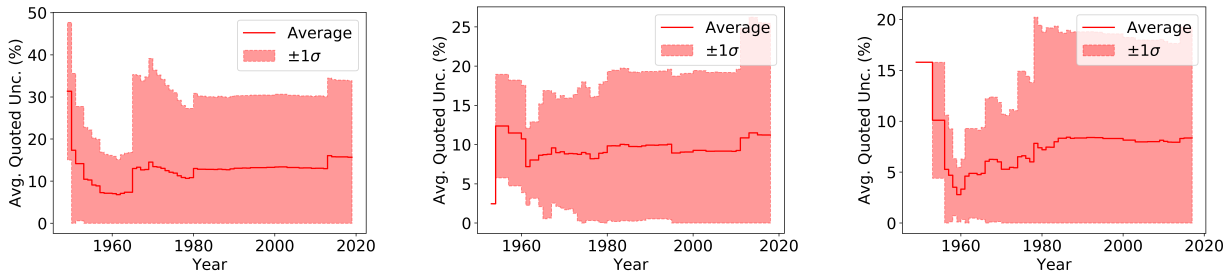

(a) ^{235}U (b) ^{238}U (c) ^{239}Pu

Figure 1.3: The average quoted uncertainty for fission yield measurements as a function of publication date. For each year on the abscissa, all values prior to and including that year are used. The error envelope is the standard deviation of the values reported.

included: activation, chemical separation, γ-ray spectroscopy, and mass spectrometry. These methods and the sources of uncertainty commonly associated with them are detailed in the template of expected measurement uncertainties presented in Chapter 3.

Figure 1.2 demonstrates the large average uncertainty in measured fission yield data. Despite these large uncertainties, Figure 1.3 shows that the precision of measured fission yields has not improved over time. However, this trend may be attributable to enhanced uncertainty reporting. Table 1.1 lists the large number of experimental techniques that are associated with fission yield measurements. Taken together, these figures show the current state of fission yield data; there remains significant uncertainty in the experimental data even with the wide variety of measurement techniques available.

1.2.1.2 Evaluations

As of early 2021, there exist three major evaluations of fission yield data: the ENDF/B-VIII.0 evaluation from the USNDP [28], the JEFF-3.3 evaluation from the NEA [29], and the JENDL-4.0 evaluation from the JAEA [30]. Table 3.2 of Sec. 3.2.2 summarizes the original sources for each of these evaluations and the years they were conducted. These evaluations and how they were conducted is discussed in greater detail in Sec. 3.2.2.

Figures 1.4 and 1.5 display histograms of the relative uncertainties in the independent and cumulative fission yields of the ENDF/B-VIII.0 and JEFF-3.3 evaluations. These figures show the large average relative uncertainties in evaluated fission yield data. This state of uncertainty in fission yield data is problematic to certain applications. Both improving the mean and width of the distributions of fission yield uncertainties shown in Figs. 1.4 and 1.5 is important to enabling applications.

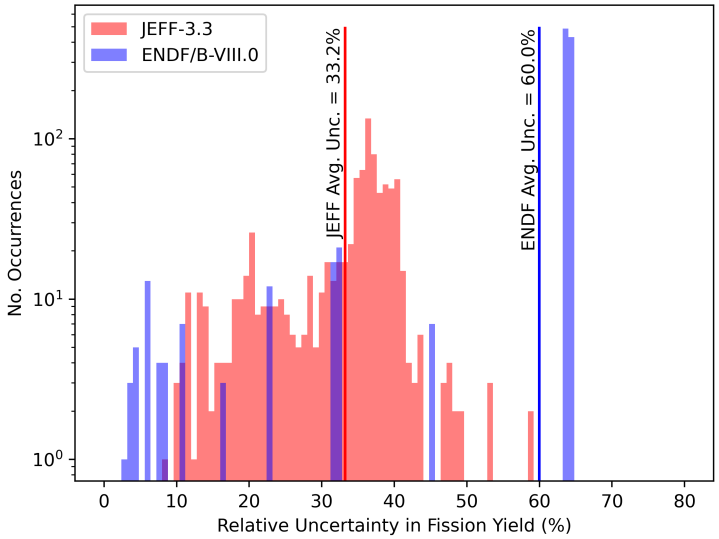

Figure 1.4: A histogram of the relative uncertainties of the independent fission yields in the ENDF/B-VIII.0 and JEFF-3.3 evaluations. Each histogram contains 100 bins. The independent yields have an average uncertainty of 33.2% and 60.0% in the JEFF-3.3 and ENDF/B-VIII.0 evaluations, respectively.

1.2.2 Improving Fission Yield Data

Given the current uncertainty in fission yield data, there is great room for improvement. To improve this uncertainty, advanced experimental techniques are required. Combining new, state-of-the-art experimental techniques with conventional measurement methods is one potential path to reducing average uncertainties. As legacy measurements did not always fully consider all sources of experimental uncertainty (as discussed in Sec. 1.2.1.1), careful characterization of uncertainties is a crucial detail in any new experiment.

One particular issue with evaluated fission yield data is that none of the existing fission yield evaluations contain information on fission yield covariances. This gap has been identified as a critical need [1, 42]. This covariance information could be useful to any calculation where fission yields are involved, but its importance to reactor antineutrino emission rate calculations [43, 44, 45, 46] and reactor decay heat calculations [47] has been specifically noted. To address this issue, a method for the estimation of fission yield covariances was developed. This method is presented in Chapter 4 as a part of the work that contributes to this dissertation.

The primary means by which uncertainties in fission yields can be improved is experimentation. To this end, two projects that seek to improve fission yield data through experimenta-

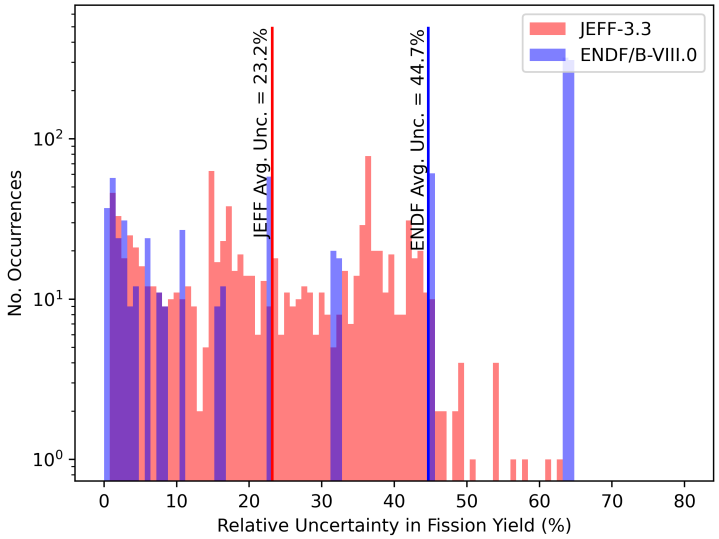

Figure 1.5: A histogram of the relative uncertainties of the cumulative fission yields in the ENDF/B-VIII.0 and JEFF-3.3 evaluations. Each histogram contains 100 bins. The cumulative yields have an average uncertainty of 23.2% and 44.7% in the JEFF-3.3 and ENDF/B-VIII.0 evaluations, respectively.

tion are presented in this dissertation. The template of expected measurement uncertainties for fission yields is presented in Chapter 3. This template provides a guide to help experimentalists fully consider their experimental uncertainties when using common fission yield measurement methods. The development of and preliminary results from the Fast Loading User Facility for Fission Yields (FLUFFY) at the 88-Inch Cyclotron at Lawrence Berkeley National Laboratory are presented in Chapter 5. The technique of cyclical activation analysis is used with FLUFFY to measure short-lived fission product yields. The measurement of fission yields has been predominately focused on the cumulative yields of longer-lived fission products. Therefore, the information provided by FLUFFY on short-lived fission product yields has the potential to improve yield data in this region of the fission product distribution.

The work that is presented in Chapters. 3, 4, and 5 makes contributions at several stages in the nuclear data pipeline. The template of expected measurement uncertainties in Chapter 3 contributes to the Experiment and Evaluation stages of the pipeline by providing a guide that can be used by both experimentalists and evaluators. The work on estimating fission yield covariances in Chapter 4 contributes to the Theory, Evaluation, and Sensitivity Studies stages of the pipeline. The experimental measurement of fission yields using FLUFFY in Chapter 5 contributes to the Experiment stage of the pipeline.

Table 1.1: All of the methods found in EXFOR-compiled measurements of fission yields of 235U, 238U, and 239Pu. The method codes and their descriptions are taken from Dictionary 21 of the EXFOR manual [41].

Method Code	Description
ABSFY	Absolute fission yield measurement
ACTIV	Activation
AMS	Accelerator mass spectrometry
ASEP	Separation by mass-separator
BGCT	Beta-gamma coincidence technique
BSPEC	Beta-ray spectrometry
CHSEP	Chemical separation
COINC	Coincidence
EDE	Particle identification by E/Delta E measurement
EXTB	Irradiation with external beam
FISCT	Absolute fission counting
FNB	Filtered neutron beam
FPGAM	Direct gamma-ray spectrometry
GSPEC	Gamma-ray spectrometry
HATOM	Hot-atom method
HEJET	Collection by He jet
INTB	Irradiation with internal beam
JET	Collection by gas jet
MASSP	Mass spectrometry of a product
MOMIX	Mixed monitor
OLMS	On-line mass separation
PHD	Pulse-height discrimination
PLSED	Pulse die-away
PSD	Pulse-shape discrimination
RCHEM	Radiochemical separation
REAC	Reactivity measurement
REC	Collection of recoils
RELFY	Relative fission yield measurement
RINGR	Ring ratio method
RVAL	R-value measurement
SITA	Single target irradiation
SLODT	Slowing-down time
STTA	Stacked-target irradiation
TOF	Time-of-flight

Chapter 2

Background

In order to understand fission yields, an understanding of the process of fission must be developed first. This chapter focuses on providing a background on fission, its observables, its discovery, its theoretical descriptions, and the experimental methods used to measure it.

2.1 The Process of Fission

Fission is the process by which an atomic nucleus undergoes a change in the configuration of its nucleons that results in its division – or "scission" – into two or more fragments. Fission can be induced by imparting excitation energy to a nucleus via an external particle or it can happen as a spontaneous decay process. A typical fission event produces two fission fragments; this is called "binary fission." Ternary and quaternary fission have been observed [48, 49], and occur in less than one in every hundred fission events. Ternary and quaternary fission fragments are typically significantly smaller than their binary counterparts with $A < 10$.

The binary fission fragments produced in fission are born with high excitation energy (tens of MeV). These fragments are neutron-rich and at such high excitation energies, the preferred de-excitation pathway is neutron emission. The fragments proceed to emit neutrons until their excitation energy has fallen below the neutron separation energy, after which neutron emission is energetically forbidden. After neutron emission has ceased, the fission fragment is now called a fission "product" and γ-ray emission begins. Gamma emission proceeds until the fission product is fully de-excited. From scission to de-excitation, several neutrons and several γ rays are emitted from each fission fragment. This de-excitation occurs in less than a nanosecond, and thus the particles resulting from it are described as "prompt."

The fission product that results after prompt de-excitation is usually itself unstable and will undergo radioactive decay. As fission products are on the neutron-rich side of the line of stability, the overwhelming majority undergo β^- decay. The most neutron-rich of these fission products have β^- decays that populate states in their daughter nucleus that are above

the neutron separation energy, allowing for further neutron emission. In addition to these neutrons, the β^- decays result in the emission of γ rays from the daughter nuclei. The neutrons and γ rays that are emitted due to these β^- decays are called "beta-delayed" or "delayed." A handful of fission products exhibit β^+, electron capture, and α decays. The $\beta^\pm$ and electron capture decays also result in the emission of antineutrinos and neutrinos. In all, the process of fission results in the emission of fission fragments/products, neutrons, γ rays, $\beta^\pm$ particles, antineutrinos and neutrinos, and α particles. Each fission event releases an average energy of roughly 200 MeV. Figure 2.1 shows the chronology of the fission process and its resulting emissions and decays.

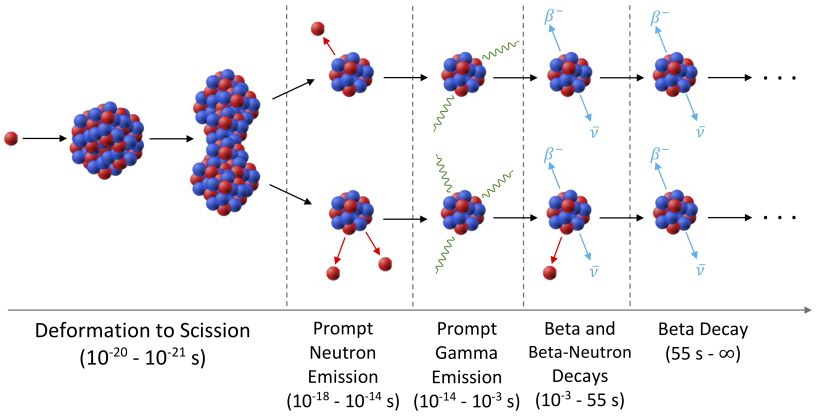

Figure 2.1: The chronology of fission, from deformation to fission product β decay. Timescale based on Ref. [50]. Atomic nucleus figure used from Ref. [51].

As will be further discussed in Sec. 2.2.1, fission occurs when the repulsive Coulombic force between the protons overcomes the attractive residual strong (nuclear) force between the nucleons. The strength of the nuclear force is considerably greater than that of the Coulombic force. Thus, in order for fission to occur, deformation to the nucleus must occur that allows the Coulombic force to overcome the nuclear force. This deformation can exist naturally, as is the case in super-heavy nuclei where spontaneous fission occurs, or it can be induced by adding excitation energy to the compound system. The energy required to induce a deformation that allows fission to proceed is called the "fission barrier."

Fission occurs in heavy nuclei. Fission is most commonly associated with actinides but has been observed in compound nuclei with A as low as 197 through the ^{181}Ta(^{16}O,f) reaction [52]. With increasing nuclear mass, the fission barrier tends to lower, and thus the probability of spontaneous fission tends to increase. In some nuclei, the fission barrier is low enough that fission can be induced by a neutron with thermal kinetic energy. The excitation energy left in the compound nucleus by the absorption of the neutron (the neutron separation energy) is sufficient to cross the fission barrier and allow fission to proceed. Such target

nuclei are referred to as "fissile." In the mass region near uranium, this effect causes target nuclei with odd neutron numbers to be fissile. This is because nucleon pairing results in a boost to the energy imparted to the compound nucleus by the absorption of a neutron that completes a pair with the odd neutron of the nucleus [11, p. 488].

In some nuclei, induced deformation can create an isomeric state. The deformation is severe enough that fission becomes possible, but not so severe that fission proceeds immediately. Because a significant change in deformation is required to either proceed to fission or revert to the ground state, the state exhibits a non-zero lifetime. These states are called "fission isomers." Fission isomers have been observed from thorium to berkelium and have lifetimes ranging from nanoseconds to tens of milliseconds [53].

2.1.1 Fission Observables

Fission is a complex process that results in the generation of several different particles in each fission event. Because of this, fission has many different observables. To generate a comprehensive list of fission observables, 300 publications in NSR on fission observables from ^{238}U(n,f) were reviewed. These publications spanned the years 1977 to 2019. In total, 32 different fission observables were found. Of these, the most commonly reported observables were the (n,f) cross section and fission yields. A list of the fission observables that were found and the number of times they were found is provided in Table 2.1.

Because the particles emitted from fission and their corresponding observables result from the same nuclear event, fission observables have strong correlations between them. These correlations can be determined experimentally or estimated from theoretical modeling. The number of times that multiple fission observables were measured in a single experiment was recorded during the review of NSR. These experiments are important because they have the potential to give information on the correlation between fission observables. Unfortunately, experiments involving fission do not often report more than one observable, making information on fission observable correlations scarce. Only 13.0% of all measurements for this compound system measured more than one observable. Figure 2.2 shows a matrix that tabulates the number of times that the fission observables listed in Table 2.1 were simultaneously measured.

2.1.2 The History of Fission

The existence of a process whereby an atomic nucleus would be split into fragments was initially posited by Ida Noddack in 1934 [54]. Between 1937 and 1938, Irene Joliot-Curie published papers that noted the presence of several chemical elements in a uranium sample that had been irradiated with neutrons [55, 56, 57]. This work prompted Lise Meitner to request additional experiments from Otto Hahn and Fritz Strassmann. The existence of the process of fission was confirmed by Hahn and Strassmann by bombarding uranium with

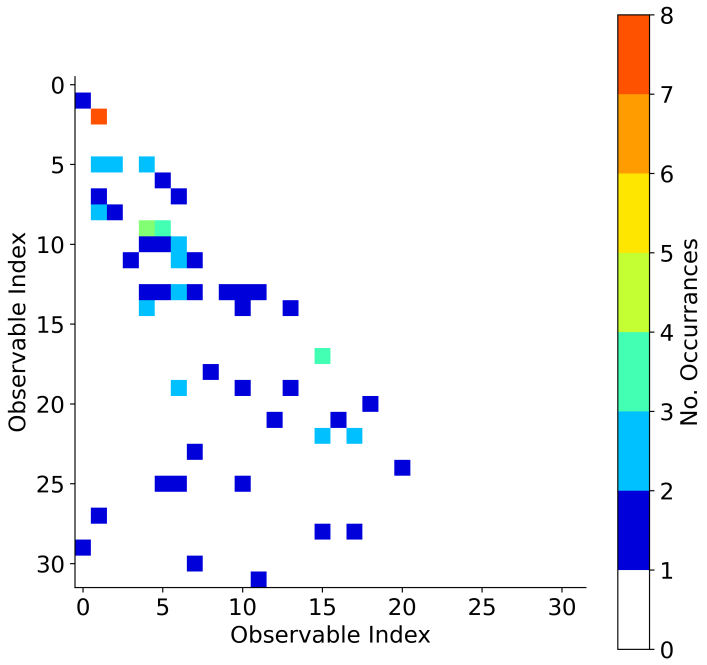

Figure 2.2: Lower triangular matrix of simultaneous measurements of the fission observables listed in Table 2.1 for neutron-induced fission of ^{238}U. The indices on the axes correspond to the matrix indices listed in Table 2.1. The diagonal is null as the diagonal of this matrix only reflects the measurement of a single observable. Only 13.0% of all measurements for this compound system measured more than one observable.

neutrons in December 1938 [58]. In this experiment, chemical analysis was used to confirm that barium was produced as a result of bombarding the uranium with neutrons. The first theoretical description of fission was offered by Meitner and Frisch in January 1939 [59]. The existence of fission was further confirmed by a team of physicists at Columbia University in late January of 1939 [60]. A uranium target was placed in an ionization chamber and bombarded with neutrons, allowing the energy released by each fission event to be measured.

Soon after its discovery, the details on the emissions from fission were clarified and the average number of neutrons emitted from each fission event was assessed [61]. A key observation was that the average number of neutrons emitted from fission was greater than one. This immediately raised the possibility that fissile actinides could be configured in a geometry that would allow a chain reaction to proceed. A controlled chain reaction, where the number of neutrons produced by fission and the number of neutrons inducing fission

remain constant in time, was recognized as a possible source of energy. An uncontrolled chain reaction, however, was recognized for its potential to create a very destructive release of energy [62].

Both controlled and uncontrolled systems were designed and tested by scientists in short order. On December 2, 1942, a research team led by Enrico Fermi achieved the first controlled nuclear chain reaction in the Chicago Pile-1 reactor at the University of Chicago [63]. Less than three years later, on July 16, 1945, the first uncontrolled nuclear chain reaction was initiated by a team of researchers led by J. Robert Oppenheimer with the Trinity nuclear test near Socorro, New Mexico [64]. The first nuclear reactor designed to produce electrical power, the Experimental Breeder Reactor I at the National Reactor Testing Station, became operational on December 20, 1951 [65].

Since these early developments, both nuclear reactors and nuclear weapons have been extensively developed and have become integral parts of society. Nuclear reactors are responsible for approximately 10% of global electricity production [66], are critical in radioisotope production, and aid basic research. Nuclear weapons are possessed by at least eight sovereign states and are a major concern for national and global security. As these two critical technologies have developed, the interest in nuclear fission – which is at their core – has continued to grow.

2.2 Descriptions of Fission

To describe the fundamental origin of fission and observed fission phenomena, a number of semi-empirical and theoretical descriptions of fission have been put forth. As time has progressed, more and more complex models have been developed, each offering more advanced descriptions of particular observables. Nevertheless, even the most simplistic model – the liquid drop model – can provide basic insights into the nature of fission. This section will review a series of fission models that are particularly useful to evaluation and applications.

2.2.1 The Liquid Drop Model

The first model that can be used to describe fission was developed in 1930, before the discovery of fission itself. This model, often referred to as the "liquid drop model", was first posited by George Gamow in order to describe empirical trends in nuclear binding energies [67]. In 1935, Carl Friedrich von Weizsäcker further developed this theory to give the formulation that is most commonly used today [68].

The model treats the nucleus as a drop of charged liquid. The charge of the liquid has a single polarity that is uniformly distributed across the volume of the drop. This creates a repulsive force within the drop that tends to drive it towards disintegration. Countering this

repulsive Coulombic force is the nuclear force that attracts the matter of the drop together. Equation 2.1 gives the Semi-Empirical Mass Formula which represents the liquid drop model [11, p. 68]:

$$E = a_V A - a_S A^{2/3} - a_C \frac{Z(Z-1)}{A^{1/3}} - a_A \frac{(A-2Z)^2}{A} + \delta(N,Z) \tag{2.1}$$

where E is the binding energy of the nucleus, A is the mass number of a particular nucleus, Z is the proton number of the nucleus, a_V is the volume term parameter, a_S is the surface term parameter, a_C is the Coulomb term parameter, a_A is the asymmetry term parameter, and δ is the pairing term which is given by:

$$\delta(A,Z) = \begin{cases} +a_P & A - Z \, and \, N \, even \\ 0 & A \, odd \\ -a_P & A - Z \, and \, N \, odd \end{cases} \tag{2.2}$$

where a_P is the pairing term parameter.

This model has five terms and five parameters, each with an underlying physical basis:

- **volume term** – $a_V A$ – this term scales with A which is directly proportional to the volume of the nucleus. The term is positive and therefore represents an attractive force that holds the nucleus together. Physically, this term represents the nuclear force: the more volume per nucleon, the greater the attractive nucleon-nucleon interactions in the nucleus.

- **surface term** – $-a_S A^{2/3}$ – this term is a correction to the volume term; it accounts for the fact that nucleons on the surface of the nucleus have fewer attractive nucleon-nucleon interactions as they are not surrounded by other nucleons on all sides. Therefore, this term is negative.

- **Coulombic term** – $-a_C \frac{Z(Z-1)}{A^{1/3}}$ – this term accounts for the repulsive force between the protons of the nucleus and is therefore negative. It is analytically derived from the energy required to add an infinitesimal shell of charge to a sphere of charge assuming Gauss's law.

- **asymmetry term** – $-a_A \frac{(A-2Z)^2}{A}$ – this term accounts for the fact that nuclear configurations with an uneven number of proton and neutron pairs are less bound than those with an even number of proton and neutron pairs. Except when the number of protons and neutrons is equal, this term is negative and thus destabilizing.

- **pairing term** – $\delta(N,Z)$ – this term accounts for the observed enhancement in stability when all nucleons are paired. The term is positive when all are paired, zero when there is one odd nucleon, and negative when there is both an odd neutron and odd proton.

While different sources list different values for the parameters of the model, commonly used values are: $a_V = 15.5$ MeV, $a_S = 16.8$ MeV, $a_C = 0.72$ MeV, $a_A = 23$ MeV, and $a_P = 34$ MeV [11, p. 68].

The utility of this model lies in its simplicity: while the model only contains five terms and parameters, it has a remarkable ability to reproduce many observed trends in nuclear binding energies. And while the model was developed to describe nuclear binding energies, it also provides insights about the energetics of fission. Consider the example of fission of the ^{235}U(n,f) compound nucleus, ^{236}U. In the case of symmetric fission, ^{236}U splits to form two ^{118}Pd fragments. Table 2.2 shows values of the individual terms of the semi-empirical mass formula and how they change after the ^{236}U fissions into symmetric fission fragments. It can be seen that the semi-empirical mass formula accurately predicts the energy release from fission. It also explains the mechanism by which fission occurs: the shape change that occurs in fission reduces the number of attractive nucleon-nucleon interactions, allowing the Coulombic force to take over and split the nucleus. This is seen in the reduction of the surface term and the increase of the Coulombic term. While the liquid drop model provides important insights about the energetics and forces that drive the fission process, it falls short of describing more advanced fission phenomena.

2.2.2 The Shell Model

In 1949, the shell model of atomic nuclei was developed by Maria Goeppert Meyer [69]. The model was developed to address the observed "magic numbers" in atomic nuclei. Nuclei with a magic number of protons or neutrons were observed to have enhanced stability and low nuclear level density. This was especially true for nuclei with both a magic number of protons and a magic number of neutrons. While this behavior had been observed in the 1930s and 1940s [70], a physical model that successfully predicted all of these magic numbers had been elusive. Figure 2.3 shows an example of enhanced stability in nuclei with a magic number of protons or neutrons.

The nuclear shell model was inspired by the atomic shell model, which had done an excellent job of describing shell effects in atoms. However, applying the atomic shell model directly to the nucleus cannot work; there is a single force that holds an atom together (the Coulombic force), whereas a nucleus has nucleons that attract each other through the nuclear force and protons that repel each other through the Coulombic force. Moreover, an atom has a central, immobile potential that is created by the charged nucleus. The potential of a nucleus is created by the nucleons themselves and is thus non-central. As a result, a multi-termed potential is required to describe a nucleus in the Schrödinger equation and that is difficult to solve analytically.

In order to form a potential that describes a nucleus in a mathematically tractable way, the assumption that the nucleons form a nearly central potential is made. This potential is

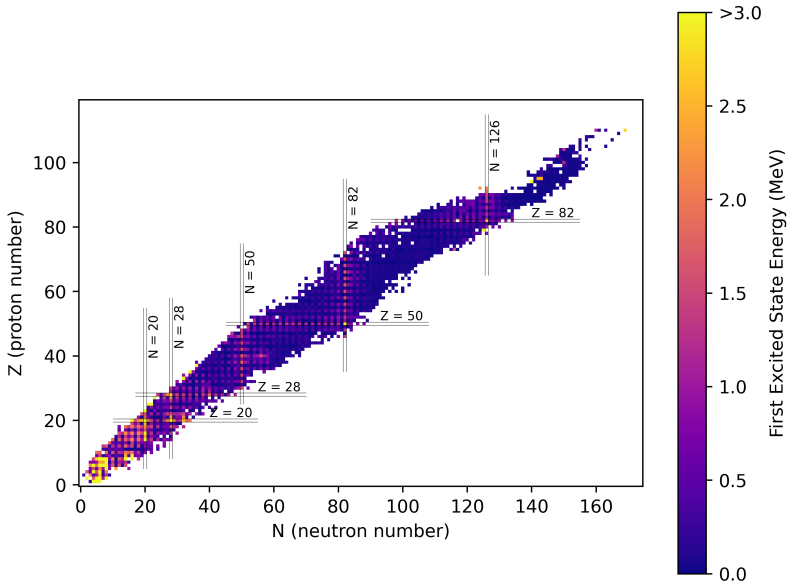

Figure 2.3: The first excited states of nuclei as a function of N and Z. Enhanced stability is observed in even-even nuclei with a magic number of protons and/or neutrons; their first excited states occur at significantly higher energies on average. The color bar is truncated at 3 MeV to enhance the visibility of the effect in nuclei with A $\geq$ 20. The data in this figure were taken from RIPL [35].

described with the Wood-Saxon potential [71], the mathematical form of which is shown in Eq. 2.3. This potential, which is a modified form of the three-dimensional harmonic oscillator potential, describes the nuclear potential as a well with a finite depth and a smooth edge or "skin." Figure 2.4 shows the Wood-Saxon potential as a function of nuclear radius and demonstrates its smooth edge.

$$V_{WS}(r) = \frac{-V_0}{1 + exp[(r - R/a)]} \tag{2.3}$$

where V_0 is the depth of the well (strength of the potential) and is commonly given the value $V_0 = 50$ MeV, R is the nuclear radius and is commonly given by $R = 1.25A^{1/3}\,[fm]$, and a describes the "thickness" of the skin at the edge of the potential and is commonly given the value $a = 0.524$ fm [11, p. 122].

The Wood-Saxon potential begins to describe the shell structure of atomic nuclei, however, it falls short of accurately predicting the experimentally observed magic numbers. The Wood-Saxon potential predicts magic numbers of 2, 8, 20, 34, 58, 92, and 138, whereas the experimentally observed magic numbers are 2, 8, 20, 28, 50, 82, and 126 [11, p. 123].

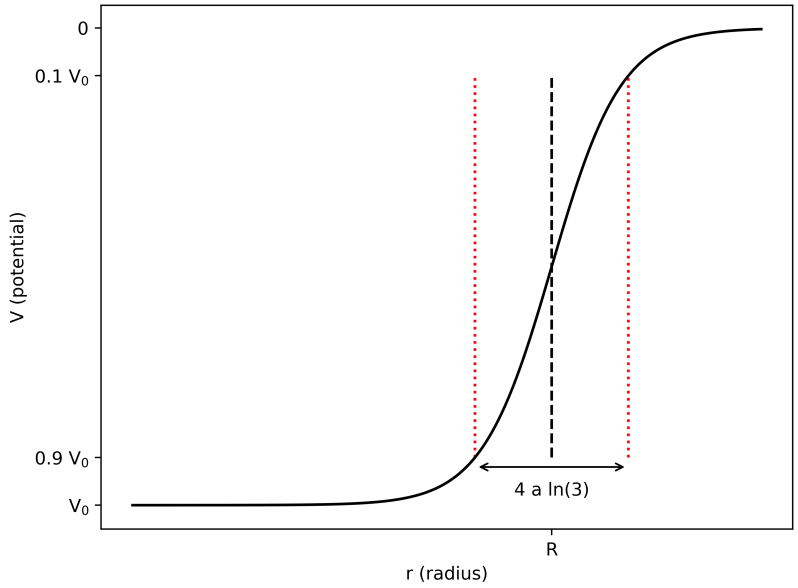

Figure 2.4: The Wood-Saxon potential as a function of nuclear radius. The "skin" of the nucleus is shown between the red dotted lines. The thickness of the skin is controlled by the parameter a. As a decreases, the skin becomes thinner.

To further modify the nuclear potential and finally describe the experimentally observed magic numbers, Mayer introduced a term to account for the interaction between the spin of the nucleons with the orbital potential – the so-called "spin-orbit" coupling. This results in the nuclear potential that is given in Eq. 2.4, where the term, $V_{so}(r)\,\boldsymbol{\ell}\cdot\boldsymbol{s}$, is the modification for the spin-orbit coupling. The form of $V_{so}(r)$ is not particularly important [11, p. 124]. What is important is the factor, $\boldsymbol{\ell}\cdot\boldsymbol{s}$, which breaks the spin degeneracies from the Wood-Saxon levels.

$$V(r) = V_{WS}(r) + V_{so}(r)\,\boldsymbol{\ell}\cdot\boldsymbol{s} \tag{2.4}$$

where $V(r)$ is the total radial nuclear potential, $V_{WS}(r)$ is the Wood-Saxon potential given in Eq. 2.3, and $V_{so}(r)\,\boldsymbol{\ell}\cdot\boldsymbol{s}$ is the modification for the spin-orbit coupling.

With the introduction of the spin-orbit coupling term to the nuclear potential, the experimentally observed magic numbers are reproduced exactly. This significant development in the description of the nuclear potential allows the origins of the shell structure in atomic nuclei to be understood. This shell structure is very important for understanding the dynamics of fission as well. At low excitation energies, binary fission produces two fragments with unequal mass; binary fission rarely produces two fragments of equal mass. This is explained by the shell model: fission preferentially produces one fragment near the doubly magic $A = 132$ ($Z = 50$, $N = 82$). The other fragment receives the remainder of the mass. Figure 2.5

demonstrates the important effect that shell structure has on the process of fission. Mass yields in low-energy fissioning systems are anchored near the doubly magic $A = 132$. Shell effects give low-energy fission its characteristic asymmetry.

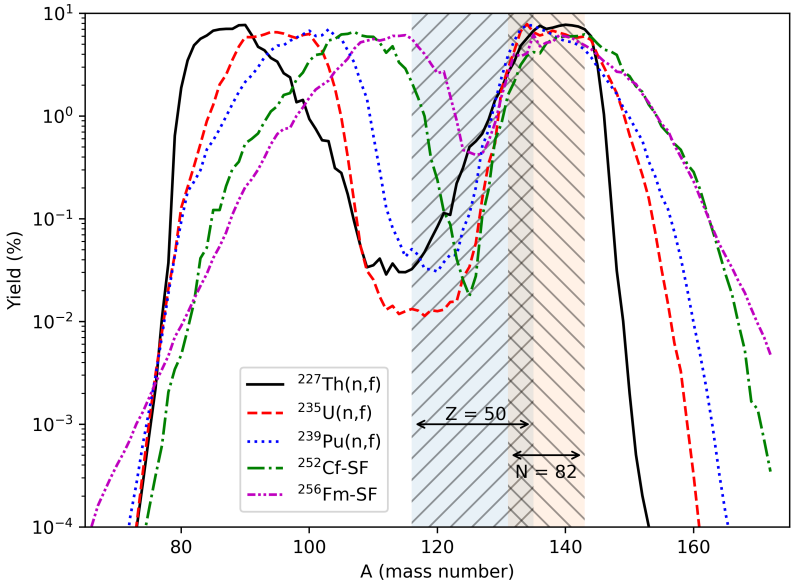

Figure 2.5: The thermal-neutron mass yields for ^{227}Th, ^{235}U, and ^{239}Pu and the spontaneous-fission mass yields for ^{252}Cf and ^{256}Fm. The shaded regions show mass yields which are contributed to by at least one product with a magic number of protons or neutrons. Note that in the doubly magic region, there is an enhancement in the mass yield curve of all five nuclei. The low-mass centroid of each mass yield curve increases with increasing nucleus mass. This occurs because the left edge of the heavy-mass centroid is anchored near the doubly magic closure. The independent mass yields were taken as the sum of the independent fission yields with a given A using the data in the fission yield evaluation of ENDF/B-VIII.0 [28].

2.2.3 The Deformed Shell Model

In the early 1950s, experimental evidence emerged that suggested the existence of static deformation in atomic nuclei [72, 73, 74, 75]. These statically deformed nuclei exhibited rotational bands in their excitation spectra. The shell model that had been proposed by Maria Goeppert Mayer in 1949 had a spherical potential and therefore described spherical nuclei. This model was not sufficient for the description of deformed nuclei and could not predict the observed rotational phenomenology.

In 1955, Sven Nilsson modified the shell model potential to account for deformation in the nuclear shape [76]. Because a non-spherical, deformed potential was used, $\boldsymbol{\ell}$ ceases to be a

good quantum number. Instead, the projection of $\boldsymbol{j}$ onto the symmetry axis of the nucleus, $\boldsymbol{\Omega}$, becomes a good quantum number. This means that the $(2j + 1)$ degeneracy of the spherical shell model is broken as the result of a non-zero deformation. As the deformation increases, the greater the energy splitting. Figure 2.6 shows energy levels for single neutrons in a deformed nucleus as a function of deformation.

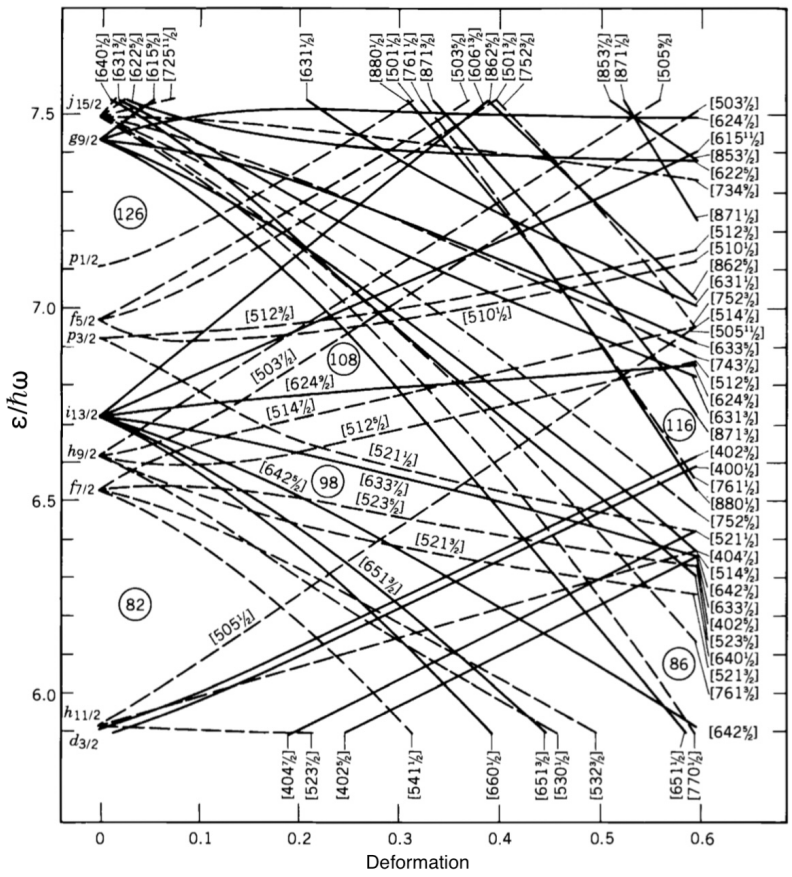

Figure 2.6: Energy levels for single neutrons in a prolate deformed potential as predicted by the Nilsson model. As deformation goes to zero, the energies and (2j+1) degeneracy of the spherical shell model are restored. This figure is reproduced from Figure 5.29 of Ref. [11, p. 155], which was produced from Ref. [77].

While this deformed shell model was successful at describing trends at small deformations, its accuracy at large deformations was poor [78]. This had made theoretical calculation and prediction of fission barrier values in heavy nuclei (which have high deformation) difficult. In 1967, Velin Strutinsky proposed a method that uses the Nilsson model to calculate a "shell correction" for the liquid drop model [79]. A deformed version of the liquid drop model was used [80]. The method suggests that this shell correction, δU, is given by Eq. 2.5:

$$\delta U = U - \tilde{U} \tag{2.5}$$

where U is the sum of the energies of the nucleons as calculated by the Nilsson model and $\tilde{U}$ is the sum of the energies of the nucleons as calculated by the deformed liquid drop model.

In addition to allowing the accurate calculation of fission barrier values, this method also provides the first theoretical description of fission isomers. The deformation energy calculated using this method as a function of deformation showed two to three minima. The ground state of the nucleus exists in the first minimum. The fission isomer exists in the next minimum. Depending on the energy surface, the fission isomer can either tunnel back to the ground state or can tunnel to even higher deformation where fission will proceed. Figure 2.7 shows an example of a fission barrier calculated with this method.

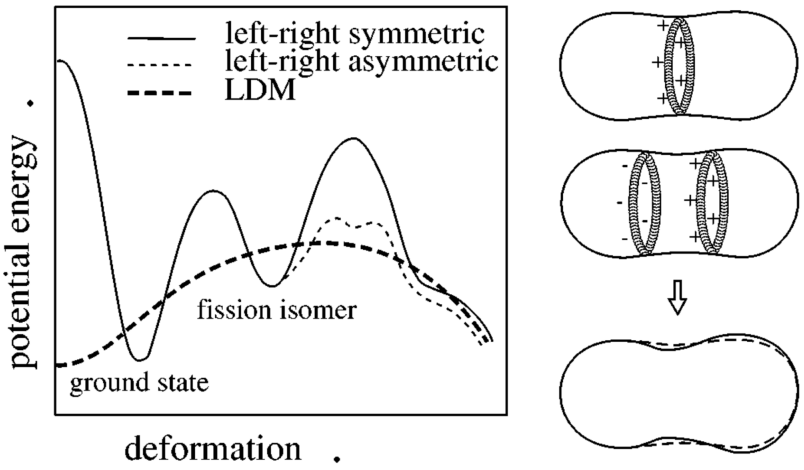

Figure 2.7: An example of a fission barrier calculated with the Strutinsky Method. The dashed line is predicted by the deformed liquid drop model. The thin dashed line is a fission barrier that is typical when asymmetric fission is observed. The thick dashed line is typical of asymmetric fission. This figure was reproduced from Figure 3 of Ref. [81].

2.2.4 Advanced Models

There exist many advanced models of atomic nuclei and some of these models can be used to investigate fission phenomenology. An extensive number of advanced models of fission have been reviewed in Refs. [82, 83]; these include statistical models, microscopic models, and *ab initio* calculations. While many models of fission exist, only a handful are useful for applications and evaluations. As this dissertation is focused on the nuclear data of fission yields, only models that are useful to fission yield evaluation and applications will be dis-

cussed specifically.

Four models, in particular, are useful to applications that use fission yield information and evaluations of fission yields: the Wahl Systematics, the General Description of Fission Observables (GEF) code, the Hauser-Feshbach Fission Fragment Decay (HF^3D) model, and the Fission Reaction Event Yield Algorithm (FREYA). Each of these models and their uses will be briefly discussed in Secs. 2.2.4.1-2.2.4.4.

2.2.4.1 Wahl Systematics

The Wahl systematics provide a set of mathematical equations that describe the charge distributions (including even-odd effects), mass distributions, and delayed-neutron yields of a fissioning system [84, 85]. The relative simplicity and limited number of parameters featured in this model make it a good candidate for use in evaluations. The model parameters can be tuned to experimental data with tractable regression methods. Because of this, the model was particularly useful in the most recent USNDP evaluation of fission yields conducted in 1994 [86]. The model was complemented with the Madland isomeric yield ratio tables [87, 88] to produce a complete evaluation. While this model has been useful to evaluation, advancements in computational resources have made the use of even more descriptive models in fission yield evaluation possible.

2.2.4.2 GEF

The General Description of Fission Observables (GEF) code is a model developed to describe the observables of fission from any compound nucleus with a given excitation energy and angular momentum [89]. Like the Wahl systematics, GEF is able to reproduce expected fission yield distributions and their even-odd effects. However, GEF not only models fission yield distributions, but it also predicts several other fission observables including prompt neutron and γ-ray distributions, fission barrier values, fission probabilities, isomeric yield ratios (a notable improvement over the Wahl systematics), and fragment kinetic energies. To accommodate such a broad range of predictive results, the model underlying the GEF code has 50 model parameters.

While GEF predicts a broad range of fission observables, it is not recommended for evaluations [89]. The GEF code and its model parameters are meant to be used to predict fission observables for several hundred fissioning systems from $Z = 80$ to $Z = 112$. Thus, by comparison to the large amount of experimental data covering this range of fissioning systems, the 50 model parameters are relatively restrictive. Therefore, at this time, GEF is only recommended for the validation of evaluations, not for the production of evaluations themselves.

2.2.4.3 HF^{3}D

The Hauser-Feshbach Fission Fragment Decay (HF^{3}D) model has been implemented as a package inside of BeoH [90, 91] – a statistical Hauser-Feshbach code developed at Los Alamos National Laboratory (LANL). HF^{3}D is a deterministic model. This makes HF^{3}D ideal for fission yield modeling as the yields to all fission fragments/products are calculated with the same precision. Moreover, the calculations performed by HF^{3}D require significantly less computational power than Monte-Carlo models of fission, making it an ideal evaluation tool [92].

Together with the Cascading Gamma-ray and Multiplicity for Fission (CGMF) code [93], HF^{3}D is being used by researchers at Los Alamos National Laboratory to generate evaluations of fission observables that are physically consistent with each other [92]. CGMF will be used for some fission observables, such as average neutron multiplicities and prompt neutron energy spectra, while HF^{3}D will be used for others, such as fission yields. The underlying models in CGMF and HF^{3}D are nearly identical, allowing the same parameters to be used for both codes. Because of this, there is a high degree of consistency between evaluations of fission observables generated using CGMF and HF^{3}D. This addresses an important problem: existing evaluations of fission observables have been conducted independently. Correlations between the observables are therefore missed and this results in the evaluations being inconsistent [94].

2.2.4.4 FREYA

As previously mentioned in Sec. 2.2.4.3, inconsistencies between fission observable evaluations exist. A similar issue was identified in event generators for nuclear transport codes: the conservation of physical quantities and correlations between observables were not properly handled. To address this problem, the Fission Reaction Event Yield Algorithm (FREYA) was developed to provide an event generator for Monte-Carlo transport codes that simulated fission events with physically consistent observables [95, 96]. FREYA has been integrated into standard Monte-Carlo transport codes such as MCNP and the Geometry and Tracking (GEANT) code [97].

While the previously mentioned models – the Wahl Systematics, GEF, and HF^{3}D – are particularly useful for evaluation efforts, FREYA is focused on use in applications. The model underlying FREYA generates a complete and fully correlated set of fission observables for individual fission events, starting from pre-fission neutron emission, following the fission event all the way through to prompt γ-ray emission from the fission products. Because FREYA is an event generator it is more appropriate for radiation transport applications than evaluation itself. This is particularly true for fission yield evaluations where an intractable number of events would need to be generated to assess the full range of fission products (which have yields ranging 21 orders of magnitude [86]).

While advanced models of nuclear fission exist, none can describe the process of fission and all of its observables with sufficient accuracy. As such, experimental measurement of fission observables is required to determine the properties of nuclear fission and to complement and inform theoretical models of fission. This dissertation focuses on the improvement of the nuclear data related to one category of fission observable: fission yields. The background presented in this chapter is complemented by the material that follows in Chapter 3, which offers a review of experimental methods used in fission yield measurements, with a particular focus given to measurement uncertainties. Together, these chapters provide a foundation for fission yield evaluation by detailing theoretical and experimental capabilities.

Matrix Index	Observable	No. Measurements
0	(n,f) Cross Section	41
1	Product Cumulative Yields	32
2	Mass Yields	12
3	Fragment Angular Correlations	12
4	Prompt Fission n Spectrum	10
5	Average n Multiplicity	10
6	Fragment TKE	8
7	Charge Yields	7
8	Product Independent Yields	6
9	Average n Energy	6
10	Fragment Mass Yields	5
11	Fragment Yields	4
12	Delayed n Group Numbers	4
13	Average TKE	4
14	Prompt n Angular Correlation	3
15	Prompt γ Spectrum (Low Res.)	3
16	Delayed n Energy Spectra	3
17	Average γ Multiplicity	3
18	Isomeric Ratios	2
19	Fragment Mass	2
20	Fragment Angular Momenta	2
21	Delayed n Yield	2
22	Average Total γ Energy per Fission	2
23	Prompt X-ray Spectra	1
24	Prompt γ Spectrum (High Res.)	1
25	Fragment Excitation Energy	1
26	Fragment γ Emission	1
27	Fractional Cumulative Yields	1
28	Average γ Energy	1
29	(nf) Cross Section Correlations	1
30	$\gamma - \gamma$ Coincidence	1
31	$\gamma - \gamma - \gamma$ Coincidences	1

Table 2.1: Observables matrix indices and number of measurements listed in NSR for the 300 measurements reviewed.

Table 2.2: Terms of the semi-empirical mass formula (Eq. 2.1) calculated for ^{236}U and two symmetric fission fragments, ^{118}Pd. The difference between these terms indicates approximately 235 MeV should be released from such a symmetric fission event.

Term (MeV)	^{236}U	$2 \times {}^{118}$Pd	Difference (MeV)
Volume	3658	3658	0
Surface	-641.6	-808.3	-166.7
Coulombic	-975.4	-607.7	367.7
Asymmetry	-263.5	-263.5	0
Pairing	34	68	-34
Total	1811.5	2046.5	235

Chapter 3

Expected Measurement Uncertainties in Fission Yield Measurements

The basis of this chapter is formed by "Templates of Expected Measurement Uncertainties" – Chapter IX – "Fission Yields" which was previously submitted to Nuclear Data Sheets [98]. Chapter IX – "Fission Yields" reviews the current state of experimental fission yield nuclear data and provides a useful guide to assist experimentalists and evaluators in their research. In particular, this work details what uncertainties should be quantified for a given measurement and what information should be provided for nuclear data evaluation purposes. This publication advances the current state of fission yield nuclear data.

3.1 Introduction

The templates of expected measurement uncertainties are a series of guides – or "templates" – which review common experimental techniques that are used for the measurement of a particular type of nuclear property. This review process generates templates on what measurement uncertainties should be reported for each of these techniques; reviewing the sources of uncertainty associated with them and, where possible, providing estimated minimum, mean, or maximum values for those uncertainties.

The need for these templates was first outlined by Dr. Denise Neudecker of Los Alamos National Laboratory [99, 100]. Since this need was identified, Neudecker has led a project to compile templates of expected measurement uncertainties for multiple measured nuclear properties. The initial efforts of this project have culminated in the aforementioned publication "Templates of Expected Measurement Uncertainties."

Each template is compiled from a variety of sources. Peer-reviewed literature and EXFOR reports are the primary sources for the templates. As these two sources have community-

wide recognition, they are preferred. However, peer-reviewed literature and EXFOR reports do not always provide enough information to compile a template. In this situation, the template in question is supplemented by consultation with experts on particular experimental methods.

The templates have a dual purpose: providing a guide for experimentalists and a guide for evaluators. As a guide for experimentalists, the templates provide a tabulation of the uncertainty sources associated with common experimental techniques and their expected values. The templates can assist experimentalists in the planning of their experiments; using the information in the templates, experimentalists can configure their experiments to appropriately track all sources of uncertainty and to minimize those sources as much as is reasonably achievable. In addition to this, the templates provide a listing of further information, beyond uncertainties, that is useful for evaluators. The templates also assist evaluators when they conduct their evaluations. As the templates provide a comprehensive listing of uncertainty sources and their expected values, evaluators can use them to assess the quality of various published measurements. As a last resort, evaluators can also use the suggested template uncertainty values to fill in missing sources of uncertainty in legacy measurements that did not fully account for all sources of uncertainty.

While the templates provide a list of uncertainty sources and their expected values, it should be clear that these values should not be viewed as immutable. Advances in technology or the implementation of existing technology can render the values in the template obsolete. It is intended that the templates will be continuously updated so that they remain current. It should also be noted that the values in the templates should not be viewed as targets; experimentalists should strive to achieve the lowest uncertainties that are reasonably possible for the techniques and technology they use. Similarly, evaluators should not use the templates in place of the uncertainties detailed in publication as the details of each individual experiment are unique.

3.2 The Fission Yields Template

In this section, neutron-induced fission yield measurements will be reviewed. Neutron-induced fission yields are measured using a number of experimental techniques that will be discussed in Sec. 3.2.1. In Sec. 3.2.2, a review of current neutron-induced fission yield evaluations is conducted and this review guided the identification of needs for future evaluations. Sec. 3.2.3 outlines the template of expected uncertainties for neutron-induced fission yields and details a review of EXFOR that was conducted to help guide the values in the template.

Fission is the process by which a nucleus crosses its fission barrier and splits into at least two fragments. These fission fragments then de-excite by the emission of neutrons and

γ rays. A fission fragment that has completed neutron emission is called a **fission product**. This chapter will focus on the assessment of **fission product yields**. A fission yield is the probability that a given fission product will be produced as the result of a fission event.

Each fission event will create two macroscopic (A>60) fission fragments/products and will occasionally also create one or two light charged particles (A<10). The yields to the macroscopic fission products are called **binary fission yields** and the yield to light charged particles are referred to as **ternary** or **quaternary fission yields**. The probability of producing ternary or quaternary fission products is small compared to binary fission, and as a result, experimental measurements have focused predominately on binary fission yields. Thus, this chapter will focus on the assessment of binary fission product yields.

Fission can occur spontaneously or it can be induced. Spontaneous fission is the decay of a nucleus via fission; it occurs in certain heavy actinides where the fission barrier is sufficiently low to allow the fission process to proceed without an external source of excitation. Fission can be induced by imparting sufficient energy to a nucleus to allow it to cross the fission barrier. Any particle can induce fission including photons, neutrons, and charged particles. Because of the importance of neutron-induced fission to applications, both measurements and evaluations have focused on neutron-induced fission yields. Therefore, this chapter will only discuss neutron-induced fission product yield measurements.

Fission yields can be measured as a function of mass number, atomic number, and isomeric state. Evaluations of independent and cumulative yields report fission yields as a function of these three quantities. There are several different types of fission product yields that are measured. There are five definitions of fission yields that will be discussed in this chapter:

- **Independent** - the probability that a given product is produced by a fission event immediately after scission and neutron emission,
- **Cumulative** - the probability that a given product will exist at some point in time after a fission event, either from direct production from the fission event itself or from the decay of another fission product,
- **Chain** - the probability that a product with a given mass number will be produced in a fission event after beta-delayed neutron emission has occurred,
- **Mass** - the probability that a product with a given mass number will be produced in a fission event before beta-delayed neutron emission has occurred,
- **Charge** - the probability that a product with a given atomic number will be produced in a fission event.

It should be noted that chain and mass yields are sometimes used interchangeably in literature, however, they are different.

In general, the specificity and immediacy of a fission yield type correlate with the uncertainty with which it can be measured. Specificity describes whether the yield is specific in mass/atomic number alone (such as mass, chain, and charge yields) or whether it is specific to atomic number, mass number, and isomeric state (such as independent and cumulative yields). Immediacy describes the time scale on which the yield must be measured. Fission yields of short-lived fission products (either independent or cumulative) require greater immediacy in the assay of the fissionable sample in measurements and thus tend to have larger uncertainty due to decay corrections.

This behavior is confirmed by the EXFOR review that is conducted in Sec. 3.2.3.1. For example, Fig. 3.5 in Sec. 3.2.3.1 shows that the measured independent yields of ^{238}U exhibit the highest average uncertainty as they are the most specific and require the greatest experimental immediacy. Cumulative yields exhibit a lower average uncertainty than independent fission yields; while they are specific in both atomic and mass numbers, they do not require the same experimental immediacy. Chain yields exhibit the lowest average uncertainty as they are specific only in mass number and allow for long periods of radioactive decay between irradiation and assay.

In addition to the above definitions of fission yield types, each type can be measured as three different quantities:

- **Absolute** - the total probability that a given fission product will be produced by a fission event,
- **Relative** - the probability that a given fission product will be produced relative to a reference fission product yield of the same type,
- **Fractional** - an independent or cumulative fission yield relative to a chain or mass yield.

Two fundamental equations define the determination of relative versus absolute fission yield measurements. In the case of an absolute fission yield measurement, the experimental data analysis process ultimately seeks to determine the fission yield using Eq. 3.1:

$$Y_f^i = \frac{N_i}{N_f} \tag{3.1}$$

where Y_f^i is the absolute fission yield of the i^{th} fission product, N_i is the number of the i^{th} fission product produced in the experiment, and N_f is the total number of fissions that occurred in the experiment.

In a relative fission yield measurement, the experimental data analysis process ultimately seeks to determine the fission yield using Eq. 3.2:

$$y_f^i = \frac{N_i}{N_{ref}} \tag{3.2}$$

where y_f^i is the relative fission yield of the i^{th} fission product, N_i is the number of the i^{th} fission product produced in the experiment, and N_{ref} is the total number of a reference fission product that was produced in the experiment.

The templates that are presented in Sec. 3.2.3 are established using a combination of information taken from an EXFOR review of fission yield measurements (Sec. 3.2.3.1), peer-reviewed literature, and private communication and consultation with experts on various techniques used in fission yield measurement. The template for activation-type fission yield measurements relied on all three of these sources. Due to its relative novelty, limited useful information on the "2E-2v" method for fission yield measurement was found in the EXFOR review. Therefore, that template only relies on peer-reviewed literature and expert consultation.

3.2.1 Measurement Types

A large number of experimental techniques have been used to measure neutron-induced fission product yields [101, 102, 103]. While some of these techniques involve unique and specialized procedures and equipment, many others – namely activation measurements – are all closely related and often only differ by assay method, neutron source, and whether a chemical separation was performed. Section 3.2.1.1 will detail the methods and techniques associated with these activation-type measurements. Section 3.2.1.5 will discuss the "2E-2v" method for fission yield measurements. This is a specialized technique that has yielded a series of important results in recent years.

3.2.1.1 Activation Measurements

Activation-type experiments for fission yield measurement employ several different experimental techniques depending on the needs and goals of the experimentalist. Figure 3.1 summarizes a generalized experimental chronology of such activation-type experiments in fission yield measurements. There are three possible stages to these experiments: irradiation, separation, and assay. The neutron source and irradiation method used to activate the sample introduces a number of uncertainties that are discussed in Sec. 3.2.1.2. The fission products from the activated sample may or may not then be separated using a chemical process. The uncertainties introduced by these separation processes are discussed in Sec. 3.2.1.3. Finally, the number of fission products produced must be assayed. Most experiments perform this assay using one or more of the following three techniques: mass spectrometry, γ spectroscopy, and β counting. The uncertainties introduced by these assay methods are

discussed in Sec. 3.2.1.4.

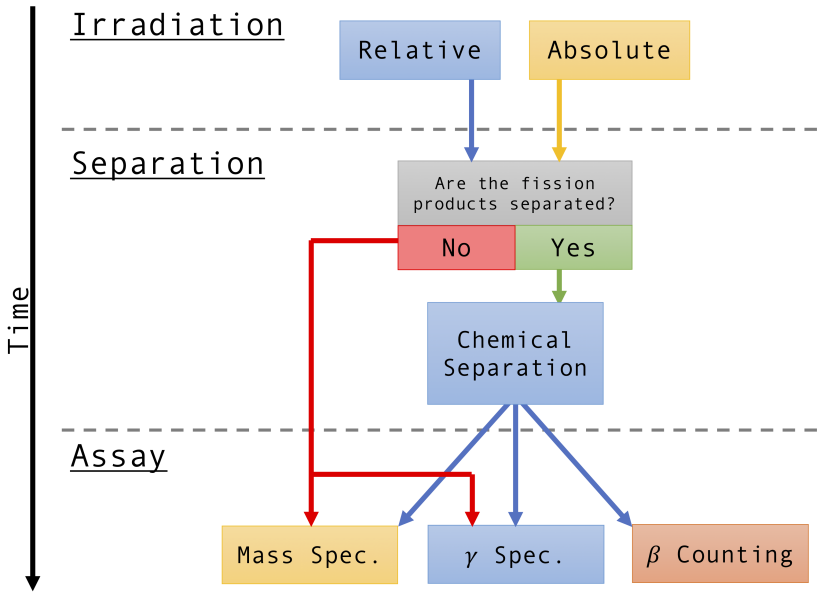

Figure 3.1: Generalized experimental chronology for activation experiments in fission yield measurements.

Many activation measurements involve a single irradiation of a sample followed by assay without chemical separation. Often the experimentalists will manually transport the irradiated sample to the detection apparatus (e.g., [104]), however, a mechanical/pneumatic device can be used to transport the sample (e.g., [105]). Depending on the method of transport and safety regulations at the facility used, the delay between the end of irradiation and the start of counting can be between seconds and hours. Usually, cumulative and chain yields are observed with these measurements, but if transport times are rapid enough, independent yields can also be observed. The transport time between the irradiation apparatus and the detection apparatus can be a source of uncertainty in these measurements, however, it is rarely a dominant source.

In recent years, cyclical neutron activation analysis (CNAA) has become a promising method for neutron-induced fission yield measurements [105, 106]. CNAA employs a mechanical/pneumatic device to rapidly and repeatedly transport the irradiated sample between the irradiation apparatus and the detection apparatus. The rapidity of the transport allows for short-lived fission products to be observed and the repeated nature of the measurement allows the counting uncertainties related to the short-lived fission products to be reduced. This ultimately allows for independent, cumulative, and chain yields to be measured. Like standard activation measurements, the transport time between the irradiation

apparatus and the detection apparatus can be a source of uncertainty in these measurements.

Because fission produces around one thousand fission products, each with their own β/γ radiations, chemical separations are often used to increase the sensitivity to products with a particular atomic number and/or mass number. Because of this increased sensitivity, the total uncertainty in fission yield measurements that employ chemical separations may be reduced relative to methods and techniques without chemical separation. Nevertheless, because they involve the alteration of the target sample, chemical separation processes introduce additional uncertainties that are not present in other methods.

3.2.1.2 Irradiation Methods

A number of neutron sources have been used to irradiate fissionable material to create fission products. Virtually any neutron source with energy sufficient to induce fission in the target is acceptable and has been used. Past measurements have focused heavily on reactor-generated thermal neutrons, fission-spectrum neutrons, and 14-MeV DT fusion neutrons. These three neutron energy spectra form the basis of all three major fission yield evaluations discussed in Sec. 3.2.2.

Any neutron source has uncertainty in its energy spectrum. Unless a monitor foil is used to determine the fluence on the target, uncertainty in the neutron energy spectrum has not traditionally contributed directly to the reported uncertainty of the measured fission product yields due to the use of the energy groupings discussed above. However, as will be discussed in Sec. 3.2.2, uncertainty in the neutron energy spectrum is potentially important information that will allow assessments of fission yield energy dependence in future nuclear data evaluations.

Two common methods for determining the incident neutron energy spectrum are neutron time-of-flight (nTOF) and foil activation spectral unfolding. In nTOF measurements, one or more neutron detectors are placed at a fixed distance from a neutron source and the time between the generation of a neutron at the source and arrival in the detector (time-of-flight) is measured. The energy of the neutron is then inferred from its time-of-flight. The major sources of uncertainty that contribute to the neutron energy spectrum resulting from nTOF include the time-of-flight length, the neutron detection system timing resolution, and counting statistics [107]. In foil activation measurements, multiple monitor foils with well-known energy-dependent cross sections are irradiated by the neutron source in question [108]. The measured activities are used in regression analysis to determine the neutron energy spectrum using their respective monitor reaction cross sections. The uncertainties in neutron energy spectra from foil activation are primarily reflective of the monitor reaction product activity uncertainties and the uncertainties in the evaluated monitor reaction cross sections.

As demonstrated by Eqs. 3.1 and 3.2, relative fission yield measurements do not need to determine the total number of fissions that occurred in the experiment, unlike absolute fission yield measurements. Relative fission yield measurements only require the number of two fission products that are produced, both of which can often be determined with the same experimental techniques. As relative fission yields are ratio values, some experimental uncertainties cancel. Absolute fission yield measurements require the total number of fissions that occurred in the experiment to be known. Determining the total number of fissions usually requires additional experimental techniques and/or the incorporation of additional nuclear data. This results in absolute fission yields having more sources of uncertainty and thus larger total uncertainties on average.

Actinide targets are required for fission yield measurements. Often these actinide targets have undergone some level of enrichment to increase the presence of the target nucleus of interest. Similarly, in the cases of Th and U, the natural abundance of a particular isotope is of importance. Both enrichment and natural isotopic abundance can contribute to the uncertainty in the number of target nuclei irradiated in a given experiment.

In absolute fission yield measurements, the total number of fissions must be determined. One common way to determine the total number of fissions in a sample is to use the neutron flux of the neutron source if this quantity is known *a priori*. Equation 3.3 gives the calculation of the total number of fissions in a sample as a function of neutron flux:

$$N_f = N t_i \phi \int \sigma_f(E_{inc}) P(E_{inc})\, dE_{inc} \tag{3.3}$$

where ϕ is the (time-averaged) neutron flux, $\sigma_f(E_{inc})$ is the fission cross section, N is the total number of target atoms in the irradiated sample, t_i is the irradiation time, and $P(E_{inc})$ is the incident neutron energy spectrum. This equation assumes a thin sample with negligible neutron attenuation across its geometry.

When the neutron flux of the neutron source is not known *a priori*, another method for determining the total number of fissions is the use of a monitor foil. In this method, a sample of material with an energy-dependent cross section that is well-known across the incident neutron energy spectrum is co-loaded with the actinide target and exposed to the same neutron source. The resulting activity of the monitor foil is determined using some assay method, often γ spectroscopy, and this is used to determine the neutron flux. This neutron flux is then used in Eq. 3.3 to determine the number of fissions that occurred. Equation 3.4 gives the (time-averaged) neutron flux that is determined with a monitor foil:

$$\phi = \frac{A}{N \lambda t_i \int \sigma(E_{inc}) P(E_{inc})\, dE_{inc}} \tag{3.4}$$

where A is the activity of the product produced in the monitor foil reaction of interest at the end of irradiation, N is the number of monitor foil nuclei present, λ is the decay constant

of the monitor reaction product, t_i is the irradiation time, $\sigma(E_{inc})$ is the monitor reaction cross section, and $P(E_{inc})$ is the incident neutron energy spectrum.

Similar to the use of a monitor foil, the number of fissions may sometimes be determined using a "monitor" fission product yield. In this case, the number of fissions that occurred in the target sample is determined from the measured activity of one particular fission product that has a well-known fission yield for the incident neutron energy spectrum used in the irradiation. When this is done, Eq. 3.4 becomes modified to be the form presented in Eq. 3.5:

$$\phi = \frac{A}{N\lambda t_i Y \int \sigma_f(E_{inc}) P(E_{inc})\, dE_{inc}} \tag{3.5}$$

where A is the produced activity of the monitor fission product at the end of irradiation, N is the number of target nuclei present, λ is the decay constant of the monitor fission product, t_i is the irradiation time, Y is the monitor fission product yield, $\sigma_f(E_{inc})$ is the fission cross section of the target nucleus, and $P(E_{inc})$ is the incident neutron energy spectrum.

The cross sections for monitor foils are generally known to within a few percent. Monitor reaction cross sections and covariance matrices can be found in specialized databases, such as the International Reactor Dosimetry and Fusion File [109], where special attention is given to their characterization. In general, the uncertainty from the use of a monitor foil will be driven by the evaluated nuclear data uncertainties in the cross section and the uncertainty in the incident neutron energy spectrum.

As thermal and fission-spectrum neutron-induced fission is of special interest to applications, many fission yield measurements have been performed using reactor beam ports as a neutron source. When this neutron source is used, the burnup of the reactor at the time of irradiation may be used to correct the neutron flux from the beam port [110]. If this is done, additional uncertainty is introduced.

Another common way to determine the total number of fissions induced is the use of a fission chamber. This technique places a target sample in a gas detector which is co-loaded with one or two thin reference samples of the same fissionable/fissile material [111, 112, 113]. The number of fissions in the target sample is then proportional to the product of the ratio of the mass of the target and the reference mass(es) and the number of high-energy pulses created by the fission fragments, as described in Eq. 3.6. Sometimes the number of high-energy signals produced is adjusted by a geometric correction factor that represents the probability that the fission fragments are emitted parallel to the plane of the target sample and thus do not produce a sufficiently large signal in the gas chamber due to Coulombic stopping. As can be seen from Eq. 3.6, the uncertainty introduced by the use of fission chambers can usually be determined from uncertainties in masses and counting statistics.

$$N_f = \frac{m_t}{m_{ref}} \frac{N_c}{\varepsilon} \tag{3.6}$$

where m_t is the mass of the target sample and m_{ref} is the total mass of the reference sample(s), N_c is the number of high-energy signals created in the gas chamber by each fission event, and ε is an optional geometric correction factor that represents the probability that the fission fragments are emitted parallel to the plane of the target sample and thus do not produce a sufficiently large signal in the gas chamber. Often it is assumed all fission fragments escape the target such that ε is equal to one.

Yet another method for determining the number of fissions that occurred in a target sample is fission fragment track counting. In this method, a target sample is placed in direct contact with a material (often CR-39 plastic) that will produce microscopic tracks for each fission fragment that travels through it. The tracks created by fission fragments in this material are then counted under magnification, either manually [114] or using an automated optical detection scheme [115]. The number of fissions that occurred in the target sample is proportional to the number of tracks seen in the tracking material scaled by a fragment escape probability/track detection efficiency. This is similar to the operation of a standard fission chamber. The uncertainties arise primarily from counting statistics and uncertainties/biases from the track detection method.

Uncertainties in the geometry of the irradiation apparatus can contribute to the net uncertainty of any of the sources listed above. This includes, but is not limited to time-of-flight length, the solid angle coverage of the target sample, the shape of the incident neutron field, fission chamber geometric correction factors, and self-shielding in thick target samples. It is difficult to broadly characterize sources of geometric uncertainty as each experiment uses different experimental apparatuses. However, geometric sources of uncertainty are generally fixed units of length/area/volume and their effect on the total experimental uncertainty can be minimized by setting the scale of the dimension in question to be much larger than its geometric uncertainty. For example, a time-of-flight length will generally have a fixed uncertainty in units of mm/cm dictated by the measurement device used, but the relative effect of this uncertainty is reduced by choosing a large time-of-flight length that is orders of magnitude larger than this fixed uncertainty.

Tables 3.3 and 3.4 in Sec. 3.2.3.2 present the template for irradiation methods in fission yield measurements. Due to the wide variety of irradiation methods that can be employed in fission yield measurements, assigning mean and/or maximum expected values to the uncertainty sources is not reasonable. Rather, only minimum expected uncertainties for each of these sources will be enumerated based on literature review and expert opinion.

3.2.1.3 Chemical Separations

The main goal of chemical separations in fission yield measurements is to separate fission products of a given element or elements with similar chemical properties for subsequent assay. Fig. 3.2 shows a general schematic for chemical separations in fission yield measurements.

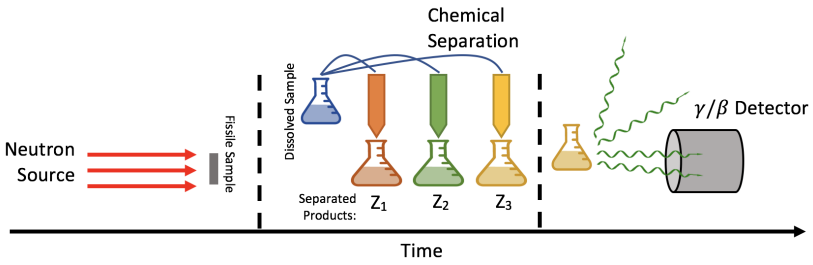

Figure 3.2: General schematic for chemical separation measurements. The fissionable/fissile sample is irradiated by a neutron source. The irradiated sample undergoes some chemical process that allows an element or set of elements to be separated. The separated fission products are then assayed using β or γ spectroscopy.

The chemical separation of fission products meets one or both of the following goals: separate fission products of a given element for yield determination via direct activity measurement (β counting) or separate fission products to allow detailed mass or γ spectroscopy of lower-yield products by reducing background and interference from high-yield products.

There is a wide variety of chemical separation techniques and methods that can be employed in fission yield measurements, each comes with its own sources of uncertainty and bias. Cumulative and chain yields can be determined using β counting of separated products for total activity determinations. Some independent fission product yields can be determined using rapid separations and on-line separators. Resin column separations can be employed to obtain high-quality elemental separations. Isotope dilution mass spectrometry can be used to determine the total number of fissions in a sample with high precision [111]. A comprehensive review of the techniques used for chemical separations in fission yield measurements is difficult due to this wide variety, however, a review article by Prakash et al. [111] offers a detailed review of some common techniques.

A review of uncertainties in radiochemical neutron activation analysis was conducted by Kučera et al. in the year 2000 and offers insight into the standard sources of uncertainty that are associated with activation-type experiments [116]. This review article acknowledges that each experiment has different sources of uncertainty but identified three commonly observed sources of uncertainty: mass determination of the stable carrier and/or radiotracer, chemical yield determination, and isotopic exchange between the radiotracer and stable carrier. This review suggested that the relative uncertainty of the radiotracer/stable carrier mass determination should be between 0.02% and 0.5%, but that if the mass was determined

gravimetrically this uncertainty value should be near 0.075%. The chemical yield of the process should have uncertainty between 0.3% and 0.5%. Finally, the review asserts that isotopic exchange should be negligible when a homogenous system is obtained by sample decomposition.

Gravimetric mass uncertainties with modern scales could be as low as 0.001%. Oxidation of metallic targets can be particularly problematic for mass determinations in the case of fission yield measurements, where metallic actinide targets are often used. This oxidation can create a bias in the measurement mass. The upper bound of this bias is determined by the stoichiometry of the oxidation reaction. For example, the upper bound of this oxidation bias for a uranium target is 17% (if the target is fully oxidized to produce UO_3). However, the degree of oxidation of a target varies due to a number of factors such as the target geometry and amount of exposure to oxygen or other reactive gases, thus determining this bias can be difficult. Metallic targets should be acid dipped and then massed to ensure the effects of oxidation bias are minimized. Further oxidation after massing can be avoided by flame sealing the target in quartz that is back-filled with inert gas or press-sealing the target in aluminum. Quartz sealing targets can introduce bias itself as a fraction of the fission products will be embedded in the quartz and thus are lost during dissolution.

The chemical yield of the separation process can be affected by the ability to fully dissolve the target. In the case of high-fired oxide targets, in particular, as much as 3% of the original target mass may fail to be dissolved. The chemistry of the separation should ideally be performed in triplicate in order to estimate the uncertainty of the chemical yield and to test the consistency of the process. Additionally, if possible, tracer and reagent blank control experiments should be performed in tandem to further test the reliability of the process. Experiments that do not execute these tasks will have uncharacterized sources of uncertainty that the evaluator will need to take into account.

There are several places where unintended uncertainty/bias can be introduced in radiochemical processing. Experimentalists need to fully document and openly publish the radiochemical methods they use so that an evaluator can assess the reliability of their measurement. A potential remedy to this issue is discussed in the following paragraph where standards for uncertainty quantification in chemical separations are discussed.

A number of community-recognized standards exist to guide uncertainty quantification in chemical separations. These documents have a broad scope and are applicable to most radiochemical separations. The most notable of these standards, ISO/TS 21748, was published by the International Organization for Standards (ISO) in 2004 and was subsequently revised in 2010 and 2017 [117]. A review of chemical separation uncertainties by Saffaj et al. recommended this standard and a number of other suitable standards [118]. Saffaj notes that while these standards exist, many laboratories have not adhered to them, due in part to their complexity. Nevertheless, experimentalists should make every reasonable effort to

follow these guidelines and fully characterize their uncertainty. Similarly, evaluators with detailed knowledge of chemical separations need to review whether proper standards on uncertainty estimation in radiochemical separations were used. While chemical separations are highly regarded in fission yield measurements due to their ability to decrease total measurement uncertainties by increasing sensitivity to selected fission products, it should be kept in mind that many legacy measurements did not fully characterize the uncertainties introduced by the chemical separations used, as noted by Saffaj.

Table 3.5 in Sec. 3.2.3.3 presents the template for chemical separations in fission yield measurements.

3.2.1.4 Assay Methods

A number of diverse assay methods have been used in fission yield measurements. While these methods differ in the tools and techniques that they employ, many of the sources of uncertainty associated with them are the same and thus they will be considered together in this section. In some measurements, assay of the fission products begins immediately after the irradiation of the target sample. In other measurements, the fission products undergo some separation process immediately after irradiation before proceeding to assay, namely measurements that include chemical separation.

Methods that undergo some separation stage tend to offer the advantage of lower assay backgrounds as the fission products have been separated from each other. However, the separation stage introduces additional sources of uncertainty and/or bias as discussed in Sec. 3.2.1.3. The separation stage will also introduce a delay between irradiation and assay, preventing the observation of short-lived fission products. Methods that do not undergo some separation stage often require less complex experimental capabilities and have the potential to observe short-lived fission products. However, these methods observe all of the fission products at once and therefore tend to have higher assay backgrounds.

Regardless of the amount of delay between the irradiation stage and assay stage of a given experiment, three assay methods appear often in fission yield measurement experiments: mass spectrometry, γ spectrometry, and β counting. Indeed, these three methods appeared most often in the EXFOR review of fission yield measurements (presented in Sec. 3.2.3.1) that was performed as a part of the background research for this chapter. The sources of uncertainties associated with each of these three methods will be detailed in the following sections:

Mass Spectrometry Mass spectrometry has been commonly used in fission yield measurements either with or without chemical separations [119]. Several mass spectrometry techniques and configurations exist. Among these techniques, the following have appeared commonly in fission yield measurements: accelerator mass spectrometry (AMS) [120], time-

of-flight mass spectrometry (TOFMS) [121], isotope dilution mass spectrometry (IDMS) [122], thermal ion mass spectrometry (TIMS) [123], inductively coupled plasma mass spectrometry (ICPMS) [124], and recoil mass spectrometry (RMS) [125].

The mass spectrometry methods that commonly appear in fission yield measurements are selected because they feature ion sources that are able to break molecular bonds that may have formed between the fission products and the medium that they were born into; mitigating multiplets in mass spectra that are commonly seen in other mass spectrometry methods that are optimized for analysis of molecules and chemical compounds. Each of these mass spectrometry techniques has particular advantages and disadvantages that are balanced when they are selected for use in a particular fission yield measurement. In general though, all mass spectroscopy methods seek to produce data that separate particles of different mass and/or charge. In most mass spectrometry methods, this is achieved by ionizing individual atoms of fission product nuclei, accelerating these ions through a magnetic field, and measuring their deflection through this field using a position-sensitive detector. In TOFMS, the mass of a particle is determined not by its deflection, but rather by its measured velocity and energy with a "start" and "stop" detector [121].

Depending on the mass/charge selectivity of the mass spectrometry technique used and the time delay between irradiation and assay, all five types of fission yields discussed in this introduction to this section can be measured. Mass spectroscopy features high sensitivity/low backgrounds allowing for mass/charge assignment with low uncertainty compared to other assay methods used in fission yield measurements. AMS in particular is known for its superior mass sensitivity and resultantly low uncertainties, as mentioned in Reference [121]. Together these factors have made this technology a staple in assay methods for fission yield measurements.

Mass spectrometry most often produces information on isotopic ratios, thus, mass spectrometry in fission yield measurements is usually used to determine the relative presence of fission products. A normalization may be used to determine absolute yields, which carries its own uncertainty (see Sec. 3.2.1.2).

Several publications have been produced on uncertainty quantification in mass spectroscopy measurements in order to reduce measurement inconsistencies between different facilities [126, 127, 128]. In recent years, enhanced focus has been placed on the "Guide to the Expression of Uncertainty in Measurements" (GUM) ISO standard [126, 127, 129]. This standard seeks to identify individual sources of uncertainty that contribute to a measured value (commonly called "forward propagation"). The uncertainty from these sources is determined where possible and propagated forward to the measured value. A second method of uncertainty quantification is the "integrated" or "repeatability" method where an identical sample is analyzed multiple times and the uncertainty in the measurement is taken from the standard deviation between these trials [126, 128]. In this way, sources of uncertainty

in the measurement are integrated together in the trial deviation rather than having their values assessed individually. This method is attractive in its simplicity and generally low uncertainty, however, it does not properly account for sources of systematic uncertainty/bias and thus does not allow for valid comparison between different facilities and experiment apparatuses.

The integrated method appears often in legacy fission yield measurements that used mass spectroscopy. Evaluators will need to be aware of this issue, which harkens back to the lack of standards in the uncertainty quantification of chemical separations that was discussed in Sec. 3.2.1.3. A strong background in or discussions with experimentalists on mass spectrometry is important to properly incorporate measurements that used the integrated method into future evaluations.

The work of Essex et al. [126] lists a number of common sources of uncertainty that can arise in these different mass spectrometry techniques including electronics gain and baseline, Faraday cup efficiency, Schottky noise, counting statistics, yield calibrations, linearity calibrations, and filament geometry. There is little published research on forward propagation uncertainty analysis in mass spectrometry as used in fission yield measurements. Reference [130] discusses forward propagation of uncertainties when measuring uranium isotope ratios with TIMS. This publication lists the electronics baseline, mass peak shaping (such as tailing and flatness), and linearity calibrations as sources of uncertainty.

Table 3.1 lists the sources of uncertainty for the two mass spectrometry uncertainty methods that were discussed above. There likely exist many additional sources of uncertainty associated with mass spectrometry depending both on the type of mass spectrometry used and the specifics of each experiment. Therefore, it is noted that this table is not exhaustive and experimentalists and evaluators need to carefully consider sources of uncertainty on a case-by-case basis.

For the "integrated"/"repeatability" uncertainty quantification method, a minimum uncertainty value of 1% is suggested. This value is taken to be consistent with the minimum value suggested for the repeatability uncertainty of AMS that was detailed in Chapter IV of "Templates of Expected Measurement Uncertainties." AMS was selected from the six methods of mass spectrometry commonly used in fission yield measurements to represent the minimum uncertainty due to its reputation in literature for producing results with low uncertainty [121]. It is stressed that this value is a minimum and that the integrated/repeatability uncertainty quantification method is discouraged over the use of the forward propagation method.

There is very limited information in currently published literature on the forward propagation/GUM method of uncertainty quantification in mass spectrometry. This is because this method has only gained traction relatively recently. Further still, there is even less in-

formation published on the forward propagation/GUM method as it applies to fission yield measurements and the specific types of mass spectrometry used in them. The EXFOR review revealed no reports of mass spectrometry uncertainty sources. Therefore, a template will not be recommended for mass spectrometry in Sec. 3.2.3. Rather this discussion is presented in order to stimulate further progress in this area of fission yield assay methods.

Table 3.1: List of uncertainty sources for mass spectrometry.

Symbol	Description
Forward Propagation (GUM):	
g	electronics gain
bl	electronics baseline
ε_{FC}	Faraday cup efficiency
n_S	Schottky noise
Y	yield calibrations
ℓ	linearity calibrations
f	filament geometry
s_{mass}	mass peak shaping
c	counting statistics
Integrated Quantification:	
σ_{MS}^{rep}	standard deviation of repeated trials

γ Spectroscopy Several γ detection methods are employed in fission yield measurements. These detection methods can generally be grouped into two categories: energy-resolved and energy-unresolved. Energy-resolved detection is the detection of γ rays with sufficient energy resolution such that source identification and quantitative activity determination are possible using at least one photopeak. Energy-unresolved detection is the detection of γ rays with limited to no energy information and is commonly used in coincidence methods for Compton scatter rejection.

Both energy-resolved and energy-unresolved detection seek to determine the number of a fission product produced, N_i, using Eq. 3.7:

$$N_i = \frac{C(E_\gamma^i)}{\varepsilon(E_\gamma^i)\, I_\gamma(E_\gamma^i)\, [-e^{-\lambda t}]_{t_0}^{t_1}} \tag{3.7}$$

where C is the number of counts from the detector, $\varepsilon(E_\gamma^i)$ is the detector efficiency for γ rays with energy E_γ^i, $I_\gamma(E_\gamma^i)$ is the decay intensity of the γ ray with energy E_γ^i, λ is the decay constant of the γ emitter, and t_0 and t_1 are the start and stop times of the detector counting,

respectively.

Commonly-used detectors in the energy-resolved category include:

- Ge - Germanium solid-state detectors
  HPGe - high-purity Germanium
  Ge(Li) - lithium drifted Germanium
- NaI - sodium iodide scintillator
- $LaBr_3$ - lanthanum bromide scintillator

These detectors are used in experiments in fundamentally the same way, the key difference between them in fission yield measurements is their efficiency and energy resolution. High energy resolution (such as that possible with HPGe detectors) allows for improved ability to identify and separate photopeaks emitted by individual fission products. Lower energy resolution makes individual photopeak identification increasingly difficult; however, decreased energy resolution typically comes with improved timing resolution, decreased dead-time, and increased detection efficiency. The specific detector used in any given fission yield measurement will be selected to balance these factors. For example, an experiment looking for γ-γ coincidences to determine fission yields might choose a $LaBr_3$ detector for its high timing resolution and detection efficiency, accepting its moderate energy resolution. Whereas, another experiment that seeks to determine fission yields from individual photopeaks in a singles spectrum might choose an HPGe detector for its high energy resolution.

Detectors in the energy-resolved category usually require an energy-dependent photopeak efficiency calibration. This efficiency calibration carries uncertainty with it, which will vary with the detector type used. Nuclear decay data relevant to the calibration source used (e.g., half-lives and γ intensities) contribute to this uncertainty. In a limited number of experiments, the γ ray(s) of interest also belong to a standard calibration source. In this situation, the detection efficiency for the γ ray(s) of interest can be obtained directly from the measurement of a calibration standard in what is often called an "internal calibration." Internal calibrations tend to have lower uncertainty than energy-dependent calibrations as they avoid model-parameter covariance and interpolation and/or extrapolation biases. The efficiency data points used for both energy-dependent calibration and internal calibration are calculated with Eqs. 3.8 and 3.9.

$$\varepsilon(E_\gamma^i) = \frac{C(E_\gamma^i)}{N(E_\gamma^i)} \tag{3.8}$$

where $C(E_\gamma^i)$ is the number of γ rays of energy E_γ^i counted by the detector and $N(E_\gamma^i)$ is the number of γ rays of energy E_γ^i emitted by the calibration source. The uncertainty in the number of γ rays counted by the detector will rarely follow Poisson statistics alone due

to background subtractions and photopeak fitting uncertainty. It should also be noted that strong correlations between efficiencies determined using different γ rays from the same calibration source will exist.

The number of γ rays emitted by a calibration source between times t_0 and t_1 is determined with:

$$N(E_\gamma^i) = I_\gamma(E_\gamma^i)\, A_0 \int_{t_0}^{t_1} e^{-\lambda t}\, dt \tag{3.9}$$

where I_γ is the intensity of calibration γ ray with energy E_γ^i, A_0 is the initial activity of the calibration source, and λ is the decay constant of the calibration source, which is inversely proportional to its half-life $T_{1/2}$.

In addition to the uncertainties that accompany the variables in Eqs. 3.8 and 3.9, there will be fit/model uncertainty and covariance associated with energy-dependent efficiency calibrations. Fit/model uncertainty in energy-dependent efficiency calibration can be particularly troubling when extrapolated to high γ-ray energies. Standard calibration sources do not usually have γ rays with energies above the 2.7-MeV ^{24}Na photopeak, thus calculating efficiencies above that energy (or the highest γ-ray energy in a particular calibration) will introduce non-trivial extrapolation bias/uncertainty.

The energy resolution of a detector and its uncertainty can be important when a dense γ-ray spectrum results from a particular measurement. In experiments where fission products are not separated and all of the fission products are observed simultaneously, the energy resolution of the detector governs the ability of photopeaks to be separated. This is important to photopeak fitting in γ-ray spectroscopy, where background subtraction and photopeak deconvolution are needed to determine the true number of events in a photopeak. These fitting processes introduce uncertainty beyond standard Poisson counting statistics and energy resolution uncertainty is generally included as a part of that γ spectroscopy fitting uncertainty. When count rates from the measured sample are high, pile-up will occur in the detector. This effect needs to be accounted for, otherwise, the photopeak area will be underestimated.

Commonly-used detectors in the energy-unresolved category include:

- BGO - bismuth germanate scintillator
- BaF_2 - barium fluoride scintillator
- Liquid scintillators
- NaI - sodium iodide scintillator

These energy-unresolved detectors are commonly used in coincidence with energy-resolved detectors for the purposes of Compton rejection. Because of this, often the efficiency of energy-unresolved detectors is not calculated directly. In this situation, their efficiency is folded into the efficiency calibration for the greater coincidence detection system and Eqs. 3.8 and 3.9 remain applicable. For example, an HPGe detector is surrounded by a BGO shield for Compton suppression. The signals from the BGO are used to veto coincident signals from the HPGe. The efficiency calibration for the system is determined using a calibration source, effectively folding together the efficiencies of both the HPGe and BGO detectors into one net efficiency.

There are uncertainty sources that affect both resolved and unresolved detection systems. The total dead time of the detection system must be assessed and corrected. When a detector array is used there may need to be a correction for correlations due to the angular distribution of γ emissions from the same nucleus.

Uncertainties in the counting geometry of the detection system may need to be accounted for. This is particularly true when Monte-Carlo simulations are used to assist the efficiency calibration. Another aspect of geometry that must be considered is self attenuation of γ rays by the source. While γ attenuation through the detector dead layer is usually captured in the efficiency calibration, γ attenuation through the source itself will not be accounted for. Thus this self attenuation must be corrected and this will impart additional uncertainty.

When observing γ-γ coincidences, accounting for angular correlation between γ rays is important. There exists limited experimental information about angular correlation between γ cascades, making accurate correction for this phenomenon difficult. Nevertheless, both experimentalists and evaluators should keep this factor in mind when assessing measured data.

Tables 3.6 and 3.7 in Sec. 3.2.3.4 present the template for γ assay in fission yield measurements.

β Counting Beta counting is a commonly used method in fission yield measurements. Beta particles are emitted with a broad spectrum of energies and β detectors often have low energy resolution. Because of this, β detectors are used primarily to assess the total activity of a sample by counting the total number of emissions rather than any energy-dependent behavior. Thus, β counting is usually used only after a chemical separation has been performed so that the observed β activity only describes one or a few fission products.

Similar to Eq. 3.7, β counting seeks to determine the number of a fission product produced, N_i, using Eq. 3.10:

$$N_i = \frac{C}{\varepsilon \, BR_\beta [-e^{-\lambda t}]_{t_0}^{t_1}} \tag{3.10}$$

where C is the number of counts from the detector, ε is the detector efficiency for β particles, BR_β is the beta decay branching ratio of the β emitter, λ is the decay constant of the β emitter, and t_0 and t_1 are the start and stop times of the counting, respectively.

Commonly-used detectors for β counting include:

- Gas-filled Detectors (e.g., ionization chamber)
- Silicon Detectors
- Solid-state Scintillators
- Liquid Scintillation Counter

Gas-filled detectors, silicon detectors, and solid-state scintillators are all used in similar ways in fission yield measurements; they are placed near the fission product sample to determine its activity. Liquid Scintillation Counting (LSC) involves the placement of the fission products directly into the active volume of the scintillator for counting, entailing additional sources of uncertainty.

Gas-filled detectors, silicon detectors, and solid-state scintillators are placed near the sample of fission products. The absolute efficiency of the detector will be a source of uncertainty. Due to the short range of β particles in matter, the absolute efficiency is largely dependent on the solid angle coverage of the detector. As with other detectors, β counters experience dead time which must be corrected for and this introduces additional uncertainty. The physical form and shape of the fission product sample will determine if a self attenuation correction is required. Again due to the short range of β particles in matter, this correction will need to be applied to most geometries.

While liquid scintillation counters can be used for beta counting, there is a lack of literature on their application to fission yield measurements. Therefore, liquid scintillation counters will not be considered in this chapter.

Tables 3.8 and 3.9 in Sec. 3.2.3.4 present the template for β assay in fission yield measurements.

3.2.1.5 The 2E-2v Method

The "2E-2v" method for fission yield measurements has gained importance due to its ability to accurately measure mass yields with several results and facility updates published in recent years [131, 132, 133, 134, 135]. This method was developed in the 1980s at the Laue-Langevin Institute (ILL) [136]. The name of the method is derived from its measurement of both the energy and velocity (through time-of-flight) for two fission products emitted from

a single fission event.

Figure 3.3 illustrates the experimental apparatus for a typical 2E-2v measurement. An actinide target is located in the center of the apparatus and fission is induced with a neutron beam. Some fission product pairs will be emitted into the solid angle of the arms of the apparatus. When a fission occurs, a "start" signal is generated. This start signal can be taken as the prompt γ-ray flash from the fission event, the sputtering of electrons from the target when a fragment is generated, the start time of a finely pulsed neutron beam, or can be determined through the use of timing detectors. The products from the fission event travel along the flight path and reach the E detectors at the end of each arm. The energy of the fission product is taken as the total energy deposited in each E detector.

Because each arm of the 2E-2v detector covers a non-trivial solid angle, the flight path that the fission products transverse from each individual fission event has variability. To correct the flight path for each fission event, each arm of the apparatus may be lined with electronics to detect the trajectory of the fission product. This trajectory is then used to correct the nominal path length to obtain the true path length for each event.

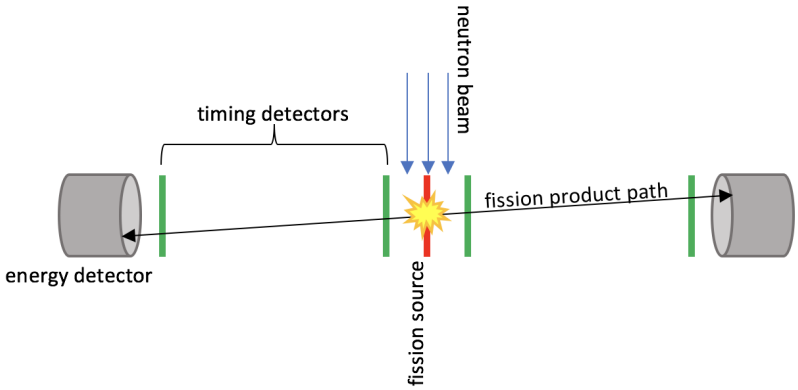

Figure 3.3: General schematic for the 2E-2v method. Fission is induced in an actinide target using a neutron beam. The energy and timing of the fission products from each fission event are detected using a two-arm apparatus. This measurement approach is also used for spontaneously fissioning actinides.

With the energy and timing information, the mass of each fission product can be determined using the non-relativistic mass-energy-velocity relationship given by Eq. 3.11:

$$m = \frac{2E}{v^2} = \frac{2Et^2}{L^2} \tag{3.11}$$

where E is the measured energy of the fission product, v is the velocity of the fission product, t is the time-of-flight of the fission product, and L is the flight path length of the fission

product.

Because Eq. 3.11 is linear, the mass resolution of the 2E-2v detection system can be determined by standard uncertainty propagation as shown in Eq. 3.12:

$$\sigma_m = m\sqrt{\left(\frac{\sigma_E}{E}\right)^2 + 4\left(\frac{\sigma_t}{t}\right)^2 + 4\left(\frac{\sigma_L}{L}\right)^2} \tag{3.12}$$

Mass yields are determined by normalizing the total number of observed events to 200%. The distribution of measured yields is fitted to a functional form that describes their physical behavior [137]. Because of its limited number of measurement parameters and experimental techniques that allow for relatively precise measurement of these parameters (as will be discussed in Sec. 3.2.3.5), the 2E-2v method offers one of the most precise capabilities for the measurement of mass yields.

While evaluated mass yields have not been directly published in the most recent fission yields evaluations, they serve as an important piece of information for both modeling fission product distributions and benchmarking evaluations of independent and cumulative yields. Because the 2E-2v method measures mass yields (before β decay) it has the potential to improve consistency between cumulative and independent fission yields. This is because independent fission yields are often inferred from cumulative yields using decay corrections. These inferred independent yields can be benchmarked using the precise mass yields measured using the 2E-2v method.

The 2E-2v method also has the potential to help address inconsistencies between evaluated fission product yields and evaluated prompt-neutron yields and distributions. The inconsistency between these two pieces of evaluated data has been noted in peer-reviewed literature [94]. The 2E-2v method has the potential to address this because the number of prompt neutrons emitted in a given fission event can be inferred from the mass difference between the compound fissioning system and the measured masses of the two fission products. This experimentally measured prompt neutron distribution could help to constrain future fission yield evaluations. However, it should be noted that non-trivial deviation from the assumption of isotropic neutron emission in the center-of-mass frame, which leads to near (but not exact) conservation of the average values of fission product velocities, has been found [132]. This does not affect the measured mass of the post-neutron-emission products, but it does alter inferred quantities such as the pre-neutron-emission mass. Corrections for this are possible [132] but will result in the inflation of reported uncertainties.

Similar to the 2E-2v method, but not included in this template, is the 2E method for fission yield measurements. In the 2E method, a pair of particle spectrometers are used to measure the total energy deposited by each fission product, and this information is used to infer the mass of the fission products. The 2E method has a mass resolution of 2-5 a.m.u.

[138, 131], approximately twice that of the 2E-2v method. Therefore, this template will focus on the 2E-2v method.

Table 3.10 in Sec. 3.2.3.5 presents the template for the 2E-2v method in fission yield measurements.

3.2.2 Information Needed for Evaluations

3.2.2.1 State of Current Evaluations

Unlike many other nuclear data quantities, fission yields have been reviewed rather infrequently and there is limited standardization in their evaluation methodology. As a result, the most current evaluations that have been conducted for three nuclear data libraries will be reviewed individually to determine what information was important to them and to infer what information will be useful to future evaluations. A fourth evaluation by M. N. Nikolaev exists for the BROND-3.1 nuclear data library, however, a report on that evaluation is not available. Table 3.2 lists these three evaluations, and the experimental data and theoretical tools required for these evaluations are detailed in the following sections.

Table 3.2: Evaluations of fission product yields included in the most current version of international nuclear data libraries.

Library	Reference(s)	Year(s)
ENDF/B-VIII.0	[86], [139]	1994, 2010
JEFF-3.3	[140], [141]	1995, 2004
JENDL-4.0	[142], [143], [144]	2001, 2011, 2016

ENDF/B-VIII.0 The last complete evaluation of fission product yields for the United States Nuclear Data Program was published in 1994 by T. R. England and B. F. Rider [86]. In 2010, an evaluation for fission yields from fission-spectrum neutrons on plutonium was performed by Chadwick et al. to update the 1994 evaluation [139].

The 1994 evaluation incorporated measured fission yield data from 1989 and prior. Independent yields were determined from a Gaussian charge distribution that was fit to match uncertainty-weighted averages of experimental independent yields. These modeled independent yields were normalized to ensure their sum along each A chain equals the chain yield. Cumulative yields were taken to be the weighted average of two different methods. One method calculated the cumulative yields by summing the independent yields along an A chain. The other method calculated the cumulative yields by subtracting independent yields

along an A chain from the chain yield.

Experimental uncertainties on the yields used in the evaluation were tabulated by the evaluators. Relative yields were converted to absolute yields using the value of a reference yield. The uncertainties of relative yield measurements were combined statistically with the uncertainty of the relevant reference yield. Absolute yield measurements were assumed to have at least 2% systematic uncertainty and the measurement uncertainties were updated to meet this minimum. Reported uncertainties were adjusted to a minimum set of values based on the detection method and year of publication. For example, Ge(Li) radiochemical measurements made after 1965 were all assigned a minimum uncertainty of 5%. This enforcement of minimum uncertainties based on the detection method is similar in philosophy to what this template seeks to foster. However, this was not undertaken at the level of partial uncertainty sources as is the case in the templates.

Light ternary fission yield data were incorporated from Madland [145] and Wahl [84, 85]. A model by Madland [87] was used to assign the isomer-to-ground state splitting of independent fission yields in cases were experimental data were not available. These calculated splittings were assigned uncertainties of $\pm 50\%$. When the angular momentum of a isomeric state of a fission product was not known, the yield to that nucleus was split evenly across the ground state and isomeric states. Pairing effects were added to the Gaussian charge distribution model using a model by Madland [88].

The decay data considered in this evaluation include half-lives, decay chains, and decay modes and branching ratios. In particular, delayed neutron emission probabilities were important to this evaluation as these probabilities were used to convert independent yields to cumulative yields. These delayed neutron probabilities were obtained from the ENDF/B-VI decay library.

The 2010 evaluation of plutonium yields was focused on improving evaluated fission yields that are important in reactor burnup calculations. Because of this goal, the evaluation was focused on relative yield quantities (so-called K-factors, Q-values, and R-values) which tend to have lower systematic uncertainty than absolute measurements. This update made the important contribution of adding energy dependence in fission yield evaluations, whereas evaluations before this update focused on fission yields in three energy-averaged groups.

JEFF-3.3 The JEFF-3.3 fission yield evaluation is based on the 1995 "UKFY3" evaluation by R. W. Mills [140]. A 2004 update to this evaluation [141] featured an updated experimental database and modifications to isomeric splitting, cumulative yield calculation, and uncertainty analysis.

The 1995 evaluation fit a five Gaussian model of chain yields [146] to statistically com-

bined experimental chain yield data. This fit was then used to calculate chain yields for A chains where experimental data were not available. This combined set of modeled and experimental chain yields were normalized and used to fit the parameters of a model similar to the Wahl Zp model [84]. Fractional independent yields were then modeled using this Wahl Zp model. Because of large discrepancies in the measured fractional independent yield data, the model was used to generate all of the fractional independent yields used in the evaluation, not just to fill in missing data. Independent yields were calculated by summing the modeled fractional independent yields. These independent yields were then used to calculate cumulative yields using the decay modes and branching ratios of the parents of each fission product. Finally, the chain yields were calculated to be the sum of the cumulative yields to the stable fission products in each A chain. Mills notes that some fission products undergo α decay with long half-lives and that the resulting diversion of yield into different A chains as a result of these decays is not corrected in measurements. As a result, corrections to cumulative and chain yields as a result of α decaying fission products were not made.

JENDL-4.0 The JENDL-4.0 fission yield evaluation is based primarily on the evaluations of J. Katakura, et al. The original evaluation was published in 2001 [142] with an update in 2011 [143] and revisions to the 2011 update performed in 2016 [144]. These documents do not detail the process followed to combine experimental fission yield data to produce the evaluation, however, they do detail the decay data that were used.

The 2001 evaluation primarily used the 1992 ENSDF library from Bhat [147] to obtain decay data for fission products in the evaluation. The report lists decay modes, branching ratios, half-lives, Q-values, and emission types, energies, and intensities as necessary quantities. The report also makes explicit mention of the "Beta Pandemonium" [148] problem as present in decay data relevant to numerous fission products with high β Q-values. The Beta Pandemonium problem affects nuclei with high Q_β values. These highly unstable nuclei populate the continuum or quasi-continuum of their daughter upon decay. As the decay daughter de-excites out of the continuum, many low-intensity γ transitions occur. These low-intensity transitions are not able to be detected over the signal produced by higher intensity transitions, and this results in the systematic underestimation of β feeding at high energies. These inaccuracies in the measured β feeding are then propagated forward when γ decay intensities are determined. Knowing these decay γ intensities accurately is vital to the determination of fission yields in activation-type experiments (see Eq. 3.7). As most fission products have high Q_β values, many fission product γ decay intensities may be affected. In this evaluation, nuclei with a maximum observed energy level that is small compared to their Q_β value were identified as nuclei that were potentially impacted by the Beta Pandemonium problem.

When the decay data of a certain nucleus were suspected to be deficient or when decay data were absent for a given nucleus, the evaluators used a theoretical estimation of the

decay data. The "Gross Theory of Beta Decay" [149] was used to estimate half-lives and average emitted β and γ energies. The Brink-Axel hypothesis [150, 151] was used to estimate the γ strength function, and the Gilbert and Cameron model [152] was used to calculate the nuclear level density.

3.2.2.2 Future Evaluation Needs

Experimental Fission Yields and Supporting Data Experimentally measured fission yield data are the central input for an evaluation. These data must include absolute independent, cumulative, and chain yields. The evaluation should also incorporate relative independent and cumulative yields as these can be converted to absolute values given a sufficiently well-known reference yield. In addition, the following supporting information is needed for each experiment: details on the uncertainty analysis, the incident neutron energy spectrum, and a record of the evaluated nuclear data values that were used in the data analysis. The uncertainty sources that should be provided for experimental results obtained with a particular measurement type are listed in the template tables in Sec. 3.2.3.

Decay Data All three of the current fission yield evaluations demonstrate the need for accurate decay data. These data are vital to ensuring the consistency between independent yields and cumulative/chain yields. These decay data are also important in the review of measured data by the evaluator; previous measurements may need to be adjusted when decay data values in the relevant experimental analysis have changed. Specific decay data quantities required are decay modes, branching ratios, half-lives, Q-values, and emission types, energies, and intensities with special attention required for delayed neutron emission probabilities and decay γ intensities.

ENSDF can provide a considerable portion of these data. However, as discussed in Sec. 3.2.2.1, the Katakura evaluation highlighted the non-trivial effect of the Beta Pandemonium problem [148] on decay γ intensities for short-lived, high Q-value fission product yields. Indeed, the Beta Pandemonium problem has been previously demonstrated as problematic for decay heat calculations [153, 154], for which fission product yields are crucial input data. Therefore, updated and improved decay γ intensities are of use to future evaluations. Due to limitations in experimental techniques and the large expanse of the issue, this problem cannot be addressed in the near future solely experimentally. Thus, improved predictive capabilities are also of use to future evaluations.

Neutron Energy Spectra The incident neutron energy spectrum used in a particular experiment is an important detail for any fission yield measurement. Previous evaluations have grouped measurements and their resulting yields into thermal, fast, and DT fusion energy-averaged groupings. Future evaluations may seek to capture the energy dependence of fission yields. In order to extract this dependence from literature, the incident neutron energy spectrum and its uncertainty must be analyzed and published. This information

has often been excluded from publication as it does not usually have a direct effect on the reported fission yield (unless a monitor foil is used). However, it is important information for future fission yield evaluations.

Covariances As none of the current fission yield evaluations include covariance data between fission yields, there is currently great interest in providing covariances for the first time in upcoming evaluations. Fission yield covariances have been identified as critically needed information for a number of applications, such as decay heat and reactor antineutrino rate calculations [44, 47]. To address this, several methods have been developed to estimate correlation/covariance matrices for existing fission yield libraries [47, 155, 156, 157, 158]. These estimated covariances are a useful starting point for applications but validating the results of these methods is important. To that end, empirical information on the covariance between experimental uncertainty sources and between fission product yields would be of great use to future evaluations. Having this information could validate fission covariance estimation methods and enhance the consistency between experimental data and evaluations. However, very few experiments provide fission yield covariance data currently.

3.2.3 Template

3.2.3.1 EXFOR Review

To help guide the assignment of uncertainty values that follow in the templates presented in Secs. 3.2.3.2, 3.2.3.3, 3.2.3.4, and 3.2.3.5, a review of the entries in the Experimental Nuclear Reaction Data library (EXFOR) for neutron-induced fission yields of ^{235}U, ^{238}U, and ^{239}Pu was conducted. This review covered 812 entries spanning the years 1943 to 2019. Within these entries were 1433 subentries which contained 18214 quoted fission yield uncertainty values. The `ERR_ANALYS` section of an EXFOR entry details sources of uncertainty that contribute to the uncertainty budget of a given measurement. This section was particularly useful in guiding uncertainty assignments for the templates. However, it should be noted that an overwhelming majority of the entries in EXFOR contain no information in the `ERR_ANALYS` section about the sources of uncertainty in the measurement due to none being reported in the relevant publication. This includes 6.8% of entries self-reporting that their quoted uncertainties only detailed statistical uncertainties. Because of this, a broader literature review and expert consultation were needed to supplement the information found in the EXFOR review. A total of 25 sources of uncertainty were found in this EXFOR review and these are discussed in the relevant templates listed below.

As mentioned in the introduction to this section, different types of fission yields can be measured with varying degrees of uncertainty. Figures. 3.4, 3.5, and 3.6 show histograms of the quoted uncertainties for the three predominant fission yield types found in this review (independent, cumulative, and chain) for the three fissioning systems that were covered. In all three cases, it can be seen that the mean quoted uncertainty for each fission yield type

ranks in descending order from independent, to cumulative, to chain.

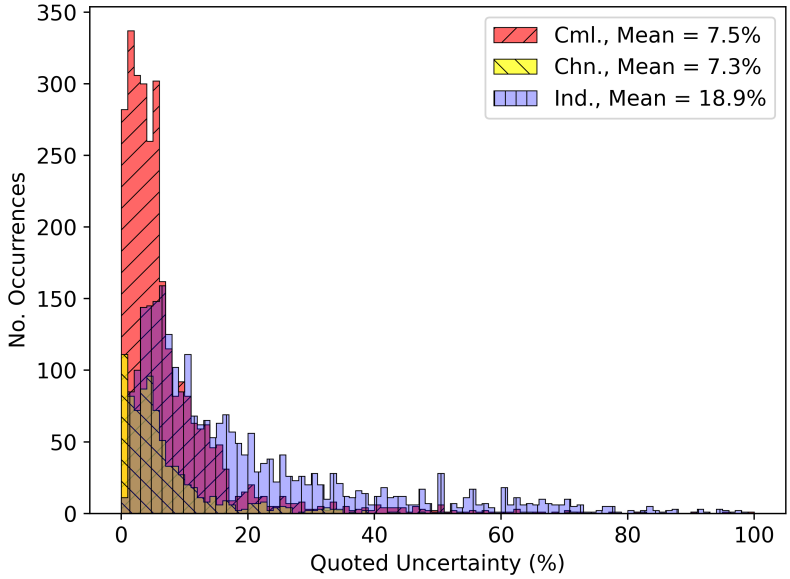

Figure 3.4: Histogram of quoted uncertainties as a function of fission yield type for ^{235}U. The types of fission yields are defined in the introduction to this chapter.

This EXFOR review also revealed an absence of covariances between different sources of uncertainty. Due to this lack of data, covariances between these sources of uncertainty will not be discussed in this chapter. Future updates to these templates may include recommendations on covariances between sources of uncertainty if subsequently published literature begins to offer more insight into these values.

3.2.3.2 Irradiation Methods

As discussed in Sec. 3.2.1.2, due to the wide variety of irradiation methods that can be employed in fission yield measurements, assigning mean and/or maximum expected values for the uncertainty sources discussed in Table 3.3 is not yet reasonable. Rather, the template for irradiation methods presented in this section will enumerate minimum expected uncertainties for each of these sources based on literature review and expert opinion. The EXFOR review was able to inform the lower bound estimates of a number of the uncertainty sources listed in Table 3.3. Recommended correlations between the fission yields of products measured within a single experiment are given for selected uncertainty sources in Table 3.4.

- **incident neutron energy spectrum** ($P(E_{inc})$) - A recommendation for the minimum uncertainty in the incident neutron energy spectrum is not offered due to the wide variety of neutron sources used in fission yield measurements. The correlation

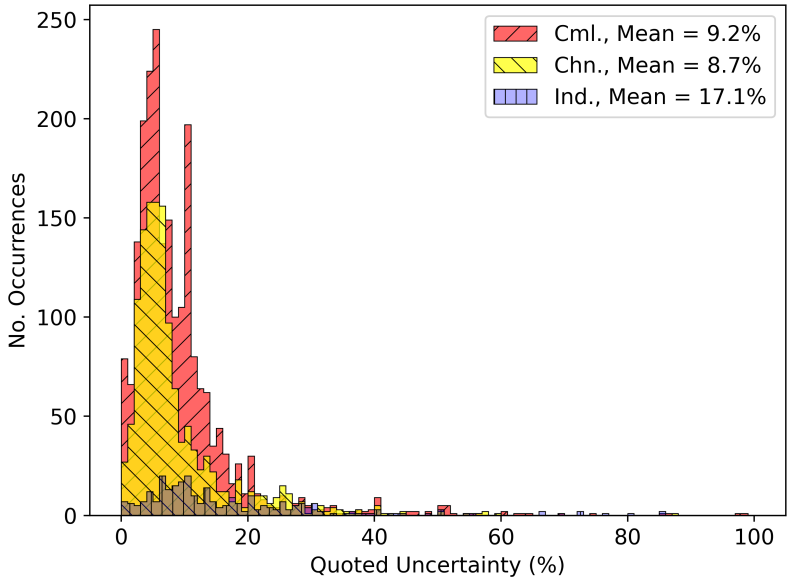

Figure 3.5: Histogram of quoted uncertainties as a function of fission yield type for ^{238}U. The types of fission yields are defined in the introduction to this chapter.

between fission yields measured in the same experiment due to the incident neutron energy source is an active area of research. Both positive and negative correlations are expected.

- **geometry ($\oslash$), solid angle (Ω), time-of-flight length (L)** - With the use of modern measurement devices, namely those that use laser positioning technologies, various dimensions can be measured to very high precision [159]. Therefore, quantities such as time-of-flight length, L, can be measured with uncertainty much less than 0.1% uncertainty. This also applies generally to other geometric measurements. However, for dimensions that are particularly small, the measurement uncertainty could be non-negligible. Therefore, the minimum geometry uncertainty, $\oslash$, and solid angle uncertainty, Ω, assigned in the template below has been set at less than 0.1%. Evaluators should remain aware of the particulars of each experiment and acknowledge that some experiments may have geometric uncertainties that are much larger than this. In nTOF measurements, the uncertainty on the time-of-flight length can be inflated by the spatial distribution of the neutron source and the neutron detector(s). Neutron time-of-flight lengths have been measured with absolute uncertainties as low as 1 mm. Therefore, the minimum uncertainty in nTOF time-of-flight length has been set to 1 mm for this template. The correlation between fission yields measured in the same experiment due to geometry depends on the specifics of each experiment and thus a recommended correlation is not offered. There is no expected correlation between fission yields measured in the same experiment due to solid angle. This is because solid

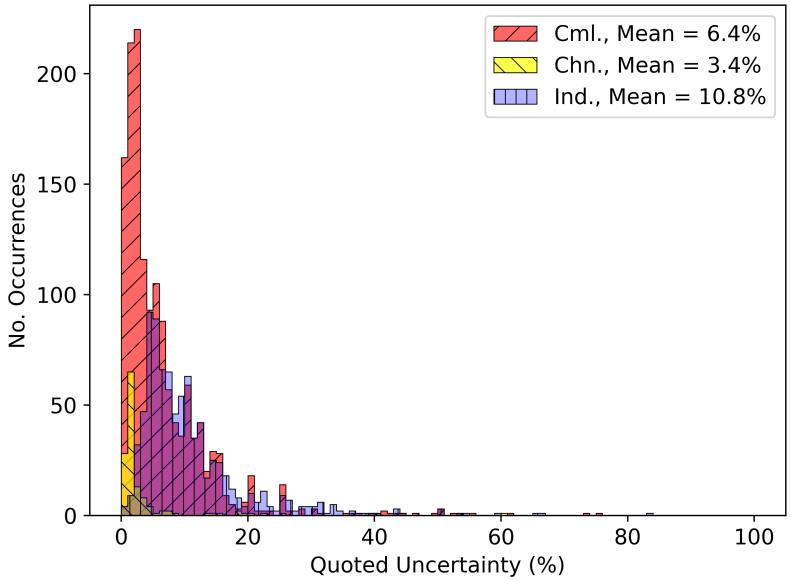

Figure 3.6: Histogram of quoted uncertainties as a function of fission yield type for ^{239}Pu. The types of fission yields are defined in the introduction to this chapter.

angle simultaneously increases both the number of products produced and the number of fissions (see Eq. 3.1).

- **timing resolution (Δt)** - The timing resolution of detectors used in neutron time-of-flight measurements can be very small in absolute terms. In most cases, the timing resolution can be measured to less than 1 ns [160, 107]. The timing resolution can be inflated by the width of the neutron pulse from the neutron source.

- **monitor reaction product activities (A_{mon})** - The uncertainty in the monitor reaction product activity from a foil irradiation can come from several different sources. Counting statistics, γ spectroscopy uncertainties, and detector efficiency often dominate this quantity. In an idealized case (where γ spectroscopy and efficiency calibration uncertainties are minimal), counting statistics represents the lower bound for this uncertainty. As mentioned below, counting statistics will follow a Poisson distribution at a minimum. Therefore, the minimum uncertainty for this quantity is set as a Poisson distribution. However, it should be noted this uncertainty will likely be larger than this.

- **number of fissions (N_f)** - The number of fissions that occurred in a target sample can be affected by one or more of the sublisted quantities in Table 3.3, depending on the measurement methodology. Therefore, taken together, the minimum values for the sources of uncertainty that contribute to the number of fissions/fission rate suggest that the lower bound for the net uncertainty on that quantity should be 1%. Equation 3.1

indicates that the correlation between fission yields measured in the same experiment due to the number of fissions should be fully correlated.

- **neutron flux (ϕ)** - Without regard to its measurement methodology, the uncertainty in the neutron flux experienced by the target material was reported in 17 measurements in the EXFOR review. The lowest such value was listed as 1% [161]. Therefore, the minimum value for this uncertainty source has been set at 1%. Equations 3.1, 3.3, 3.4, and 3.5 indicate that the correlation between fission yields measured in the same experiment due to the neutron flux should be fully correlated.

- **fission cross section (σ_f)** - The fission cross section is generally taken from evaluation and therefore its uncertainty should be taken from the corresponding evaluation. Equations 3.1, 3.3, 3.4, and 3.5 indicate that the correlation between fission yields measured in the same experiment due to the fission cross section should be fully correlated.

- **number of atoms/mass (N)** - As was discussed in Sec. 3.2.1.3, the number of atoms/mass present in a sample can be determined using gravimetric scaling with uncertainties as low as 0.001%. Therefore, the minimum value for this uncertainty source has been set at 0.001%. However, other methods of mass/number determination may be less accurate. Equations 3.1, 3.3, 3.4, and 3.5 indicate that the correlation between fission yields measured in the same experiment due to the number of atoms/mass of the target should be fully correlated. If different targets are used for the two measurements, a strong correlation is still expected.

- **isotopic abundance (w)** - Databases of isotopic abundances and their uncertainties are maintained by various scientific institutions such as the National Institute of Standards and Technology (NIST) [162] and the International Union of Pure and Applied Chemistry (IUPAC) [163]. These database values should be used in calculations where relevant. For non-natural sources, isotopic abundance is often the result of an enrichment process. These uncertainties should be given by the manufacturer and are expected to be relatively small ($< 0.1\%$).

- **irradiation time (t_i)** - Modern computers and electronic stopwatches can be used to track intervals of time, such as irradiation time, with a precision of less than 1 ms. Therefore, it is often acceptable to treat the uncertainty on those time intervals as negligible relative to other sources of uncertainty. Equations 3.1 and 3.3 indicate that the correlation between fission yields measured in the same experiment due to the irradiation time should be fully correlated.

- **reactor burn-up (B_u)** - The EXFOR review found a single fission yield measurement that reported the uncertainty on the reactor burn-up value, B_u, included in their calculations as 1.3% [110]. Therefore, the minimum value for this uncertainty source has been set at 1%. When reactor burn-up increases, the calibrated neutron flux of a beam port will need to be decreased; making these two quantities strongly correlated.

As the correlation between fission yields measured in the same experiment due to neutron flux should be fully correlated, the correlation due to reactor burn-up should be strongly correlated.

- **fission fragment track counting (c_T)** - Track counting uncertainties were found twice in the EXFOR review, with the lowest reported uncertainty being 1.5% [164]. Therefore, the minimum value for this uncertainty source has been set at 1.5%. As the number of fission fragment tracks counted in an experiment increases, the number of fissions in the target increases (within counting statistics uncertainty); making these two quantities strongly correlated. As the correlation between fission yields measured in the same experiment due to the number of fissions should be fully correlated, the correlation due to fission fragment track counting should be strongly correlated.

- **fission chambers (F_C)** - Uncertainties due to the use of fission chambers were found twice in the EXFOR review, with the lowest reported uncertainty being 1.5% [164]. Therefore, the minimum value for this uncertainty source has been set at 1.5%. Equations 3.1 and 3.6 indicate that the correlation between fission yields measured in the same experiment due to fission chamber counting should be fully correlated.

- **counting statistics (c)** - In general, counting statistics will follow a Poisson distribution at a minimum. However, some counting systems/methodologies may introduce non-Poisson elements to their counting statistics, increasing their counting uncertainty. In general, the correlation between data points due to counting statistics is expected to be uncorrelated.

3.2.3.3 Chemical Separations

Table 3.5 lists the expected range of values for the sources of uncertainty for chemical separations that were discussed in Sec. 3.2.1.3. The chemical separations discussed in this chapter are used to separate fission products, not to directly assay the quantity of those fission products. Therefore, correlations between fission product yields that result from chemical separations will vary from experiment to experiment. Thus, recommended correlations between fission yields as a result of chemical separation are not offered.

- **number of atoms/mass (N)** - As discussed in Sec. 3.2.1.3, the number of atoms/mass can be determined gravimetrically to within uncertainties as low as 0.001%. The publication by Kučera et al. [116] suggests the upper limit for these uncertainties to be 0.5%, however, this could be larger if oxidation bias is not corrected.

- **isotopic abundance (w)** - Section 3.2.3.2 discussed the uncertainties present in sample enrichment/isotopic abundance. The uncertainty in the isotopic abundance in a sample is given by databases for a natural sample or given by the manufacturer when using an enriched sample.

Table 3.3: List of uncertainty sources associated with the irradiation methods detailed in Sec. 3.2.1.2. δ denotes relative uncertainties given in % and Δ notes absolute uncertainties with units. Uncertainties are relative to each source listed.

Symbol	**Minimum σ**
Relative and Absolute:	
$\delta P(E_{inc})$	
nTOF	
-ΔL	1 mm
-Δt	1 ns
-δc	Poisson dist.
Foil Act.	
-δA_{mon}	Poisson dist.
-δc	Poisson dist.
-$\delta\sigma_{mon}$	given by evaluation
Absolute Only:	
δN_f	1
-$\delta\phi$	1
-$\delta\sigma_f$	given by evaluation
-δN	0.001
- δw	abundance: See databases or given by enrichment
- δt_i	$\sim$0
-δB_u	1
-δc_T	1.5
-δF_C	1.5
$\delta\oslash$	<0.1
δN	0.001
- δw	enrichment: given by manufacturer abundance: See databases
$\delta\Omega$	<0.1
δc	Poisson dist.

- **oxidation bias (o)** - Section 3.2.1.3 gives the upper limit for oxidation bias in number/mass is determined by stoichiometry, but could be negligible if proper chemical protocols are followed.
- **chemical yield (y)** - The publication from Kučera et al. [116] suggests the lower limit for chemical yield uncertainty to be 0.3% and the upper limit to be 0.5%. However,

Table 3.4: Recommended correlations for the uncertainty sources in Table 3.3. These correlations are between fission yields of products measured in the same experiment.

Symbol	Correlation
Relative and Absolute:	
$P(E_{inc})$	–
Absolute Only:	
N_f	Fully Correlated
ϕ	Fully Correlated
σ_f	Fully Correlated
N	Fully Correlated (strongly if different targets)
t_i	Fully Correlated
B_u	Strongly Correlated
c_T	Strongly Correlated
F_C	Fully Correlated
$\oslash$	–
Ω	Uncorrelated
c	Uncorrelated

a higher upper limit of 3% is possible if full dissolution of the target sample is not achieved.

- **isotopic exchange (x)** - Kučera et al. assert that uncertainty induced by isotopic exchange should be negligible if a homogenous system is achieved. However, there is insufficient literature material to assign an upper limit for this uncertainty.

Finally, the importance of adherence to established chemical uncertainty protocols is stressed. The use of these standards is encouraged in the publication by Saffaj et al. [118]. This publication also notes that these standards are often ignored. This will impact legacy fission yield measurements that include chemical separations in untold ways. An evaluator with experience in radiochemistry is needed to assess the quality of each publication. The list of sources of uncertainty presented in Table 3.5 only seeks to detail common and predominate sources of uncertainty and thus is not exhaustive. The judgment of a qualified evaluator is needed to properly incorporate fission yield measurements with chemical separations into future evaluations.

Table 3.5: List of uncertainty sources associated with chemical separations in fission measurements as detailed in Sec. 3.2.1.3. Uncertainties are relative to each source listed. "–" indicates an upper bound is not recommended due to lack of information.

Symbol	**Min. σ (%)**	**Max. σ (%)**
δN	0.001	0.5
- δw	abundance: See databases or given by enrichment	
- δo	$\sim$0	stoichometry ($\sim$17 for O_2)
δy	0.3	3
δx	$\sim$0	–

3.2.3.4 Assay Methods

γ Spectroscopy Table 3.6 lists the expected range of values for the sources of uncertainty in γ assay methods that were discussed in Sec. 3.2.1.4. Recommended correlations between the fission yields of products measured within a single experiment are given for these uncertainty sources in Table 3.7.

- **γ detection efficiency (ε)** - The EXFOR review found 43 reports of efficiency uncertainties with the mean of these values equaling 5%. Energy-resolved γ spectroscopy produced lower uncertainty values on average than energy-unresolved spectroscopy. The largest uncertainties in efficiency calibration values generally result from energy-unresolved measurements before the wide-spread adoption of Ge-based detectors in the late-1960s. Energy-resolved detection efficiency values ranged from 0.51% [113] to 20% [165]. Energy-unresolved detection efficiency ranged from 1.9% to 50% both in Reference [166]. The lower and upper bounds for efficiency uncertainty values in energy-resolved and energy-unresolved spectroscopy were set to these values. Equations 3.1 and 3.2 with Eq. 3.7 indicate that the correlation between fission yields measured in the same experiment due to the γ detection efficiency should be fully correlated.

- **γ decay intensity (I_γ)** - The uncertainty in a decay γ intensity is generally taken from evaluation. Equations 3.1 and 3.2 with Eq. 3.7 indicate that the correlation between fission yields measured in the same experiment due to the γ decay intensity should be fully correlated.

- **half-life ($T_{1/2}$)** - The uncertainty in a half-life is generally taken from evaluation. $T_{1/2}$ appears in the exponential term of Eq. 3.7 (through λ). Therefore, the correlation

between fission yields measured in the same experiment due to the half-life should be strongly (not fully) correlated, as indicated by Eq. 3.7 with Eqs 3.1 and 3.2.

- **calibration source activity (A_0)** - The uncertainties in the activity of calibration sources are generally given in the calibration certificate provided by the manufacturer. For most standard calibration source isotopes, the associated activity will have uncertainty between 1-2%. Equations 3.1 and 3.2 with Eqs. 3.7, 3.8, and 3.9 indicate that the correlation between fission yields measured in the same experiment due to the calibration source activity should be fully correlated.

- **gamma spectroscopy (g)** - Gamma spectroscopy fitting methods are often used in fission yield measurements to separate overlapping photopeaks in dense fission product γ-ray spectra. These methods introduce uncertainty in the extracted photopeak area that is beyond standard Poisson counting statistics. The EXFOR review found four reports for γ spectroscopy uncertainties, ranging from 0.18% [113] to 5% [124]. Reference [113] could represent a reasonable lower bound for γ spectroscopy uncertainties (in spectra where counting statistics are high and photopeak shapes are well defined). However, in γ-ray spectra with low counting statistics and/or poor photopeak shaping, these γ spectroscopy uncertainties could be larger than 5%. Because of this, an upper limit for the uncertainty in γ-ray spectroscopy is not set in this template. The correlation between fission yields measured in the same experiment due to γ spectroscopy fitting could be positive or negative depending on the specifics of the spectrum being analyzed. Therefore, a recommendation on this correlation is not offered in Table 3.7.

- **dead-time (τ)** - Uncertainties in assay counting related dead-times were found in the EXFOR review in only one publication, with values ranging from 0.5% to 2.0% [105]. Several dead-time models predict that given the correct conditions, the dead-time uncertainty can be equal to or less than the uncertainty given by Poisson counting statistics [167]. Thus, it is theoretically possible to obtain negligible dead-time uncertainty if the counting system used is well-optimized and sufficient counting statistics are obtained during the calibration. This also suggests dead-time uncertainty could be very large if the counting system is unoptimized and low counting statistics are obtained during the calibration. Therefore, the lower limit for dead-time uncertainty has been set near zero and an upper limit is not suggested for this template. As a dead-time correction can be seen as a correction to the γ detection efficiency, and as the correlation between fission yields measured in the same experiment due to the γ detection efficiency should be fully correlated, the correlation due to dead-time is also expected to be fully correlated.

- **geometry ($\oslash$, η) and solid angle (Ω)** - As discussed in Sec. 3.2.3.2, with modern measurement technologies, geometry uncertainties can often be very small in relation to their respective dimensions (<0.1%). It is difficult to assign a reasonable upper bound to geometry uncertainties as some experimental apparatuses may have dimensions that

are small relative to their uncertainty. Therefore, an upper limit is not assigned in this template. The correlation between fission yields measured in the same experiment due to geometry depends on the specifics of each experiment and thus a recommended correlation is not offered. The correlation between fission yields measured in the same experiment due to counting geometry/solid angle is expected to be uncorrelated as both of these quantities simultaneously increase the number of products produced and the number of fissions (see Eq. 3.1).

- **self-shielding (ξ)** - Closely related to geometry and of particular concern to fission yield measurements (where high-Z actinide targets are used) are self-shielding/self-attenuation corrections. The EXFOR review found 11 reports of self-shielding correction uncertainties, ranging from 0.18% [168] to 10% [105]. These values have been set as the lower and upper bounds for the template. As a self-shielding correction can be seen as a correction to the γ detection efficiency, and as the correlation between fission yields measured in the same experiment due to the γ detection efficiency should be fully correlated, the correlation due to self-shielding is also expected to be fully correlated.

- **counting statistics (c)** - As discussed in Sec. 3.2.3.2, counting statistics will at a minimum follow a Poisson distribution. However, some counting systems may introduce non-Poisson elements to their counting statistics, increasing their counting uncertainty. In general, the correlation between data points due to counting statistics is expected to be uncorrelated.

Section. 3.2.1.4 discussed that throughout this publication it has been noted that there are limited data available about γ angular correlation shapes. Moreover, these angular correlations only become important when observing γ-γ coincidences in fission yield measurements. While observing these coincidences is a powerful tool that can limit backgrounds, it is not often used. Given this and the lack of detailed information about γ angular correlations, this template will not make a recommendation about lower or upper bounds for angular correlation uncertainties.

β Counting Table 3.8 lists the expected range of values for the sources of uncertainty in γ assay methods that were discussed in Sec. 3.2.1.4. Recommended correlations between the fission yields of products measured within a single experiment are given for these uncertainty sources in Table 3.9.

- **β detection efficiency (ε)** - Of the 43 efficiency values that were found in the EXFOR review, none were related to β counting. Because of the short range of β particles in matter and the fact that β counting does not require energy deposition information, the efficiencies of β counters are very closely related to their solid angle coverage. A correction to solid angle is usually required to account for stopping of low-energy β particles in the dead layer/air between the source and the counter. Also, some β

Table 3.6: List of uncertainty sources associated with the γ assay methods detailed in Sec. 3.2.1.4. Uncertainties are relative to each source listed. "–" indicates an upper bound is not recommended due to lack of information.

Symbol	Min. σ (%)	Max. σ (%)
Resolved Only:		
$\delta\varepsilon$	0.5	20
-δI_γ	given by evaluation	
-$\delta T_{1/2}$	given by evaluation	
-δA_0	calib. certificate	
-δg	0.2	–
-δc	Poisson dist.	–
δg	0.2	–
Unresolved Only:		
$\delta\varepsilon$	2	50
Unresolved and Resolved:		
$\delta\tau$	$\sim$0	–
$\delta\eta/\Omega$	$<$0.1	–
$\delta\xi$	0.2	10
δc	Poisson dist.	–

counters may have limited γ efficiency. In this case, if a β emitter that also emits γ rays is counted, a correction for signals produced by γ rays will need to be applied. Because of the issues related to energy-dependent corrections and γ sensitivity, an upper bound for β counting efficiency uncertainty is not recommended in this template. The lower limit for this uncertainty is set to match that of counting geometry/solid angle at 0.1%. However, it should be noted that most β counters will have uncertainty greater than this and that this value is only a lower limit. Equations 3.1 and 3.2 with Eq. 3.10 indicate that the correlation between fission yields measured in the same experiment due to the β detection efficiency should be fully correlated.

- **dead-time (τ)** - The lower limit for dead-time uncertainty has been set near zero and an upper limit is not suggested for this template. This lower limit is based on the γ assay template as dead-time uncertainties should be similar for γ and β detectors. As a dead-time correction can be seen as a correction to the β detection efficiency, and as the correlation between fission yields measured in the same experiment due to the β detection efficiency should be fully correlated, the correlation due to dead-time is also expected to be fully correlated.

- **counting geometry (η) and solid angle (Ω)** - As discussed in previous sections,

Table 3.7: Recommended correlations for the uncertainty sources in Table 3.6. These correlations are between fission yields of products measured in the same experiment.

Symbol	Correlation
Resolved Only:	
ε	Fully Correlated
-I_γ	Fully Correlated
-$T_{1/2}$	Strongly Correlated
-A_0	Fully Correlated
g	–
Unresolved Only:	
ε	Fully Correlated
Unresolved and Resolved:	
τ	Fully Correlated
η/Ω	Uncorrelated
ξ	Fully Correlated
c	Uncorrelated

counting geometries and solid angles can often be determined with very low relative uncertainty. The lower bound for counting geometries and solid angles is thus set to the previously suggested lower limit of 0.1%. However, it should be noted that β counting geometries often feature small dimensions as β particles are highly attenuated in matter and air. Therefore, relative geometric uncertainties in β counting experiments are likely to be larger on average than in the other assay methods detailed in this template. The correlation between fission yields measured in the same experiment due to counting geometry/solid angle is expected to be uncorrelated as both of these quantities simultaneously increase both the number of products produced and the number of fissions (see Eq. 3.1).

- **self-shielding (ξ)** - The self-shielding/self-attenuation correction in β counting is almost certainly present in any β counting experiment due to the very low range of β particles in matter and the high-Z of actinide targets. These corrections are closely related to those for γ spectroscopy that were discussed in Sec. 3.2.3.4. Therefore, the lower limit for these uncertainties is set equal to those of γ spectroscopy at 0.2%. However, because β particles are much more quickly attenuated in matter than γ rays, an upper bound is not set for this uncertainty. As a self-shielding correction can be seen as a correction to the β detection efficiency, and as the correlation between fission yields measured in the same experiment due to the β detection efficiency should be fully correlated, the correlation due to self-shielding is also expected to be fully correlated.

- **counting statistics** (c) - As discussed in previous sections, counting statistics is at a minimum described by a Poisson distribution, and no upper limit for this is set in this template. In general, the correlation between data points due to counting statistics is expected to be uncorrelated.

Table 3.8: List of uncertainty sources associated with the β assay methods detailed in Sec. 3.2.1.4. Uncertainties are relative to each source listed.

Symbol	**Min. σ (%)**
$\delta\varepsilon$	0.1
$\delta\tau$	$\sim$0
$\delta\eta/\delta\Omega$	0.1
$\delta\xi$	0.2
δc	Poisson dist.

Table 3.9: Recommended correlations for the uncertainty sources in Table 3.8. These correlations are between fission yields of products measured in the same experiment.

Symbol	**Correlation**
ε	Fully Correlated
τ	Fully Correlated
η/Ω	Uncorrelated
ξ	Fully Correlated
c	Uncorrelated

3.2.3.5 2E-2v Method

Because of the relatively recent popularity of the 2E-2v method and the new construction of 2E-2v devices, only minimum values for the uncertainty sources for this method will be suggested in this template. The 2E-2v method determines the masses of fission products on an event-by-event basis; each product mass is measured independently of others. Therefore, recommended correlations between fission yields measured using the 2E-2v method are not offered.

- **fission product energy** (E) - The energy detectors usually used in the 2E-2v method are ionization chambers, though Si detectors can be used. The energy resolution for the

fission products varies with mass. For ionization chambers, it is estimated that 0.5% energy resolution can be achieved for the lightest fission products, while 1% can be achieved for the heaviest. For Si detectors, peer-reviewed publications have indicated that an energy resolution of 0.3% can be achieved for the lightest fission products [135].

- **fission product time-of-flight (t)** - For the SPIDER 2E-2v spectrometer, the timing electronics have a resolution of 150 ps for each arm. This timing resolution needs to be added in quadrature for each arm, for a total uncertainty of 210 ps. With a flight path length of approximately 70 cm, this would amount to a timing resolution of 0.5% for the lightest fission products. This value is consistent with the timing resolution claimed by the VERDI spectrometer [135]. In the case that sputtered electrons from the target are used as the start signal in the time-of-flight determination (as is done with the VERDI spectrometer), there will be a plasma delay time that results from the bending of the sputtered electrons through an electrostatic mirror into a micro-channel plate (MCP) detector.

- **fission product flight path length (L)** - The flight path length of each arm of the apparatus is often calibrated using an α-emitting source with a known energy. This allows the flight path to be determined to within approximately 1 mm. For the SPIDER spectrometer, this would be a relative uncertainty of approximately 0.1%. However, it should be noted that the flight path of the fission products from each fission event will be different. This is due to both the angle that the products are emitted at and the extended geometry of the target sample. Corrections for these factors can be made if electronics are implemented to track the trajectory of the fission products, however, these corrections will inflate the uncertainty in the flight path length.

- **counting statistics (c)** - As discussed in Sec. 3.2.1.5, the uncertainty in the number of fissions observed is determined by counting. At the very minimum, this uncertainty will be given by Poisson counting statistics.

3.3 Conclusions

This work provides a summary of the current state of fission product yield measurements. In providing this summary, the above set of templates provides a number of benefits to the scientific community: a general guide to help develop an understanding of experimental fission yield data, a guide to help experimentalists fully document their uncertainties, and a guide to help evaluators appropriately compile experimental fission yield data into their evaluations.

The templates are a community-based effort and the community can continuously use, critique, and update the templates. In the near future, NNDC will host a condensed version

Table 3.10: List of uncertainty sources associated with the 2E-2v method detailed in Sec. 3.2.1.5. Uncertainties are relative to each source listed.

Symbol	**Min. σ (%)**
δE	
Ion. Cham.	0.5
Si	0.3
δt	0.5
δL	0.1
δc	Poisson dist.

of the templates on its homepage, providing quick access to the templates for the scientific community. Journal editors are being engaged in the hopes that reviewers can be provided with the templates for use in their peer-review process. Subgroup 50 of the Working Party on International Nuclear Data Evaluation Cooperation at the Organization for Economic Cooperation and Development (OECD) at the NEA, has been assembled with the goal of developing a comprehensive and machine-readable database of experimental reaction data (similar to EXFOR). Such an advancement would enable the uncertainty sources listed in the templates and their expected values to be more consistently and easily updated.

Again it should be noted that these templates are not an immutable set of rules. The templates serve as a guideline based on the state-of-the-art at the time of their publication. As new technologies or the employment of existing technologies advance, the values listed in the templates may become obsolete. For this reason, the templates should only be viewed as a guide; the expected values in the templates can be exceeded. Similarly, the templates should not discourage further advancements in experimental methods by setting an "acceptable" level for uncertainties that no one endeavors to surpass. Experimentalists should always strive to produce measurements with uncertainties that are as low as is physically achievable. As experimental methods advance, the templates will need to be updated and it is planned that future publications will be released to continuously update the templates.

The presented template of expected measurement uncertainties in fission product yields improves the overall understanding of experimental fission yield data. As the template comes into use by the scientific community, it will improve the quality of future fission yield evaluations and experiments.

Chapter 4

Estimation of Independent and Cumulative Fission Yield Covariances

As was discussed in Sec. 1.2.2, no existing fission yield evaluation includes information on the covariance between fission product yields and this information has been identified as a critical need. To address this need, a Monte-Carlo method for the generation of correlation and covariance matrices for independent and cumulative fission yields has been developed. The method uses a constrained Monte-Carlo resampling structure in order to vary evaluated fission yield libraries in a way that meets basic conservation principles. This results in the generation of correlation/covariance matrices with limited model bias and uncertainty; the matrices are primarily reflective of the evaluated fission yield uncertainties and correlations that arise from the evaluation process. This method has been applied to generate correlation and covariance matrices for all of the fissioning systems of the ENDF/B-VIII.0 and JEFF-3.3 evaluations, marking the first time such matrices have been generated for all of these systems. These covariance matrices have been published online for immediate public use. These correlation and covariance matrices can be used to improve uncertainty estimation in calculations of reactor antineutrino emission rates, decay heat problems, and nuclear forensics. This method, and the results thereof, were published as a peer-reviewed article "Stochastically Estimated Covariance Matrices for Independent and Cumulative Fission Yields in the ENDF/B-VIII.0 and JEFF-3.3 Evaluations" in Atomic Data and Nuclear Data Tables [169].

4.1 Motivation

In fission, a nucleus undergoes a deformation that leads to the scission of the nucleus into at least two fragments. These fragments have high excitation energy and undergo prompt neutron and photon emission. When the prompt neutron emission has ceased, the fragments are referred to as "products." The probability that a particular fission product will be produced directly from a fission event is called an "independent yield." The probability that a

particular fission product will exist at some point in time after fission, either due to direct production from fission or due to production from the decay of a parent fission product, is called a "cumulative yield."

The measurement and evaluation of independent and cumulative fission yields is the result of decades of exceptional research by scientists from across the globe. Continued research in this area is needed to meet the ever-advancing needs of users. Neither the fission yield evaluation (based on Refs. [86, 139]) in the ENDF/B-VIII.0 (Evaluated Nuclear Data File) evaluated library [28] nor the fission yield evaluation (based on Refs. [140, 170]) in the JEFF-3.3 (Joint Evaluated File for Fission and Fusion) evaluated library [29] contain an estimation of correlation/covariance between fission product yields. These covariance and correlation matrices for independent and cumulative fission product yields have been identified as a pressing nuclear data need [1, 42, 28]. These matrices are needed for applications in reactor antineutrino rate calculations [43, 44, 45, 46], decay heat calculations [47], and any other calculations that incorporate fission yield data such as nuclear forensics.

Nuclear data libraries that are used in applications, such as those listed above, are produced by scientists with specialized skills in a process called "evaluation". The evaluation process brings together experimental measurements of nuclear properties, nuclear physics modeling, and the expertise of the evaluator to produce these nuclear data libraries. Therefore, there are three keys sources where correlation arises from in evaluated nuclear data libraries: **physics, experiment,** and **evaluation**.

Each of these three sources introduces a unique set of errors and correlations and all three of these sources are present in all evaluated nuclear data libraries to some degree. In an ideal case – if experimental capabilities and measurements were perfect and errorless and the evaluation was conducted flawlessly with exact modeling capabilities – the correlation between the values in a nuclear data library would be purely physical (i.e., those that arise from the underlying physics of the measured property). However, this ideal case does not occur in reality and consideration of correlations arising from experimental and evaluation sources is required in order provide users of nuclear data libraries with realistic uncertainties and covariance matrices.

Ideally, fission yield covariances would be generated with the evaluation in order to maximize consistency. In the interim, methods for estimating fission product yield covariance matrices have been proposed [47, 171, 155, 172, 156]. These methods rely on an underlying model of the fission process to determine correlations between fission products and therefore give an estimation of the physical correlations that are discussed above. For example, the works of Rochman et al. [171] and Leray et al. [155] use the GEF code [173, 174] to generate their matrices. These methods require that the model of fission is reliably accurate and that model parameters exist for a compound system of interest. Often parameters for these models have been determined for only a small number of well-known compound sys-

tems [155, 172], limiting their scope to be less than that of the compound systems currently listed in the ENDF/B-VIII.0 and JEFF-3.3 evaluations. These model-based methods are an important component of determining fission yield covariance matrices; they estimate the physical component of correlations in evaluated nuclear data libraries. Nevertheless, these only provide a part of the correlation information that users need and must be complemented with estimations of the experimental and evaluation components.

The fact that these model-based methods do not take experimental correlations fully into consideration has been previously noted in literature [175]. It should also be noted that the evaluation process and its potential to introduce additional error and correlation into evaluated fission yield libraries has been previously observed through inconsistencies between evaluated fission yields and fission neutron multiplicity distributions [94]. This observed inconsistency, and the evaluation correlation introduced by it, is captured by the new method presented in this publication, as will be detailed in Sec. 4.2.3.

In order to address the topics discussed above, the method presented was formulated. It seeks to limit model dependence and focuses primarily on correlations that arise from the ENDF/B-VIII.0 and JEFF-3.3 evaluations and the experimental data that underlie them. In addition to this, this publication also seeks to ensure open access to the correlation and covariance matrices resulting from this method. While the alternative methods listed above for covariance/correlation matrix generation exist, the results of these methods have not been made publicly available. To address this issue, the matrices that result from the method presented have been made immediately available to the nuclear science community at `nucleardata.berkeley.edu/FYCoM`. In the interest of reproducible science, a workflow for the calculation of these matrices has been preserved in Ref. [158].

4.2 Method

4.2.1 Independent Yields

Independent fission yield libraries should obey a number of conserved relationships. The following Monte-Carlo resampling method is structured to conserve the five conditions given below. These conditions are modified from similar conditions proposed by Fiorito et al. [47].

In a fission event, at least two fission products must be produced. Therefore, binary fission yields should sum to two:

$$\sum_i Y_i = 2 \tag{4.1}$$

where Y_i is the independent yield of nuclide i.

The total charge must be conserved, therefore the total charge of the compound system, Z_{CN}, should be recovered:

$$\sum_i Y_i Z_i = Z_{CN} \tag{4.2}$$

where Z_i is the atomic number of nuclide i.

The total baryon number must be conserved, therefore the total baryon number of the compound system, A_{CN}, less the average number of fission neutrons emitted, $\bar{\nu}$, should be recovered:

$$\sum_i Y_i A_i = A_{CN} - \bar{\nu} \tag{4.3}$$

where A_i is the mass number of nuclide i.

Assuming charged particle emission from fission fragments is negligible, the net yield to products with a particular atomic number, Z, should be equal to the net yield to products with the complementary atomic number, $Z_{CN} - Z$:

$$\sum_i Y(Z, A_i) = \sum_j Y(Z_{CN} - Z, A_j) \tag{4.4}$$

For a given fission yield library there should exist some midpoint mass number, A_{mid}, such that yields on either side of this midpoint should sum to one:

$$\sum_{A_i > A_{mid}} Y(A_i) = \sum_{A_i \leq A_{mid}} Y(A_i) = 1 \tag{4.5}$$

Equation 4.5 determines which nuclei are heavy ($A > A_{mid}$) and which are light ($A \leq A_{mid}$) in the resampling method. It also states the midpoint of the fission product distribution is constant. This is expected even in the extreme case of symmetric fission as changing this midpoint also changes the total mass distributed to the fission fragments from the compound nucleus. In reality, Eq. 4.5 may only be approximately true due to mass number being an integer and not a continuous variable. However, exploiting this condition allows the Monte-Carlo resampling method to be structured such that the conditions in Eqs. 4.1, 4.2, 4.3, and 4.4 are also conserved. In this method, A_{mid} is selected by finding the A in each fission yield library that best reproduces Eq. 4.5.

The following steps give the method that is used to produce resampled fission yield libraries that meet the conditions given in Eqs. 4.1, 4.2, 4.3, 4.4, and 4.5:

1. Select a random number, X, between 0 and 1. If X is less than 0.5, the yields on the 'light' side ($A \leq A_{mid}$) will be resampled. Otherwise, yields on the 'heavy' side ($A > A_{mid}$) will be resampled.

2. For each A chain on the selected side, randomly select a fission product yield to be resampled. The probability that a given product is selected should be set such that high-yield, low-uncertainty products are preferentially selected. Resample that yield about a normal distribution with a centroid equal to its evaluated yield and width equal to its evaluated yield uncertainty.

3. Scale the other fission product yields in the A chain by the same percent change realized for the product yield in Step 2.

4. Normalize the yields on the selected side such that their sum equals 1.

5. Generate fission yields on the complementary side using the fission neutron multiplicity distribution, $P(\nu, A)$:

$$Y_{frac}(Z_{CN} - Z, A_{CN} - A - \nu) = P(\nu, A)Y(Z, A) \tag{4.6}$$

$$\begin{aligned} Y(Z, A) &= \sum_{A} \sum_{\nu} Y_{frac}(Z_{CN} - Z, A_{CN} - A - \nu) \\ Y(Z, A) &= \sum_{A} \sum_{\nu} \Big[P(\nu, A_{CN} - A - \nu) \\ &\quad \times Y(Z_{CN} - Z, A_{CN} - A - \nu) \Big] \end{aligned} \tag{4.7}$$

6. Repeat Steps 1-5 N times. Select N such that statistical noise is minimized.

7. Calculate the resulting correlation and covariance matrices from the N trials.

Conservation of Eq. 4.5 is a given of the method. The conservation of Eq. 4.1 and Eq. 4.4 can be proven analytically. Equations 4.2 and 4.3 are numerically verified to be conserved to within 0.01% for the ENDF/B-VIII.0 evaluation and to within 0.05% for the JEFF-3.3 evaluation. In principle, one can combine Steps 2 and 3 and simply resample each fission product yield about its evaluated yield and yield uncertainty. However, the ENDF/B-VIII.0 evaluation assumed a Gaussian distribution of yield in Z for each A chain [86]. Therefore, Step 3 is justified as it introduces the positive correlation between product yields within a given A chain that the ENDF/B-VIII.0 evaluation process would have introduced. Step 5 relies on the accuracy of the $P(\nu, A)$ data used, and Sec. 4.2.3 will address how $P(\nu, A)$ data are obtained for all of the compound systems in the evaluations. For Step 6, this study used $N = 10000$ to produce the presented matrices. The Mersenne Twister pseudo-random number generator with a seed of 0 was used for each matrix generated.

As will be detailed in Sec. 4.2.3, the fission yield evaluations did not take into consideration the consistency of fission neutron multiplicity distributions with independent fission yields. Because of this, the covariance matrix that is directly obtained from Step 7 gives variances in the yields that are larger than their corresponding evaluated variances. The

correlation and covariance matrices obtained from Step 7 will be called "primary" matrices throughout this publication as they are the matrices that are obtained directly from the method presented.

The covariance matrices that result from this process exhibit variances in the independent yields that are larger than those in the evaluations. In order to address this, a pair of "normalized" correlation and covariance matrices are calculated. The fission yield variances in the normalized covariance matrix are equal to those in the evaluation. The normalized covariance matrix is calculated as the product of the primary correlation matrix and the evaluated fission yield uncertainties. In order to conserve total yield, the sum of the normalized covariance matrix must be zero (as it is in the primary covariance matrix). For all of the compound systems considered, the sum of the covariance matrix obtained by simply taking the product of the primary correlation matrix and the evaluated fission yield uncertainties was greater than zero. To enforce that the sum of the normalized covariance matrix is zero, the negative correlations in the primary correlation matrix were scaled slightly. This scaling was less than 2% in all cases. Both the primary and normalized correlation and covariance matrices are presented to the user at `nucleardata.berkeley.edu/FYCoM`.

4.2.2 Cumulative Yields

Correlation and covariance matrices can be generated for cumulative yields using the covariance matrices generated for the independent yields. In order to do this, the transformation of independent yields into a given cumulative yield must be known. Evaluations make specific adjustments to these transformations. For example, the ENDF/B-VIII.0 evaluation obtained cumulative yields from independent yields by taking a weighted average of two different methods [86]. Replicating these adjustments would enhance the consistency of this method with the evaluations, however, a full tabulation of these specific adjustments is not readily available. Instead, this method transformed the independent yields to cumulative yields directly using evaluated decay data. The cumulative yields were obtained by calculating the probability that an independent product will follow a decay path leading to a cumulative product using Eq. 4.8:

$$Y_C(Z,A) = \sum_i \left[Y_I(Z_i, A_i) \prod_{k=1}^{i} \beta_{k\rightarrow k+1} \right] \tag{4.8}$$

where $Y_C(Z,A)$ is the cumulative yield being calculated, $Y_I(Z_i,A_i)$ are the independent yields that contribute to the cumulative yield, and $\prod_{k=1}^{i}\beta_{k\rightarrow k+1}$ represents the probability that product (Z_i,A_i) follows a decay path to product (Z,A) where each $\beta_{k\rightarrow k+1}$ is the decay branching ratio of the k^{th} product into the $(k+1)^{th}$ product in the decay chain.

The decay chains required for Eq. 4.8 are generated using the Fission Induced Electromagnetic Response code (FIER) [176]. The decay chains generated by FIER include all possible

decay paths for each fission product. FIER also provides a table of decay branching ratios parsed from ENDF/B-VIII.0 File 8 [28]. The independent yields are statistically resampled about a multivariate normal distribution using their evaluated values and their covariance matrices generated from the process in Sec. 4.2.1. Cumulative yields are then calculated from these resampled independent yields using Eq. 4.8. This is repeated N times such that statistical noise is minimized and the correlation and covariance matrices are calculated from the resulting N trials. In this study, $N = 10000$ was used to produce the presented matrices.

It was again seen that the covariance matrices that result from this process exhibit variances that are larger than those of the evaluated variances in the cumulative yields. This is because the cumulative yield covariance matrices are generated from the primary independent yield covariance matrix. Evaluated independent yields generally have larger evaluated uncertainties than cumulative yields and, as mentioned in Sec 4.2.1, the primary independent yield covariance matrix has larger variances than the evaluation. Therefore, a normalized cumulative yield covariance matrix is also produced using the correlation matrix and the evaluated variances in the cumulative yields. This normalized covariance matrix is simply the product of the correlation matrix and the evaluated uncertainties. Both the primary and normalized cumulative yield covariance matrices are presented to the user at `nucleardata.berkeley.edu/FYCoM`.

4.2.3 Generation of Consistent $P(\nu, A)$ Data

Neither the ENDF/B-VIII.0 nor JEFF-3.3 evaluations enforced consistency between fission neutron multiplicity distributions and independent fission yields. Because of this, there is no evaluated or experimental dataset that gives $P(\nu, A)$ values that are fully consistent with the independent yields in the evaluation, nor is there complete $P(\nu, A)$ data that cover all of the compound systems in the evaluation. In order to address this issue, a procedure was developed to obtain $P(\nu, A)$ data that have the greatest degree of consistency possible with evaluated yields. Perfect consistency would be achieved if each independent fission yield in the library could be reproduced using Eq. 4.7. This is the basis for the χ^2 metric in Eq. 4.9 which judges the consistency between evaluated independent fission yields and those generated using $P(\nu, A)$ data and Eq. 4.7; perfect consistency would result in $\chi^2 = 0$.

$$\chi^2 = \sum_i \frac{[Y_{eval}(Z_i, A) - Y_{gen}(Z_i, A)]^2}{Y_{eval}(Z_i, A)} \tag{4.9}$$

where Y_{eval} are the evaluated independent yields in a given A chain and Y_{gen} are those same yields that are generated using $P(\nu, A)$ data using Eq. 4.7.

The χ^2 metric in Eq. 4.9 was minimized for each A chain in each of the fissioning systems in the evaluations in order to generate a set of $P(\nu, A)$ data for use in the method presented in Sec. 4.2.1. An example of this minimization technique is shown in Fig. 4.1 which shows

the result of minimizing χ^2 in Eq. 4.9 to obtain $P(\nu, A)$ data for the $A = 135$ chain of the ^{235}U fast fission ENDF/B-VIII.0 evaluation.

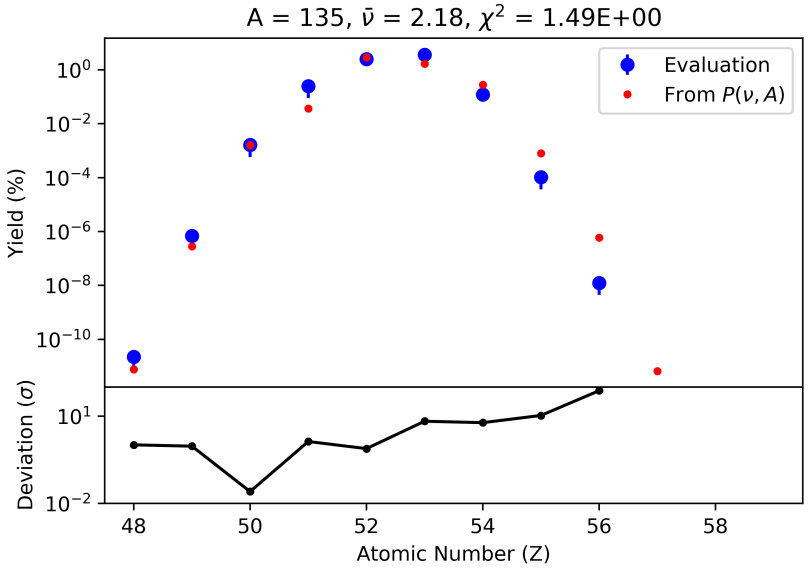

Figure 4.1: Result of the minimization of χ^2 in Eq. 4.9 for the $A = 135$ chain of the ^{235}U fast fission ENDF/B-VIII.0 evaluation. The blue data are the evaluated yields and the red data are yields generated using Eq. 4.7 and $P(\nu, A)$ data that minimized Eq. 4.9.

In order to conserve mass, $P(\nu, A)$ should ideally obey the physical condition that $P(\nu, A) = P(\nu, A_{CN} - A - \nu)$. An attempt was made to introduce a term to minimize the differences between $P(\nu, A)$ and $P(\nu, A_{CN} - A - \nu)$ in Eq. 4.9, however, this introduction made the minimization of Eq. 4.9 intractable. An iterative normalization method was developed in an attempt to force $P(\nu, A) = P(\nu, A_{CN} - A - \nu)$, however, this resulted in the χ^2 metric becoming unacceptably large. Future work could include attempts to improve the minimization method and metric such that $P(\nu, A) = P(\nu, A_{CN} - A - \nu)$ is met.

It should again be noted that inconsistency between the evaluated yields and those generated using the $P(\nu, A)$ data results directly from the evaluation itself and the fact that it did not take fission neutron multiplicity data into consideration. This inconsistency has been previously noted by Jaffke et al. [94]. These $P(\nu, A)$ data are generated to mitigate the effects of this inconsistency on the method presented in Sec. 4.2.1. An example of how these generated $P(\nu, A)$ data improve this method is presented in Fig. 4.2. It can be seen that a simplistic choice of $P(\nu)$ creates a bimodal distribution when resampling fission yields: one peak is seen when the heavy side of the fission product distribution is chosen in Step 1 of the method and another when the light side is chosen. Using these generated $P(\nu, A)$ data

yield much-improved results.

The use of these generated $P(\nu, A)$ data for other applications is not recommended. Certainly ensuring consistency between fission neutron multiplicity data and independent fission yields would add to the complexity of an evaluation and may very well be impractical. Future evaluations could attempt to address this by reporting "event" yields rather than independent yields. The "event" yields would report the probability that a given pair of fission products and number of prompt fission neutrons are produced from a given fission event.

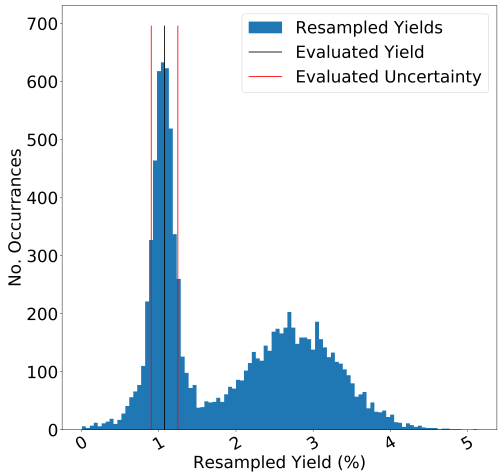

(a) The independent yield of ^{132}Te resampled 10000 times using this method. Here the choice of the $P(\nu)$ distribution used in the method was an A-independent distribution for ^{235}U(n,f) taken from Ref. [177].

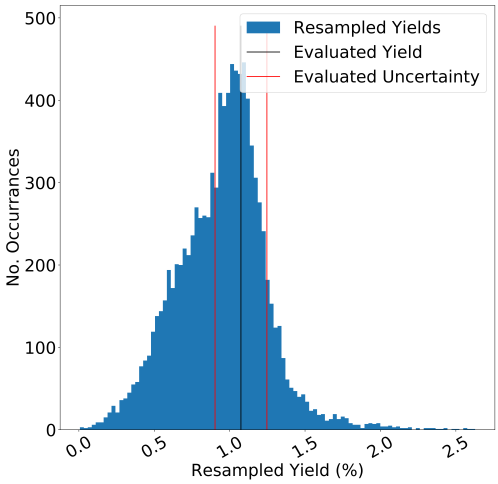

(b) The independent yield of ^{132}Te resampled 10000 times using this method. Here the $P(\nu, A)$ distributions used in the method are the generated distributions described in Sec. 4.2.3.

Figure 4.2: Histograms of resampled yields for ^{132}Te with different choices of $P(\nu, A)$. Each histogram contains 10000 entries. The evaluated yields are shown at the black line, banded by red lines representing the evaluated uncertainty of that yield.

4.2.4 Limitations and Benchmarking

This method is able to capture fission yield correlations within a given A chain through Step 3 and correlations between complementary fission products through the use of $P(\nu, A)$ data in Step 5. However, this method does not fully capture correlations between A chains on the same side of the fission product distribution. This is because those yields are resampled independently of each other. As a result of this deficit, the correlations calculated using

this method are expected to be somewhat underestimated.

Without an underlying model of fission, it is difficult to conceive how these correlations would be introduced. This method should be viewed as complementary to the model-based methods mentioned in Sec. 4.1. Where this method offers the capability to focus on correlations from the evaluation itself, model-based methods offer the ability to see physical correlations, such as those existing between A chains.

In order to assess the efficacy of the method and the effect of the limitations that are acknowledged above, a benchmarking of the method was performed with a model of mass yields. This simple model is detailed in Eq. 4.10 and consists of two Gaussians, one for the heavy peak and one for the light peak of the fission product distribution.

$$Y(A) = \frac{1}{\sqrt{2\pi}} e^{(A-\mu)^2/2\sigma^2} + \frac{1}{\sqrt{2\pi}} e^{(A-(A_{CN}-\mu-\bar{\nu}))^2/2\sigma^2} \tag{4.10}$$

where μ is the centroid of the heavy-product Gaussian, A_{CN} is the mass of the compound nucleus, $\bar{\nu}$ is the average neutron multiplicity of the fissioning system, and σ is the width of both Gaussians.

The neutron multiplicity distribution in this model was set to be a Poisson distribution with a mean of 2.0 for each mass number. This ensures the important condition discussed in Sec. 4.2.3 that $P(\nu, A) = P(\nu, A_{CN} - A - \nu)$ is met.

This model of fission has three parameters: μ, σ, and $\bar{\nu}$. Reasonable selections for the values of these three parameters are $\mu = 132 \pm 0.5$, $\sigma = 5 \pm 0.1$, and $\bar{\nu} = 2.0 \pm 0.1$. Using the model in Eq. 4.10, the mass yields for each A were calculated. A Monte-Carlo resampling of the covariances between the mass yields was then performed: the model parameters were varied about their uncertainties 10000 times, the mass yields were recalculated on each of these trials, and the correlations between the mass yields were assessed from these trial results. Figure 4.3 shows the correlation matrix between the mass yields calculated from the model given in Eq. 4.10.

To benchmark the efficacy of the method presented, the yields from Eq. 4.10 were input to the method to see if their known correlations could be reproduced. In the first test, Step 3 was modified such that the mass yields on the selected side of the fission product distribution were varied using their respective half of the correlation matrix shown in Fig. 4.3. This was done because of the above-stated limitation that correlations between mass chains are underestimated. By using half of the model correlation matrix in this test, this known limitation is compensated for, thus offering a more direct comparison for benchmarking. The correlation matrix that results from this test is shown in Fig. 4.4 and the difference between this correlation matrix and the model correlation matrix is shown in Fig. 4.5. The average

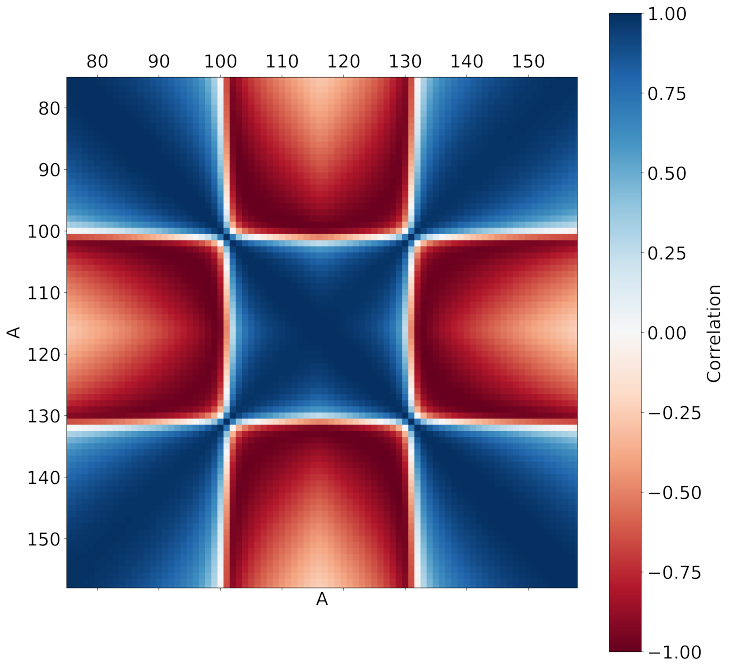

Figure 4.3: Correlations between the mass yields calculated from the model given by Eq. 4.10.

absolute difference between the model correlations and these correlations was 9%.

In the second test, the method was not modified as in the first test; the model yields and their uncertainties were input to the method without any prior knowledge of their correlations. This reflects the same situation as when the evaluated yields are used: only their uncertainties are known, not their correlations. In this test, it is expected that the correlations will be underestimated due to the above-stated limitation that correlations between mass chains are underestimated. The correlation matrix that results from this test is shown in Fig. 4.6 and the difference between this correlation matrix and the model correlation matrix is shown in Fig. 4.7. The average absolute difference between the model correlations and these correlations was 18%. On average, the correlations from the method were 15% less than those of the model, reflecting the known limitation of the method.

This benchmarking demonstrates the overall efficacy of this method. The first test demonstrates that the method is able to reproduce known model correlations. The second test demonstrates the limitation of the method. It shows that while the known limitation is non-trivial, it is still reasonably small for a first-order estimate of fission yield correlations.

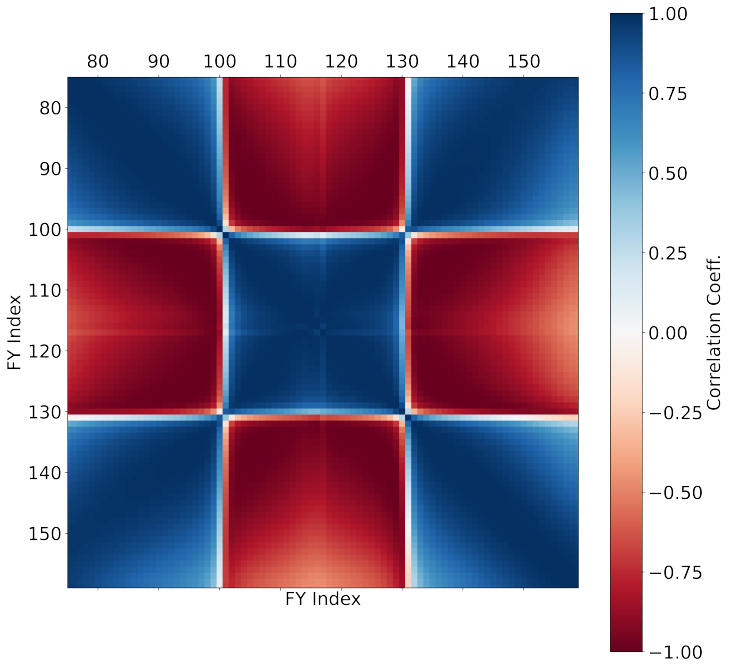

Figure 4.4: Correlations between the mass yields generated from this method with resampling of half the model correlation matrix (Fig. 4.3).

4.3 Results

Figure 4.8 shows the independent fission yield correlation matrix that was calculated for fast fission of ^{235}U from the ENDF/B-VIII.0 evaluation. Both positive and negative correlations can be seen and indeed the diagonal is identically one. Figure 4.9 shows a more illustrative subset of these data; it shows the covariance between the independent yield of ^{135}Te and those of other fission products as a function of Z and A. A number of expected trends can be seen in this figure. First, the yields along the $A = 135$ axis are all positively correlated; this is expected as the method varies all yields in a given A chain in tandem. Second, this positive correlation is reflected strongly along the $A = 99$ axis; this is expected as this A chain corresponds to the most probable complementary mass number for the $A = 135$ chain, $A_{CN} - A - 2$. Finally, negative covariance can be seen surrounding each voxel of strong positive covariance along each Z axis. For example, the $Z = 39$ axis features positive covariance at $A = 98$ and $A = 99$ with all other A on that axis exhibiting negative covariance. This is expected in order to conserve the normalization of $P(\nu, A)$ distributions; if the yield to one complementary product in the $P(\nu, A)$ distribution is increased the yield to other

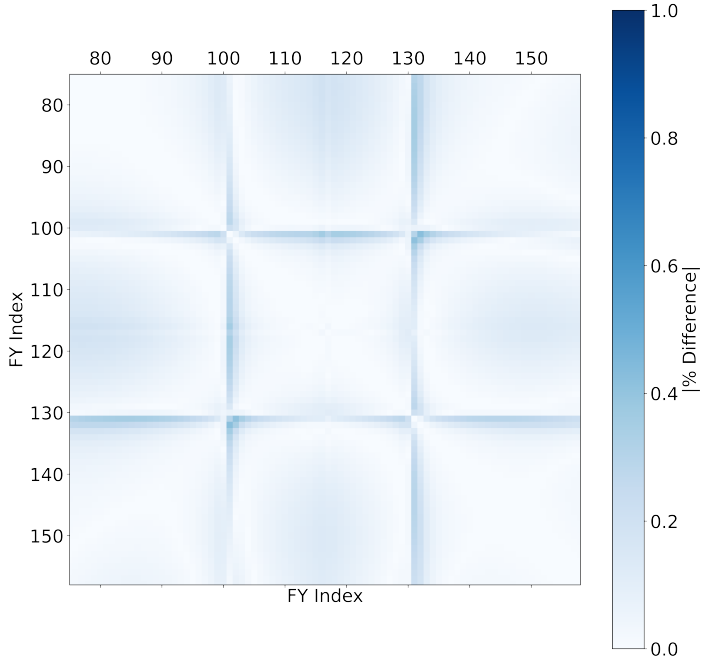

Figure 4.5: Comparison between the model correlation (Fig. 4.3) and method correlation (Fig. 4.4).

complementary products must be decreased.

Because this method does not require an underlying model of fission, it is able to be applied to any fission yield library with uncertainties. This method was successfully applied to all of the target nuclei and energy groups in the ENDF/B-VIII.0 and JEFF-3.3 evaluations. Table 4.1 lists the systems to which this method was applied.

4.4 Conclusions

The method presented in Sec. 4.2 has been applied to all compound systems in the current ENDF/B-VIII.0 and JEFF-3.3 evaluations to produce independent and cumulative yield correlation and covariance matrices. This method has been benchmarked and code to generate the consistent $P(\nu, A)$ data and calculate these matrices has been preserved in Ref. [158] as an annotated reproducible workflow. In addition to this, these matrices have been published online at `nucleardata.berkeley.edu/FYCoM`, making them available for immediate

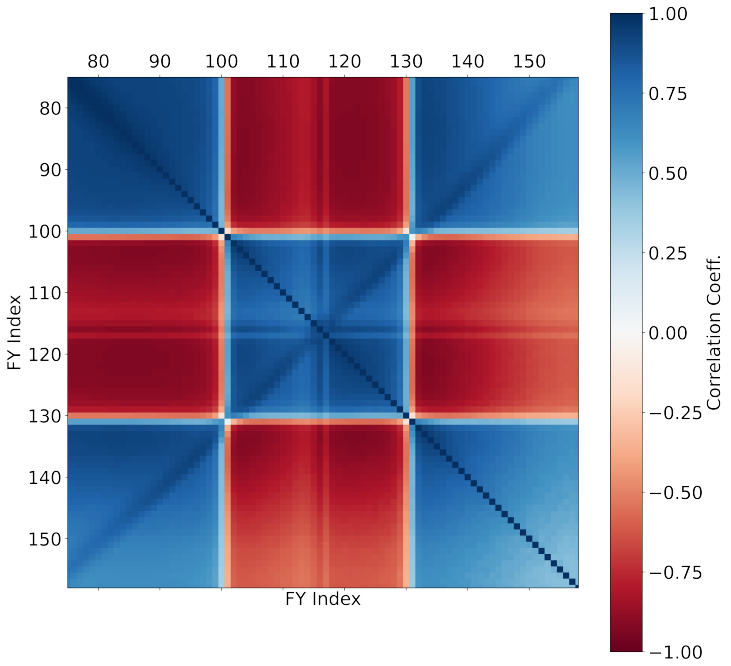

Figure 4.6: Correlations between the mass yields generated from this method (without modifications to the method).

use in applications and calculations by the nuclear science community. This marks the first time that correlation and covariance matrices have been produced for both the independent and cumulative fission product yields for all of the fissioning systems in the ENDF/B-VIII.0 and JEFF-3.3 evaluations. The presented matrices offer a first-order estimate of correlation/covariance between evaluated fission yields and serve as an interim solution until a new evaluation with a full treatment of these correlations and covariances is conducted.

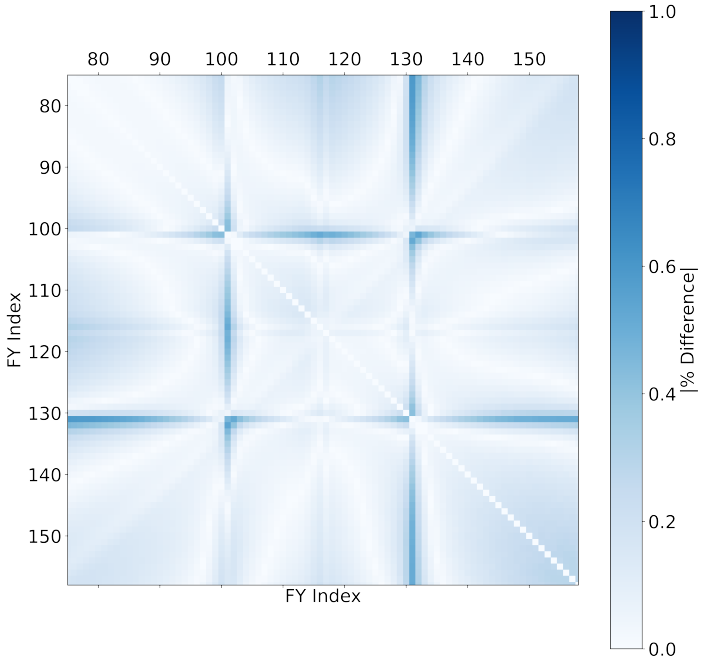

Figure 4.7: Comparison between the model correlation (Fig. 4.3) and method correlation (Fig. 4.6).

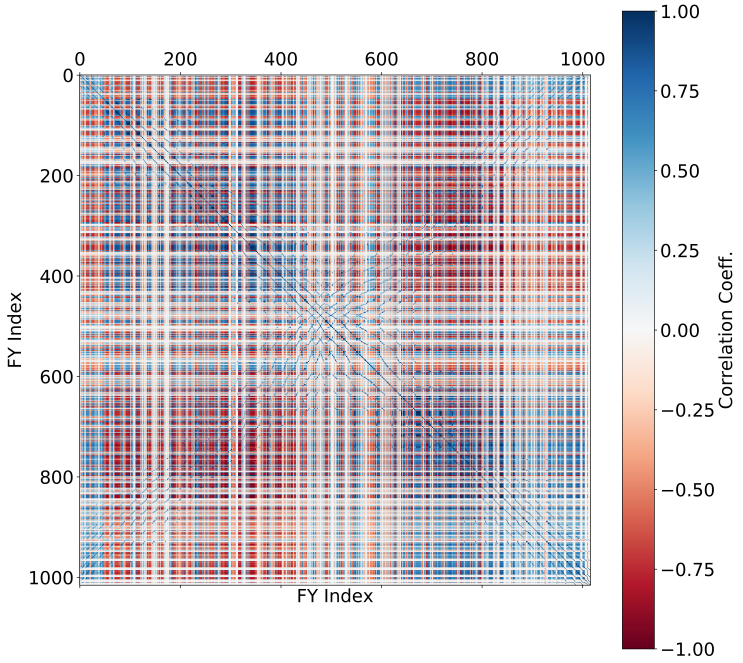

Figure 4.8: The primary correlation matrix for the independent fission yields of the ^{235}U fast fission ENDF/B-VIII.0 evaluation. "FY Index" is an index assigned to each fission product and is sorted by atomic number, mass number, and isomeric number in descending order. Thus FY Index 0 has the heaviest Z and A while FY Index 1016 has the lightest Z and A.

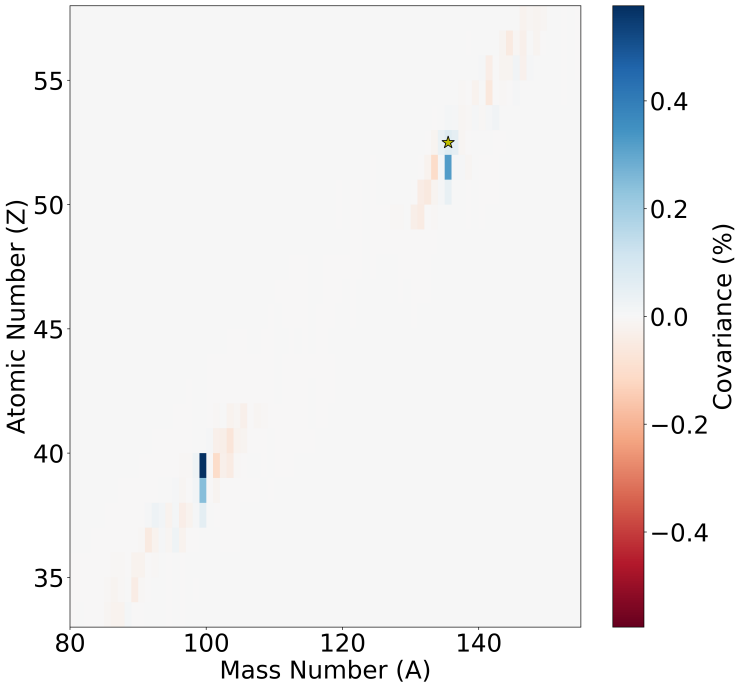

Figure 4.9: A plot of the covariance between the independent yield of ^{135}Te and those of other fission products as a function of Z and A for the ^{235}U fast fission ENDF/B-VIII.0 evaluation.

	ENDF/B-VIII.0	**JEFF-3.3**
Compound System	**Energy Group**	
^{227}Th	thermal	
^{229}Th	thermal	
^{232}Th	fast DT neutrons (14 MeV)	fast DT neutrons (14 MeV)
^{231}Pa	fast	
^{232}U	thermal	
^{233}U	thermal fast DT neutrons (14 MeV)	thermal fast DT neutrons (14 MeV)
^{234}U	fast DT neutrons (14 MeV)	fast
^{235}U	thermal fast DT neutrons (14 MeV)	thermal fast DT neutrons (14 MeV)
^{236}U	fast DT neutrons (14 MeV)	fast
^{237}U	fast	
^{238}U	fast DT neutrons (14 MeV) spontaneous fission	fast DT neutrons (14 MeV)
^{237}Np	thermal fast DT neutrons (14 MeV)	thermal fast
^{238}Np	fast	thermal fast
^{238}Pu	fast	thermal fast
^{239}Pu	thermal fast DD neutrons (2 MeV) DT neutrons (14 MeV)	thermal fast
^{240}Pu	thermal fast DT neutrons (14 MeV)	fast
^{241}Pu	thermal fast	thermal fast
^{242}Pu	thermal fast DT neutrons (14 MeV)	fast
^{241}Am	thermal fast DT neutrons (14 MeV)	thermal fast
^{242m}Am	thermal	thermal fast
^{243}Am	fast	thermal fast
^{242}Cm	fast	spontaneous fission
^{243}Cm	thermal fast	thermal fast
^{244}Cm	fast spontaneous fission	thermal fast spontaneous fission
^{245}Cm	thermal	thermal fast
^{246}Cm	fast spontaneous fission	
^{248}Cm	fast spontaneous fission	
^{249}Cf	thermal	
^{250}Cf	spontaneous fission	
^{251}Cf	thermal	
^{252}Cf	spontaneous fission	spontaneous fission
^{253}Es	spontaneous fission	
^{254}Es	thermal	
^{254}Fm	spontaneous fission	
^{255}Fm	thermal	
^{256}Fm	spontaneous fission	

Table 4.1: The target nuclei and energy groups in the ENDF/B-VIII.0 and JEFF-3.3 evaluations. This method was successfully applied to all of the systems listed in this table.

Chapter 5

Short-lived Fission Product Yield Measurements Using the Fast Loading User Facility for Fission Yields

5.1 Introduction

This chapter will detail the construction, commissioning, and operation of FLUFFY and will detail some initial results from ^{238}U fission yield measurements using FLUFFY. As was discussed in Chapter 1, fission product yields are important to a wide variety of applications, yet they suffer from large uncertainties and gaps in knowledge. Chapter 4 presented a method to estimate fission yield covariances and Chapter 3 worked to assist the standardization of future fission yield evaluations. This chapter will detail experimental efforts to make improved measurements of fission yields, particularly those of short-lived fission products. This new measurement of fission product yields offers additional information that contributes to the current understanding of fission product yields through experimentation.

In recent years, cyclical neutron activation analysis (CNAA) has been identified as a particularly powerful technique by which to measure short-lived fission product yields [105, 106]. In CNAA, an actinide target is repeatedly and rapidly transported between a γ-ray detection apparatus and a neutron source. Generally, the irradiation period is short (seconds to tens of seconds) and the subsequent counting period is long (tens of seconds to minutes), allowing for saturation of short-lived activities while mitigating the build-up of intermediate- to long-lived fission products. To facilitate new CNAA fission yield measurements, FLUFFY was constructed at the 88-Inch Cyclotron at Lawrence Berkeley National Laboratory (LBNL).

This chapter will first detail the design and construction of FLUFFY, offering insight about the quantities that it is tailored to measure and the experimental data that it produces. Results from the measurement of ^{238}U(n,f) fission yields using FLUFFY are then

presented. During this presentation, a new method for fission yield determination using the FIER code is described. Together with the results of the measurement itself, this information advances the current state of experimental fission yield data.

5.2 Design and Construction

FLUFFY is a pneumatic system that shuttles a high-density polyethylene capsule between a high-purity germanium (HPGe) detector array and a high-intensity deuteron breakup neutron source. Construction of FLUFFY began in early 2019 at the 88-Inch Cyclotron at LBNL. FLUFFY is located at the high-radiation level cave ("Cave 0") of the 88-Inch Cyclotron (shown in Fig. 5.1). This cave was selected because capabilities for neutron production via deuteron breakup have been extensively developed there and because the concrete shielding of the cave features a cable porthole through which the FLUFFY pneumatic tube was placed. The thick concrete shielding of Cave 0 is useful for shielding the HPGe detector array from neutron damage while the neutron beam is on and for reducing backgrounds from activation products of the neutron beam.

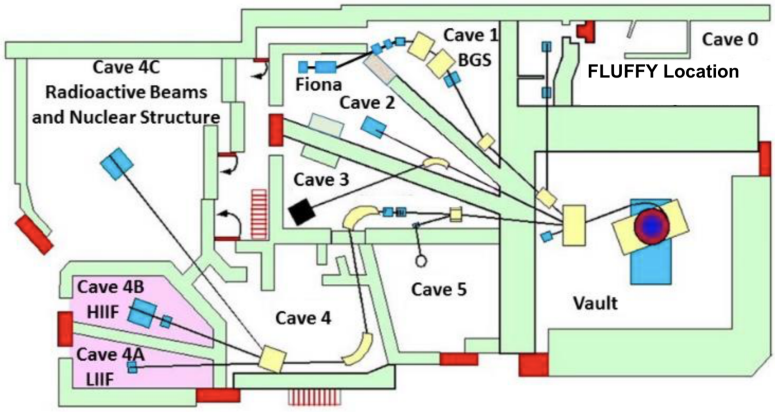

Figure 5.1: Schematic of the 88-Inch Cyclotron at Lawrence Berkeley National Laboratory. FLUFFY was constructed in Cave 0, which is shown in the upper right-hand corner of this figure. This figure was modified from the publication "The 88-Inch Cyclotron: A One-Stop Facility for Electronics Radiation and Detector Testing" by M. Kireeff Covo et al. [178]

FLUFFY, the neutron source, and the detection array it uses are shown in Fig. 5.2. The neutron source used in FLUFFY experiments is a high-purity graphite deuteron breakup target. A deuteron beam is extracted from the 88-Inch Cyclotron, directed to Cave 0 by a bending magnet, and impinges on the 6-mm thick graphite target that is located in a beam box at the end of the beam pipe. Deuteron breakup produces a forward-focused neutron beam that is incident upon the beam-side end of the FLUFFY pneumatic tube. The location

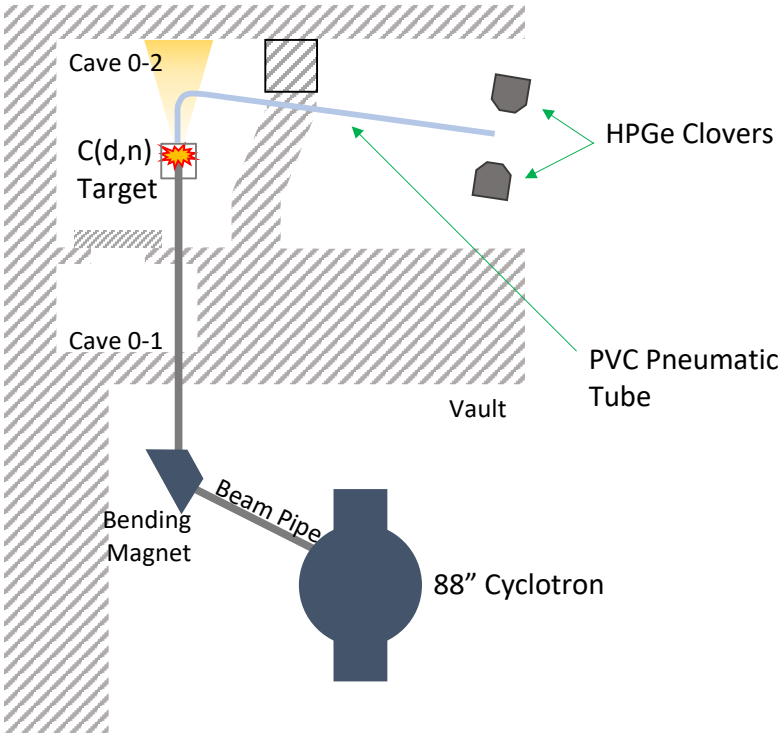

Figure 5.2: Schematic of FLUFFY within Cave 0 of the 88-Inch Cyclotron at Lawrence Berkeley National Laboratory.

of the actinide sample inside of the capsule is 17 cm back from the graphite target, a solid angle coverage of 0.013 steradians, spanning $\pm 1.8°$. Further details on the characterization of the energy spectrum of the neutron beam using a neutron time-of-flight measurement and foil-pack spectral adjustment are presented in Sec. 5.3.3.

The detector array used by FLUFFY consists of two segmented HPGe "clover" detectors with accompanying 16-segment BGO Compton-suppression shields. Figure 5.3 shows a 3-D model of the detector end of FLUFFY. The clovers were each set back approximately 20 cm from the location of the target inside of the capsule. This was done both to accommodate the incoming bend of the FLUFFY tube and to eliminate coincidence summing. The signals from the HPGe clovers and BGO shields were read by a data acquisition system (DAQ) based on the Mesytec MDPP16 digitizer [179]. This DAQ records filtered detector signals and timestamps for the logic signals produced by the capsule-positioning lasers, allowing for precise tracking of the capsule location as a function of time.

The FLUFFY pneumatic tube is constructed of transparent PVC tubing. This tubing was selected so that the capsule can be quickly located in the event that it jams. The joints of the tube were fitted with 3D-printed rings to fill the gap that was present at each cou-

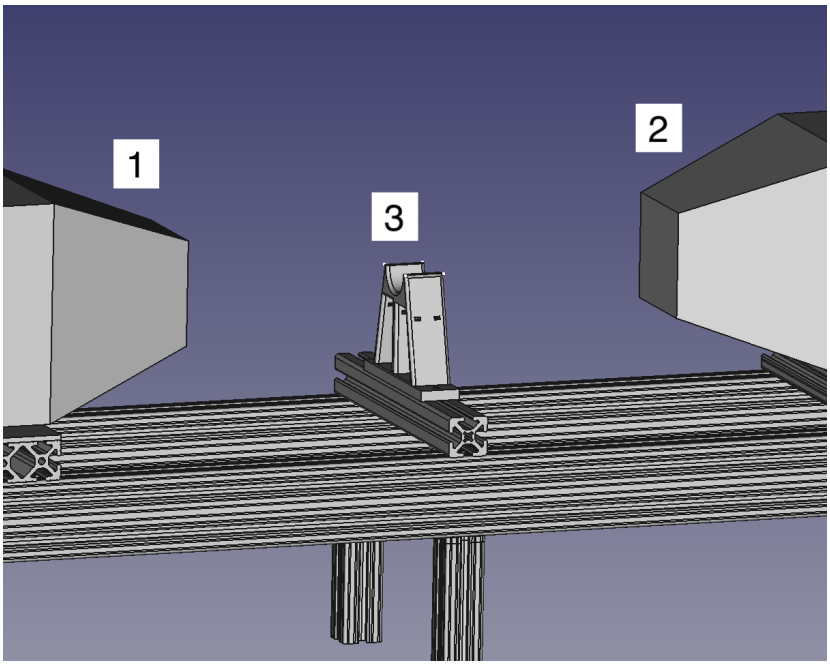

Figure 5.3: Three-dimensional model of the HPGe clover array used in FLUFFY. Labels 1 and 2 show the locations of the HPGe clovers, which are supported by an aluminum frame. Label 3 shows the cuff that holds one end of the FLUFFY pneumatic tube (not shown). When the capsule is at rest, the target is located in the middle of the cuff. Figure courtesy of Dr. Joshua Brown of the University of California, Berkeley.

pling; this prevents clipping and catching of the capsule. Each end of the pneumatic tube was connected to two solenoids: one for input air pressure and one for air pressure outlet. A 3D-printed cuff was placed at each end of the tube. This cuff held a laser-photodiode pair. When the capsule reaches the end of the tube, it breaks the laser beam into the photodiode, creating a readable electronic signal indicating that the capsule is at one end of the tube.

The capsule that is transported through the FLUFFY pneumatic tube is made of high-density polyethylene (HDPE). This material was chosen due to its high mechanical durability and resistance to fracture. This is important because the capsule is not slowed before stopping against each end of the pneumatic tube, and thus the capsule must be robust against repeated, sudden impacts (in this experiment the capsule experienced over 7000 impacts from 3659 cycles). The choice of HDPE has the added benefit of limiting backgrounds due to activation of the capsule material; HPDE is composed solely of C and H. The top end of the capsule screws on and contains a recess that can hold a foil with an 11 mm diameter and 1.25 mm thickness. Figure 5.4 shows the design of this capsule.

The 88-Inch Cyclotron is equipped with a beam chopper that can be rapidly ($<$10 μs)

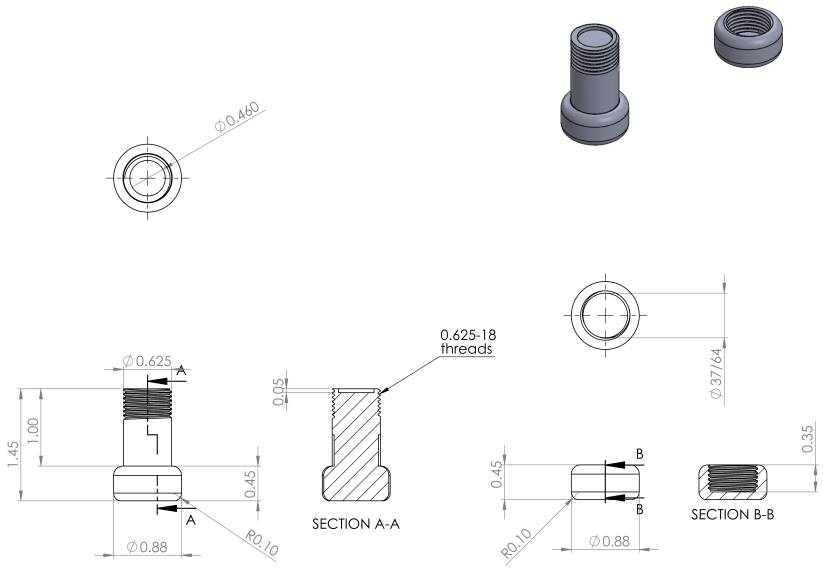

Figure 5.4: The design of the capsule used in the FLUFFY pneumatic tube. Figure courtesy of Dr. Jonathan Morrell of Los Alamos National Laboratory (formerly the University of California, Berkeley).

triggered/inhibited by a TTL logic signal [178]. This beam chopper is controlled by FLUFFY to turn the neutron beam off when the capsule is not present at the beam-side end of the pneumatic tube. This greatly reduces the γ background seen by the HPGe clover array while the capsule is being counted.

FLUFFY is controlled by a Raspberry-Pi single-board computer. The Raspberry-Pi is able to read/output 3.3 V logic signals on 18 pins. A short program reads input signals from the laser-photodiode pairs at each end of the pneumatic tube, outputs logic signals to the pressure/outlet solenoid to control the movement of the capsule, and outputs logic signals to the beam chopper to turn the neutron beam on and off. The program executes the following process:

1. Shuttle the capsule to the beam-side end of FLUFFY.
    a) Send high signals to open both the detector-side pressure solenoid and the beam-side outlet solenoid.
    b) Wait for the beam-side laser signal to read high, indicating the arrival of the capsule.
    c) Immediately send a high signal to the beam chopper to turn the beam on and start a countdown for the user-specified irradiation period.

d) Send a low signal to the detector-side pressure solenoid to close it. Wait 100 ms and send a low signal to the beam-side outlet solenoid to close it (this delay prevents excess tube pressure).

e) After the countdown is complete, send a low signal to the beam chopper to turn the beam off.

2. Shuttle the capsule to the detector-side end of FLUFFY.

a) Send high signals to open both the beam-side pressure solenoid and the detector-side outlet solenoid.

b) Wait for the detector-side laser signal to read high, indicating the arrival of the capsule.

c) Start a countdown for the user-specified counting period.

d) Send a low signal to the beam-side pressure solenoid to close it. Wait 100 ms and send a low signal to the detector-side outlet solenoid to close it.

e) After the countdown is complete, if the user has not terminated the program, return to Step 1.

5.3 Measurement of ^{238}U Fission Yields

A series of experiments to measure fission yields on ^{238}U using FLUFFY were conducted between July 20-26, 2020. In these experiments, a 455.3 $\pm$ 0.5 mg highly-enriched ^{238}U sample was irradiated. First, a 24-hour irradiation comprised of cycles of 1 s of irradiation followed by 25 s of counting ("1 s–25 s") was conducted. This timing scheme was chosen to maximize the visibility of the shortest-lived ($t_{1/2} < 2$ s) fission products in the resulting fission product γ-ray spectrum. Next, a 24-hour irradiation comprised of cycles of 5 s of irradiation followed by 125 s of counting ("5 s–125 s") was conducted. This timing scheme was chosen to maximize the visibility of short-lived (2 s $< t_{1/2} <$ 10+ s) fission products in the resulting fission product γ-ray spectrum. Both the 1 s–25 s scheme and the 5 s–125 s scheme featured a 1:25 duty cycle to allow for significant decay of intermediate-half-life fission products between each cycle.

The lengths of the 1 s and 5 s irradiation periods maximized sensitivity to the shortest-lived fission products in each mass chain. Approximately 80% of the independent yield to a given mass chain occurs in fission products with half-lives less than a few tens of seconds (see Figs. 5.14, 5.15, 5.16, and 5.17). This is because fission minimizes the total nuclear binding energy by favoring the formation of fragments with a Z/A ratio similar to the compound system. This tends to lead to the production of neutron-rich fission fragments with high Q_{β^-} and half-lives on the order of a few seconds. In contrast, longer-lived lower Q_{β^-} products are more likely to be the product of the β-decay rather than directly formed in the fission

process itself.

It should be noted that measurements conducted using FLUFFY and its deuteron breakup source are energy-integral measurements, not energy-differential measurements. While energy-differential measurements are useful in assessing the energy dependence of fission yields, the high fluxes produced by deuteron breakup paired with the rapid transport times of FLUFFY maximize sensitivity to short-lived fission yields with short irradiation periods and long counting/decay periods. It is this sensitivity that allows for approximately 80% of the independent yield to a given mass chain to be measured. This is the value these measurements provide to future fission yield evaluations. Additionally, these measurements may also serve as an integral benchmark once energy-differential data are produced [106].

The ^{238}U target was co-loaded with a high-purity synthetic sapphire (Al_2O_3) disc. The mass of the disc was 391.4 $\pm$ 0.5 mg. This sapphire disc provided an *in situ* neutron flux monitor with the ^{27}Al(n,α) and ^{27}Al(n,p) reactions together with a high energy calibration via the observation of the 6128.63-keV and 7115.15-keV γ rays that result from the decay of ^{16}N produced in the ^{16}O(n,p) reaction.

The detector array used in the experiment consisted of two HPGe clover detectors each surrounded by a bismuth germanate (BGO) scintillator. The HPGe crystals in the clover detectors were used to detect the energy of the γ emissions from the fission products with high energy resolution. The primary purpose of the BGO detectors was to provide active Compton suppression capabilities (further discussed in Sec. 5.3.1). The BGO detectors also provided a monitor of the cycle-by-cycle flux that was incident on the target. Because of their high detection efficiency, the count rate of the BGO shields during irradiation was used to monitor prompt γ rays produced during deuteron breakup and secondary reactions between the neutrons and the environment. This information, together with the timestamps from the laser positioning system, allowed for a full reconstruction of the irradiation scheme of the experiment. A fully detailed account of the irradiation scheme for the ^{238}U target used in this experiment is given in Appendix B as a formatted input deck for FIER. Figure 5.5 shows a graphical representation of this irradiation scheme. The average transport time for the capsule from the neutron source to the HPGe detector array was 1.22 s.

In addition to the irradiation of the ^{238}U target, a neutron time-of-flight (nTOF) irradiation and a foil-pack irradiation were conducted. The purpose of these two irradiations was to determine the neutron energy spectrum from the graphite deuteron breakup source. The nTOF irradiation used an EJ-309 scintillator [180] with a 1"$\times$1" right cylindrical geometry to measure the time-of-flight of neutrons from each cyclotron pulse. The activation analysis irradiated foils of natural abundance Au, Al, V, Zr, and In. The activation information from reactions on these foils was input to the spectral adjustment code STAYSL [108] with the nTOF spectrum as an initial guess. The details of this neutron energy spectrum characterization are further detailed in Sec. 5.3.3.

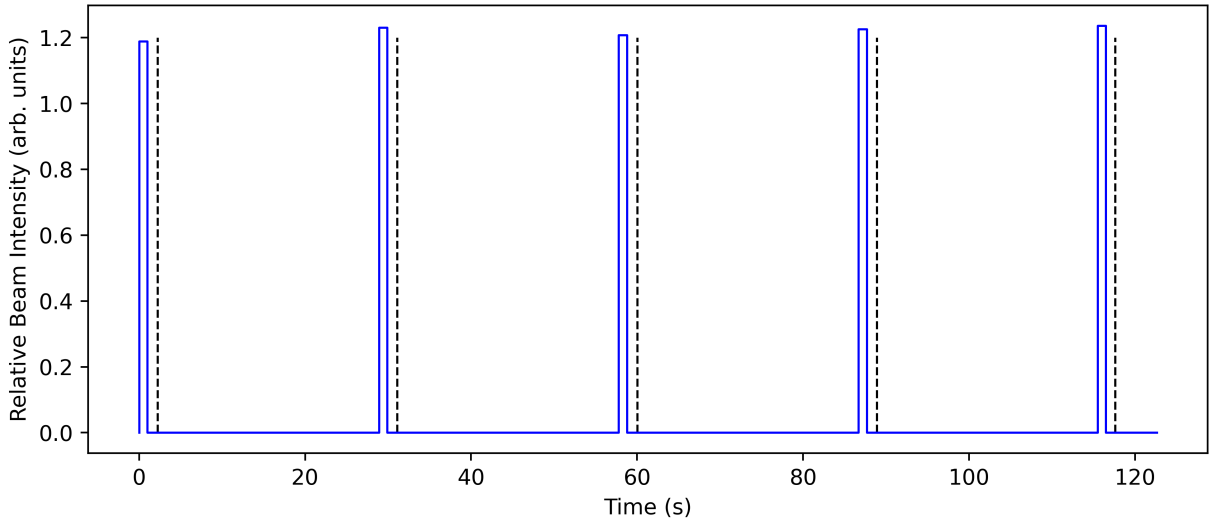

Figure 5.5: Graphical representation of the first five cycles of the 1 s–25 s irradiation scheme. The dashed lines represent the time at which the capsule returned to the HPGe array, illustrating the transport time for each cycle.

5.3.1 Gamma-ray Spectral Data Processing

Data parsing and processing software was collaboratively written with Dr. Joshua Brown of the University of California, Berkeley. This software reads the raw output of the aforementioned Mesytec MDPP16 DAQ and reduces that data to γ-ray spectra stored in ROOT TTree data files [181]. This software performs two processes: add-back between the crystals of each clover and Compton suppression using the BGO detector signals. These processes are detailed below:

Add-Back - When two or more signals are generated in different crystals of the same HPGe clover within a given timeframe, the energies of those signals are added together and reported as a single energy deposition event. This is performed to maximize the photopeak efficiency of each HPGe clover; γ rays that undergo multiple scatters but deposit their full energy in the HPGe crystals are reconstructed into one event that records the full energy of the γ-ray.

Compton Suppression - When one or more signals are generated in the crystals of an HPGe clover within a given timeframe of a signal in the surrounding BGO detector, the event is rejected. This constraint is applied to minimize the number of events in the spectrum that did not deposit the full energy of the γ ray in the HPGe crystals; if a BGO signal occurs

in coincidence with an HPGe signal, then it is likely the γ ray scattered and deposited a part of its energy in the BGO (which does not have sufficient energy resolution for add-back).

A ^{152}Eu source was used to obtain calibration constants for the add-back and Compton suppression processes. A γ-γ time-difference distribution was assembled for each HPGe crystal and the BGO detector of each clover. The centroid of the distribution was used as the time offset for each detector and the full width of the distribution was used to set the coincidence window for add-back and Compton suppression. Figure 5.6 shows an example fission product γ-ray spectrum from the 1 s– 25 s ^{238}U data with add-back and Compton suppression applied.

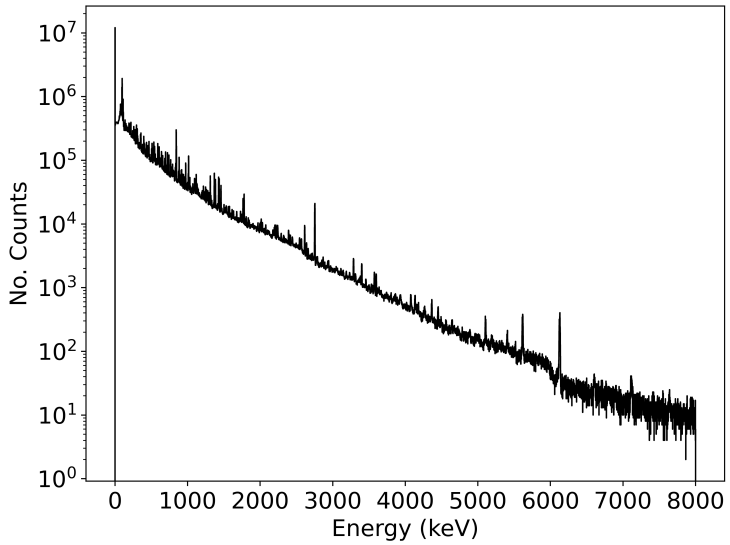

Figure 5.6: An example fission product γ-ray spectrum from the 1 s–25 s ^{238}U data. Particularly strong photopeaks from the decay of ^{16}N, ^{24}Na, and ^{27}Mg activation products formed in the co-loaded sapphire disc can be seen at 843.76 keV, 1368.626 keV, 2754.007 keV, 6128.63 keV, and 7115.15 keV.

5.3.2 Detector Array Calibration

The HPGe clover array used in FLUFFY was calibrated using two calibration sources designed to fit inside of the FLUFFY capsule so that their geometry would match that of the ^{238}U target. One calibration source was a custom-ordered, NIST-traceable ^{152}Eu source. This source has several strong γ-ray emissions up to 1408 keV.

The other calibration source was made at the 88-Inch Cyclotron by irradiating a natural Fe foil with protons to produce ^{56}Co via the ^{56}Fe(p,n) reaction. ^{56}Co offers the advantage of allowing high-energy γ efficiency calibrations due to its strong γ-ray emissions up to 3273 keV. The activity of ^{56}Co present in this source was determined by a cross-calibration with a NIST-traceable ^{60}Co source. The cross-calibration was performed with the ratio given in Eq. 5.1:

$$A_{Co56} = A_{Co60} \frac{I_{\gamma}^{1173} N_{1175}}{I_{\gamma}^{1175} N_{1173}} \tag{5.1}$$

where A_{Co56} is the activity of ^{56}Co that was produced, A_{Co60} is the activity of the ^{60}Co calibration source, I_{γ}^{1173} and I_{γ}^{1175} are the evaluated decay γ intensities for the 1173-keV γ from ^{60}Co and the 1175-keV γ from ^{56}Co, and N_{1173} and N_{1175} are the number of photopeak counts in 1173-keV and 1175-keV photopeaks, respectively.

Equation 5.1 is valid because the detection efficiency for the 1173-keV and 1175-keV photopeaks are nearly identical and thus an efficiency correction is not needed. The efficiencies for these two γ rays were determined to be within 0.1%.

In addition to the HPGe clover array that was used in FLUFFY, a different single-crystal HPGe detector was used for counting the foil pack and the sapphire monitor. This detector was calibrated with NIST-traceable ^{152}Eu, ^{133}Ba, ^{137}Cs, and ^{60}Co sources. Table 5.1 summarizes the calibration sources and activities used in the calibration of the HPGe detectors.

Table 5.1: Calibration sources used in the calibration of HPGe detectors used in this experiment.

Source	Activity (μCi)	Calibration Date
Clovers:		
^{152}Eu	10.56 ± 0.11	July 1, 2020
^{56}Co	1.65 ± 0.02	July 15, 2020
Single Crystal:		
^{152}Eu	1.033 ± 0.011	March 1, 2019
^{133}Ba	1.043 ± 0.011	March 1, 2019
^{137}Cs	0.9920 ± 0.0099	March 1, 2019
^{60}Co	1.041 ± 0.011	March 1, 2019

The energy calibrations of the HPGe detectors were fit using the linear form in Eq. 5.2:

$$E = B_0 + B_1 x \tag{5.2}$$

where E is the energy of the channel, x, and B_0 and B_1 are the parameters of the linear model. An energy calibration for each of the individual crystals of the HPGe clover array was obtained and these were used in the add-back stage of the γ-ray spectrum processing detailed in Sec. 5.3.1. Non-negligible non-linearities were observed in the energy calibrations for the HPGe clover crystals, making precise energy determination difficult for γ-rays with energies less than 800 keV. These non-linearities were not resolved with a quadratic calibration model. Therefore, the decision was made to remove calibration data points below 800 keV in the energy calibration of the HPGe clover leaves. This means those energy calibrations cannot be safely extrapolated below 800 keV. However, this is of limited consequence to the analysis of the data as fission product γ-ray spectra are often too crowded below 1 MeV to be successfully analyzed.

A single efficiency calibration for the HPGe clover array as a system was determined. The calibration γ-ray spectrum was reduced from the data using the same add-back and Compton suppression settings as were used for the fission product γ-ray spectra. The functional form used for the efficiency calibrations of the HPGe detectors is given in Eq. 5.3 which is modified from the form proposed in Ref. [182]:

$$\varepsilon(E_\gamma) = B_0 e^{-B_1 E_\gamma^{B_2}} \tag{5.3}$$

where $\varepsilon(E_\gamma)$ is the detection efficiency for a γ ray with energy E_γ, B_0, B_1, and B_2 are the parameters of the model, and E_γ is the energy of the incident γ ray. The parameters of this form were determined by fitting to the experimental data using the Differential Evolution heuristic global optimization algorithm [183] as implemented in the Scientific Python (SciPy) package [184]. The uncertainties and covariance in the parameters were determined by varying the experimental data 10000 times, refitting the parameters, and calculating the covariance matrix from the trial results. Figure 5.7 shows the net efficiency calibration for the HPGe clover array used in FLUFFY. Figure 5.8 shows the efficiency calibration for the single-crystal HPGe detector used for foil counting.

The Mesytec MDPP16 DAQ does not perform automatic detector dead-time recording. Therefore, a dead-time calibration was performed to determine if there was appreciable dead-time in the HPGe clover array system. A set of ^{137}Cs sources were counted in between the two HPGe clovers. Thirteen different permutations of these sources were counted, with net ^{137}Cs activities ranging from 0.96 μCi to 31.71 μCi. The net count rate for the HPGe clovers was measured for each permutation. These net count rate versus ^{137}Cs activity data were fit to the functional form given in Eq. 5.4. Equation 5.4 describes the theoretical count rate as a function of event rate for a system that is α% paralyzable and $(1-\alpha)$% non-paralyzable:

$$m = \alpha\Big(\frac{n}{n\tau + 1}\Big) + (1-\alpha)(n\ exp(-n\tau)) \tag{5.4}$$

where m is the observed count rate on the detector array, α is a coefficient describing how paralyzable the detection system is, τ is the dead-time of the detection system, and n is the

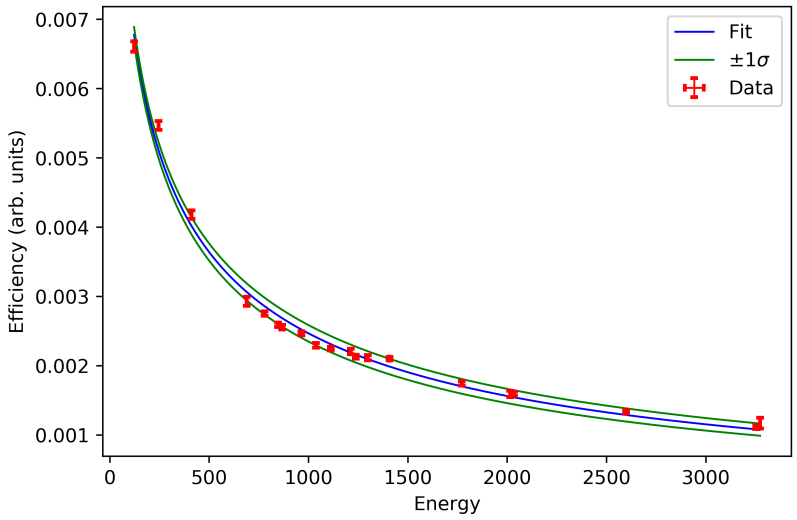

Figure 5.7: Net efficiency calibration for the HPGe clover array system used in FLUFFY.

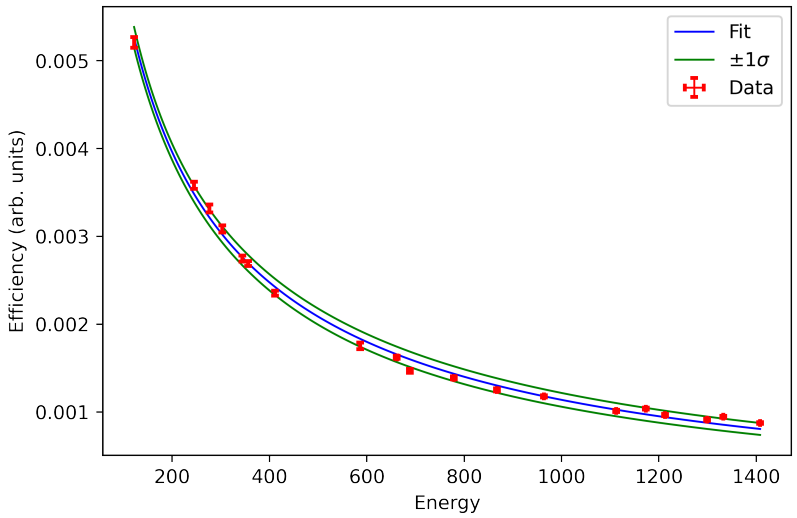

Figure 5.8: Efficiency calibration for the single-crystal HPGe detector used for foil counting.

event rate on the detector array, which is given by Eq. 5.5:

$$n = \varepsilon A + B \tag{5.5}$$

where A is the activity of the source being counted, ε is the net efficiency for detecting γ emissions from that source (both photopeak and Compton), and B is the background event rate of the environment. This model is based on the paralyzable and non-paralyzable models given in Ref. [185, p. 122].

The result of fitting these data is shown in Fig. 5.9. The optimal model parameters were determined to be: $\tau = 8$ μs, $\varepsilon = 0.0076$, $\alpha = 0.1$, and $B = 285$ counts/s. The fitted net detection efficiency for the 661.657-keV γ from ^{137}Cs is consistent with the efficiency curve determined for the HPGe clover system. However, there was limited sensitivity for the paralyzable coefficient, α. This is because the data did not extend to high enough activities to see the expected shape of either the paralyzable or non-paralyzable models. The activity of fission products produced during the FLUFFY irradiations was well below the highest activity measured in this dataset. Therefore, interpolation with this model should be reliable.

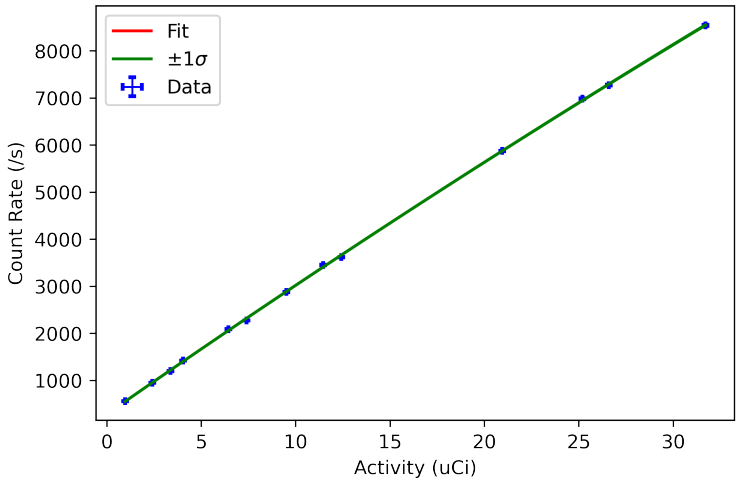

Figure 5.9: Count rate versus source activity on the HPGe clover array system. These data were fit using the functional form given in Eq. 5.4.

5.3.3 Neutron Energy Spectrum Characterization

To characterize the neutron energy spectrum that was incident upon the ^{238}U target, two experiments were conducted: a neutron time-of-flight (nTOF) measurement and a foil-pack activation measurement. These two measurements were performed to supply information about the incident neutron energy spectrum across the full energy range of interest. Single nTOF measurements are limited in the scope of their energy by the wraparound effect [186]. Due to the short flightpath in Cave 0, this nTOF measurement does not report neutron energies below 1.75 MeV. Foil pack activation allows for the measurement of the magnitude of the flux and can be used in spectral adjustment analysis codes such as STAYSL [108]. However, the spectral adjustment analysis in STAYSL requires a reasonable initial guess of the incident neutron energy spectrum. Together nTOF and foil pack activation can give an

estimate of the incident neutron energy spectrum; nTOF provides a reasonable initial guess of the incident neutron energy spectrum for spectral adjustment analysis using the foil-pack activation measurement results.

5.3.3.1 Neutron Time-of-Flight

To provide a measurement of the incident neutron energy spectrum in the energy region without wraparound effects, an nTOF measurement was conducted. An EJ-309 scintillator [180] with a 1"×1" right cylindrical geometry was placed 210.4 cm away from the location of interaction in the graphite deuteron breakup target. The scintillator was placed at 0° and was aligned using a laser leveling device. A 10 nA deuteron beam was run on the graphite deuteron breakup target for 30 minutes to enable the collection of an nTOF spectrum with sufficient statistics.

The same Mesytec MDPP16 module that was used for data acquisition on the HPGe clover arrays was used for the nTOF measurement. The charge-to-digital converter (QDC) settings of the module were used to perform pulse shape discrimination (PSD) on signals from the EJ-309 scintillator using the charge integration method [187] [185, p. 700]. The short integration time was set to 12.5 ns and the long integration time was set to 312.5 ns for the PSD.

An energy was calculated for each event with a PSD signature characteristic of a neutron using Eq. 5.6 for relativistic kinetic energy:

$$E_n = m_n c^2 \left(\sqrt{\frac{1}{1 - v^2/c^2}} - 1 \right) \tag{5.6}$$

where m_n is the rest mass of a neutron, c is the speed of light, and v is the measured velocity which is given by Eq. 5.7:

$$v = \frac{L}{t} \tag{5.7}$$

where L is the length of the neutron flight path and t is the measured time-of-flight for the neutron.

The measured neutron energies were histogrammed to obtain a raw neutron energy spectrum. This raw spectrum was then corrected with a simulated detector efficiency curve [188]. A GEANT4 simulation impinged neutrons with a uniform energy distribution on the detector volume. Each neutron in the simulation was tracked through the detector volume and recoil events were recorded. Using the light yield relation in Refs. [189, 190], the energy deposited by the recoiling particle in each recoil event was converted to a relative light

unit. The light produced by the individual recoil events was summed to give the total light produced by the neutron. A ^{137}Cs calibration spectrum was used to calibrate the experimental data to quantify a user-defined light detection threshold. This threshold was then applied to the simulation to reject low-light events that would not have been detectable in the experiment. The efficiency curve was then determined as the ratio of the number of neutrons of a given energy that were detectable over the number of neutrons of that energy that were impinged on the detector. The efficiency-corrected spectrum was used as the estimate of the incident neutron energy spectrum above 1.75 MeV, as shown in Fig. 5.10.

5.3.3.2 Foil Pack Activation

A foil pack containing thin foils of Au, Al, V, Zr, and In was irradiated for 8 hours, 11 minutes, and 58 seconds. These foils were 1 cm circular disks with varying thicknesses (which are specified in Table 5.2). The foils were placed inside the FLUFFY capsule and were shuttled into Cave 0 using FLUFFY. This was done so that the foil pack location matched that of the ^{238}U foil. Once the irradiation was complete, the foil pack was shuttled back out using FLUFFY and was rapidly transported to the single-crystal HPGe for assay; the counting of the foil began less than five minutes after the end of irradiation.

The photopeaks from the γ-ray signatures of each reaction product were fit to determine their net area. This net area was then used to determine the activity using Eq. 5.8:

$$A_0 = \frac{C(E_\gamma)\,\lambda}{I_\gamma \varepsilon(E_\gamma)\,(e^{-\lambda t_0} - e^{-\lambda t_1})} \tag{5.8}$$

where $C(E_\gamma)$ is the number of observed counts in the γ-ray spectrum for the γ-ray signature with energy E_γ, λ is the decay constant of the reaction product, I_γ is the decay γ intensity of the γ-ray signature, $\varepsilon(E_\gamma)$ is the detection efficiency for the γ-ray signature, t_0 is the time between the end of irradiation and the start of counting, and t_1 is the time between the end of irradiation and the end of counting.

The reaction product activities were then input to the SigPhi calculator that is a part of the STAYSL software package. SigPhi applies various corrections to the activities, namely neutron attenuation, γ-ray self-absorption, and flux history corrections [108]. Table 5.2 summarizes the SigPhi-processed activities from the foil pack irradiation. These activities were input to STAYSL to perform the spectral adjustment calculation on the input trial neutron energy spectrum.

Table 5.2: Foil pack activation products and activities. The produced activities are given in units of atoms of the product per atom of the target per second as these are the units that are required for use in STAYSL. All of the foils had a circular disk geometry with a 1 cm diameter.

Product	Reaction	Foil Thickness (mm)	Foil Mass (g)	Gamma Signature (keV)	Produced Activity (atom/atom/s)
^{89}Zr	^{90}Zr(n,2n)	0.5	0.2568 ± 0.0005	909.15	$7.93 \pm 0.20 \times 10^{-20}$
^{27}Mg	^{27}Al(n,p)	1.0	0.2317 ± 0.0005	843.76	$1.39 \pm 0.03 \times 10^{-17}$
^{24}Na	^{27}Al(n,α)	1.0	0.2317 ± 0.0005	1368.626	$2.48 \pm 0.06 \times 10^{-18}$
^{48}Sc	^{51}V(n,α)	1.0	0.5130 ± 0.0005	983.526	$3.84 \pm 0.13 \times 10^{-20}$
^{198}Au	^{197}Au(n,γ)	0.1	0.1525 ± 0.0005	411.80205	$1.79 \pm 0.05 \times 10^{-17}$
^{196}Au	^{197}Au(n,2n)	0.1	0.1525 ± 0.0005	355.73	$2.15 \pm 0.06 \times 10^{-18}$
^{116m}In	^{115}In(n,γ)	0.1	0.0582 ± 0.0005	1293.56	$3.27 \pm 0.10 \times 10^{-16}$
^{115m}In	^{115}In(n,n')	0.1	0.0582 ± 0.0005	336.241	$7.13 \pm 0.24 \times 10^{-17}$

5.3.3.3 Estimate of Incident Neutron Energy Spectrum

The incident neutron energy spectrum from the experiment was determined using an nTOF-informed trial spectrum and the foil pack activation data as inputs to the spectral adjustment analysis code STAYSL [108]. STAYSL uses evaluated neutron activation cross sections to calculate the expected activities of reaction products. These calculated activities are then compared against the measured activities using the χ^2 statistic. The incident neutron energy spectrum is adjusted in a least-squares routine until χ^2 is minimized.

The user specifies the binning of the neutron energy spectrum that is to be produced by STAYSL. Generally, the binning consists of 100-140 bins. This means that in most cases the problem STAYSL solves is severely under-constrained with a few knowns (i.e., the foil pack activation data) and 100-140 unknowns (i.e., the flux in each bin of the neutron energy spectrum). STAYSL uses evaluated correlations between energy groupings of the activation reaction cross section data to reduce the total number of degrees of freedom in the problem. However, for most problems, even this reduction is not enough to make the problem constrained or over-constrained. Therefore, STAYSL does not necessarily produce a unique solution for the incident neutron energy spectrum. Furthermore, the solution that STAYSL produces is highly dependent on the user-provided initial guess of the incident neutron energy spectrum.

To provide STAYSL with a reasonable trial input for the neutron energy spectrum, the nTOF-measured neutron energy spectrum was used as a basis. However, as previously

mentioned, the nTOF measurement only produces a spectrum with neutron energies above 1.75 MeV. Therefore, an estimate of the low-energy portion of the neutron energy spectrum is required. The low-energy portion of the neutron energy spectrum was assumed to take the form of a Maxwell-Boltzmann distribution with a centroid temperature of 0.0253 eV (i.e., room temperature). The form of the Maxwell-Boltzmann distribution that was used is given in Eq. 5.9:

$$N(E) = \sqrt{\frac{2}{\pi}} \frac{E^2 e^{-E^2/2a^2}}{a^3} \tag{5.9}$$

where a is given by Eq. 5.10:

$$a = \frac{E_0}{2\sqrt{2/\pi}} \tag{5.10}$$

where E_0 is the mean energy of the distribution.

This Maxwell-Boltzmann distribution spanned energies ranging from 10^{-5} eV to 0.1 eV and its magnitude was estimated using the measured activity from the ^{115}In(n,γ) reaction. In the epithermal region (0.1 eV to 1.75 MeV), a reasonable guess of the neutron energy was difficult to make. This is because this region spans many resolved resonances in the activation cross sections of the foil pack materials. Therefore, a simple log-log line between the Maxwell-Boltzmann distribution and the measured nTOF spectrum was used. The initial guess of the neutron spectrum that was supplied to STAYSL is shown in Fig. 5.10.

The SigPhi-processed activities given in Table 5.2 and the initial guess of the incident neutron energy spectrum shown in Fig. 5.10 were input to STAYSL. STAYSL was used to perform the spectral adjustment and determine the neutron energy spectrum shown in Fig. 5.11. It can be seen that STAYSL produces a neutron energy spectrum that is similar in shape to the initial guess spectrum. The χ^2 metric between the measured foil pack activities and the STAYSL calculated activities was 4.2. There is very limited thermalization of the neutrons produced from the deuteron breakup target; less than 0.001% of the total flux occurs below 1 eV.

5.3.3.4 Spectrum-Averaged Fission Cross Section

The spectrum-averaged neutron-induced fission cross section for ^{238}U was calculated with the above neutron energy spectrum and the ENDF/B-VIII.0 ^{238}U(n,f) point-wise cross section [28] using Eq. 5.11:

$$\bar{\sigma} = \int_0^\infty \sigma_{n,f}(E) \times P(E)\, dE \tag{5.11}$$

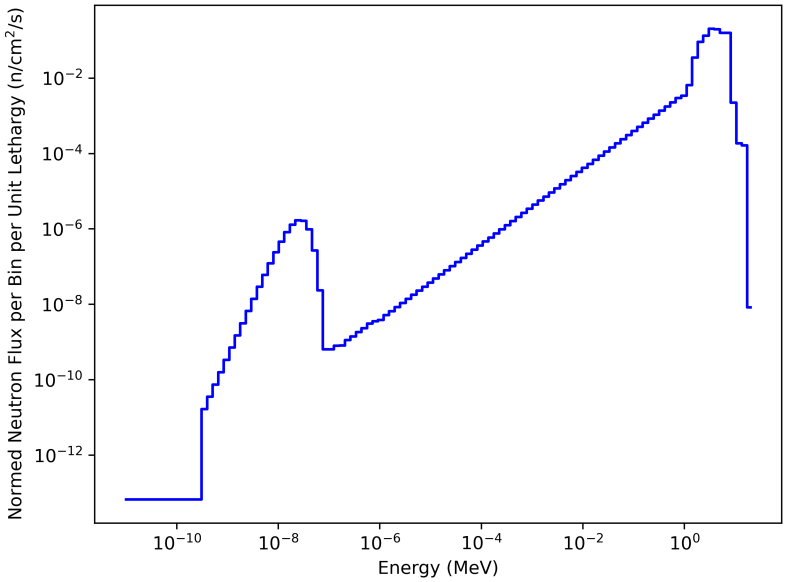

Figure 5.10: The initial guess of the incident neutron energy spectrum that was supplied to STAYSL. The spectrum is normalized such that the sum of the bins in the spectrum is 1 n/cm^2/s.

where $\sigma_{n,f}(E)$ is the ^{238}U(n,f) cross section and $P(E)$ is the measured incident neutron energy spectrum.

The point-wise ^{238}U(n,f) cross section from the ENDF/B-VIII.0 evaluation with the neutron energy spectrum overlaid is shown in Fig. 5.12. Using these data, the spectrum-averaged ^{238}U(n,f) cross section was determined to be 0.586 ± 0.015 b. Figure 5.13 shows the ^{238}U(n,f) cross section and neutron energy spectrum above 0.1 MeV. This figure shows that the neutron energy spectrum mostly covers the domain of first-chance fission. Only 2×10^{-5}% of the spectrum-averaged fission cross section is due to neutrons below 0.1 MeV.

5.3.4 Data Analysis Using the Fission Induced Electromagnetic Response Code

Historically, measured fission product yields are often reported as cumulative yields (see definition in Sec. 3.2.3). This is because transport times between the end of irradiation and the beginning of assay are often long, resulting in the complete decay of short-lived fission products before assay. This results in the cumulative yields to long-lived ($t_{1/2} > 1$ h) fission products being most commonly reported in literature. Thus, measurement of short-lived fission product yields and independent yields are less common.

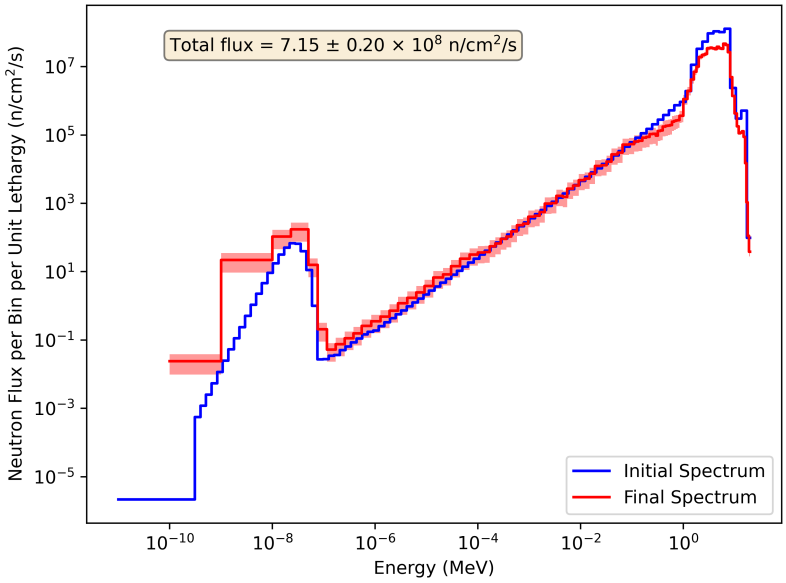

Figure 5.11: The incident neutron energy spectrum determined by STAYSL. The initial guess of the spectrum is shown for comparison. The total neutron flux was determined to be $7.15 \pm 0.20 \times 10^8$ n/cm^2/s.

Because FLUFFY features such rapid transport times, it is possible to observe γ-ray emissions from very short-lived ($t_{1/2} > 0.5$ s) fission products. This means that cumulative yields can be determined for the shortest-lived fission products and independent yields can be determined for any subsequent fission products in the mass chain. However, this can only be done if the appropriate decay corrections are applied, and the decay networks that exist at the neutron-rich end of mass chains are generally complex due to in-feeding from other mass chains caused by β-delayed neutron emission. Figure 5.14 shows an example of such a decay network.

5.3.4.1 Minimization Method

To apply the aforementioned decay correction accurately, the Fission Induced Electromagnetic Response code [176] was used. FIER uses evaluated nuclear data and analytical solutions to the Bateman equations to calculate the expected delayed γ-ray spectra that result from a user-specified irradiation scheme. FIER uses the nuclei decay modes that are listed in its input libraries (which are generated from ENDF File-8 [28, 191]) to generate the decay chains and networks that exist for the fission products. Therefore, in-feeding to a given mass chain from other mass chains is automatically accounted for. However, because FIER uses evaluated nuclear data as inputs to the solutions to the Bateman equations, the spectra output by FIER are only as accurate as the evaluated input nuclear data.

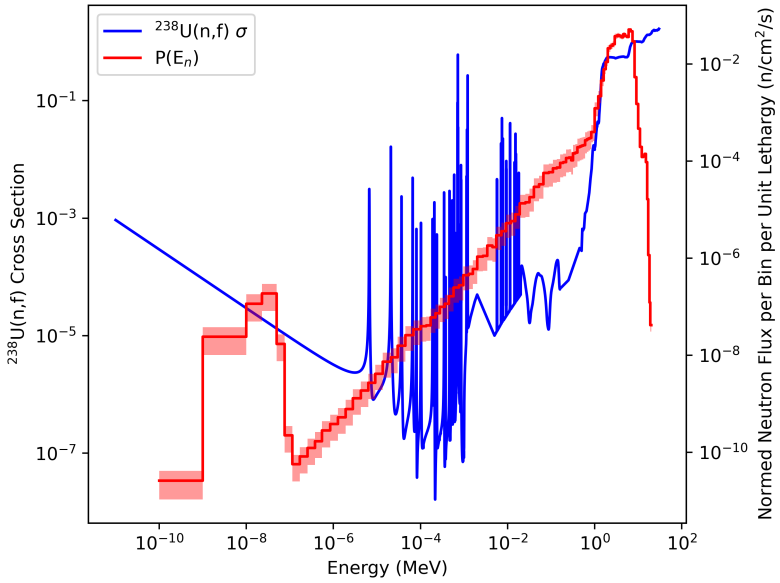

Figure 5.12: ^{238}U(n,f) cross section as a function of incident neutron energy. The data in this plot are taken from the ENDF/B-VIII.0 evaluation [28].

An example of how FIER can be used in fission yield determination using measured γ-ray emission data was offered in Sec. 4 of Ref. [176]. Fission yields (or other nuclear data values) can be determined by varying them in a minimization method that compares the output data from FIER with experimentally measured fission product γ-ray spectra. This technique is possible because the output from FIER is in units of number of γ-ray emissions and the efficiency-corrected photopeak count data from the FLUFFY experiment is also in units of number of γ-ray emissions, allowing for a one-to-one comparison in the minimization routine.

This minimization routine was developed for the purposes of analyzing the data from FLUFFY. The minimization routine that was used was the Differential Evolution heuristic global optimization algorithm [183] as implemented in the pagmo C++ software package [192]. A basic χ^2 metric was used as the objective for the minimization routine as shown in Eq. 5.12:

$$\chi^2 = \frac{N_\gamma(Z, A, I, t_0, t_1, c) - FIER(Z, A, I, t_0, t_1, c)}{\sigma^2_{N_\gamma}} \tag{5.12}$$

where N_γ is the number experimentally observed γ-ray emissions (as a function of Z product atomic number, A product mass number, I product isomeric state, t_0 time between the capsule arrival at the HPGe clover array and the start of counting, t_1 time between the capsule arrival at the HPGe clover array and the end of counting, and c number of cycles), $FIER$ is the number of γ-ray emissions predicted by FIER (as a function of Z, A, I, t_0, t_1,

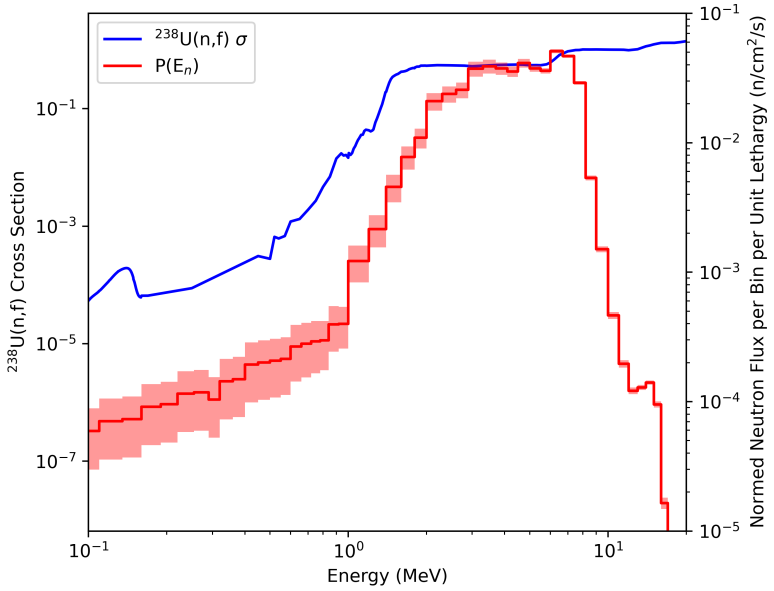

Figure 5.13: Figure 5.12 zoomed to neutron energies above 0.1 MeV.

and c), and σ_{N_γ} is the experimental uncertainty in N_γ. N_γ is determined from photopeak counts observed in the fission product γ-ray spectrum and the HPGe clover array efficiency curve using Eq. 5.13:

$$N_\gamma = \frac{C_\gamma}{\varepsilon(E_\gamma)} \tag{5.13}$$

where C_γ is the number of photopeak counts observed in the fission product γ-ray spectrum for a particular γ ray of energy E_γ and $\varepsilon(E_\gamma)$ is the absolute detection efficiency for that γ.

To enable this minimization routine, modifications were made to the version of FIER that was published in Ref. [176]. These modifications are as follows:

- The ability to track γ-ray emissions during and in between irradiation cycles was added. This is important because counting occurs in between irradiation cycles in FLUFFY experiments.
- A module was developed to implement temporal constraints on the FIER output that match the temporal constraints of the experimental data.
- A minimization program was written that calls the aforementioned module to determine optimal fission yields. This program reads in the provided experimental data for a given mass chain, sets a user-specified list of nuclear data properties (such as fission yields and decay γ intensities) as free parameters, and truncates decay chains at user-specified points where necessary.

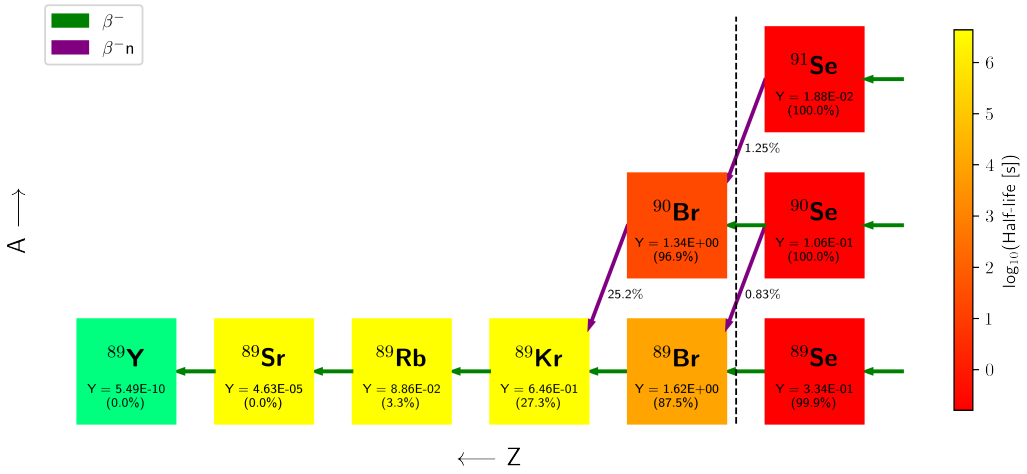

Figure 5.14: The decay network of fission products connected to the $A = 89$ mass chain. The fission yields for the nuclei to the immediate left of the dashed line were set as cumulative in the benchmarking example presented in Sec. 5.3.4.3. The purple arrows represent $\beta^- n$ decay and the branching ratio of that decay mode is written below each arrow. Each nucleus is labelled with its independent fission yield in units of percent from the ^{238}U fast fission ENDF/B-VIII.0 evaluation. Beneath that yield is a percentage, which represents that total independent yield remaining in the mass chain up to that nucleus.

- The internal operations of the FIER code needed significant optimization to make the minimizer run in a tractable amount of time. FIER now runs approximately 50-80× faster than the version in Ref. [176].

5.3.4.2 Benefits of the Method

This method of fission yield determination is computationally expensive; however, it has a number of novel and specific benefits that can advance the state of experimental fission yield nuclear data:

Complete Decay Corrections - Because FIER does an analytical treatment of the Bateman equations for complete decay chains, decay corrections to the fission yields are determined automatically via the minimization process.

Experimental Fission Yield Covariances - Covariances between fission yields in a given measurement are rarely, if ever, reported (see Sec. 3.2.2.2). Generally, fission yields are calculated from the measured fission product γ-ray spectrum independently and thus covari-

ances are not determined. Because this minimization technique determines the fission yields together and in a correlated fashion, covariances can be assessed either by deterministic error estimation or by Monte-Carlo covariance estimation.

Corrections to Discrepant Nuclear Decay Data - The minimizer used in FIER allows for any input nuclear data property to be set as a free parameter. This means that not only fission yields can be determined, but so can half-lives, decay γ intensities, and branching ratios. This is particularly useful in the case of decay γ intensities as these are subject to Beta Pandemonium errors (see Secs. 3.2.2.1 and 3.2.2.2).

5.3.4.3 Benchmarking

To test the validity of this method, a benchmarking test was developed to test the ability of the minimizer to produce expected values. FIER was run to produce expected γ-ray emission data for the 1031.92-keV γ from ^{89}Rb, the 3532.88-keV γ from ^{89}Kr, and the 3231.3-keV γ from ^{90}Br. These three nuclei are connected to the $A = 89$ mass chain, which is shown in Fig. 5.14. In the FIER calculation, the decay chains were truncated for ^{89}Kr and ^{90}Br in order to effectively make their yields cumulative. The default values in the FIER input libraries were used to generate these data and those values are summarized in Table 5.3.

This FIER-produced output was used as a test dataset and was input to the minimizer. The minimizer was run with the nuclear data properties in Table 5.3 set as free parameters. The optimal values that the minimizer determined for these free parameters are also shown in Table 5.3. The minimizer successfully reproduced the default value of all seven free parameters to within their evaluated uncertainties. Further still, the minimizer was able to reproduce the γ-ray emissions test data set accurately, as shown in Appendix Figs. A.1, A.2, and A.3.

Table 5.3: Free parameters used in the minimizer benchmarking test and their default and fitted values.

Free Parameter	Default Value	Minimizer Result
^{90}Br FY	1.34%	1.34%
^{90}Br $t_{1/2}$	1.92 s	1.92 s
^{89}Br FY	1.62%	1.60%
^{89}Br $t_{1/2}$	4.40 s	4.36 s
^{89}Kr FY	0.646%	0.650%
^{89}Kr $t_{1/2}$	189 s	186 s
^{89}Rb FY	0.0886%	0.0852%

5.3.4.4 Uncertainty Estimation

As will be discussed in Sec. 5.3.6, Monte-Carlo uncertainty and covariance estimation is not yet possible with this method. Additional computational optimizations and software will need to be made to enable this. Instead, the uncertainties on the results presented in Sec. 5.3.5 are estimated with the generalized uncertainty propagation formula given in Eq. 5.14:

$$\sigma_f^2 = \left(\frac{\partial f}{\partial x_0}\right)^2 \sigma_{x_0}^2 + \left(\frac{\partial f}{\partial x_1}\right)^2 \sigma_{x_1}^2 + \left(\frac{\partial f}{\partial x_2}\right)^2 \sigma_{x_2}^2 + ... \tag{5.14}$$

where f is the objective function that has variables $\{x_0,\ x_1,\ x_2,\ ...\}$ with uncertainties $\{\sigma_{x_0},\ \sigma_{x_1},\ \sigma_{x_2},\ ...\}$.

The objective function in Eq. 5.14 is the solutions to the Bateman equations (given in Eqs. 3 and 4 of Ref. [176]) solved for the nuclear data parameter in question. The variables of the objective function are the nuclear data properties of the mass chain and the number of γ emissions. The partial differentials in Eq. 5.14 were solved numerically using a difference quotient.

5.3.5 Results and Discussion by Mass Number

The following are initial results from the analysis of the July 2020 ^{238}U(n,f) fission yield measurement experiment with FLUFFY. These results are presented to demonstrate the type of fission yield measurements that can be performed with FLUFFY and to demonstrate the potential of the analysis method discussed above in Sec. 5.3.4.

The analysis focused on high-energy γ signatures when available. There were two primary reasons for this focus: there is a lower density of γ rays at high energies in fission product γ-ray spectra and high-energy γ rays are more penetrating and thus are of particular interest to nuclear forensics and safeguards applications.

A discussion of the results from each mass chain is offered. The results are compared to the ENDF/B-VIII.0 and JEFF-3.3 fission yield evaluations and previous measurements where available. For the comparison to experimental data, EXFOR-compiled measurements were used. Only fission yield measurements with incident neutron energies of "fast" ($\sim$0.5 MeV) or above were used in the comparison. This is because the mean of the incident neutron energy spectrum measured in this experiment is 4.1 MeV, which is between the fast and 14-MeV energies of the two evaluations. It is known that fission yields change considerably between thermal and fast energies and therefore a comparison to thermal energies would not be appropriate. The comparison of the fission yields measured in this experiment with other

measurements is not necessarily one-to-one because no other measurement that is discussed features an incident neutron energy spectrum similar to this experiment.

5.3.5.1 A = 86

Results:

The $A = 86$ mass chain was analyzed using the FIER minimization method. The decay network for the fission products connected to the $A = 86$ mass chain is shown in Fig. 5.15. Three photopeaks from products attached to this mass chain were identified and fit to extract their net areas: the 1564.60-keV photopeak from ^{86}Br, the 2660.0-keV photopeak from ^{86}Se, and the 4180.54-keV photopeak from ^{87}Br. Because of the half-lives of these three nuclei, the fission product γ-ray spectrum from the 5 s–125 s irradiation scheme was used for this analysis. Because the half-life of ^{86}Se is much shorter than the 125 s decay interval of the irradiation scheme, the ^{86}Se photopeak was fit as a function of time since capsule arrival; t_0 from Eq. 5.12 was set to 0 s and t_1 was variable. The half-lives of ^{86}Br and ^{87}Br are on the same order of the 125 s decay interval of the irradiation scheme, thus their photopeaks were fit as a function of cycle number with t_0 and t_1 constant at 0 s and 125 s, respectively. Appendix Figs. A.4, A.5, and A.6 show examples of these photopeak fits.

The 2660.0-keV photopeak from ^{86}Se was found to have significant contamination from an unknown γ ray. This was discovered because the half-life curve of the 2660.0-keV photopeak deviated significantly from the 14.3 s half-life of ^{86}Se. To separate the contribution for ^{86}Se from the unknown contaminant, the data were fit to the form given in Eq. 5.15, which is the sum of two decay curves (one for ^{86}Se and one for the contaminant):

$$N_\gamma(t) = A(1 - e^{-\lambda_{86Se}t}) + B(1 - e^{-\lambda_{cont}t}) \tag{5.15}$$

where A and B are the relative intensities of the decay curves, λ_{86Se} is the decay constant of ^{86}Se, and λ_{cont} is the decay constant on the contaminant. A, B, and λ_{cont} are free parameters, while λ_{86Se} is fixed at 14.3 s. The results of this fitting process are shown in Appendix Fig. A.7.

The photopeak data were input to the minimizer. Because the preceding nuclei are short-lived and did not have γ-ray emissions observable in the fission product γ-ray spectrum, the decay network in Fig. 5.15 was truncated at ^{86}Se and ^{87}Br. This effectively makes the fission yields determined for ^{86}Se and ^{87}Br cumulative. The nuclear data properties and free parameters related to this analysis are given in Table 5.4. Appendix Figs. A.8, A.9, and A.10 show fits of the experimentally measured γ-ray emission data to FIER.

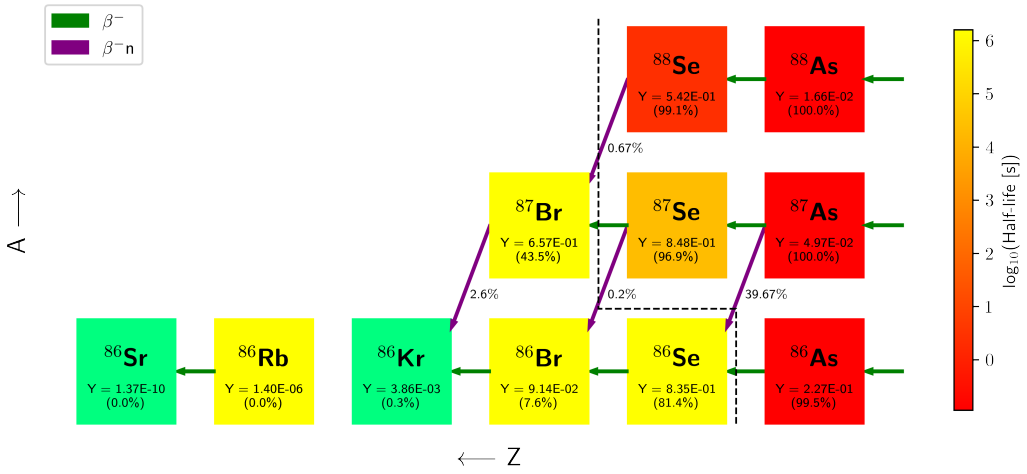

Figure 5.15: The decay network of fission products connected to the $A = 86$ mass chain. Nuclei to the right of the dashed line did not have detectable γ-ray signatures. The purple arrows represent $\beta^- n$ decay and the branching ratio of that decay mode is written below each arrow. Each nucleus is labeled with its independent fission yield in units of percent from the ^{238}U fast fission ENDF/B-VIII.0 evaluation. Beneath that yield is a percentage, which represents the total independent yield remaining in the mass chain up to that nucleus.

Discussion:

Table 5.5 compares the fission yields measured for the $A = 86$ mass chain to the ENDF/B-VIII.0 and JEFF-3.3 evaluations and Table 5.6 compares them to EXFOR-compiled measurements. The measured fission yields for the $A = 86$ mass chain have generally good agreement with both evaluation and measurements.

The quoted 69% relative uncertainty in the measured independent fission yield for ^{86}Br is relatively large as it inherits the uncertainty from the cumulative yield of its parent ^{86}Se. This large uncertainty results in 1σ agreement with all evaluated yields except for the JEFF-3.3 fast evaluation. The 0.45(31)% measured yield is in best agreement with the JEFF-3.3 14-MeV evaluation value of 0.31(11)%. No EXFOR-compiled measurements of this yield were found, likely owing to the low independent yield and short half-life of this nucleus. It should be noted that the ENDF/B-VIII.0 evaluation lists an isomer for ^{86}Br and splits the total yield to ^{86}Br evenly. However, neither ENSDF nor the JEFF-3.3 show an extant isomeric state for ^{86}Br. Indeed, the experimental data in this study did not yield evidence of an isomeric state for ^{86}Br either. Therefore, it is concluded that no such state exists.

Table 5.4: Free parameters and nuclear data properties used in the analysis of the $A = 86$ mass chain. Fission yield free parameters that are marked with an asterisk are cumulative rather than independent. Default values are taken from ENDF/B-VIII.0 File-8 and the ENDF/B-VIII.0 ^{238}U fast fission yield evaluation.

Property	Default Value	Minimizer Result
Free Parameters:		
^{86}Br FY	0.18 ± 0.08%	0.45 ± 0.31%
^{86}Se FY*	1.07 ± 0.24%	1.05 ± 0.17%
^{87}Br FY*	1.54 ± 0.09%	1.83 ± 0.29%
^{86}Se I_γ(2660.0 keV)	22.6 ± 2.3%	24.9 ± 4.0%
Fixed Values:		
^{86}Br $t_{1/2}$	55.1 ± 0.4 s	
^{86}Se $t_{1/2}$	14.3 ± 0.3 s	
^{87}Br $t_{1/2}$	55.65 ± 0.13 s	
^{86}Br I_γ(1564.60 keV)	62 ± 5%	
^{87}Br I_γ(4180.54 keV)	4.0 ± 0.3%	
^{87}Br $\beta^- n$ BR	2.60 ± 0.04%	

The 1.05(17)% measured cumulative yield for ^{86}Se is in excellent agreement with both the ENDF/B-VIII.0 and JEFF-3.3 evaluations; there is 1σ agreement between the measured yield and all four evaluated yields. The measured yield falls between the yields listed at fast and 14 MeV for both evaluations, suggesting a gradual energy dependence for this yield as a function of compound nucleus energy (though the ENDF/B-VIII.0 and JEFF-3.3 evaluations disagree on the direction of this trend). However, this measurement disagrees with the only other EXFOR-compiled measurement of this yield, which reported a value of 0.56(8)%, by nearly a factor of two.

Finally, the 1.83(29)% measured cumulative yield for ^{87}Br is in good agreement with both the ENDF/B-VIII.0 and JEFF-3.3 evaluations. In particular, there is excellent agreement between the JEFF-3.3 14-MeV evaluation value of 1.78(8)%. The comparison to the EXFOR-compiled measurements is also good with the measured yield falling within the range of the measurements: 0.7% to 1.94%. The measurement by Roshchenko et al. [193] reported a yield of 1.77(13)%, which has excellent agreement with this study. This is perhaps explained due to the similarity in the mean incident neutron energies of the two measurements: 4.1 MeV and 4.20 MeV.

In addition to the fission yields that were determined in this mass chain, the decay γ intensity of the 2660.0-keV γ from ^{86}Se was determined. While the measured value is within 1σ

Table 5.5: Comparison of the fission yields measured for the $A = 86$ mass chain in this work and the ENDF/B-VIII.0 [28] and JEFF-3.3 [29] evaluations. All values in this table are in units of %. Note: the yields for ^{86}Br are taken as the sum of the yield to the ground state and isomeric state in the ENDF/B-VIII.0 evaluation.

Property	This Work	ENDF Fast	ENDF 14 MeV	JEFF Fast	JEFF 14 MeV
^{86}Br IFY	0.45(31)	0.18(8)	4.8(22)	0.187(61)	0.31(11)
^{86}Se CFY	1.05(17)	1.07(25)	1.02(46)	0.927(56)	1.46(15)
^{87}Br CFY	1.83(29)	1.54(9)	1.55(9)	1.57(7)	1.78(8)

Table 5.6: Comparison of the fission yields measured for the $A = 86$ mass chain in this work and EXFOR-compiled measurements by Pierson et al. [105], Roshchenko et al. [193], Gudkov et al. [194], and Filatenkov et al. [195]. The errorbars on the average incident neutron energy represent the full width at half maximum of the neutron energy spectrum where given. All property values are in units of %.

Study	This Work	Pierson	Roshchenko	Gudkov	Filatenkov
Neutron Source	Deuteron Breakup	DT Fusion	^{3}H(p,n)	DT Fusion	Unknown
$\bar{E}_n$ (MeV) / Property	4.1 $^{+2.9}_{-2.2}$	14.7 $^{+0.2}_{-0.2}$	4.20 $^{+0.17}_{-0.17}$	14.7	3.0
^{86}Br IFY	0.45(31)	–	–	–	–
^{86}Se CFY	1.05(17)	0.56(8)	–	–	–
^{87}Br CFY	1.83(29)	1.17(9)	1.77(13)	1.94(31)	0.7(3)

of the evaluated value, the change is a 10% increase. This example is illustrative of how the FIER minimization method presented in Sec. 5.3.4 is useful in correcting discrepant nuclear decay data. In a standard analysis of fission yields, γ emission data are used to determine the yield of a fission product independently of other γ emission data. However, using this new method, the information on the γ emission from ^{86}Br was used to constrain the total fission yield that is passed from ^{86}Se to ^{86}Br. Analyzing the fission product γ emission data using this correlated method offers sensitivity to nuclear data decay.

5.3.5.2 A = 98

Results:

The decay network for the fission products connected to the $A = 98$ mass chain is shown in Fig. 5.16. Three photopeaks from products associated with this mass chain were identified: the 1024.4-keV photopeak from ^{98}Nb, the 1222.9-keV photopeak from ^{98}Y, and the 724.4-keV photopeak from ^{99}Y. Because of the short half-lives of these three nuclei, the fission product γ-ray spectrum from the 1 s–25 s irradiation scheme was used for this analysis. Because the half-lives of all three nuclei are much shorter than the 25 s decay interval of the irradiation scheme, their photopeaks were fit as a function of time since capsule arrival; t_0 from Eq. 5.12 was set to 0 s and t_1 was variable. Appendix Figs. A.11, A.12, and A.13 show examples of these photopeak fits.

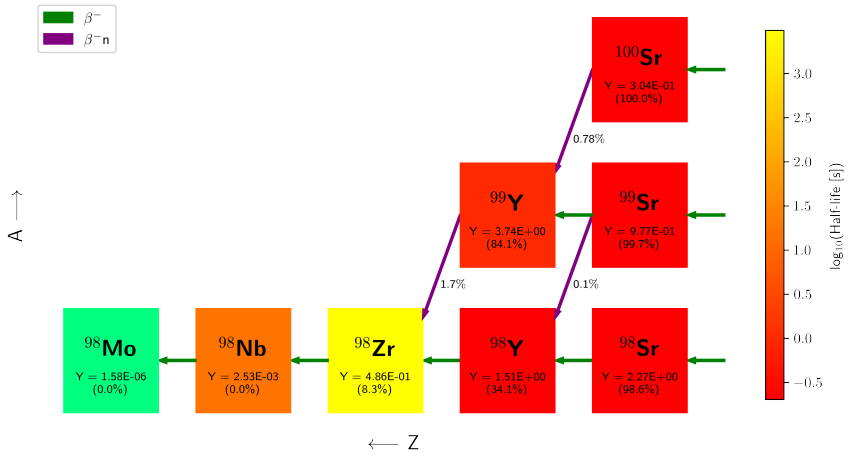

Figure 5.16: The decay network of fission products connected to the $A = 98$ mass chain. Nuclei to the right of the dashed line did not have sufficiently detectable γ-ray signatures. The purple arrows represent $\beta^- n$ decay and the branching ratio of that decay mode is written below each arrow. Each nucleus is labeled with its independent fission yield in units of percent from the ^{238}U fast fission ENDF/B-VIII.0 evaluation. Beneath that yield is a percentage, which represents that total independent yield remaining in the mass chain up to that nucleus.

The 1024.4-keV photopeak from ^{98}Nb was very weak; its location in the fission product γ-ray spectrum is very crowded with photopeaks from other fission products. An attempt to fit the photopeak was made, as is shown in Appendix Fig. A.11. Because the photopeak is one of the weakest in the energy region, it could not be fit with reasonable accuracy/uncer-

tainty; large fluctuations in the photopeak area as a function of t_1 occurred. This indicates there was poor sensitivity to the photopeak shape because it sits on the shoulder of a larger photopeak. Thus it is not included in the analysis of the $A = 98$ mass chain.

The 724.4-keV photopeak from ^{99}Y (shown in Appendix Fig. A.13) was found to have significant contamination from another photopeak. This was discovered because the half-life curve of the 724.4-keV photopeak deviated significantly from the 1.47 s half-life of ^{99}Y. It is suspected that this contaminant is the 724.33-keV γ ray from ^{145}Ce, which is another fission product with a significant cumulative yield. This contamination issue is similar to that which was discovered for the 2660.0-keV γ from ^{86}Se in Sec. 5.3.5.1. To separate the contribution for ^{99}Y from the contaminant, the data were fit to the form given in Eq. 5.15. The results of this fitting process are shown in Appendix Fig. A.14.

Zirconium-98 does not emit a strong γ-ray signature and a γ-ray signature from ^{98}Nb could not be reasonably ascertained. Because of this, there is no information on the nuclei that follow ^{98}Y in the $A = 98$ mass chain, and thus the information from the γ-ray signature from ^{99}Y is not needed. Because the only useable γ-ray signature is from ^{98}Y, the FIER minimization method is not needed to determine the fission yield to ^{98}Y. Instead, the fission yield was determined by fitting the 1222.9-keV γ-ray emission day to the form in Eq. 5.16:

$$N_\gamma = \frac{I_\gamma A_0}{\lambda}(1 - e^{-\lambda t_1}) \tag{5.16}$$

where I_γ is the decay γ intensity for the γ-ray signature, λ is the decay constant of the γ emitter, t_1 is the time since capsule arrival, and A_0 is the initial activity of the γ emitter and is given by Eq. 5.17:

$$A_0 = N_c R_f Y (1 - e^{-\lambda t_{irrad}}) e^{-\lambda \bar{t}_{trans}} \tag{5.17}$$

where N_c is the number of irradiation cycles conducted, R_f is the fission rate in the target, Y is the fission yield to the γ emitter, t_{irrad} is the irradiation time, and $\bar{t}_{trans}$ is the average transport time of the capsule between the neutron source and detector array.

The fitting process determined a fission yield for ^{98}Y of 5.13 $\pm$ 0.39%. The half-life in Eq. 5.16 was set as a free parameter because the apparent half-life of ^{98}Y is a combination of its own half-life and the half-life of its parent ^{98}Sr which has a half-life of 0.653 s. The fitted half-life was determined to be 1.028 $\pm$ 0.071 s, which is comparable to the combined half-life of the ^{98}Y/^{98}Sr system. The fit that was obtained is shown in Appendix Fig. A.15.

The fission yield determined for ^{98}Y is ascribed entirely to the ground state. This is because the apparent half-life from the γ-ray emission is significantly shorter than the 2.32 s half-life of ^{98m}Y. Furthermore, no γ-ray signatures that are unique to ^{98m}Y (namely the 1801.6-keV γ) were detected elsewhere in the spectrum. Finally, in an attempt to verify the

absence of a contribution from ^{98m}Y, the 1222.9-keV emissions were fit to the form given in Eq. 5.18:

$$N_\gamma^{tot} = N_\gamma^g + N_\gamma^m \tag{5.18}$$

where N_γ^g is the γ emissions calculated using Eq. 5.16 with the I_γ and λ relevant to the ground state of ^{98}Y and N_γ^m is the γ emissions calculated with the I_γ and λ relevant to the metastable state. This fit produced a yield for ^{98m}Y that was zero.

Discussion:

Table 5.7 compares the fission yield measured for ^{98}Y to the ENDF/B-VIII.0 and JEFF-3.3 evaluations. There are no measurements of this fission yield compiled in EXFOR for ^{238}U(n,f). EXFOR-compiled measurements for this yield exist for ^{235}U(n,f) and ^{239}Pu(n,f). However, only one of these measurements obtained the ^{98m}Y yield [196] and none measured both the ^{98g}Y and ^{98m}Y yields together.

The measurement of this fission yield offers a particularly interesting result: there was no detectable yield to the isomeric state of ^{98}Y. While the 5.13(39)% measured yield to ^{98g}Y agrees within 1σ of the sum of ^{98g}Y and ^{98m}Y yields in the ENDF/B-VIII.0 and JEFF-3.3 fast evaluations, the isomer-to-ground state ratios disagree. The fitted half-life for the in-growth of this γ ray (shown in Appendix Fig. A.15) matches exceptionally well with the joint half-life of the ^{98}Y/^{98}Sr system. This also allows significant contamination from the 1222.9-keV γ from ^{96m}Y to be ruled out.

This result is not surprising; without a measurement to guide the evaluation, there will be great uncertainty in the isomer-to-ground state ratio. A possible explanation for the lack of direct population of ^{98m}Y from fission could be the strong deformation of this isomer [197]. While deformation in fission fragments/products is common, the population of ^{98g}Y may be favored due to its enhanced stability having $Z = 39$ near $Z = 40$. $Z = 40$ is described as "semi-magic" in the region of $N = 50$–64 due to a large shell gap between the $1p_{1/2}$ and $0g_{9/2}$ states [198]. Thus, the enhanced stability of the ground state may be favored in fission, similar to the enhanced population of fission products near the doubly-magic $A = 132$.

5.3.5.3 A = 136

Results:

The $A = 136$ mass chain was analyzed using the FIER minimization method. The decay network for the fission products connected to the $A = 136$ mass chain is shown in Fig. 5.17. Three photopeaks from products attached to this mass chain were identified and successfully fit to extract their net areas: the 2077.9-keV photopeak from ^{136}Te, the 1321.08-keV

Table 5.7: Comparison of the fission yields measured for the $A = 98$ mass chain in this work and the ENDF/B-VIII.0 [28] and JEFF-3.3 [29] evaluations. All values in this table are in units of %. The yield listed for ^{98}Y is the sum of the ^{98g}Y and ^{98m}Y yields in each evaluation.

Property	This Work	ENDF Fast	ENDF 14 MeV	JEFF Fast	JEFF 14 MeV
^{98g}Y IFY	5.13(39)	3.85(62)	2.78(45)	2.62(32)	1.60(48)
^{98}Y IFY	5.13(39)	5.37(71)	4.38(58)	5.24(43)	4.09(85)

photopeak from ^{136g}I, and the 1313.02-keV photopeak from ^{136g}I and ^{136m}I. Given the half-lives of these three nuclei, the fission product γ-ray spectrum from the 5 s–125 s irradiation scheme was used for this analysis. Because the half-life of ^{136}Te is much shorter than the 125 s decay interval of the irradiation scheme, the ^{136}Te photopeak was fit as a function of time since capsule arrival; t_0 from Eq. 5.12 was set to 0 s and t_1 was variable. Though not as short as the half-life of ^{136}Te, the half-lives of ^{136g}I and ^{136m}I are still shorter than the 125 s decay interval of the irradiation scheme. In order to separate the time signature of their 1313.02-keV photopeak, they too were fit as a function of time since capsule arrival. Appendix Figs. A.16 and A.17 show examples of these photopeak fits.

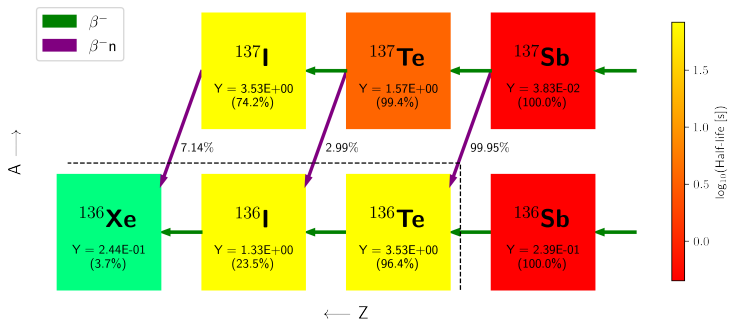

Figure 5.17: The decay network of fission products connected to the $A = 136$ mass chain. Nuclei to the right of the dashed line did not have sufficiently detectable γ-ray signatures. The purple arrows represent $\beta^- n$ decay and the branching ratio of that decay mode is written below each arrow. Each nucleus is labeled with its independent fission yield in units of percent from the ^{238}U fast fission ENDF/B-VIII.0 evaluation. Beneath that yield is a percentage, which represents that total independent yield remaining in the mass chain up to that nucleus.

The photopeak data were input to the minimizer. Because the preceding nuclei are short-

lived and did not have γ-ray emissions observable in the fission product γ-ray spectrum, the decay network in Fig. 5.17 was truncated at ^{136}Te. This effectively makes the fission yield determined for ^{136}Te cumulative. Similarly, because a γ-ray signature for ^{137}Te was not detected, the 2.99% β^-n branching ratio of ^{137}Te to ^{136}I was set to zero. As this branching ratio is small, the resulting bias is also small. The nuclear data properties and free parameters related to this analysis are given in Table 5.8. Appendix Figs. A.18, A.19, and A.20 show fits of the experimentally measured γ-ray emission data to FIER.

Table 5.8: Free parameters and nuclear data properties used in the analysis of the $A = 136$ mass chain. Fission yield free parameters that are marked with an asterisk are cumulative rather than independent. Default values are taken from ENDF/B-VIII.0 File-8 and the ENDF/B-VIII.0 ^{238}U fast fission yield evaluation. Values with a † are set differently than their evaluation.

Property	Default Value	Minimizer Result
Free Parameters:		
^{136m}I FY	1.34 ± 0.43%	0.59 ± 0.18%
^{136g}I FY	1.33 ± 0.43%	0.78 ± 0.34%
^{136}Te FY*	3.70 ± 0.85%	0.67 ± 0.20%
Fixed Values:		
^{136}Te $t_{1/2}$	17.63 ± 0.08 s	
^{136g}I $t_{1/2}$	83.4 ± 1.0 s	
^{136m}I $t_{1/2}$	46.9 ± 1.0 s	
^{136}Te I_γ(2077.9 keV)	22.1%	
^{136g}I I_γ(1321.08 keV)	24.8 ± 1.8%	
^{136g}I I_γ(1313.02 keV)	66.7%	
^{136m}I I_γ(1313.02 keV)	100%	
^{137}Te $\beta^- n$ BR	0%†	

Discussion:

The $A = 136$ mass chain offers a particularly compelling measurement of the isomer-to-ground fission yield ratio for ^{136}I. This is because ^{136g}I emits two γ rays that are very close in energy: 1313.02 keV and 1321.08 keV. Because they are so close in energy, concerns about detection efficiency bias are alleviated. Iodine-136m also emits the 1313.02-keV γ but does not emit the 1321.08-keV γ. This makes it possible to use 1321.08-keV γ to subtract the contribution of the ground state to the 1313.02-keV photopeak. The measured isomer-to-ground fission yield ratio is 0.76 ± 0.40. This ratio falls between the values of the ENDF/B-VIII.0 evaluation (0.5 for both fast and 14 MeV) and the JEFF-3.3 evaluation (2.73 for fast and

4.5 for 14 MeV).

Table 5.9 compares the fission yields measured for the $A = 136$ mass chain to the ENDF/B-VIII.0 and JEFF-3.3 evaluations and Table 5.10 compares them to EXFOR-compiled measurements. The 0.78(34)% measured independent fission yield to ^{136g}I is lower than the fast and 14-MeV ENDF/B-VIII.0 evaluations by more than a factor of two. However, it has excellent agreement with both the fast and 14-MeV JEFF-3.3 evaluations. There is significant scatter between the measurements of the ^{136g}I yield, spanning the range from 0.10% to as high as 2.5%.

The 0.59(18)% measured independent fission yield of ^{136m}I is lower than both the ENDF/B-VIII.0 and JEFF-3.3 evaluations. The measurement is in better agreement with the ENDF/B-VIII.0 evaluation with 1.2-1.4σ differences. As was the case with the ^{136g}I yield, the measurement falls within the wide range of yields reported in other measurements which span 0.141% to 1.90%.

Finally, the 0.67(20)% measured cumulative yield for ^{136}Te is in disagreement with both measurements and evaluations by a factor of about two. A specific explanation for this discrepancy is not immediately apparent, however, it should again be noted that the incident neutron energy spectrum is not identical to the evaluations or other measurements.

Table 5.9: Comparison of the fission yields measured for the $A = 136$ mass chain in this work and the ENDF/B-VIII.0 [28] and JEFF-3.3 [29] evaluations. All values in this table are in units of %.

Property	This Work	ENDF Fast	ENDF 14 MeV	JEFF Fast	JEFF 14 MeV
^{136g}I IFY	0.78(34)	1.33(43)	1.58(51)	0.70(14)	0.630(90)
^{136m}I IFY	0.59(18)	1.34(43)	1.58(51)	1.91(39)	2.84(41)
^{136}Te CFY	0.67(20)	3.70(85)	1.39(45)	4.13(46)	1.83(32)

5.3.6 Future Work

The results present both new measurements of short-lived fission yields and a demonstration of how FIER can be employed in the analysis of fission yield measurements. Below is a list of possible future work that could improve and/or expand the present results:

Detector Efficiency Calibrations - The detector efficiency calibrations presented in Sec. 5.3.2 need to be improved. The energy-dependent efficiency model given by Eq. 5.3 only

Table 5.10: Comparison of the fission yields measured for the $A = 136$ mass chain in this work and EXFOR-compiled measurements by Pierson et al. [105], Wilson et al. [165], Campbell et al. [199], and Lhersonneau et al. [200]. The errorbars on the average incident neutron energy represent the full width at half maximum of the neutron energy spectrum where given. All values in this table are in units of %.

Study	This Work	Pierson	Wilson	Campbell	Lhersonneau
Neutron Source	Deuteron Breakup	DT Fusion	p(^{7}Li,n)	Reactor Core Port	Deuteron Breakup
$\bar{E}_n$ (MeV) / Property	4.1 $^{+2.9}_{-2.2}$	14.7 $^{+0.2}_{-0.2}$	1.72 $^{+0.5}_{-0.5}$	"Fast"	20 $^{+9}_{-12}$
^{136g}I IFY	0.78(34)	0.28(15)	–	0.10(17)	2.5(6)
^{136m}I IFY	0.59(18)	1.90(16)	–	0.141(13)	
^{136}Te CFY	0.67(20)	1.29(15)	3.91(9)	2.56(19)	2.0(6)

features three model parameters and is thus too rigid to fully describe the energy-dependent efficiency of the detection system. While the centroid fit of the efficiency curve is reasonable, the Monte-Carlo estimated covariance matrix for the model parameters results in calculated uncertainties for the efficiency curve that are larger than the uncertainties in the measured efficiency data. This is particularly true at high energies. Using a more descriptive model for the efficiency calibration should resolve this problem. Additional work should be performed to assess the ability of the efficiency curve to be extrapolated beyond the energy domain of the measured efficiency data. While extrapolation should always be avoided when possible, the ability to extrapolate would allow the use of photopeaks from very high-energy γ rays in limited circumstances.

Neutron Energy Spectrum Characterization - Additional work on the characterization of the incident neutron energy spectrum would enable FLUFFY and its neutron source to be used for fission yield measurements on fissile targets. The spectrum presented in Sec. 5.3.3 serves as a reasonable initial result. However, a more thorough characterization of the spectrum at thermal and epithermal energies will be necessary to accurately interpret data collected on fissile actinide targets.

A forward model fit is being developed that propagates a trial neutron flux through a modeled detector response function in a χ^2 minimization. This would provide an improved statistical estimate of the neutron flux at the target location.

As mentioned in the analysis of the nTOF measurement presented in Sec. 5.3.3, the nTOF measurement does not give information about the spectrum below 1.75 MeV. In order to

estimate the shape of the incident neutron energy spectrum below the limits of the nTOF measurement, a model of deuteron breakup is being developed by Dr. Jonathan Morrell of Los Alamos National Laboratory (formerly of the University of California, Berkeley). The parameters of this model will be fit to the nTOF spectrum above 1.75 MeV and the model will then be used to estimate the neutron energy spectrum below 1.75 MeV by extrapolation. Having a careful characterization of the low-energy portion of the neutron energy spectrum is critical to enable future measurements on fissile targets. However, it should be noted that it has little to no effect on the presented ^{238}U(n,f) measurement as less than 2×10^{-5}% of the spectrum-averaged fission cross section is due to neutrons below 0.1 MeV.

Further study of the spectral adjustment performed by STAYSL is required. In particular, STAYSL is very sensitive to the initial guess of the neutron energy spectrum that it is provided, especially in the epithermal region where there are few suitable monitor reactions to provide sensitivity. This can be seen in Fig. 5.11 where the initial guess of the neutron energy spectrum in the epithermal region remains relatively unchanged by STAYSL. This is because STAYSL uses a least-squares minimization approach that is prone to settling on local minima in the χ^2 space. Improving the initial guess (such as in the plans described above) will improve the results produced by STAYSL. Other methods of spectral adjustment that may be less prone to settling on local minima or do not require an initial guess should be investigated. One such method may be maximum likelihood and maximum entropy methods [201, 202, 203]. Finally, reducing the number of energy bins in the epithermal region may enhance the sensitivity of STAYSL to those bins and allow for more realistic results in that energy region. Fortunately, because ^{238}U(n,f) cross section thresholds at approximately 1 MeV the presented results are not affected.

Data Analysis Using FIER - The method of determining fission yields using χ^2 minimization against FIER presented in Sec. 5.3.4 is a novel advancement in fission yield measurements. The benchmarking example presented in Sec. 5.3.4.3 and the examples of its use in the analysis of the $A = 86$ and $A = 136$ mass chains demonstrate the efficacy of this method.

Further benchmarking of the method should be conducted. Investigation of the sensitivity of the method to settle on local minima in the χ^2 minimization should be performed. Finally, further optimization of the FIER code is required to enable fully Monte Carlo estimation of uncertainties and covariances.

Finally, in addition to the above-listed improvements in the analysis of the experimental data, expansion of the results to more mass chains would be valuable to the nuclear data community. Quantification of the maximum sensitivity and minimum observable fission yield of the FLUFFY pneumatic system would help establish its value for fission yield measurements.

5.4 Conclusions

Short-lived fission product yields have been measured for neutron-induced fission of ^{238}U. At present, eight fission yields, two isomer-to-ground state ratios, and one decay γ intensity have been measured in the $A = 86$, 98, and 136 mass chains. Of these eight reported fission yields, three have not been previously measured. In particular, this work offers a measurement of the ^{98}Y fission yield and its isomer-to-ground state ratio, for which there exist no EXFOR-compiled measurements. The fission yields of ^{98g}Y and ^{98m}Y have been identified as contributors to the reactor antineutrino anomaly [204] and this new information may contribute to a better understanding of that problem.

The presented results were compared to the ENDF/B-VIII.0 and JEFF-3.3 evaluations and EXFOR-compiled measurements where available. The analysis of these data showcases a new method of fission yield determination. The FIER code is used as a model of time-dependent fission product γ-ray emission and a χ^2 minimization is performed to determine fission yield and nuclear decay data values simultaneously. This novel method automatically implements complete decay corrections, allows the investigation and correction of discrepant decay data (namely decay γ intensities), and has the potential to provide fission yield covariance information.

An important value of this work is that a detailed characterization of the incident neutron energy spectrum is provided. As was mentioned in Sec. 3.2.2 of the fission yields template, a majority of legacy fission yield measurements have not reported detailed information on the incident neutron energy spectrum. This has resulted in limiting the energy dependence of past fission yield evaluations to three loosely defined energy groupings. For future fission yield evaluations to properly assess energy dependence, scientists must provide detailed information on the incident neutron energy spectra used in measurements. This work provides that information.

This experiment provides an energy-integral measurement of fission yields. Other efforts are being made to measure energy-differential fission yields using quasi-monoenergetic neutron sources [106]. The results of those measurements can be compared with the energy-integral measurements reported in this work as a validation step in fission yield evaluation.

While this measurement does not provide energy-differential fission yield information, the use of a high-flux neutron source allows sufficient statistics to be generated with short burst irradiation periods (1 s and 5 s) and long counting/decay periods (25 s and 125 s). This allows high sensitivity to very short-lived fission product yields. The value of the FLUFFY pneumatic system has been validated by the ability to measure very short-lived fission yields. The yields for fission products with half-lives as low as 0.5 s were measured.

This dataset contains a rich array of information available for further analysis. Possible

future work to enable the use of FLUFFY and its neutron source for fissile actinide measurements and to expand the number of mass chains analyzed was discussed in Sec. 5.3.6. The results presented offer new measurements of fission product yields and validate the efficacy of a novel fission yield analysis method.

Chapter 6

Conclusions

Despite being discovered less than a century ago, the fission process is already used in a number of applications with important societal benefits. However, there remains significant uncertainty in the nuclear data related to fission. This is particularly true of the nuclear data of fission yields, as was discussed in Sec. 1.2. This work has improved the state of fission yield nuclear data through three original research projects: a template of expected measurement uncertainties in fission yields, a method for the estimation of fission yield covariances, and a measurement of short-lived fission product yields.

First, the template of expected measurement uncertainties in fission yields provides an extensive review of the current state-of-the-art in fission yield measurement. Using this review, a series of templates of expected measurement uncertainties was assembled. These templates offer an extensive listing of the sources of uncertainty that are expected to be present in commonly used techniques for fission yield measurement. Peer-reviewed literature, the EXFOR database, and expert consultation were used to compile a set of expected minimum values for these uncertainty sources.

Together, the templates and their expected values offer both experimentalists and evaluators a manual to guide their research. For experimentalists, the templates can be used in planning experiments and the subsequent analysis of the data. Experimentalists can further use the templates to configure their experiments to enable accurate estimation of all sources of uncertainty. For evaluators, the templates can be used to aid the understanding of the sources of uncertainty that are expected from different measurement types. It can also help in assessing the quality of different measurements and, as a last resort, can be used to fill in missing uncertainty information in legacy measurements. Though it should be used as a final recourse, the ability to assign reasonable values in the case of missing measurement uncertainty for legacy data is particularly important in the case of fission yields, as many legacy measurements only reported statistical uncertainties. Journal editors are being engaged to establish procedures for using the templates in their peer-review processes. As the templates come into use, they will improve the quality of both experiments and evaluations

and thus will improve the state of fission yield nuclear data as a whole.

Second, a pressing fission yield nuclear data need has been met: estimated covariance information for evaluated fission yields. Neither the most recent ENDF/B-VIII.0 nor JEFF-3.3 fission yield evaluations contain covariance information. This nuclear data need has been identified as crucial for reactor decay heat and reactor antineutrino emission rate calculations. To address this need, a method for fission-model-independent estimation of fission yield covariances was developed. This method uses a Monte-Carlo resampling structure that produces fission yields varied from their evaluated values.

While other fission yield covariance estimation methods have been proposed (as discussed in Sec. 4.1), these methods are based on different models of fission and thus are only applicable where model parameters are available. Because the method presented in this dissertation does not have an underlying model of fission, it was successfully applied to all of the nuclei in the ENDF/B-VIII.0 and JEFF-3.3 evaluations. Moreover, none of these previous publications provided open access to their covariance matrices. The presented covariance matrices have been made publicly available for use by the nuclear science community.

Finally, a new measurement of fission product yields using cyclical neutron activation analysis with the recently constructed FLUFFY was performed. Eight fission yields, including two isomer-to-ground state ratios, were reported. Three of these fission yields do not have EXFOR-compiled previous measurements.

In addition to the reported fission yields, a new method for fission yield determination was presented. This method used the FIER code as a model for fission product γ-ray emission and a χ^2 minimization is performed to determine optimal fission yields and nuclear decay data. A number of benefits are offered by this novel method: complete decay corrections, correction of discrepant decay data, and fission covariance estimation within the same experiment.

Continuous improvement of fission yield nuclear data is vital to enabling applications such as reactor design, nuclear forensics and safeguards, nuclear medicine, and stockpile stewardship. The three research projects presented in this dissertation all make contributions toward the current understanding of fission yields. Taken together, these results advance the current state of fission yield nuclear data.

Bibliography

[1] L. A. Bernstein et al. *Nuclear Data Needs for Capabilities and Applications*. Tech. rep. LLNL-CONF-676585. Berkeley, CA: Lawrence Livermore National Laboratory, 2015. DOI: 10.2172/1234359. arXiv: 1511.07772.

[2] C. E. Romano et al. *Proceedings of the Workshop for Applied Nuclear Data: WANDA 2020*. Tech. rep. ORNL/TM-2020/1617. Oakridge National Laboratory, Aug. 2020. DOI: 10.2172/1649010.

[3] L. A. Bernstein et al. "Our Future Nuclear Data Needs". In: *Annual Review of Nuclear and Particle Science* 69.1 (2019), pp. 109–136. DOI: 10.1146/annurev-nucl-101918-023708.

[4] *The TRIGRESS Array at TRIUMF*. 2010. URL: http://www.sfu.ca/~caa12/NuclearScienceSFU/tigress.html (visited on 04/03/2021).

[5] *How Complex Is the Nuclear Fission Barrier? A Challenge for Nuclear Fission Theory*. 2016. URL: https://ec.europa.eu/jrc/en/science-update/how-complex-nuclear-fission-barrier-challenge-nuclear-fission-theory (visited on 04/03/2021).

[6] V. V. Zerkin. *Evaluated Nuclear Data File (ENDF)*. 2018. URL: https://www.nndc.bnl.gov/exfor/endf00.jsp (visited on 04/03/2021).

[7] R. Mosteller and J. M. Goda. "Analysis of Godiva-IV Delayed-Critical and Static Super-prompt-critical Conditions". In: 2009. URL: https://www.semanticscholar.org/paper/Analysis-of-Godiva-IV-delayed-critical-and-static-Mosteller-Goda/019e6c49ee78a3e3f5e93ce72ecc7b947c4a5ec6.

[8] J. Sanborn. *Sanborn Critical Assembly Installation*. 2007. URL: https://commons.wikimedia.org/wiki/File:Sanborn_Critical_Assembly_Installation.jpg (visited on 04/03/2021).

[9] P. Romojaro et al. "Nuclear Data Sensitivity and Uncertainty Analysis of Effective Neutron Multiplication Factor in Various MYRRHA Core Configurations". In: *Annals of Nuclear Energy* 101 (2017), pp. 330–338. ISSN: 0306-4549. DOI: 10.1016/j.anucene.2016.11.027.

[10] R. ul Khaliq. *South Korea: Nuclear Reactor Shut After "Malfunction"*. 2019. URL: https://www.aa.com.tr/en/asia-pacific/south-korea-nuclear-reactor-shut-after-malfunction-/1419440 (visited on 04/03/2021).

[11] K. S. Krane and D. Halliday. *Introductory Nuclear Physics*. 3rd ed. Wiley, 1988.

[12] B. Pritychenko et al. "The Nuclear Science References (NSR) Database and Web Retrieval System". In: *Nuclear Instruments and Methods in Physics Research Section A: Accelerators, Spectrometers, Detectors and Associated Equipment* 640.1 (2011), pp. 213–218. ISSN: 0168-9002. DOI: 10.1016/j.nima.2011.03.018.

[13] V. V. Zerkin and B. Pritychenko. "The Experimental Nuclear Reaction Data (EXFOR): Extended Computer Database and Web Retrieval System". In: *Nuclear Instruments and Methods in Physics Research Section A: Accelerators, Spectrometers, Detectors and Associated Equipment* 888 (2018), pp. 31–43. DOI: 10.1016/j.nima.2018.01.045.

[14] D. F. Winchell. "New Web-Based Access to Nuclear Structure Datasets". In: *AIP Conference Proceedings*. Vol. 769. 1. American Institute of Physics. 2005, pp. 578–581. DOI: 10.1063/1.1945076.

[15] A. J. Koning and D. Rochman. "Modern Nuclear Data Evaluation with the TALYS Code System". In: *Nuclear Data Sheets* 113.12 (2012). Special Issue on Nuclear Reaction Data, pp. 2841–2934. ISSN: 0090-3752. DOI: 10.1016/j.nds.2012.11.002.

[16] T. Kawano. *Unified Coupled-Channels and Hauser-Feshbach Model Calculation for Nuclear Data Evaluation*. 2019. URL: https://arxiv.org/abs/1901.05641.

[17] M. Herman et al. "EMPIRE: Nuclear Reaction Model Code System for Data Evaluation". In: *Nuclear Data Sheets* 108.12 (2007). Special Issue on Evaluations of Neutron Cross Sections, pp. 2655–2715. ISSN: 0090-3752. DOI: 10.1016/j.nds.2007.11.003.

[18] R. Capote et al. "Inter-comparison of Hauser-Feshbach Model Codes Toward Better Actinide Evaluations". In: *EPJ Web Conf.* 146 (2017), p. 12034. DOI: 10.1051/epjconf/201714612034.

[19] L. P. Kabina, A. A. Rodionov, and Yu L. Khazov. "Improvement of the Algorithm for the Analysis of Level Schemes in the GTOL Code". In: *Bulletin of the Russian Academy of Sciences: Physics* 73.11 (2009), pp. 1469–1471. DOI: 10.3103/S1062873809110094.

[20] T. W. Burrows. *Program RULER*. Tech. rep. Brookhaven National Laboratory, 1984. URL: https://www-nds.iaea.org/public/ensdf_pgm/analysis/ruler/ruler.pdf.

[21] T. Kibèdi, F. G. Kondev, and B. Tee. *GABS v12*. Tech. rep. Australian National University, 2019. URL: https://www-nds.iaea.org/public/ensdf_pgm/analysis/gabs_test/2019_NSDD_GABS_Kibedi.pdf.

[22] T. Kibédi et al. "Evaluation of Theoretical Conversion Coefficients Using BrIcc". In: *Nuclear Instruments and Methods in Physics Research Section A: Accelerators, Spectrometers, Detectors and Associated Equipment* 589.2 (2008), pp. 202–229. ISSN: 0168-9002. DOI: 10.1016/j.nima.2008.02.051.

[23] N. B. Gove and M. J. Martin. "Log-f Tables for Beta Decay". In: *Atomic Data and Nuclear Data Tables* 10.3 (1971), pp. 205–219. ISSN: 0092-640X. DOI: 10.1016/S0092-640X(71)80026-8.

[24] S. Singh et al. "Nuclear Radius Parameters (r_0) for Even-Even Nuclei from Alpha Decay". In: *Nuclear Data Sheets* 167 (2020), pp. 1–35. ISSN: 0090-3752. DOI: 10.1016/j.nds.2020.07.001.

[25] V. McLane. *ENDF-102 Data Formats and Procedures for the Evaluated Nuclear Data File ENDF-6*. Tech. rep. Brookhaven National Laboratory, 2001. DOI: 10.2172/781830.

[26] J. K. Tuli. "Evaluated Nuclear Structure Data File". In: *Nuclear Instruments and Methods in Physics Research Section A: Accelerators, Spectrometers, Detectors and Associated Equipment* 369.2 (1996), pp. 506–510. ISSN: 0168-9002. DOI: 10.1016/S0168-9002(96)80040-4.

[27] D. A. Brown et al. *Specifications for the Generalised Nuclear Database Structure (GNDS)-Version 1.9*. Tech. rep. NEA–7519. Nuclear Energy Agency - Organization for Economic Co-Operation and Development, 2020. URL: https://inis.iaea.org/search/search.aspx?orig_q=RN:51092137.

[28] D. A. Brown et al. "ENDF/B-VIII.0: The 8th Major Release of the Nuclear Reaction Data Library with CIELO-project Cross Sections, New Standards and Thermal Scattering Data". In: *Nuclear Data Sheets* 148 (2018). Special Issue on Nuclear Reaction Data, pp. 1–142. ISSN: 0090-3752. DOI: 10.1016/j.nds.2018.02.001.

[29] A. J. M. Plompen et al. "The Joint Evaluated Fission and Fusion Nuclear Data Library, JEFF-3.3". In: *The European Physical Journal A* 56.7 (2020), pp. 1–108. DOI: 10.1140/epja/s10050-020-00141-9.

[30] K. Shibata et al. "JENDL-4.0: A New Library for Nuclear Science and Engineering". In: *Journal of Nuclear Science and Technology* 48.1 (2011), pp. 1–30. DOI: 10.1080/18811248.2011.9711675.

[31] Z. G. Ge et al. "The Updated Version of Chinese Evaluated Nuclear Data Library (CENDL-3.1)". In: *J. Korean Phys. Soc* 59.2 (2011), pp. 1052–1056. DOI: 10.3938/jkps.59.1052.

[32] Z. G. Ge et al. "CENDL-3.2: The New Version of Chinese General Purpose Evaluated Nuclear Data Library". In: *EPJ Web of Conferences*. Vol. 239. EDP Sciences. 2020, p. 09001. DOI: 10.1051/epjconf/202023909001.

[33] A. I. Blokhin et al. "New Version of Neutron Evaluated Data Library BROND-3.1". In: *Yad. Reak. Konst* 2.2 (2016), p. 62. URL: https://vant.ippe.ru/images/pdf/2016/2-5.pdf.

[34] A. J. Koning et al. "TENDL: Complete Nuclear Data Library for Innovative Nuclear Science and Technology". In: *Nuclear Data Sheets* 155 (2019). Special Issue on Nuclear Reaction Data, pp. 1–55. ISSN: 0090-3752. DOI: 10.1016/j.nds.2019.01.002.

[35] R. Capote et al. "RIPL - Reference Input Parameter Library for Calculation of Nuclear Reactions and Nuclear Data Evaluations". In: *Nuclear Data Sheets* 110.12 (2009). Special Issue on Nuclear Reaction Data, pp. 3107–3214. ISSN: 0090-3752. DOI: 10.1016/j.nds.2009.10.004.

[36] R. B. Firestone et al. "The Evaluated Gamma-ray Activation File (EGAF)". In: *AIP Conference Proceedings*. Vol. 769. 1. American Institute of Physics. 2005, pp. 219–224. DOI: 10.1063/1.1944994.

[37] T. Goorley et al. "Initial MCNP6 Release Overview". In: *Nuclear Technology* 180.3 (2012), pp. 298–315. DOI: 10.13182/NT11-135.

[38] S. M. Bowman. "SCALE 6: Comprehensive Nuclear Safety Analysis Code System". In: *Nuclear Technology* 174.2 (2011), pp. 126–148. DOI: 10.13182/NT10-163.

[39] J. J. Duderstadt. *Nuclear Reactor Analysis*. Wiley, 1976.

[40] J. B. Briggs, J. D. Bess, and J. Gulliford. "Integral Benchmark Data for Nuclear Data Testing Through the ICSBEP and IRPhEP". In: *Nuclear Data Sheets* 118 (2014), pp. 396–400. ISSN: 0090-3752. DOI: 10.1016/j.nds.2014.04.090.

[41] O. Schwerer. *EXFOR Formats Description for Users (EXFOR Basics)*. Tech. rep. IAEA-NDS-206. International Atomic Energy Agency, 2008. URL: https://www-nds.iaea.org/nrdc/nrdc_doc/iaea-nds-0206-200806.pdf.

[42] R. W. Mills. *WPEC Subgroup Proposal*. Tech. rep. Nuclear Energy Agency - Organization for Economic Co-operation and Development, 2012. URL: https://www.oecd-nea.org/science/wpec/sg37/SG37.pdf.

[43] G. Fabricante et al. "Cumulative Fission Yield Correlations". In: *US National Nuclear Data Week*. 2019. URL: https://indico.bnl.gov/event/6642/contributions/32356/.

[44] A. A. Sonzogni and E. A. McCutchan. "Uncertainty Quantification in the Summation Method for Nuclear Reactor Antineutrinos". In: *American Physical Society April Meeting*. Denver, Colorado: American Physical Society, 2019. URL: http://meetings.aps.org/Meeting/APR19/Session/H12.5.

[45] F. P. An et al. "Measurement of the Reactor Antineutrino Flux and Spectrum at Daya Bay". In: *Physical Review Letters* (2016). ISSN: 10797114. DOI: 10.1103/PhysRevLett.116.061801.

[46] F. P. An et al. "Evolution of the Reactor Antineutrino Flux and Spectrum at Daya Bay". In: *Physical Review Letters* (2017). ISSN: 10797114. DOI: 10.1103/PhysRevLett.118.251801.

[47] L. Fiorito et al. "Generation of Fission Yield Covariances to Correct Discrepancies in the Nuclear Data Libraries". In: *Annals of Nuclear Energy* (2016). ISSN: 18732100. DOI: 10.1016/j.anucene.2015.10.027.

[48] T. San-Tsiang et al. "Ternary and Quaternary Fission of Uranium Nuclei". In: *Nature* 159.4049 (1947), pp. 773–774. DOI: 10.1038/159773a0.

[49] F. Gönnenwein. "Ternary and Quaternary Fission". In: *Nuclear Physics A* 734 (2004), pp. 213–216. DOI: 10.1016/j.nuclphysa.2004.01.037.

[50] S. Pomp. *Fission (A Brief Introduction)*. 2018. URL: https://indico.cern.ch/event/677259/contributions/2786820/attachments/1585962/2507547/n_TOF_2018_-_Fission_Intro.pdf.

[51] *Nucleus Drawing*. URL: https://commons.wikimedia.org/wiki/File:Nucleus_drawing.svg#metadata (visited on 06/04/2021).

[52] F. Videbæk et al. "Elastic Scattering, Transfer Reactions, and Fission Induced by ^{16}O ions on ^{181}Ta and ^{208}Pb". In: *Phys. Rev. C* 15 (3 Mar. 1977), pp. 954–971. DOI: 10.1103/PhysRevC.15.954.

[53] B. Singh, R. Zywina, and R. B. Firestone. "Table of Superdeformed Nuclear Bands and Fission Isomers: Third Edition (October 2002)". In: *Nuclear Data Sheets* 97.2 (2002), pp. 241–592. ISSN: 0090-3752. DOI: 10.1006/ndsh.2002.0018.

[54] I. Noddack. "Über das Element 93". In: *Angew. Chem* 47.37 (1934), pp. 653–656.

[55] I. Curie and P. Savitch. "Sur les radioéléments formés dans l'uranium irradié par les neutrons". In: *Journal de Physique et le Radium* 8.10 (1937), pp. 385–387. DOI: 10.1051/jphysrad:01937008010038500.

[56] I. Curie and P. Savitch. "Sur le radioélément de période 3, 5 heures formé dans l'uranium irradié par les neutrons". In: *CR Acad. Sci* 206 (1938), p. 906.

[57] I. Curie and P. Savitch. "Sur les radioéléments formés dans l'uranium irradié par les neutrons. II". In: *Journal de Physique et le Radium* 9.9 (1938), pp. 355–359. DOI: 10.1051/jphysrad:0193800909035500.

[58] O. Hahn and F. Strassmann. "Über den Nachweis und das Verhalten der bei der Bestrahlung des Urans mittels Neutronen entstehenden Erdalkalimetalle". In: *Naturwissenschaften* 27.1 (1939), pp. 11–15. DOI: 10.1007/BF01488241.

[59] L. Meitner and O. R. Frisch. "Disintegration of Uranium by Neutrons: A New Type of Nuclear Reaction". In: *Nature* 143.3615 (1939), pp. 239–240. DOI: 10.1038/143239a0.

[60] H. L. Anderson et al. "The Fission of Uranium". In: *Phys. Rev.* 55 (5 Mar. 1939), pp. 511–512. DOI: 10.1103/PhysRev.55.511.2.

[61] H. Von Halban, F. Joliot, and L. Kowarski. "Number of Neutrons Liberated in the Nuclear Fission of Uranium". In: *Nature* 143.3625 (1939), pp. 680–680. DOI: 10.1038/143680a0.

[62] L. Szilárd and A. Einstein. *Einstein–Szilárd Letter*. Private Communication. Franklin D. Roosevelt Presidential Library and Museum. URL: https://commons.wikimedia.org/wiki/File:Einstein-Roosevelt-letter.png.

[63] C. Allardice and E. R. Trapnell. *The First Pile*. Vol. 292. US Atomic Energy Commission. Technical Information Division, 1949.

[64] K. T. Bainbridge. *Trinity*. Tech. rep. Los Alamos Scientific Lab., NM (USA), 1976. DOI: 10.2172/5306263.

[65] R. Michal. "Fifty Years Ago in December: Atomic Reactor EBR-I Produced First Electricity". In: *Nuclear News* 44.12 (2001), pp. 28–29. URL: https://www.ne.anl.gov/About/reactors/ebr1/2001-11-2.pdf.

[66] S. Krikorian. *Preliminary Nuclear Power Facts and Figures for 2019*. 2020. URL: https://www.iaea.org/newscenter/news/preliminary-nuclear-power-facts-and-figures-for-2019 (visited on 06/16/2021).

[67] G. Gamow. "Mass Defect Curve and Nuclear Constitution". In: *Proceedings of the Royal Society of London. Series A, Containing Papers of a Mathematical and Physical Character* 126.803 (1930), pp. 632–644. DOI: 10.1098/rspa.1930.0032.

[68] C. F. von Weizsäcker. "Zur theorie der kernmassen". In: *Zeitschrift für Physik* 96.7-8 (1935), pp. 431–458. DOI: 10.1007/BF01337700.

[69] M. G. Mayer. "On Closed Shells in Nuclei. II". In: *Phys. Rev.* 75 (12 June 1949), pp. 1969–1970. DOI: 10.1103/PhysRev.75.1969.

[70] M. G. Mayer. "On Closed Shells in Nuclei". In: *Phys. Rev.* 74 (3 Aug. 1948), pp. 235–239. DOI: 10.1103/PhysRev.74.235.

[71] R. D. Woods and D. S. Saxon. "Diffuse Surface Optical Model for Nucleon-Nuclei Scattering". In: *Phys. Rev.* 95 (2 July 1954), pp. 577–578. DOI: 10.1103/PhysRev.95.577.

[72] J. Rainwater. "Nuclear Energy Level Argument for a Spheroidal Nuclear Model". In: *Phys. Rev.* 79 (3 Aug. 1950), pp. 432–434. DOI: 10.1103/PhysRev.79.432.

[73] A. Bohr and B. R. Mottelson. "Rotational States in Even-Even Nuclei". In: *Phys. Rev.* 90 (4 May 1953), pp. 717–719. DOI: 10.1103/PhysRev.90.717.2.

[74] A. Bohr and B. R. Mottelson. "Interpretation of Isomeric Transitions of Electric Quadrupole Type". In: *Phys. Rev.* 89 (1 Jan. 1953), pp. 316–317. DOI: 10.1103/PhysRev.89.316.

[75] T. Huus and C. Župančić. *Excitation of Nuclear Rotational States by the Electric Field of Impinging Particles*. Munksgaard, 1953.

[76] S. G. Nilsson. *Binding States of Individual Nucleons in Strongly Deformed Nuclei*. Tech. rep. CERN-55-30. The European Organization for Nuclear Research, 1955, pp. 1–69. URL: https://cds.cern.ch/record/212345?ln=en.

[77] C. Gustafson et al. "Nuclear Deformabilities in the Rare-Earth and Actinide Regions with Excursions Off the Stability Line and into the Super-heavy Region". In: *Ark. Fys.* 63 (1967).

[78] S. A. E. Johansson. "Nuclear Octupole Deformation and the Mechanism of Fission". In: *Nuclear Physics* 22.4 (1961), pp. 529–552. ISSN: 0029-5582. DOI: 10.1016/0029-5582(61)90467-9.

[79] V. M. Strutinsky. "Shell Effects in Nuclear Masses and Deformation Energies". In: *Nuclear Physics A* 95.2 (1967), pp. 420–442. ISSN: 0375-9474. DOI: 10.1016/0375-9474(67)90510-6.

[80] S. Frankel and N. Metropolis. "Calculations in the Liquid-Drop Model of Fission". In: *Phys. Rev.* 72 (10 Nov. 1947), pp. 914–925. DOI: 10.1103/PhysRev.72.914.

[81] A. G. Magner et al. "Shell Structure and Orbit Bifurcations in Finite Fermion Systems". In: *Physics of Atomic Nuclei* 74.10 (2011), pp. 1445–1477. DOI: 10.1134/S1063778811100061.

[82] N. Schunck and L. M. Robledo. "Microscopic Theory of Nuclear Fission: A Review". In: *Reports on Progress in Physics* 79.11 (Oct. 2016), p. 116301. DOI: 10.1088/0034-4885/79/11/116301.

[83] K.-H. Schmidt and B. Jurado. "Review on the Progress in Nuclear Fission - Experimental Methods and Theoretical Descriptions". In: *Reports on Progress in Physics* 81.10 (Sept. 2018), p. 106301. DOI: 10.1088/1361-6633/aacfa7.

[84] A. C. Wahl. *Nuclear-charge Distribution and Delayed-neutron Yields for Thermal-neutron-induced Fission of 235U, 233U, and 239Pu and for Spontaneous Fission of 252Cf*. 1988. DOI: 10.1016/0092-640X(88)90016-2.

[85] A. C. Wahl and A. D. Carlson. "Nuclear-charge and Mass Distributions from Fission". In: *Fifty Years with Nuclear Fission*. American Nuclear Society, 1989. URL: https://inis.iaea.org/search/searchsinglerecord.aspx?recordsFor=SingleRecord&RN=23024110.

[86] T. R. England and B. F. Rider. *Evaluation and Compilation of Fission Product Yields*. Tech. rep. LA-UR-94-3106. Los Alamos National Laboratory, 1994. URL: https://t2.lanl.gov/nis/publications/endf349.pdf.

[87] D. G. Madland and T. R. England. *Distribution of Independent Fission-Product Yields to Isomeric States*. Tech. rep. LA-6595-MS. Los Alamos National Laboratory, 1976. DOI: 10.2172/7222873.

[88] D. G. Madland and T. R. England. "Influence of Isomeric States on Independent Fission Product Yields". In: *Nuclear Science and Engineering* 64 (1977), pp. 859–865. ISSN: 00295639. DOI: 10.13182/NSE77-A14501.

[89] K.-H. Schmidt et al. "General Description of Fission Observables: GEF Model Code". In: *Nuclear Data Sheets* 131 (2016). Special Issue on Nuclear Reaction Data, pp. 107–221. ISSN: 0090-3752. DOI: 10.1016/j.nds.2015.12.009.

[90] S. Okumura et al. "235U(n, f) Independent Fission Product Yield and Isomeric Ratio Calculated with the Statistical Hauser–Feshbach Theory". In: *Journal of Nuclear Science and Technology* 55.9 (2018), pp. 1009–1023. DOI: 10.1080/00223131.2018.1467288.

[91] A. E. Lovell et al. "Extension of the Hauser-Feshbach Fission Fragment Decay Model to Multichance Fission". In: *Phys. Rev. C* 103 (1 Jan. 2021), p. 014615. DOI: 10.1103/PhysRevC.103.014615.

[92] A. E. Lovell. *Towards a Consistent Evaluation of Fission Observables*. Tech. rep. LA-UR-21-21339. Los Alamos National Laboratory, 2020. URL: https://ncsp.llnl.gov/TPRAgendas/2021/50_NSCPTRP_FY20_Lovell.pdf.

[93] P. Talou, T. Kawano, and I. Stetcu. *CGMF User Manual*. Tech. rep. LA-UR-14-24031. Los Alamos National Laboratory, 2014. URL: https://readthedocs.org/projects/cgmf-documentation/downloads/pdf/latest/.

[94] P. Jaffke. "Identifying Inconsistencies in Fission Product Yield Evaluations with Prompt Neutron Emission". In: *Nuclear Science and Engineering* 190.3 (2018), p. 258. ISSN: 00295639. DOI: 10.1080/00295639.2018.1429173.

[95] J. M. Verbeke, J. Randrup, and R. Vogt. "Fission Reaction Event Yield Algorithm, FREYA — For Event-by-Event Simulation of Fission". In: *Computer Physics Communications* 191 (2015), pp. 178–202. ISSN: 0010-4655. DOI: 10.1016/j.cpc.2015.02.002.

[96] J. M. Verbeke, J. Randrup, and R. Vogt. "Fission Reaction Event Yield Algorithm FREYA 2.0.2". In: *Computer Physics Communications* 222 (2018), pp. 263–266. ISSN: 0010-4655. DOI: 10.1016/j.cpc.2017.09.006.

[97] S. Agostinelli et al. "GEANT4—A Simulation Toolkit". In: *Nuclear Instruments and Methods in Physics Research Section A: Accelerators, Spectrometers, Detectors and Associated Equipment* 506.3 (2003), pp. 250–303. ISSN: 0168-9002. DOI: 10.1016/S0168-9002(03)01368-8.

[98] D. Neudecker et al. "Templates of Expected Measurement Uncertainties". Submitted.

[99] D. Neudecker et al. "The Need for Precise and Well-documented Experimental Data on Prompt Fission Neutron Spectra from Neutron-induced Fission of 239Pu". In: *Nuclear Data Sheets* 131 (2016). Special Issue on Nuclear Reaction Data, pp. 289–318. ISSN: 0090-3752. DOI: 10.1016/j.nds.2015.12.005.

[100] D. Neudecker et al. "Applying a Template of Expected Uncertainties to Updating 239Pu(n,f) Cross-section Covariances in the Neutron Data Standards Database". In: *Nuclear Data Sheets* 163 (2020), pp. 228–248. ISSN: 0090-3752. DOI: 10.1016/j.nds.2019.12.005.

[101] A. N. Andreyev, K. Nishio, and K. H. Schmidt. "Nuclear Fission: A Review of Experimental Advances and Phenomenology". In: *Reports on Progress in Physics* 81 (2018), p. 106301. ISSN: 00344885. DOI: 10.1088/1361-6633/aa82eb.

[102] K.-H. Schmidt and B. Jurado. "Review on the Progress in Nuclear Fission - Experimental Methods and Theoretical Descriptions". In: *Reports on Progress in Physics* 81 (2018), p. 106301. ISSN: 00344885. DOI: 10.1088/1361-6633/aacfa7.

[103] W. Younes, J. J. Ressler, and J. A. Becker. *Survey of Fission-yield Studies Based on Non-destructive Gamma-ray Spectrometry*. Tech. rep. LLNL-TR-648488. Lawrence Livermore National Laboratory, 2014.

[104] S. Stave et al. "Reducing Uncertainties for Short Lived Cumulative Fission Product Yields". In: *Journal of Radioanalytical and Nuclear Chemistry* 307.3 (2016), pp. 2221–2225. ISSN: 1588-2780. DOI: 10.1007/s10967-015-4436-3.

[105] B. D. Pierson et al. "Fission Product Yields from 232Th, 238U, and 235U Using 14 MeV Neutrons". In: *Nuclear Data Sheets* 139 (2017), pp. 171–189. ISSN: 00903752. DOI: 10.1016/j.nds.2017.01.004.

[106] M. A. Stoyer et al. "Fission Product Yield Measurements from Neutron-Induced Fission of 235,238 U and 239 Pu". In: *EPJ Web of Conferences* 232 (2020), p. 03006. DOI: 10.1051/epjconf/202023203006.

[107] M. A. Cognet and V. Gressier. "Development of a Measurement Reference Standard for Neutron Energies between 1 MeV and 20 MeV Using Time of Flight Method at the AMANDE Facility". In: *Metrologia* 47.4 (2010), pp. 377–386. ISSN: 00261394. DOI: 10.1088/0026-1394/47/4/004.

[108] L. R. Greenwood and C. D. Johnson. *User Guide for the STAYSL PNNL Suite of Software Tools*. Tech. rep. PNNL-22253. 2013. URL: https://www.pnnl.gov/main/publications/external/technical_reports/pnnl-22253.pdf.

[109] A. Trkov et al. "IRDFF-II: A New Neutron Metrology Library". In: *Nuclear Data Sheets* 163 (2020), pp. 1–108. ISSN: 00903752. DOI: 10.1016/j.nds.2019.12.001. arXiv: 1909.03336.

[110] A. Bail et al. "Isotopic Yield Measurement in the Heavy Mass Region for 239Pu Thermal Neutron Induced Fission". In: *Physical Review C - Nuclear Physics* 84 (2011), p. 034605. ISSN: 1089490X. DOI: 10.1103/PhysRevC.84.034605.

[111] S. Prakash and S. B. Manohar. "Radiochemical Methods of Measurements of Fission Products Yields". In: *Journal of Radioanalytical and Nuclear Chemistry Articles* 142.1 (1990), pp. 119–133. ISSN: 02365731. DOI: 10.1007/BF02039457.

[112] C. Bhatia et al. "Dual-fission Chamber and Neutron Beam Characterization for Fission Product Yield Measurements Using Monoenergetic Neutrons". In: *Nuclear Instruments and Methods in Physics Research, Section A: Accelerators, Spectrometers, Detectors and Associated Equipment* 757 (2014), pp. 7–19. ISSN: 01689002. DOI: 10.1016/j.nima.2014.03.022.

[113] C. Bhatia et al. "Exploratory Study of Fission Product Yields of Neutron-induced Fission of 235U, 238U, and 239Pu at 8.9 MeV". In: *Physical Review C* 91 (2015), p. 064604. ISSN: 0556-2813. DOI: 10.1103/PhysRevC.91.064604.

[114] D. Chaillou and A. Chambaudet. "Statistics of Uranium Fission-track Counting". In: *Nuclear Tracks* 5 (1981), pp. 93–98. ISSN: 0191278X. DOI: 10.1016/0191-278X(81)90031-7.

[115] J. Lippold et al. "Automatic Counting of Fission Tracks Using Object-based Image Analysis for Dating Applications". In: *International Geoscience and Remote Sensing Symposium (IGARSS)*. 2007, pp. 440–443. ISBN: 1424412129. DOI: 10.1109/IGARSS.2007.4422825.

[116] J. Kučera, P. Bode, and Stepanek V. "The 1993 ISO Guide to the Expression of Uncertainty in Measurement Applied to NAA". In: *Journal of Radioanalytical and Nuclear Chemistry* 245.1 (2000), pp. 115–122. DOI: 10.1023/A:1006760726572.

[117] *ISO 21748:2017 - Guidance for the Use of Repeatability, Reproducibility and Trueness Estimates in Measurement Uncertainty Evaluation*. Tech. rep. ISO 21748:2017. International Organization for Standardization, 2017. URL: https://www.iso.org/standard/71615.html.

[118] T. Saffaj et al. "An Overall Uncertainty Approach for the Validation of Analytical Separation Methods". In: *Analyst* 138.16 (2013), pp. 4677–4691. ISSN: 13645528. DOI: 10.1039/c3an00519d.

[119] J. A. Petruska, H. G. Thode, and R. H. Tomlinson. "The Absolute Fission Yields of Twenty-eight Mass Chains in the Thermal Neutron Fission of U235". In: *Canadian Journal of Physics* 33 (1955), pp. 693–706. ISSN: 0008-4204. DOI: 10.1139/p55-085.

[120] K. Knie et al. "Search for A = 60 Fragments from Neutron-induced Fission with Accelerator Mass Spectrometry". In: *Nuclear Physics A* 723 (2003), pp. 343–353. ISSN: 03759474. DOI: 10.1016/S0375-9474(03)01435-0.

[121] S. Ayet San Andrés et al. "High-resolution, Accurate Multiple-reflection Time-of-flight Mass Spectrometry for Short-lived, Exotic Nuclei of a Few Events in Their Ground and Low-lying Isomeric States". In: *Physical Review C* 99 (2019), p. 064313. ISSN: 24699993. DOI: 10.1103/PhysRevC.99.064313.

[122] F. L. Lisman et al. "Fission Yields of Over 40 Stable and Long-Lived Fission Products for Thermal Neutron Fissioned 233U, 235U, 239Pu, and 241Pu and Fast Reactor Fissioned 235U and 239Pu". In: *Nuclear Science and Engineering* 42 (1970), pp. 191–214. ISSN: 0029-5639. DOI: 10.13182/nse70-a19500.

[123] W. J. Maeck et al. *The Measurement of Ruthenium in Uranium Ores and 238U Spontaneous Fission Yields*. International Atomic Energy Agency (IAEA): International Atomic Energy Agency, 1978. ISBN: 92-0-051078-7. URL: http://inis.iaea.org/search/search.aspx?orig_q=RN:10479619.

[124] I. Glagolenko et al. "Fission Yield Measurements by Inductively Coupled Plasma Mass-spectrometry". In: *Journal of Radioanalytical and Nuclear Chemistry* 282.2 (2009), p. 651. ISSN: 1588-2780. DOI: 10.1007/s10967-009-0209-1.

[125] C. Schmitt et al. "Fission Yields at Different Fission-product Kinetic Energies for Thermal-neutron-induced Fission of 239Pu". In: *Nuclear Physics, Section A* 430 (1984), pp. 21–60. ISSN: 03759474. DOI: 10.1016/0375-9474(84)90191-X.

[126] R. M. Essex and S. A. Goldberg. "Calculating Measurement Uncertainties for Mass Spectrometry Data". In: *AGU Fall Meeting Abstracts*. Vol. 2006. Dec. 2006, V11E–07. URL: https://ui.adsabs.harvard.edu/abs/2006AGUFM.V11E..07E.

[127] R. B. Thomas, R. M. Essex, and S. A. Goldberg. "Alternative Approaches to Uncertainty Calculations for TIMS Isotopic Measurements". In: *AGU Fall Meeting Abstracts*. Vol. 2006. Dec. 2006, V21A–0554. URL: https://ui.adsabs.harvard.edu/abs/2006AGUFM.V21A0554T.

[128] Jochen Vogl. "Measurement Uncertainty in Single, Double and Triple Isotope Dilution Mass Spectrometry". In: *Rapid Communications in Mass Spectrometry* 26.3 (Feb. 2012), pp. 275–281. ISSN: 0951-4198. DOI: 10.1002/rcm.5306.

[129] T. Williams et al. *Evaluation of Measurement Data — An Introduction to the "Guide to the Expression of Uncertainty in Measurement" and Related Documents*. Tech. rep. JCGM 100:2008. International Organization for Standardization Geneva, 2008. URL: https://www.bipm.org/documents/20126/2071204/JCGM_100_2008_E.pdf.

[130] S. Bürger et al. "Implementation of Guide to the expression of Uncertainty in Measurement (GUM) to multi-collector TIMS uranium isotope ratio metrology". In: *International Journal of Mass Spectrometry* 294 (2010), pp. 65–76. ISSN: 13873806. DOI: 10.1016/j.ijms.2010.05.003.

[131] K. Meierbachtol et al. "The SPIDER Fission Fragment Spectrometer for Fission Product Yield Measurements". In: *Nuclear Instruments and Methods in Physics Research, Section A: Accelerators, Spectrometers, Detectors and Associated Equipment* 788 (2015), pp. 59–66. ISSN: 01689002. DOI: 10.1016/j.nima.2015.02.032.

[132] K. Jansson et al. "The Impact of Neutron Emission on Correlated Fission Data from the 2E-2v Method". In: *European Physical Journal A* 54.6 (2018). ISSN: 1434601X. DOI: 10.1140/epja/i2018-12544-0.

[133] A. Al-Adili et al. "Impact of Prompt-neutron Corrections on Final Fission-fragment Distributions". In: *Physical Review C - Nuclear Physics* 86 (2012), p. 054601. ISSN: 1089490X. DOI: 10.1103/PhysRevC.86.054601.

[134] A. Al-Adili et al. "Studying Fission Neutrons with 2E-2v and 2E". In: *EPJ Web of Conferences*. Vol. 169. 2018, pp. 1–6. ISBN: 9782759890316. DOI: 10.1051/epjconf/201816900002.

[135] M. O. Frégeau and S. Oberstedt. "The Fission-fragment Spectrometer VERDI". In: *Physics Procedia*. Vol. 64. 2015, pp. 197–203. DOI: 10.1016/j.phpro.2015.04.027.

[136] A. Oed et al. "A Mass Spectrometer for Fission Fragments Based on Time-of-flight and Energy Measurements". In: *Nuclear Instruments and Methods In Physics Research* 219 (1984), pp. 569–574. ISSN: 01675087. DOI: 10.1016/0167-5087(84)90232-1.

[137] M. O. Frégeau et al. "First Results from the New Double Velocity-Double Energy Spectrometer VERDI". In: *Nuclear Instruments and Methods in Physics Research Section A* 817 (2016), pp. 35–41. ISSN: 0168-9002. DOI: 10.1016/j.nima.2016.02.011.

[138] A. Al-Adili et al. "Prompt Fission Neutron Yields in Thermal Fission of ^{235}U and Spontaneous Fission of ^{252}Cf". In: *Phys. Rev. C* 102 (6 Dec. 2020), p. 064610. DOI: 10.1103/PhysRevC.102.064610.

[139] M. B. Chadwick et al. "Fission Product Yields from Fission Spectrum n+239Pu for ENDF/B-VII.1". In: *Nuclear Data Sheets* 111.12 (2010), pp. 2923–2964. ISSN: 00903752. DOI: 10.1016/j.nds.2010.11.003.

[140] R. W. Mills. "Fission Product Yield Evaluation". PhD thesis. University of Birmingham, 1995. URL: http://etheses.bham.ac.uk/id/eprint/4353/.

[141] R. W. Mills. *Status of the UKFY3 Fission Yield Evaluation*. Tech. rep. The Nuclear Energy Agency, 2004. URL: https://www.oecd-nea.org/dbdata/nds_jefdoc/jefdoc-1031.pdf.

[142] J. Katakura et al. *JENDL FP Decay Data File 2000*. Tech. rep. 1343. Japan Atomic Energy Research Institute, 2001. URL: https://inis.iaea.org/collection/NCLCollectionStore/_Public/37/001/37001609.pdf.

[143] J. Katakura. *JENDL FP Decay Data File 2011 and Fission Yields Data File 2011*. Tech. rep. 2011-025. Japan Atomic Energy Agency, 2011. URL: https://jopss.jaea.go.jp/pdfdata/JAEA-Data-Code-2011-025.pdf.

[144] J. Katakura, F. Minato, and K. Ohgama. "Revision of the JENDL FP Fission Yield Data". In: *EPJ Web of Conferences* 111 (2016), pp. 2–7. ISSN: 2100014X. DOI: 10.1051/epjconf/201611108004.

[145] D. G. Madland and L. Stewart. *Light Ternary Fission Products: Probabilities and Charge Distributions*. Tech. rep. LA–6783-MS. Los Alamos National Laboratory, 1977. URL: https://inis.iaea.org/search/search.aspx?orig_q=RN:8342460.

[146] A. R. Musgrove, J. L. Cook, and G. D. Trimble. In: *Panel on Fission Product Nuclear Data*. 1973.

[147] M. R. Bhat. "Evaluated Nuclear Structure Data File (ENSDF)". In: *Nuclear Data for Science and Technology: Proceedings of an International Conference, held at the Forschungszentrum Jülich, Fed. Rep. of Germany, 13–17 May 1991*. Springer Berlin Heidelberg, 1992, pp. 817–821. ISBN: 978-3-642-58113-7. DOI: 10.1007/978-3-642-58113-7_227.

[148] J. C. Hardy et al. "The Essential Decay of Pandemonium: A Demonstration of Errors in Complex Beta-decay Schemes". In: *Physics Letters B* 71 (1977), pp. 307–310. ISSN: 03702693. DOI: 10.1016/0370-2693(77)90223-4.

[149] K. Takahashi, M. Yamada, and T. Kondoh. "Beta-decay Half-lives Calculated on the Gross Theory". In: 12 (1973), pp. 101–142. ISSN: 10902090. DOI: 10.1016/0092-640X(73)90015-6.

[150] D. M. Brink. PhD thesis. Oxford University, 1955.

[151] P. Axel. "Electric Dipole Ground-state Transition Width Strength Function and 7-MeV Photon Interactions". In: *Physical Review* 126 (1962), p. 671. ISSN: 0031899X. DOI: 10.1103/PhysRev.126.671.

[152] A. Gilbert and A. G. W. Cameron. "A Composite Nuclear-level Density Formula with Shell Corrections". In: *Canadian Journal of Physics* 43 (1965), pp. 1446–1496. ISSN: 0008-4204. DOI: 10.1139/p65-139.

[153] T. Yoshida, Y. Wakasugi, and N. Hagura. "Pandemonium Problem in Fission-product Decay Heat Calculations Revisited". In: *Journal of Nuclear Science and Technology* 45 (2008), pp. 713–717. ISSN: 00223131. DOI: 10.1080/18811248.2008.9711471.

[154] A. Algora et al. "Reactor Decay Heat in Pu239: Solving the Gamma Discrepancy in the 4-3000-s Cooling Period". In: *Physical Review Letters* 105 (2010), p. 202501. ISSN: 00319007. DOI: 10.1103/PhysRevLett.105.202501.

[155] O. Leray et al. "Fission Yield Covariances for JEFF: A Bayesian Monte Carlo Method". In: *EPJ Web of Conferences*. 2017. ISBN: 9782759890200. DOI: 10.1051/epjconf/201714609023.

[156] M. T. Pigni et al. "Applications of Decay Data and Fission Product Yield Covariance Matrices in Uncertainty Quantification on Decay Heat". In: *WPEC - Subgroup 37*. Nuclear Energy Agency - Organisation for Economic Co-operation and Development, 2013. URL: %7Bhttps://www.oecd-nea.org/science/wpec/sg37/Meetings/2013_May/32_Pigni_Cov.pdf%7D.

[157] T. Kawano and M. B. Chadwick. "Estimation of 239Pu Independent and Cumulative Fission Product Yields from the Chain Yield Data Using a Bayesian Technique". In: *Journal of Nuclear Science and Technology* 50 (2013), pp. 1034–1042. ISSN: 00223131. DOI: 10.1080/00223131.2013.830580.

[158] E. F. Matthews. *Reproducible Workflow for "Stochastically Estimated Covariance Matrices for Independent and Cumulative Fission Yields in the ENDF/B-VIII.0 and JEFF 3.1 Evaluations"*. 2020. DOI: 10.5281/zenodo.4580536. URL: https://github.com/efmatthews/FYCoM.

[159] W. Land. *Laser Interferometer Feedback Machine Positioning Uncertainty*. Tech. rep. Aerotech, 2016, pp. 1–8.

[160] A. Brusegan, G. Noguere, and F. Gunsing. "A Noise Analysis Approach for Measuring the Decay Constants and the Relative Abundance of Delayed Neutrons in a Zero Power Critical Facility". In: *Journal of Nuclear Science and Technology* 39 (2002), pp. 685–688. ISSN: 00223131. DOI: 10.1080/00223131.2002.10875192.

[161] S. Katcoff and W. Rubinson. "Yield of Xe133 in the Thermal Neutron Fission of U235". In: *Physical Review* 91 (1953), p. 1458. ISSN: 0031899X. DOI: 10.1103/PhysRev.91.1458.

[162] J. S. Coursey et al. *Atomic Weights and Isotopic Compositions (version 4.1)*. 2015. URL: https://www.nist.gov/pml/atomic-weights-and-isotopic-compositions-relative-atomic-masses.

[163] J. Meija et al. *Isotopic Compositions of the Elements 2013 (IUPAC Technical Report)*. 2016. DOI: 10.1515/pac-2015-0503.

[164] J. G. Cuninghame, J. A. B. Goodall, and H. H. Willis. "Absolute Yields in the Fission of 235U by Mono-energetic Neutrons of Energy 130-1700 keV". In: *Journal of Inorganic and Nuclear Chemistry* 36 (1974), pp. 1453–1457. ISSN: 00221902. DOI: 10.1016/0022-1902(74)80604-4.

[165] J. N. Wilson et al. "Anomalies in the Charge Yields of Fission Fragments from the 238U(n,f) Reaction". In: *Physical Review Letters* 118.22 (2017), p. 222501. ISSN: 10797114. DOI: 10.1103/PhysRevLett.118.222501.

[166] R. W. Peelle and F. C. Maienschein. "Spectrum of Photons Emitted in Coincidence with Fission of U235 by Thermal Neutrons". In: *Physical Review C* 3 (1971), p. 373. ISSN: 05562813. DOI: 10.1103/PhysRevC.3.373.

[167] S. Pommé, R. Fitzgerald, and J. Keightley. "Uncertainty of Nuclear Counting". In: *Metrologia* 52.3 (2015), S3–S17. ISSN: 16817575. DOI: 10.1088/0026-1394/52/3/S3.

[168] J. Feng et al. "Absolute Measurement of 99Mo Fission Yields of 235U Induced by 0.57, 1.0 and 1.5 MeV Neutrons". In: *Yuanzineng Kexue Jishu/Atomic Energy Science and Technology* 47 (2013), pp. 1473–1478. ISSN: 10006931. DOI: 10.7538/yzk.2013.47.09.1473.

[169] E. F. Matthews, L. A. Bernstein, and W. Younes. "Stochastically Estimated Covariance Matrices for Independent and Cumulative Fission Yields in the ENDF/B-VIII.0 and JEFF-3.3 Evaluations". In: *Atomic Data and Nuclear Data Tables* (2021), p. 101441. ISSN: 0092-640X. DOI: 10.1016/j.adt.2021.101441.

[170] M. A. Kellett, O. Bersillon, and R. W. Mills. *The JEFF-3.1/-3.1.1 Radioactive Decay Data and Fission Yields Sub-libraries - JEFF Report 20*. The Nuclear Energy Agency - Organization for Economic Cooperation and Development, 2009. ISBN: 978-92-64-99087-6. URL: https://www.oecd-nea.org/jcms/pl_14322.

[171] D. Rochman et al. "A Bayesian Monte Carlo Method for Fission Yield Covariance Information". In: *Annals of Nuclear Energy* (2016). ISSN: 18732100. DOI: 10.1016/j.anucene.2016.05.005.

[172] N. Terranova et al. "Fission Yield Covariance Matrices for the Main Neutron-induced Fissioning Systems Contained in the JEFF-3.1.1 Library". In: *Annals of Nuclear Energy* (2017). ISSN: 18732100. DOI: 10.1016/j.anucene.2017.05.052.

[173] K.-H. Schmidt, B. Jurado, and C. Amouroux. *General Description of Fission Observables - GEF Model*. Tech. rep. NEA/DB/DOC(2014)1. The Nuclear Energy Agency - Organization for Economic Cooperation and Development, 2014. URL: https://www.oecd-nea.org/jcms/pl_19520.

[174] K.-H. Schmidt and B. Jurado. *GEFY : GEF-based Fission-fragment Yield Library in ENDF-format*. 2020. URL: https://www.cenbg.in2p3.fr/GEFY-GEF-based-fission-fragment (visited on 03/17/2021).

[175] B. Voirin et al. "From Fission Yield Measurements to Evaluation: Status on Statistical Methodology for the Covariance Question". In: *EPJ Nuclear Sciences and Technologies* 4 (2018), p. 26. ISSN: 2491-9292. DOI: 10.1051/epjn/2018030.

[176] E. F. Matthews et al. "FIER: Software for Analytical Modeling of Delayed Gamma-ray Spectra". In: *Nuclear Instruments and Methods in Physics Research, Section A: Accelerators, Spectrometers, Detectors and Associated Equipment* 891 (2018), pp. 111–117. ISSN: 01689002. DOI: 10.1016/j.nima.2018.02.072.

[177] J. P. Lestone. *Energy and Isotope Dependence of Neutron Multiplicity Distributions*. 2014. URL: https://arxiv.org/abs/1409.5346.

[178] M. Kireeff Covo et al. "The 88-Inch Cyclotron: A One-stop Facility for Electronics Radiation and Detector Testing". In: *Measurement* 127 (2018), pp. 580–587. ISSN: 0263-2241. DOI: 10.1016/j.measurement.2017.10.018.

[179] A. Ruben et al. "A New, Versatile, High-performance Digital Pulse Processor with Application to Neutron/Gamma-ray Pulse-shape Discrimination in Scintillator Detectors". In: *Proc. Nima_Sorma XVII*. 2018. URL: http://mesytec.de/products/appnotes/MDPP16_SORMA_2018.pdf.

[180] A. Enqvist et al. "Neutron Light Output Response and Resolution Functions in EJ-309 Liquid Scintillation Detectors". In: *Nuclear Instruments and Methods in Physics Research Section A: Accelerators, Spectrometers, Detectors and Associated Equipment* 715 (2013), pp. 79–86. ISSN: 0168-9002. DOI: 10.1016/j.nima.2013.03.032.

[181] R. Brun and F. Rademakers. "ROOT—An Object Oriented Data Analysis Framework". In: *Nuclear Instruments and Methods in Physics Research Section A: Accelerators, Spectrometers, Detectors and Associated Equipment* 389.1-2 (1997), pp. 81–86. DOI: 10.1016/S0168-9002(97)00048-X.

[182] W. J. Gallagher and S. J. Cipolla. "A Model-based Efficiency Calibration of a Si(Li) Detector in the Energy Region from 3 to 140 keV". In: *Nuclear Instruments and Methods* 122 (1974), pp. 405–414. ISSN: 0029-554X. DOI: 10.1016/0029-554X(74)90508-4.

[183] R. Storn and K. Price. "Differential Evolution - A Simple and Efficient Heuristic for Global Optimization over Continuous Spaces". In: *Journal of Global Optimization* (1997). ISSN: 09255001. DOI: 10.1023/A:1008202821328.

[184] P. Virtanen et al. "SciPy 1.0: Fundamental Algorithms for Scientific Computing in Python". In: *Nature Methods* 17 (2020), pp. 261–272. DOI: 10.1038/s41592-019-0686-2.

[185] G. F. Knoll. *Radiation Detection and Measurement*. 4th ed. John Wiley and Sons, 2010.

[186] K. P. Harrig et al. "Neutron Spectroscopy for Pulsed Beams with Frame Overlap Using a Double Time-of-flight Technique". In: *Nuclear Instruments and Methods in Physics Research Section A: Accelerators, Spectrometers, Detectors and Associated Equipment* 877 (2018), pp. 359–366. ISSN: 0168-9002. DOI: 10.1016/j.nima.2017.09.051.

[187] L. J. Heistek and L. van der Zwan. "Pulse Shape Discrimination with a Comparator Circuit". In: *Nuclear Instruments and Methods* 80.2 (1970), pp. 213–216. ISSN: 0029-554X. DOI: 10.1016/0029-554X(70)90764-0.

[188] J. A. Brown. Private Communication. University of California - Berkeley. Dec. 2020.

[189] J. A. Brown et al. "Proton Light Yield in Organic Scintillators Using a Double Time-of-flight Technique". In: *Journal of Applied Physics* 124.4 (2018), p. 045101. DOI: 10.1063/1.5039632.

[190] T. A. Laplace et al. "Comparative Scintillation Performance of EJ-309, EJ-276, and a Novel Organic Glass". In: *Journal of Instrumentation* 15.11 (Nov. 2020), P11020–P11020. DOI: 10.1088/1748-0221/15/11/p11020.

[191] M. Herman and A. Trkov. *ENDF-6 Formats Manual*. Tech. rep. BNL-90365-2009. Brookhaven National Laboratory, 2010. URL: https://www.bnl.gov/isd/documents/70393.pdf.

[192] F. Biscani and D. Izzo. "A Parallel Global Multiobjective Framework for Optimization: pagmo". In: *Journal of Open Source Software* 5.53 (2020), p. 2338. DOI: 10.21105/joss.02338.

[193] V. A. Roshchenko, V. M. Piksaykin, G. G. Korolev, et al. "Cumulative Yields of Delayed Neutrons Precursors in Neutron Induced Fission of 237-Np and 238-U in the Energy Range from 0.5 up to 5.0 MeV". In: *Yad. Konst* 1.2 (2006), p. 43.

[194] A. N. Gudkov et al. "Yields of Delayed Neutron Precursors in the Fission of Actinides". In: *Radiochimica Acta* 57.2-3 (1992), pp. 69–76. DOI: doi:10.1524/ract.1992.57.23.69.

[195] A. A. Filatenkov. "Energies and Yields of Prompt Gamma-Rays from Fission Fragments in 235U and 238U Fission by 3 MeV Neutrons". PhD thesis. 1988, p. 127.

[196] H. D. Schuessler and G. Herrmann. "Main Components of the Delayed-neutron Precursors in the Fission of 235U by Thermal Neutrons". In: *Radiochimica Acta* 18.3 (1972), pp. 123–133. DOI: 10.1524/ract.1972.18.3.123.

[197] B. Cheal et al. "The Shape Transition in the Neutron-rich Yttrium Isotopes and Isomers". In: *Physics Letters B* 645.2 (2007), pp. 133–137. ISSN: 0370-2693. DOI: 10.1016/j.physletb.2006.12.053.

[198] H. Grawe et al. "Nuclear Structure Far Off Stability–Implications for Nuclear Astrophysics". In: *The European Physical Journal A-Hadrons and Nuclei* 27.1 (2006), pp. 257–267. DOI: 10.1140/epja/i2006-08-040-7.

[199] J. M. Campbell. "Yields of Short-lived Fission Products Following Fast Fission of U-238". PhD thesis. University of Massachusetts Lowell, 1997.

[200] G. Lhersonneau et al. "Production of Neutron-rich Isotopes in Fission of Uranium Induced by Neutrons of 20 MeV Average Energy". In: *The European Physical Journal A-Hadrons and Nuclei* 9.3 (2000), pp. 385–396. DOI: 10.1007/s100500070023.

[201] J. Cvachovec and F. Cvachovec. "Maximum Likelihood Estimation of a Neutron Spectrum and Associated Uncertainties". In: *Advances in Military Technology* 1.2 (2008), pp. 67–79.

[202] S. Maeda et al. "Fundamental Study on Neutron Spectrum Unfolding Using Maximum Entropy and Maximum Likelihood Method". In: *Progress in Nuclear Science and Technology* 1 (2011), pp. 233–236. URL: https://www.aesj.net/document/pnst001/233.pdf.

[203] S. Maeda and T. Iguchi. "A New Unfolding Code Combining Maximum Entropy and Maximum Likelihood for Neutron Spectrum Measurement". In: *Journal of Nuclear Science and Technology* 50.4 (2013), pp. 381–386. DOI: 10.1080/00223131.2013.773162.

[204] A. A. Sonzogni, T. D. Johnson, and E. A. McCutchan. "Nuclear Structure Insights into Reactor Antineutrino Spectra". In: *Phys. Rev. C* 91 (1 Jan. 2015), p. 011301. DOI: 10.1103/PhysRevC.91.011301.

Appendix A

Appendix of Figures for Short-lived Fission Product Yield Measurements Using the Fast Loading User Facility for Fission Yields

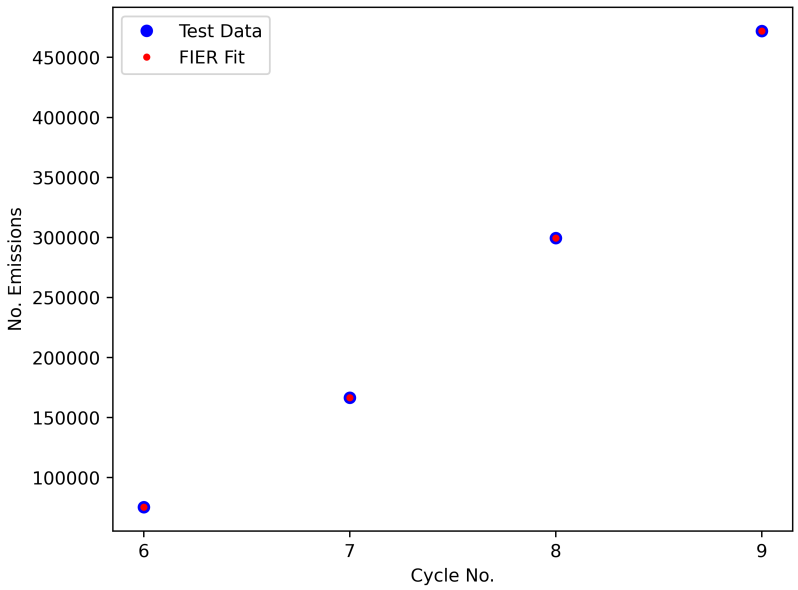

Figure A.1: Minimizer Benchmarking: The number of 1031.92-keV γ emissions from ^{89}Rb as a function of cycle number.

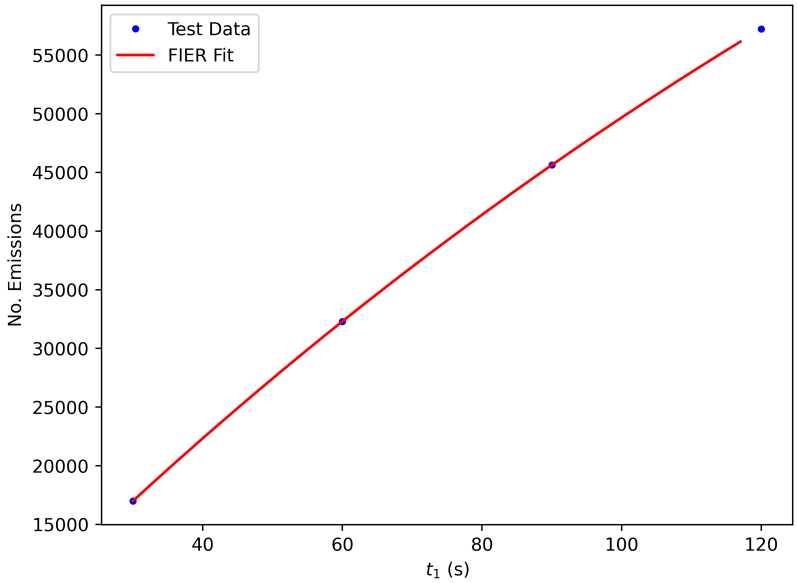

Figure A.2: Minimizer Benchmarking: The number of 3532.88-keV γ emissions from ^{89}Kr as a function of time since capsule arrival, t_1.

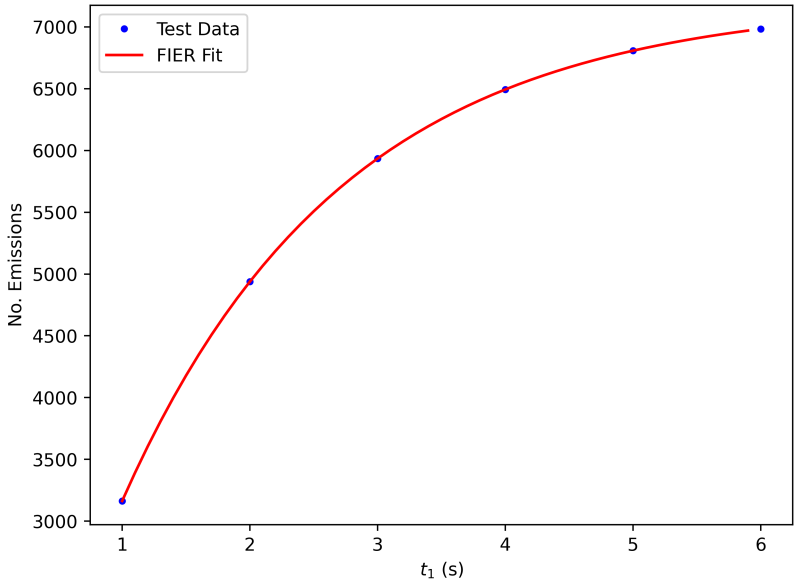

Figure A.3: Minimizer Benchmarking: The number of 3231.3-keV γ emissions from ^{90}Br as a function of time since capsule arrival, t_1.

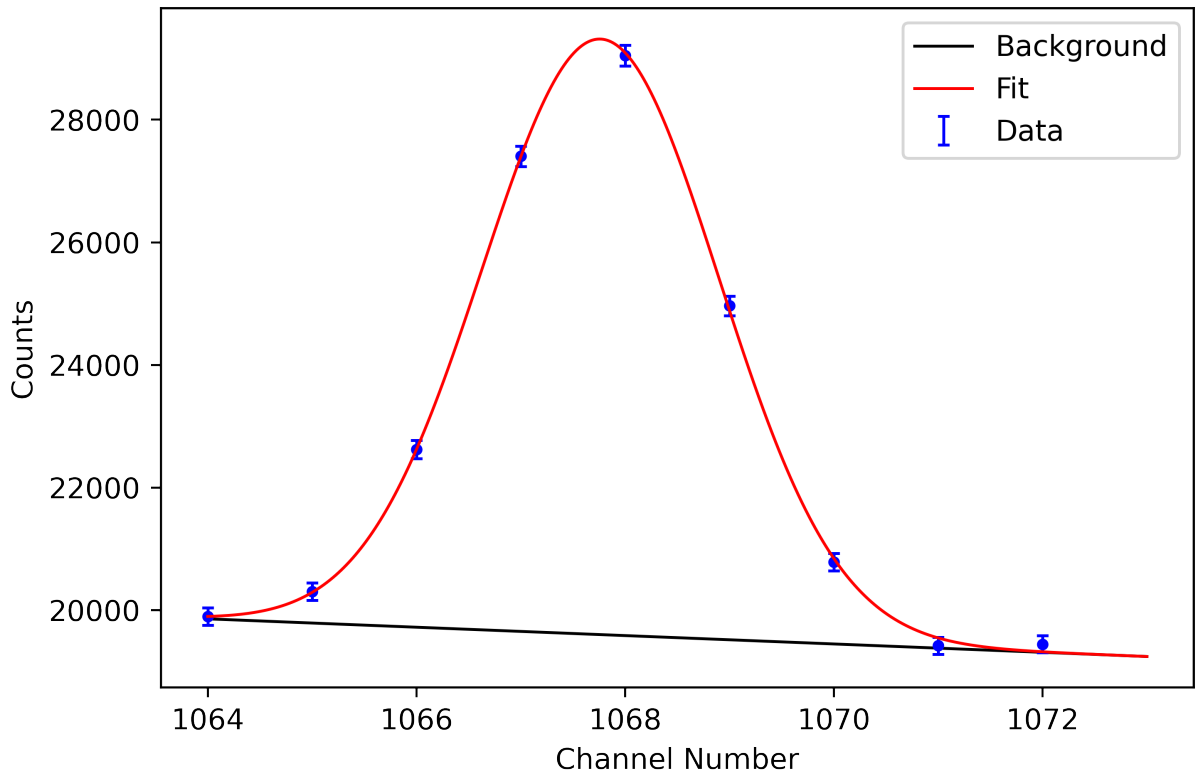

Figure A.4: An example of the fitted photopeak for 1564.60-keV γ from ^{86}Br in the fission product γ-ray spectrum from the 5 s–125 s irradiation scheme. The spectrum shown in this figure includes all cycles and spans $t_0 = 0$ s to $t_1 = 125$ s.

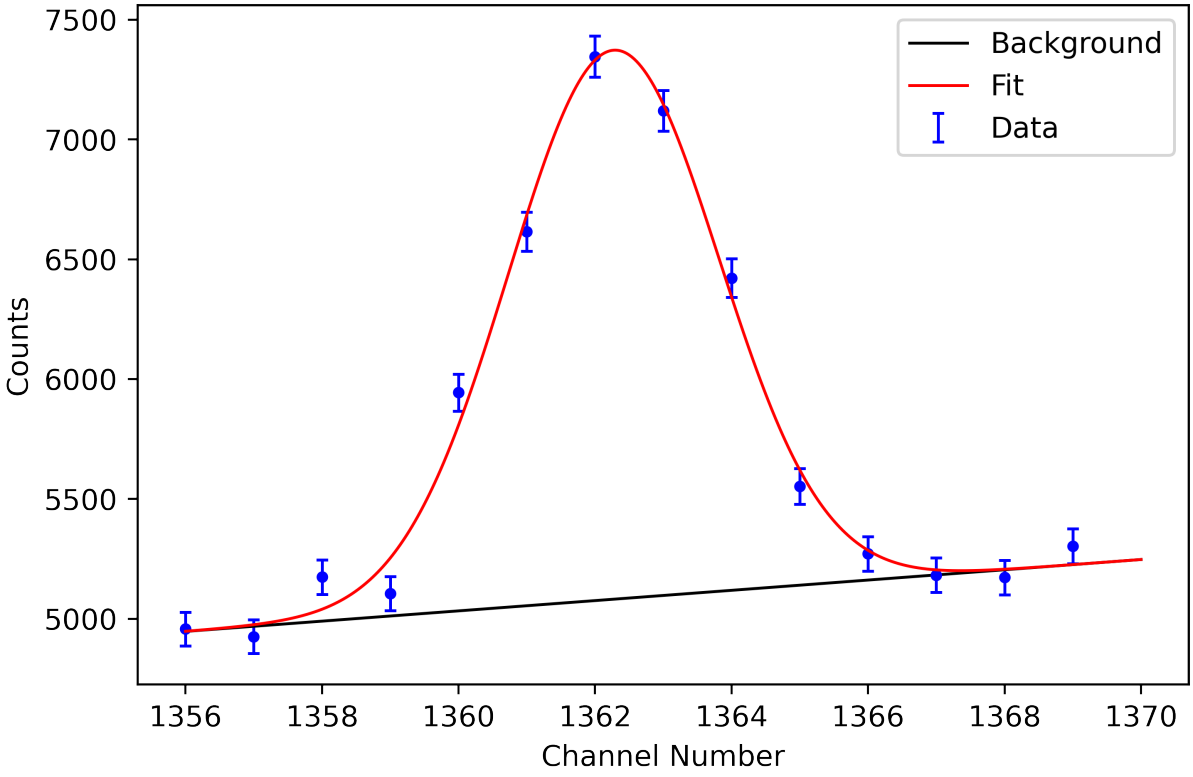

Figure A.5: An example of the fitted photopeak for 2660.0-keV γ from ^{86}Se in the fission product γ-ray spectrum from the 5 s–125 s irradiation scheme. The spectrum shown in this figure includes all cycles and spans $t_0 = 0$ s to $t_1 = 100$ s.

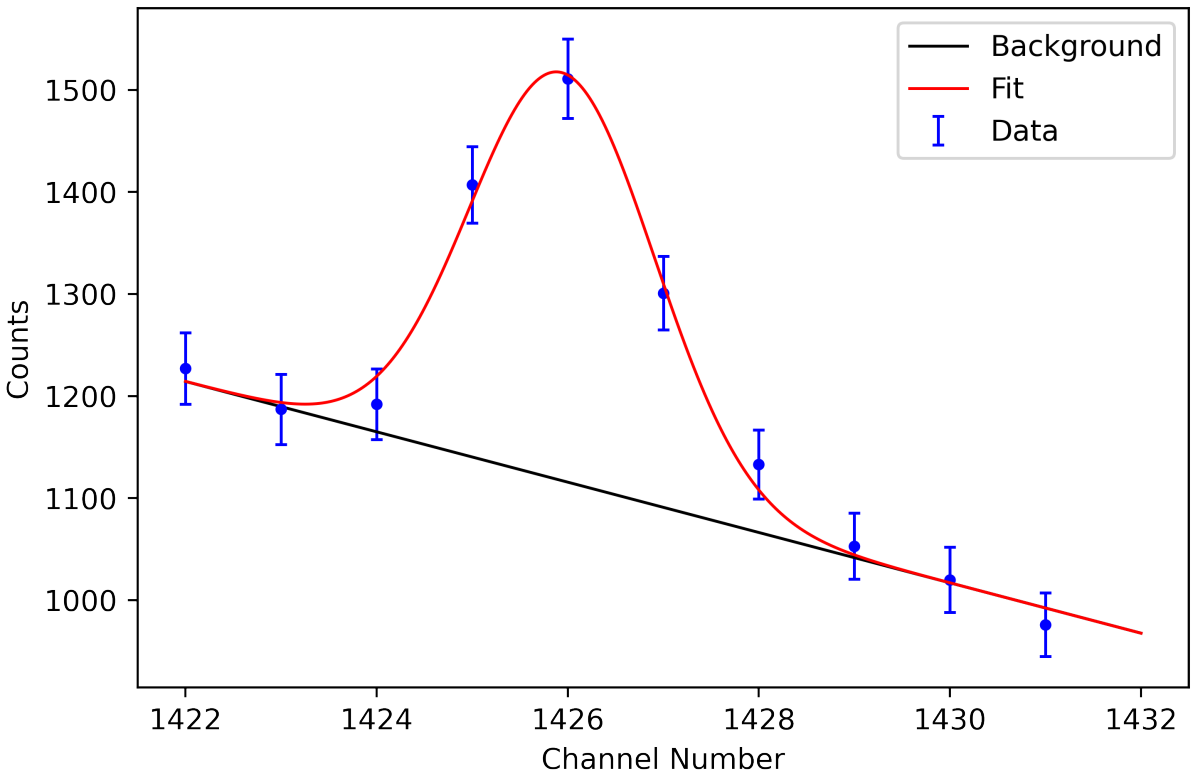

Figure A.6: An example of the fitted photopeak for 4180.54-keV γ from ^{87}Br in the fission product γ-ray spectrum from the 5 s–125 s irradiation scheme. The spectrum shown in this figure includes all cycles and spans $t_0 = 0$ s to $t_1 = 125$ s.

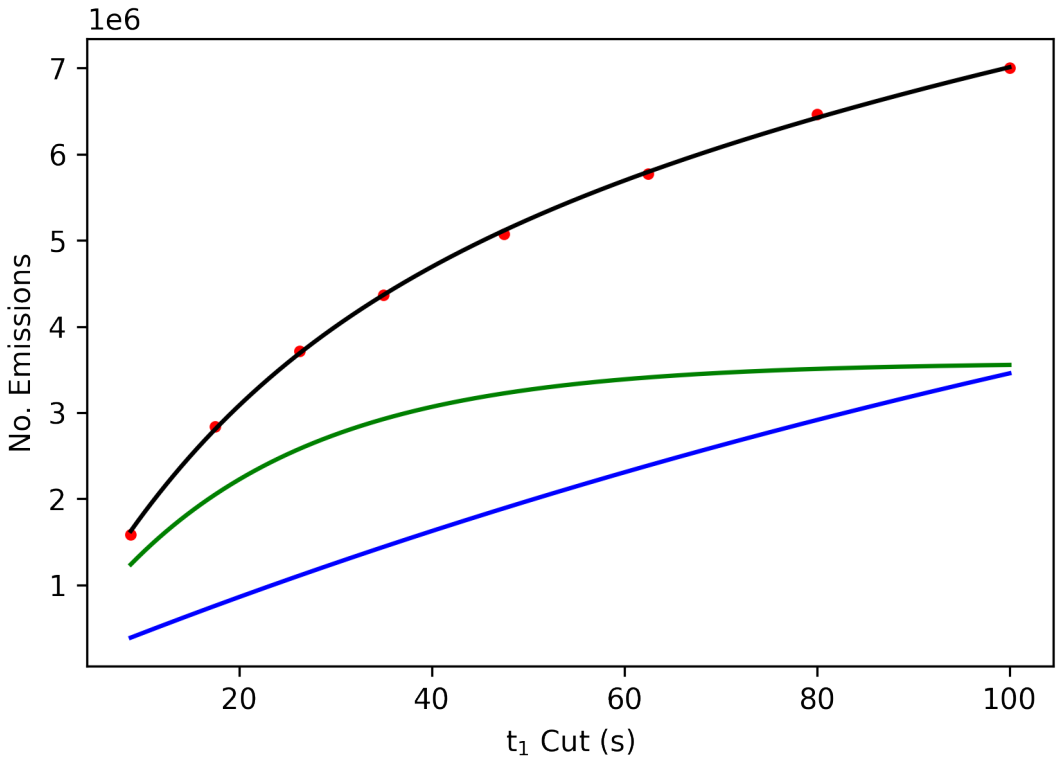

Figure A.7: Time separation of the 2660.0-keV photopeak into components from ^{86}Se and an unknown contaminant. The black line is the total fit, the green line is the component from ^{86}Se, and the blue line is the component from the contaminant.

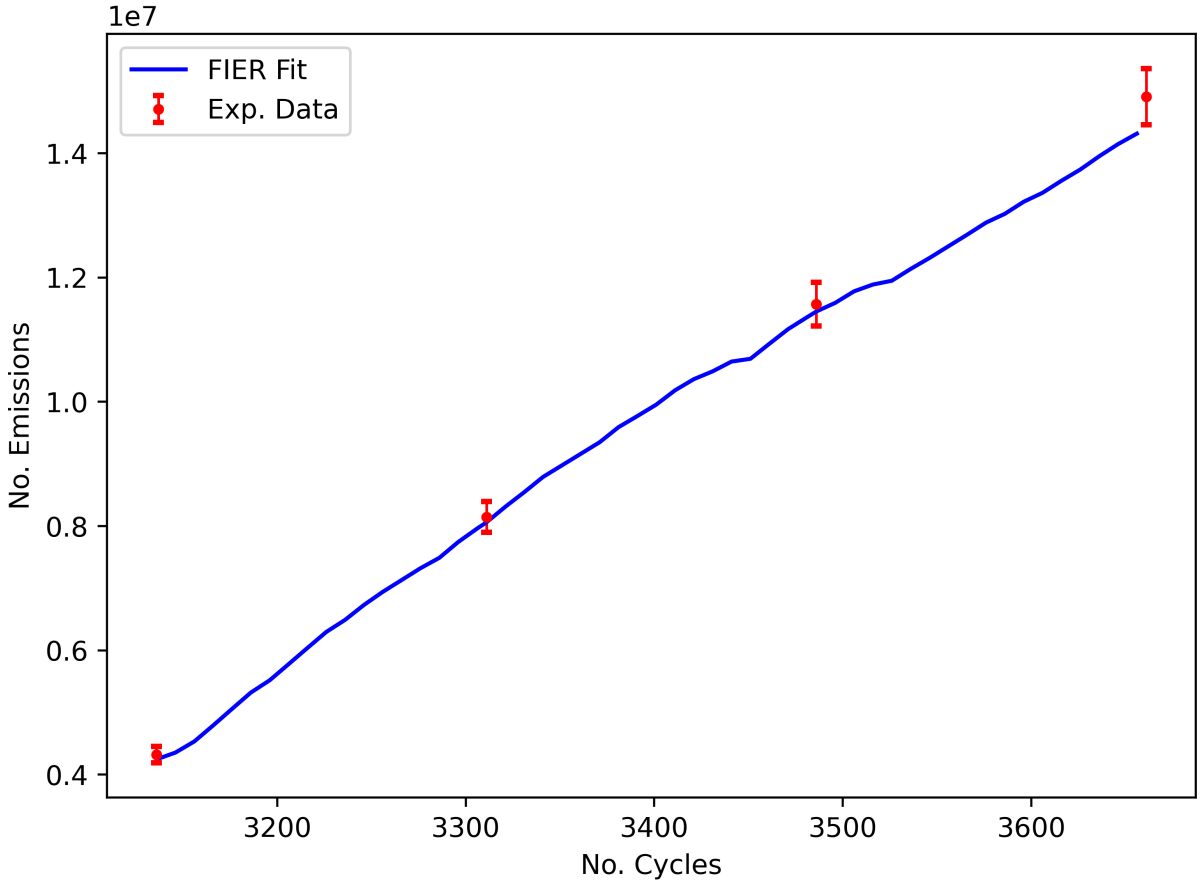

Figure A.8: Fit of the 1564.60-keV γ-ray emissions from ^{86}Br to FIER. It was determined the independent fission yield of ^{86}Br was 0.45%.

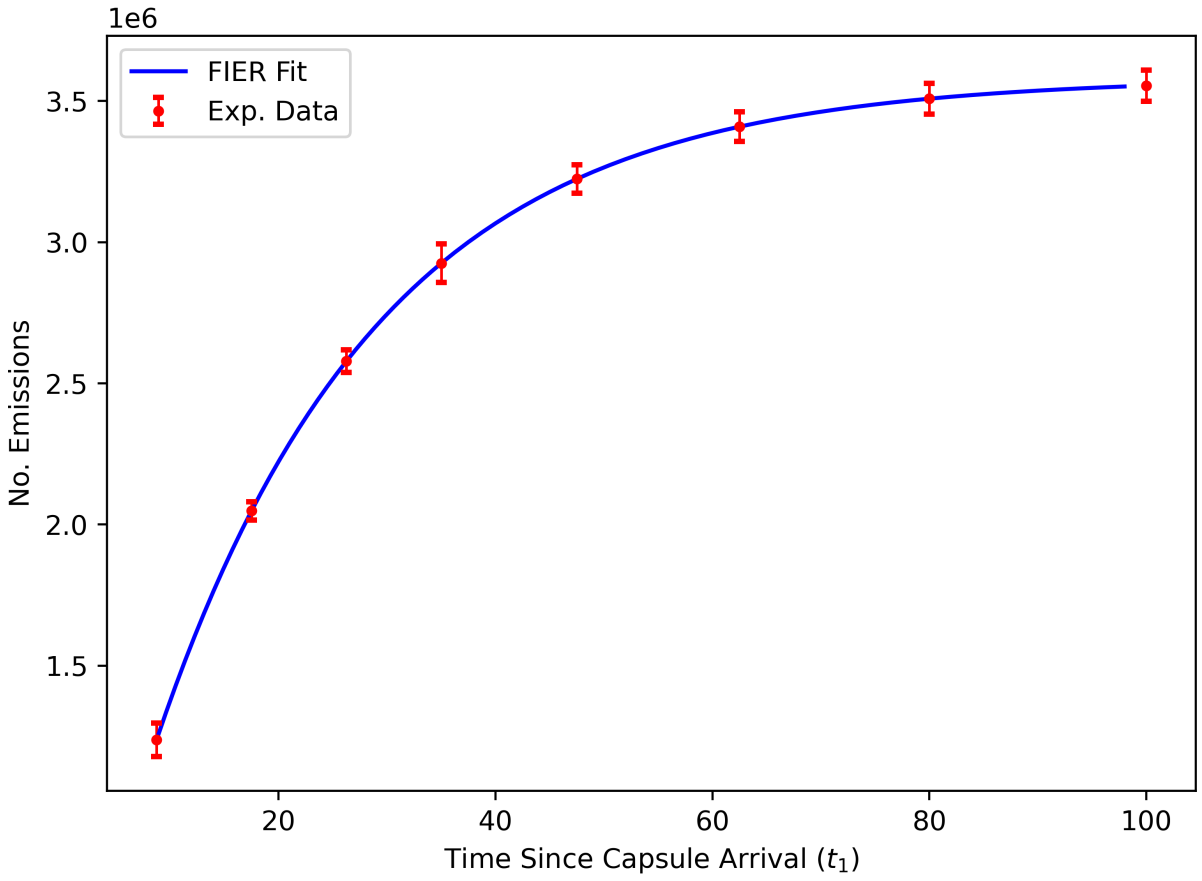

Figure A.9: Fit of the 2660.0-keV γ-ray emissions from ^{86}Se to FIER. It was determined the cumulative fission yield of ^{86}Se was 1.05% and the decay γ intensity of its 2660.0-keV emission was 24.9%.

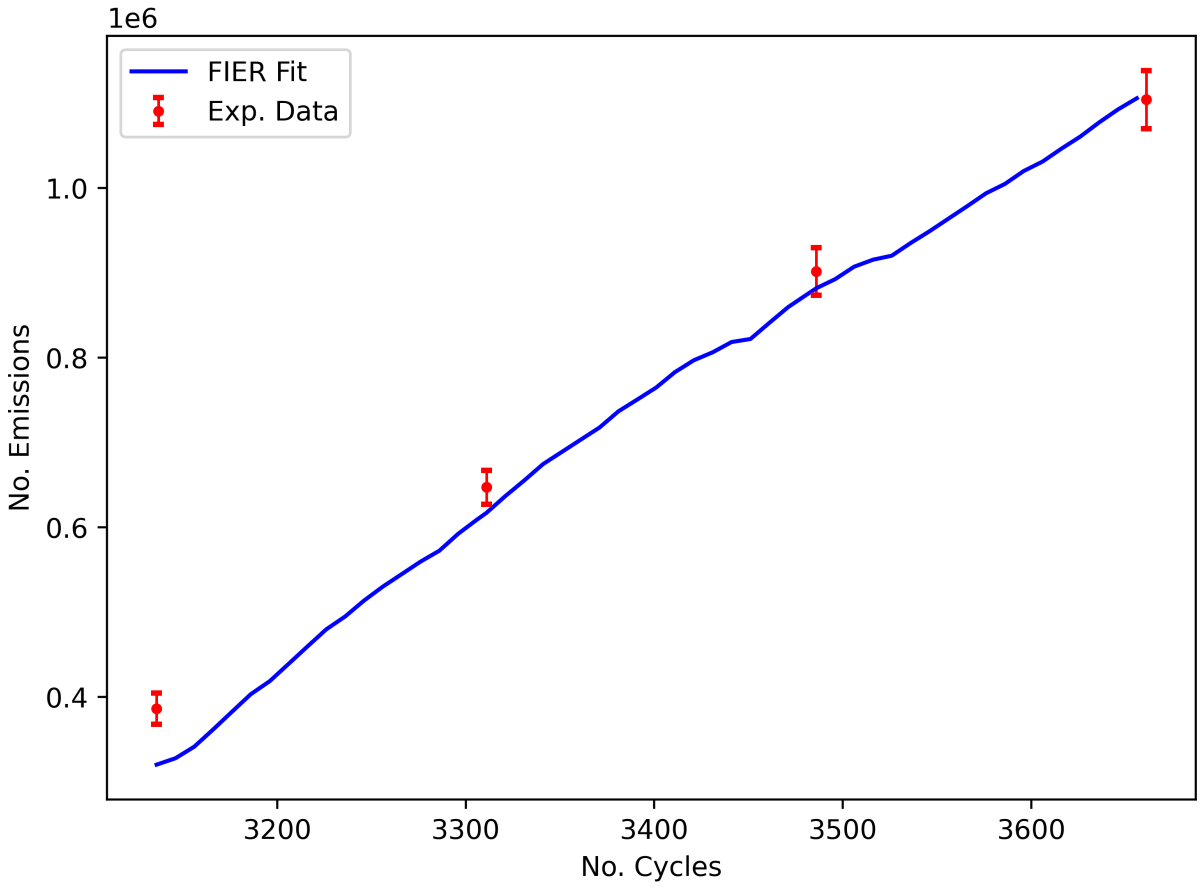

Figure A.10: Fit of the 4180.54-keV γ-ray emissions from ^{87}Br to FIER. It was determined the independent fission yield of ^{87}Br was 1.83%.

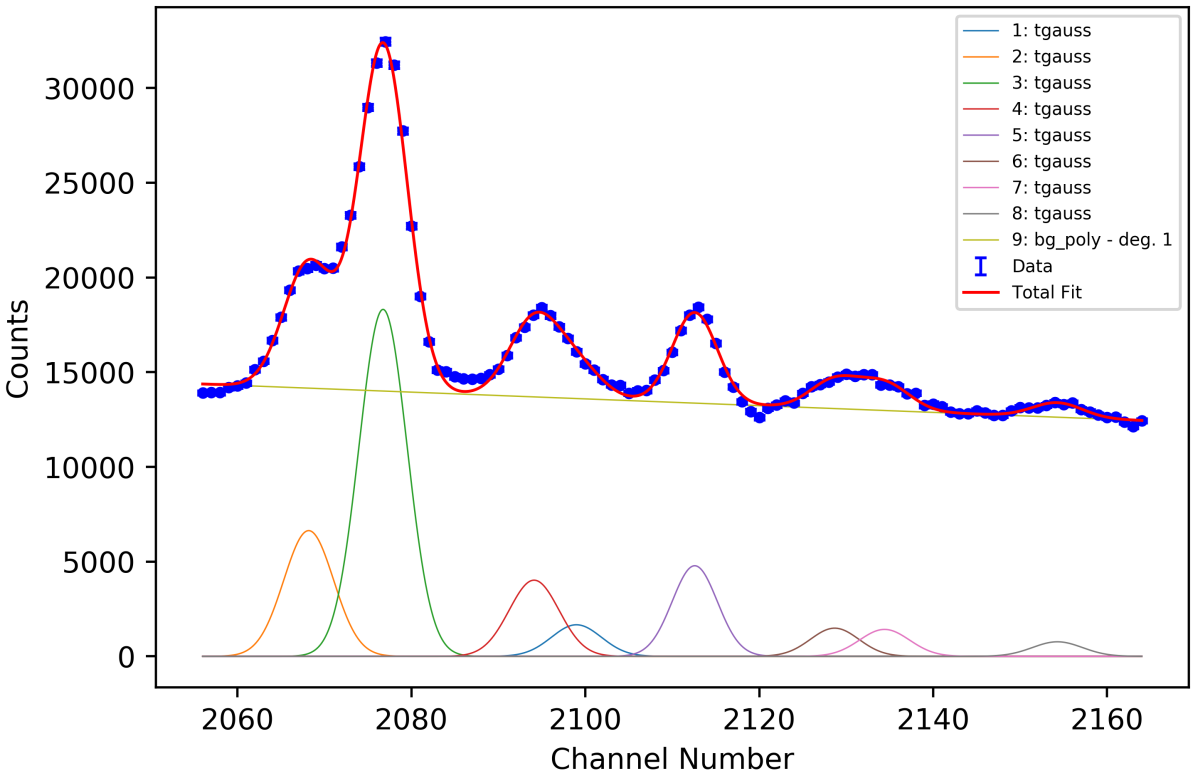

Figure A.11: An example of the fitted photopeak for 1024.4-keV γ from ^{98}Nb (shown in curve 1, the blue line) in the fission product γ-ray spectrum from the 1 s–25 s irradiation scheme. The spectrum shown in this figure includes all cycles and spans $t_0 = 0$ s to $t_1 = 12$ s. This photopeak is small relative to the photopeaks near it, requiring a complex photopeak fit. As a result, there is large uncertainty in this photopeak area.

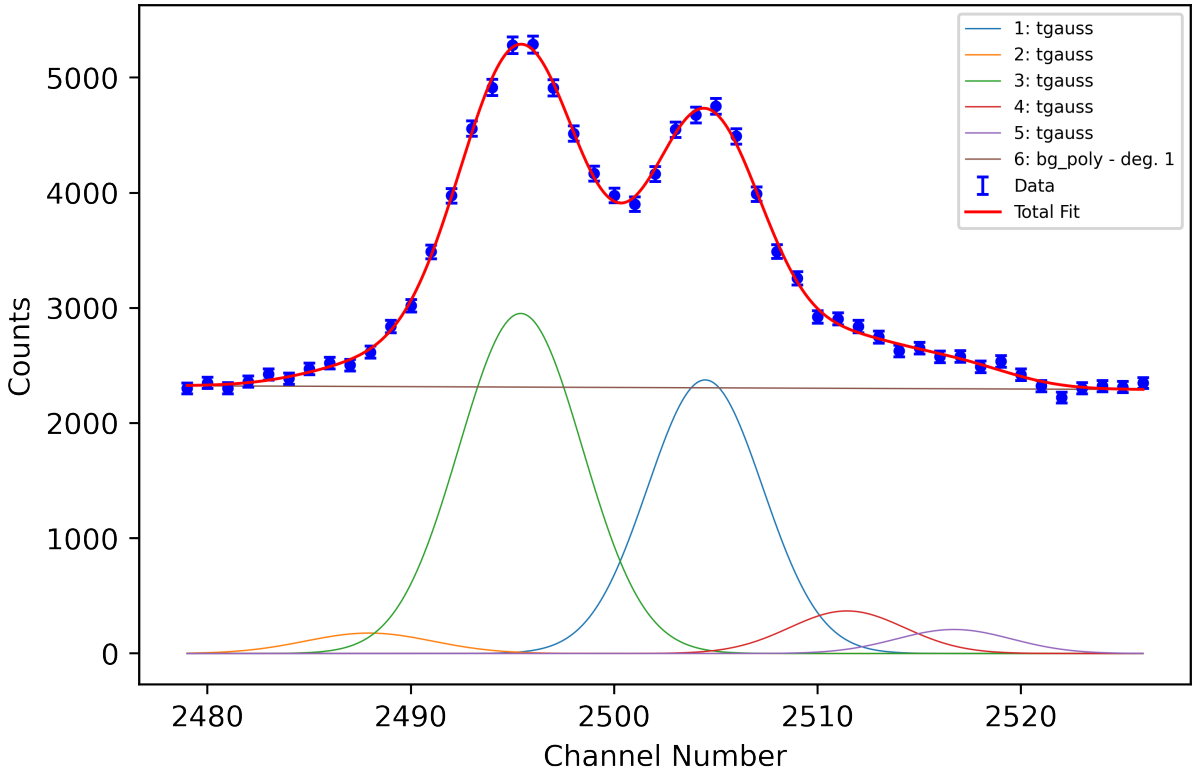

Figure A.12: An example of the fitted photopeak for 1222.9-keV γ from ^{98}Y (shown in curve 1, the blue line) in the fission product γ-ray spectrum from the 1 s–25 s irradiation scheme. The spectrum shown in this figure includes all cycles and spans $t_0 = 0$ s to $t_1 = 3.5$ s.

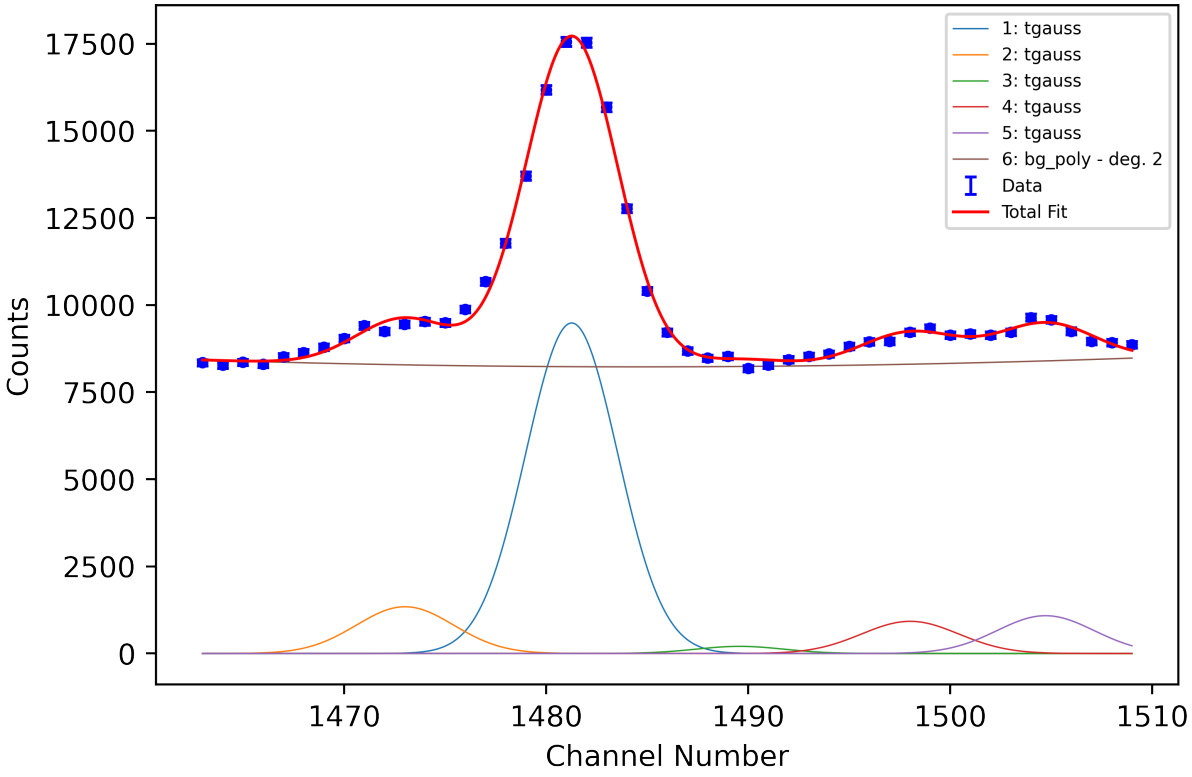

Figure A.13: An example of the fitted photopeak for 724.4-keV γ from ^{99}Y (shown in curve 1, the blue line) in the fission product γ-ray spectrum from the 1 s–25 s irradiation scheme. The spectrum shown in this figure includes all cycles and spans $t_0 = 0$ s to $t_1 = 6$ s.

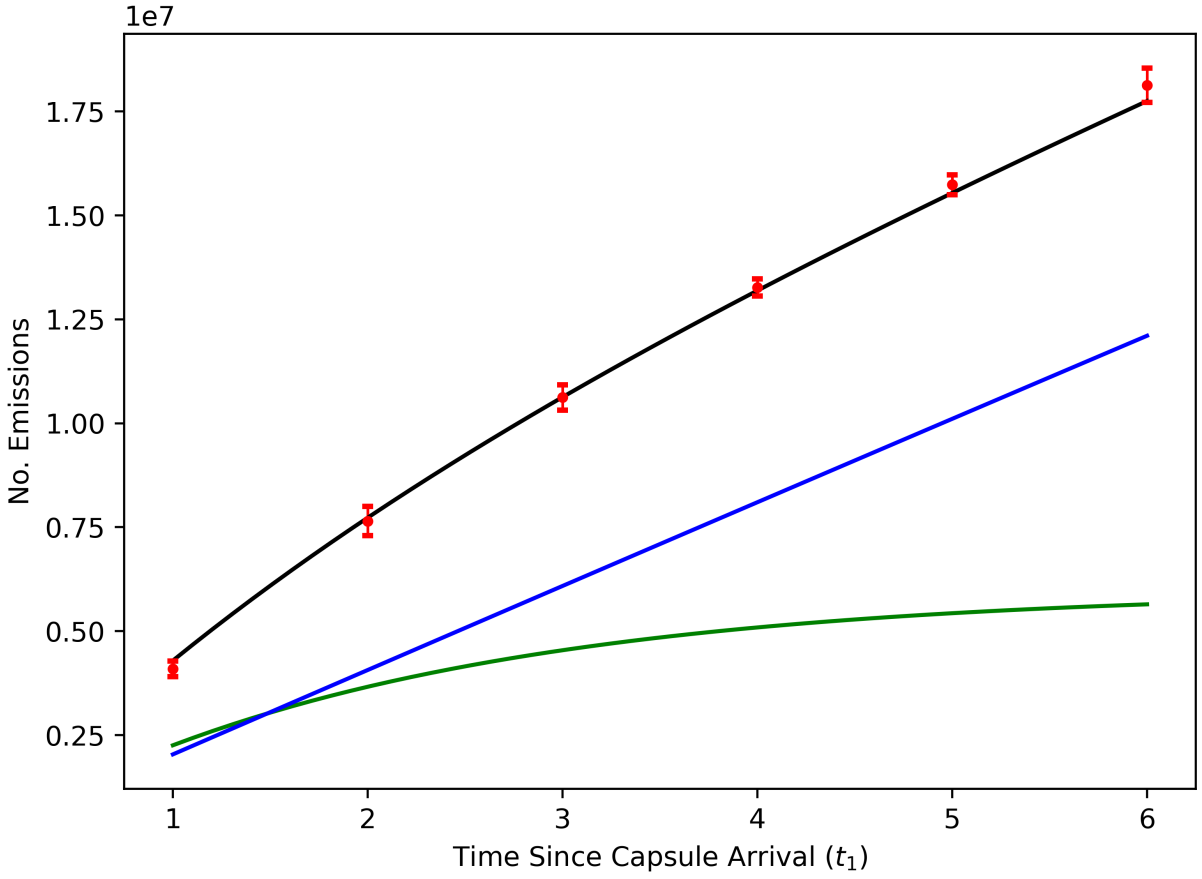

Figure A.14: Time separation of the 724.4-keV photopeak into components from ^{99}Y and an unknown contaminant. The black line is the total fit, the green line is the component from ^{99}Y, and the blue line is the component from the contaminant.

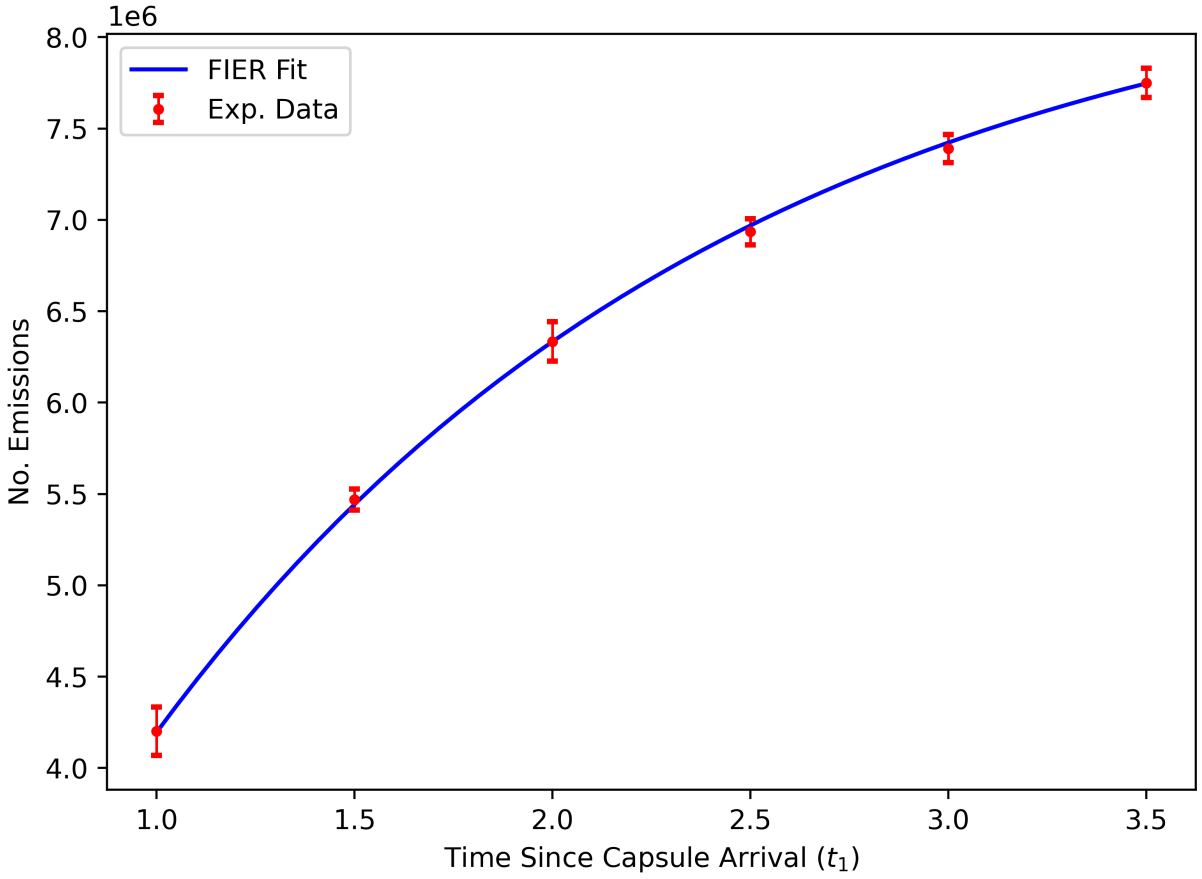

Figure A.15: Fit of the 1222.9-keV γ-ray emissions from ^{98}Y to Eq. 5.16. It was determined the cumulative fission yield of ^{98}Y was 5.13 $\pm$ 0.39%.

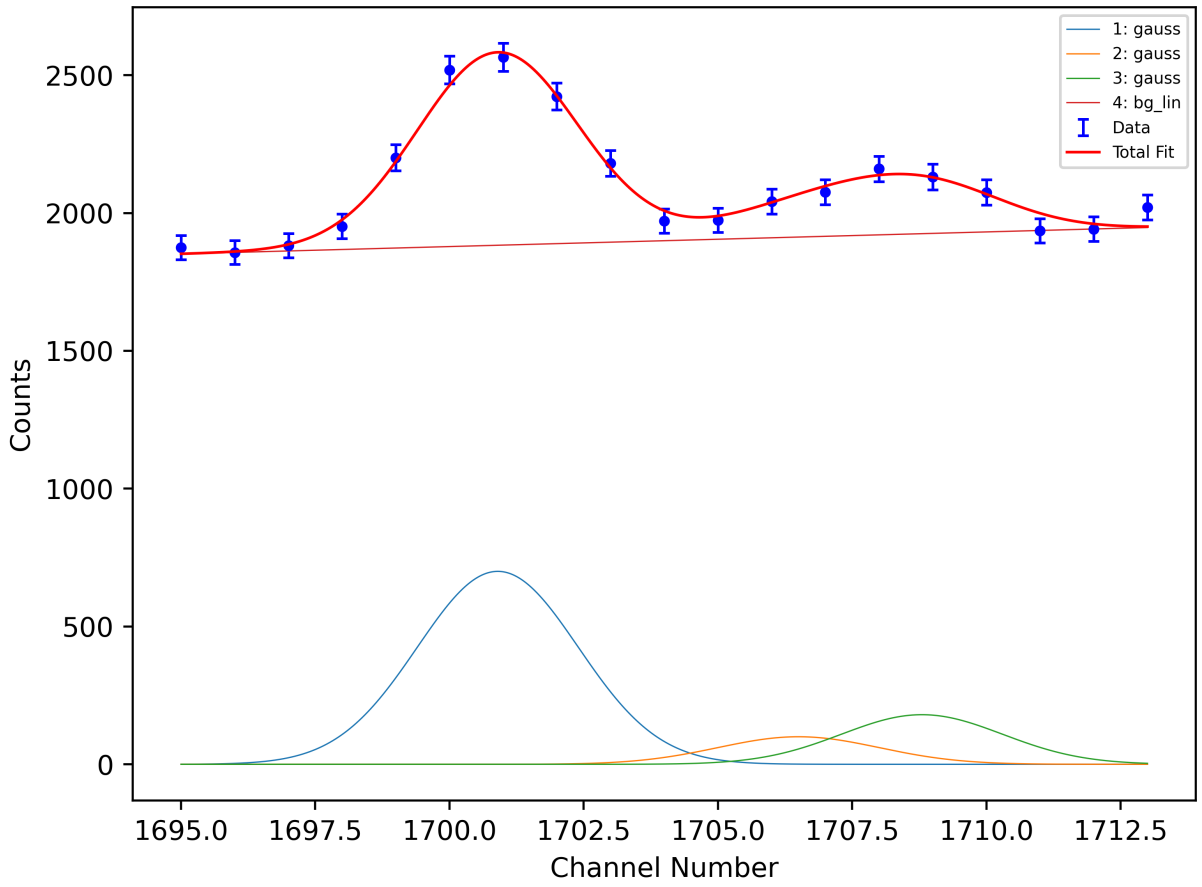

Figure A.16: An example of the fitted photopeak for the 2077.9-keV γ from ^{136}Te (shown in curve 1, the blue line) in the fission product γ-ray spectrum from the 5 s–125 s irradiation scheme. The spectrum shown in this figure includes all cycles and spans $t_0 = 0$ s to $t_1 = 40$ s.

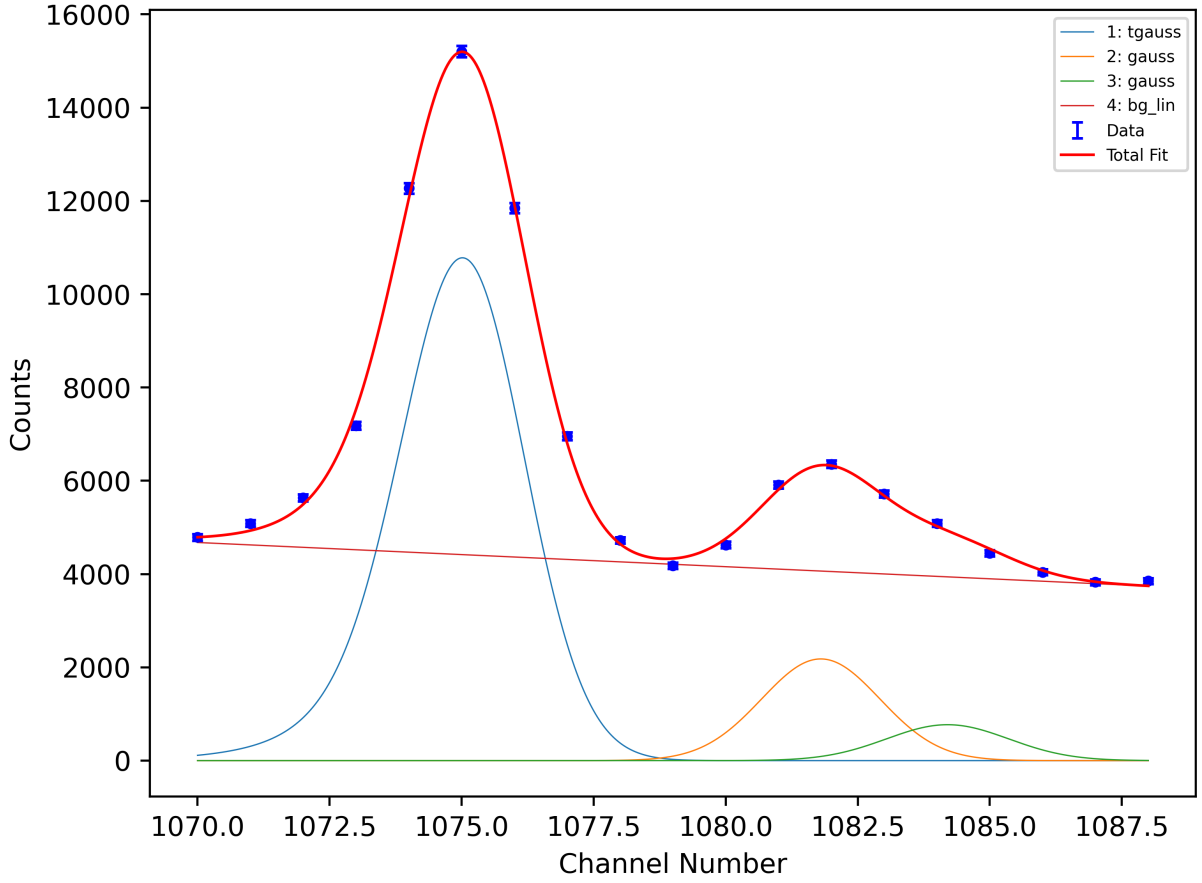

Figure A.17: An example of the fitted photopeaks for the 1313.02-keV γ from ^{136g}I and ^{136m}I (shown in curve 1, the blue line) and the 1321.08-keV γ from ^{136g}I (shown in curve 2, the orange line) in the fission product γ-ray spectrum from the 5 s–125 s irradiation scheme. The spectrum shown in this figure includes all cycles and spans $t_0 = 0$ s to $t_1 = 104.2$ s. The photopeak to the left (shown in curve 2, the green line) is the 1324.0-keV photopeak from ^{95}Y.

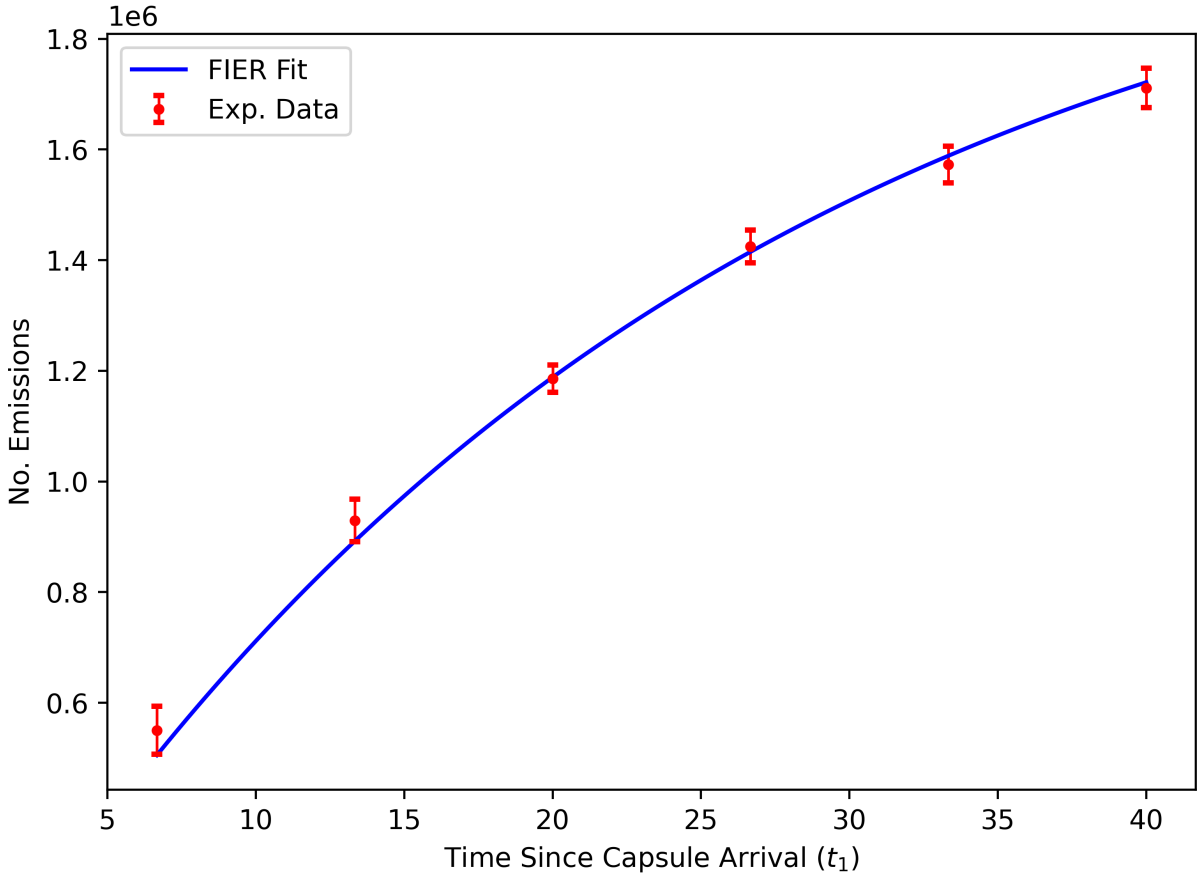

Figure A.18: Fit of the 2077.9-keV γ-ray emissions from ^{136}Te to FIER. It was determined the cumulative fission yield of ^{136}Te was 0.67%.

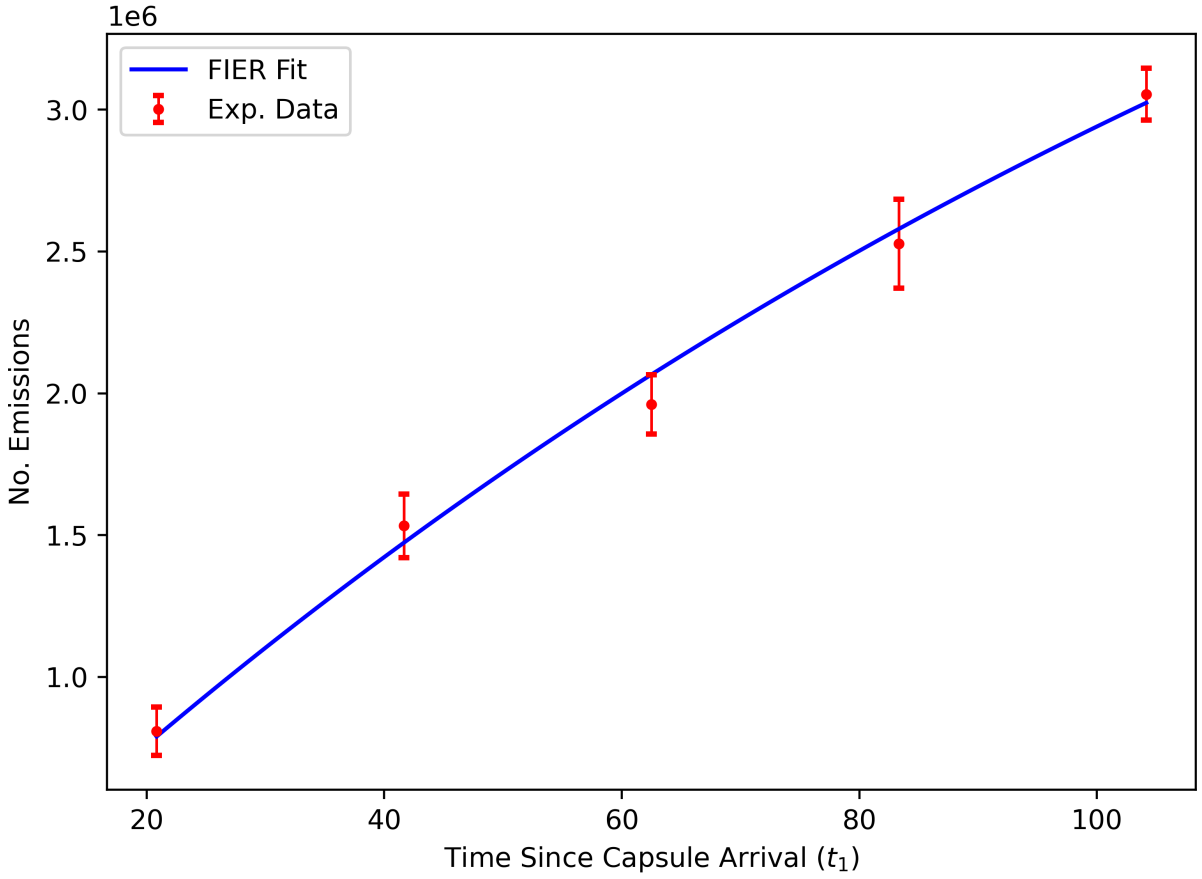

Figure A.19: Fit of the 1321.08-keV γ-ray emissions from ^{136g}I to FIER. It was determined the independent fission yield of ^{136g}I was 0.78%.

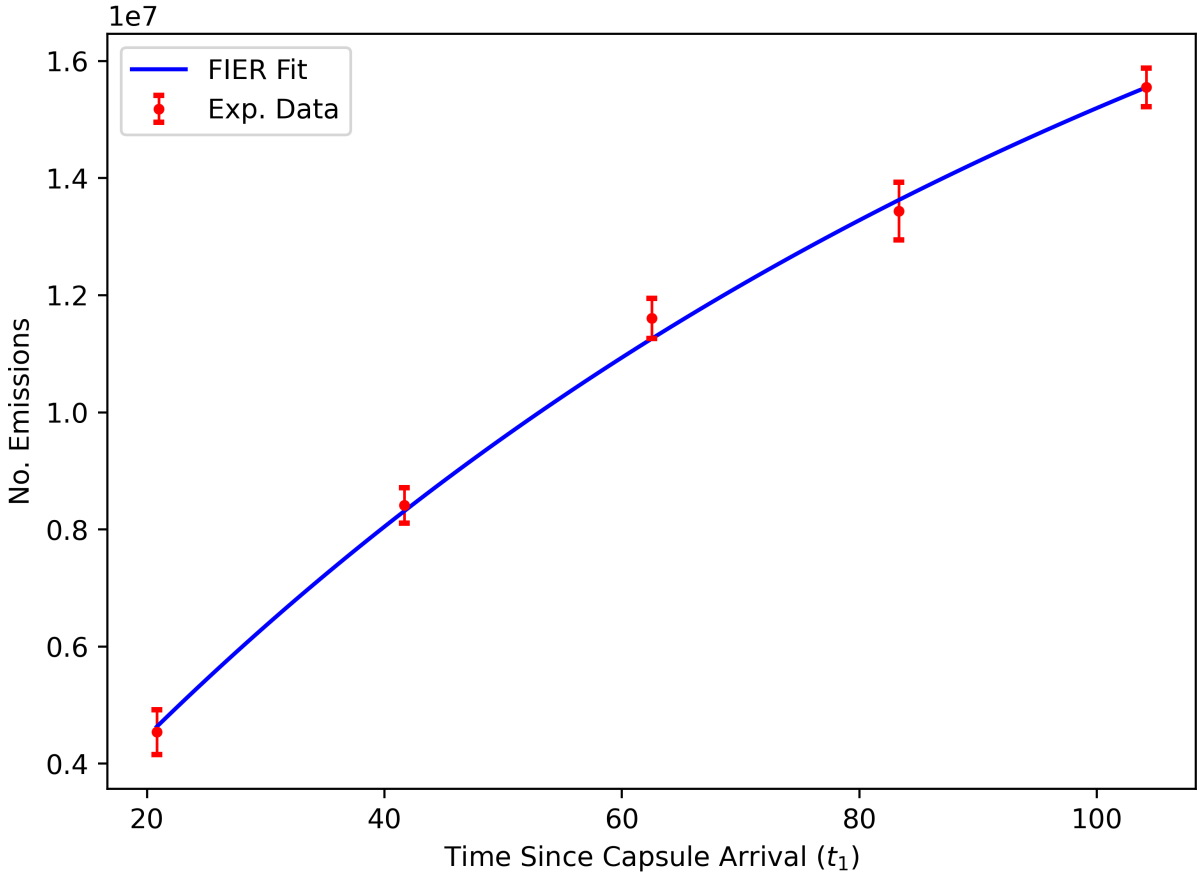

Figure A.20: Fit of the 1313.02-keV γ-ray emissions from ^{136g}I and ^{136m}I to FIER. It was determined the independent fission yield of ^{136g}I was 0.78% and the independent fission yield of ^{136m}I was 0.59%.

Appendix B

Appendix of Detailed Irradiation Scheme for ^{238}U Target

Listing B.1: Formatted FIER input deck for the irradiation scheme of the ^{238}U target. The number displayed in the even-numbered columns is the end time of the current stage of the irradiation scheme (in units of seconds). The number displayed in odd-numbered columns is the relative intensity of the neutron source during the current stage of the irradiation scheme. All "//" symbols should be replaced with a carriage return for use as input to FIER.

```
MODE:SINGLE
ON DECAY PREDICTION
isotopes.csv ISOTOPES FILE
decays.csv DECAYS FILE
gammas.csv GAMMAS FILE
YIELDS:ER
U,238,fission YIELDS FILE
NONE CHAINS OUTPUT
NONE STEMS OUTPUT
NONE POPS OUTPUT
output/U238_FIER_gamma_output.csv GAMMAS OUTPUT
NONE ERROR LOG
INITIALIZE
IRRADIATION
 1.000, 1.189 // 2.215, 0.000 // 28.896, 0.000 // 29.896, 1.230 // 31.095, 0.000
57.771, 0.000 // 58.771, 1.208 // 60.010, 0.000 // 86.684, 0.000 // 87.684, 1.226
88.872, 0.000 // 115.479, 0.000 // 116.479, 1.236 // 117.615, 0.000 // 144.155, 0.000
145.155, 1.231 // 146.364, 0.000 // 172.975, 0.000 // 173.975, 1.231 // 175.190, 0.000
201.945, 0.000 // 202.945, 1.195 // 204.167, 0.000 // 230.863, 0.000 // 231.863, 1.184
233.066, 0.000 // 259.965, 0.000 // 260.965, 1.215 // 262.205, 0.000 // 288.980, 0.000
289.980, 1.171 // 291.200, 0.000 // 317.937, 0.000 // 318.937, 1.177 // 320.139, 0.000
346.770, 0.000 // 347.770, 1.189 // 348.944, 0.000 // 375.650, 0.000 // 376.650, 1.208
377.858, 0.000 // 404.612, 0.000 // 405.612, 1.200 // 406.827, 0.000 // 433.538, 0.000
434.538, 1.209 // 435.740, 0.000 // 462.346, 0.000 // 463.346, 1.228 // 464.571, 0.000
491.147, 0.000 // 492.147, 1.202 // 493.322, 0.000 // 520.017, 0.000 // 521.017, 1.188
522.211, 0.000 // 549.002, 0.000 // 550.002, 1.186 // 551.225, 0.000 // 577.986, 0.000
578.986, 1.202 // 580.167, 0.000 // 606.794, 0.000 // 607.794, 1.191 // 609.023, 0.000
635.696, 0.000 // 636.696, 1.201 // 637.885, 0.000 // 664.558, 0.000 // 665.558, 1.187
666.759, 0.000 // 693.526, 0.000 // 694.526, 1.199 // 695.746, 0.000 // 722.464, 0.000
723.464, 1.186 // 724.804, 0.000 // 751.576, 0.000 // 752.576, 1.206 // 753.828, 0.000
780.645, 0.000 // 781.645, 1.206 // 782.963, 0.000 // 809.627, 0.000 // 810.627, 1.197
811.860, 0.000 // 838.619, 0.000 // 839.619, 1.185 // 840.860, 0.000 // 867.500, 0.000
```

868.500, 1.171 // 869.757, 0.000 // 896.517, 0.000 // 897.517, 1.190 // 898.824, 0.000
925.599, 0.000 // 926.599, 1.169 // 927.936, 0.000 // 954.506, 0.000 // 955.506, 1.169
956.676, 0.000 // 983.441, 0.000 // 984.441, 1.192 // 985.751, 0.000 // 1012.381, 0.000
1013.381, 1.178 // 1014.600, 0.000 // 1041.261, 0.000 // 1042.261, 1.185 // 1043.470, 0.000
1070.178, 0.000 // 1071.178, 1.192 // 1072.347, 0.000 // 1099.034, 0.000 // 1100.034, 1.196
1101.235, 0.000 // 1128.031, 0.000 // 1129.031, 1.189 // 1130.302, 0.000 // 1157.062, 0.000
1158.062, 1.216 // 1159.289, 0.000 // 1185.954, 0.000 // 1186.954, 1.196 // 1188.161, 0.000
1214.883, 0.000 // 1215.883, 1.189 // 1217.098, 0.000 // 1243.815, 0.000 // 1244.815, 1.184
1246.065, 0.000 // 1272.810, 0.000 // 1273.810, 1.171 // 1274.990, 0.000 // 1301.695, 0.000
1302.695, 1.174 // 1303.897, 0.000 // 1330.621, 0.000 // 1331.621, 1.179 // 1332.794, 0.000
1359.518, 0.000 // 1360.518, 1.183 // 1361.691, 0.000 // 1388.428, 0.000 // 1389.428, 1.194
1390.606, 0.000 // 1417.310, 0.000 // 1418.310, 1.206 // 1419.530, 0.000 // 1446.241, 0.000
1447.241, 1.192 // 1448.401, 0.000 // 1475.017, 0.000 // 1476.017, 1.164 // 1477.255, 0.000
1503.860, 0.000 // 1504.860, 1.176 // 1506.062, 0.000 // 1532.767, 0.000 // 1533.767, 1.210
1534.937, 0.000 // 1561.686, 0.000 // 1562.686, 1.180 // 1563.894, 0.000 // 1590.682, 0.000
1591.682, 1.160 // 1592.952, 0.000 // 1619.824, 0.000 // 1620.824, 1.170 // 1622.037, 0.000
1648.560, 0.000 // 1649.560, 1.183 // 1650.774, 0.000 // 1677.497, 0.000 // 1678.497, 1.183
1679.698, 0.000 // 1706.483, 0.000 // 1707.483, 1.183 // 1708.686, 0.000 // 1735.436, 0.000
1736.436, 1.173 // 1737.667, 0.000 // 1764.455, 0.000 // 1765.455, 1.173 // 1766.771, 0.000
1793.450, 0.000 // 1794.450, 1.182 // 1795.642, 0.000 // 1822.300, 0.000 // 1823.300, 1.181
1824.488, 0.000 // 1851.201, 0.000 // 1852.201, 1.203 // 1853.412, 0.000 // 1880.156, 0.000
1881.156, 1.172 // 1882.372, 0.000 // 1909.037, 0.000 // 1910.037, 1.197 // 1911.233, 0.000
1937.864, 0.000 // 1938.864, 1.171 // 1940.032, 0.000 // 1966.753, 0.000 // 1967.753, 1.161
1968.919, 0.000 // 1995.695, 0.000 // 1996.695, 1.195 // 1997.870, 0.000 // 2024.524, 0.000
2025.524, 1.178 // 2026.727, 0.000 // 2053.334, 0.000 // 2054.334, 1.169 // 2055.542, 0.000
2082.142, 0.000 // 2083.142, 1.211 // 2084.320, 0.000 // 2111.096, 0.000 // 2112.096, 1.194
2113.271, 0.000 // 2140.043, 0.000 // 2141.043, 1.178 // 2142.249, 0.000 // 2168.989, 0.000
2169.989, 1.189 // 2171.293, 0.000 // 2198.005, 0.000 // 2199.005, 1.181 // 2200.174, 0.000
2226.926, 0.000 // 2227.926, 1.165 // 2229.089, 0.000 // 2255.739, 0.000 // 2256.739, 1.192
2257.990, 0.000 // 2284.677, 0.000 // 2285.677, 1.185 // 2286.896, 0.000 // 2313.638, 0.000
2314.638, 0.910 // 2316.276, 0.000 // 2342.890, 0.000 // 2343.890, 1.187 // 2345.303, 0.000
2371.898, 0.000 // 2372.898, 1.202 // 2374.164, 0.000 // 2400.983, 0.000 // 2401.983, 1.218
2403.195, 0.000 // 2429.849, 0.000 // 2430.849, 1.191 // 2432.123, 0.000 // 2458.993, 0.000
2459.993, 1.201 // 2461.297, 0.000 // 2487.956, 0.000 // 2488.956, 1.202 // 2490.185, 0.000
2516.908, 0.000 // 2517.908, 1.195 // 2519.095, 0.000 // 2545.707, 0.000 // 2546.707, 1.195
2547.902, 0.000 // 2574.664, 0.000 // 2575.664, 1.182 // 2576.835, 0.000 // 2603.549, 0.000
2604.549, 1.208 // 2605.947, 0.000 // 2632.667, 0.000 // 2633.667, 1.179 // 2634.964, 0.000
2661.710, 0.000 // 2662.710, 1.166 // 2663.933, 0.000 // 2690.803, 0.000 // 2691.803, 1.170
2693.071, 0.000 // 2719.678, 0.000 // 2720.678, 1.176 // 2721.959, 0.000 // 2748.744, 0.000
2749.744, 1.168 // 2751.097, 0.000 // 2777.776, 0.000 // 2778.776, 1.168 // 2779.958, 0.000
2806.703, 0.000 // 2807.703, 1.157 // 2808.867, 0.000 // 2835.635, 0.000 // 2836.635, 1.199
2837.811, 0.000 // 2864.336, 0.000 // 2865.336, 1.177 // 2866.586, 0.000 // 2893.305, 0.000
2894.305, 1.174 // 2895.500, 0.000 // 2922.188, 0.000 // 2923.188, 1.180 // 2924.337, 0.000
2951.062, 0.000 // 2952.062, 1.186 // 2953.262, 0.000 // 2979.971, 0.000 // 2980.971, 1.166
2982.195, 0.000 // 3008.918, 0.000 // 3009.918, 1.170 // 3011.099, 0.000 // 3037.782, 0.000
3038.782, 1.127 // 3039.987, 0.000 // 3066.620, 0.000 // 3067.620, 1.184 // 3068.848, 0.000
3095.535, 0.000 // 3096.535, 1.177 // 3097.724, 0.000 // 3124.277, 0.000 // 3125.277, 1.198
3126.505, 0.000 // 3153.131, 0.000 // 3154.131, 1.219 // 3155.312, 0.000 // 3181.989, 0.000
3182.989, 1.195 // 3184.182, 0.000 // 3210.832, 0.000 // 3211.832, 1.174 // 3213.025, 0.000
3239.694, 0.000 // 3240.694, 1.191 // 3241.875, 0.000 // 3268.624, 0.000 // 3269.624, 1.185
3270.853, 0.000 // 3297.568, 0.000 // 3298.568, 1.183 // 3299.737, 0.000 // 3326.494, 0.000
3327.494, 1.198 // 3328.750, 0.000 // 3355.547, 0.000 // 3356.547, 1.169 // 3357.754, 0.000
3384.393, 0.000 // 3385.393, 1.181 // 3386.553, 0.000 // 3413.323, 0.000 // 3414.323, 1.180
3415.522, 0.000 // 3442.230, 0.000 // 3443.230, 1.200 // 3444.424, 0.000 // 3471.221, 0.000
3472.221, 1.194 // 3473.406, 0.000 // 3500.101, 0.000 // 3501.101, 1.180 // 3502.296, 0.000
3528.927, 0.000 // 3529.927, 1.185 // 3531.090, 0.000 // 3557.801, 0.000 // 3558.801, 1.202
3559.994, 0.000 // 3586.609, 0.000 // 3587.609, 1.177 // 3588.830, 0.000 // 3615.477, 0.000
3616.477, 1.200 // 3617.669, 0.000 // 3644.446, 0.000 // 3645.446, 1.165 // 3646.664, 0.000
3673.360, 0.000 // 3674.360, 1.178 // 3675.562, 0.000 // 3702.236, 0.000 // 3703.236, 1.181
3704.381, 0.000 // 3731.039, 0.000 // 3732.039, 1.160 // 3733.211, 0.000 // 3759.882, 0.000
3760.882, 1.179 // 3762.101, 0.000 // 3788.796, 0.000 // 3789.796, 1.176 // 3791.008, 0.000
3817.816, 0.000 // 3818.816, 1.172 // 3820.057, 0.000 // 3846.781, 0.000 // 3847.781, 1.174
3848.989, 0.000 // 3875.612, 0.000 // 3876.612, 1.197 // 3877.768, 0.000 // 3904.438, 0.000

```
3905.438, 1.182 // 3906.620, 0.000 // 3933.325, 0.000 // 3934.325, 1.207 // 3935.541, 0.000
3962.104, 0.000 // 3963.104, 1.200 // 3964.354, 0.000 // 3991.034, 0.000 // 3992.034, 1.200
3993.277, 0.000 // 4020.029, 0.000 // 4021.029, 1.170 // 4022.317, 0.000 // 4049.023, 0.000
4050.023, 1.227 // 4051.224, 0.000 // 4077.753, 0.000 // 4078.753, 1.197 // 4079.942, 0.000
4106.619, 0.000 // 4107.619, 1.194 // 4108.786, 0.000 // 4135.457, 0.000 // 4136.457, 1.189
4137.615, 0.000 // 4164.342, 0.000 // 4165.342, 1.207 // 4166.521, 0.000 // 4193.243, 0.000
4194.243, 1.197 // 4195.427, 0.000 // 4222.064, 0.000 // 4223.064, 1.203 // 4224.254, 0.000
4251.013, 0.000 // 4252.013, 1.196 // 4253.222, 0.000 // 4279.886, 0.000 // 4280.886, 1.180
4282.117, 0.000 // 4308.705, 0.000 // 4309.705, 1.193 // 4310.934, 0.000 // 4337.612, 0.000
4338.612, 1.181 // 4339.813, 0.000 // 4366.538, 0.000 // 4367.538, 1.178 // 4368.829, 0.000
4395.536, 0.000 // 4396.536, 1.174 // 4397.779, 0.000 // 4424.542, 0.000 // 4425.542, 1.190
4426.729, 0.000 // 4453.416, 0.000 // 4454.416, 1.178 // 4455.582, 0.000 // 4482.335, 0.000
4483.335, 1.177 // 4484.568, 0.000 // 4511.278, 0.000 // 4512.278, 1.173 // 4513.508, 0.000
4540.159, 0.000 // 4541.159, 1.188 // 4542.430, 0.000 // 4569.173, 0.000 // 4570.173, 1.196
4571.390, 0.000 // 4598.028, 0.000 // 4599.028, 1.182 // 4600.183, 0.000 // 4626.759, 0.000
4627.759, 1.182 // 4628.982, 0.000 // 4655.715, 0.000 // 4656.715, 1.201 // 4657.897, 0.000
4684.479, 0.000 // 4685.479, 1.192 // 4686.693, 0.000 // 4713.361, 0.000 // 4714.361, 1.196
4715.554, 0.000 // 4742.281, 0.000 // 4743.281, 1.195 // 4744.523, 0.000 // 4771.307, 0.000
4772.307, 1.180 // 4773.572, 0.000 // 4800.166, 0.000 // 4801.166, 1.176 // 4802.371, 0.000
4828.939, 0.000 // 4829.939, 1.190 // 4831.114, 0.000 // 4857.864, 0.000 // 4858.864, 1.190
4860.029, 0.000 // 4886.606, 0.000 // 4887.606, 1.188 // 4888.765, 0.000 // 4915.420, 0.000
4916.420, 1.197 // 4917.599, 0.000 // 4944.353, 0.000 // 4945.353, 1.196 // 4946.604, 0.000
4973.324, 0.000 // 4974.324, 1.170 // 4975.549, 0.000 // 5002.344, 0.000 // 5003.344, 1.201
5004.536, 0.000 // 5031.234, 0.000 // 5032.234, 1.186 // 5033.414, 0.000 // 5060.045, 0.000
5061.045, 1.183 // 5062.233, 0.000 // 5088.969, 0.000 // 5089.969, 1.193 // 5091.122, 0.000
5117.750, 0.000 // 5118.750, 1.190 // 5119.926, 0.000 // 5146.496, 0.000 // 5147.496, 1.203
5148.671, 0.000 // 5175.312, 0.000 // 5176.312, 1.189 // 5177.487, 0.000 // 5204.187, 0.000
5205.187, 1.161 // 5206.395, 0.000 // 5233.248, 0.000 // 5234.248, 1.195 // 5235.492, 0.000
5262.248, 0.000 // 5263.248, 1.188 // 5264.466, 0.000 // 5291.171, 0.000 // 5292.171, 1.199
5293.407, 0.000 // 5319.994, 0.000 // 5320.994, 1.186 // 5322.319, 0.000 // 5349.079, 0.000
5350.079, 1.210 // 5351.292, 0.000 // 5377.989, 0.000 // 5378.989, 1.178 // 5380.206, 0.000
5406.874, 0.000 // 5407.874, 1.188 // 5409.059, 0.000 // 5435.797, 0.000 // 5436.797, 1.193
5438.019, 0.000 // 5464.748, 0.000 // 5465.748, 1.182 // 5466.925, 0.000 // 5493.706, 0.000
5494.706, 1.182 // 5495.823, 0.000 // 5522.593, 0.000 // 5523.593, 1.192 // 5524.892, 0.000
5551.554, 0.000 // 5552.554, 1.196 // 5553.803, 0.000 // 5580.654, 0.000 // 5581.654, 1.194
5582.913, 0.000 // 5609.593, 0.000 // 5610.593, 1.186 // 5611.780, 0.000 // 5638.383, 0.000
5639.383, 1.183 // 5640.578, 0.000 // 5667.216, 0.000 // 5668.216, 1.180 // 5669.379, 0.000
5695.907, 0.000 // 5696.907, 1.197 // 5698.106, 0.000 // 5724.674, 0.000 // 5725.674, 1.193
5726.855, 0.000 // 5753.477, 0.000 // 5754.477, 0.813 // 5756.262, 0.000 // 5783.063, 0.000
5784.063, 1.209 // 5785.263, 0.000 // 5811.959, 0.000 // 5812.959, 1.207 // 5814.207, 0.000
5840.756, 0.000 // 5841.756, 1.194 // 5842.945, 0.000 // 5869.568, 0.000 // 5870.568, 1.211
5871.757, 0.000 // 5898.543, 0.000 // 5899.543, 1.175 // 5900.761, 0.000 // 5927.564, 0.000
5928.564, 1.171 // 5929.805, 0.000 // 5956.509, 0.000 // 5957.509, 1.191 // 5958.809, 0.000
5985.568, 0.000 // 5986.568, 1.168 // 5987.788, 0.000 // 6014.395, 0.000 // 6015.395, 1.168
6016.568, 0.000 // 6043.248, 0.000 // 6044.248, 1.170 // 6045.489, 0.000 // 6072.229, 0.000
6073.229, 1.149 // 6074.466, 0.000 // 6101.157, 0.000 // 6102.157, 1.177 // 6103.340, 0.000
6130.052, 0.000 // 6131.052, 1.173 // 6132.206, 0.000 // 6158.988, 0.000 // 6159.988, 1.181
6161.229, 0.000 // 6187.890, 0.000 // 6188.890, 1.162 // 6190.085, 0.000 // 6216.855, 0.000
6217.855, 1.140 // 6219.093, 0.000 // 6245.772, 0.000 // 6246.772, 1.174 // 6247.950, 0.000
6274.759, 0.000 // 6275.759, 1.171 // 6276.939, 0.000 // 6303.580, 0.000 // 6304.580, 1.174
6305.788, 0.000 // 6332.276, 0.000 // 6333.276, 1.154 // 6334.450, 0.000 // 6361.111, 0.000
6362.111, 1.174 // 6363.291, 0.000 // 6389.884, 0.000 // 6390.884, 1.190 // 6392.055, 0.000
6418.666, 0.000 // 6419.666, 1.186 // 6420.882, 0.000 // 6447.459, 0.000 // 6448.459, 1.202
6449.792, 0.000 // 6476.411, 0.000 // 6477.411, 1.193 // 6478.580, 0.000 // 6505.296, 0.000
6506.296, 1.168 // 6507.504, 0.000 // 6534.224, 0.000 // 6535.224, 1.174 // 6536.455, 0.000
6563.156, 0.000 // 6564.156, 1.172 // 6565.319, 0.000 // 6591.985, 0.000 // 6592.985, 1.194
6594.145, 0.000 // 6620.760, 0.000 // 6621.760, 1.173 // 6622.937, 0.000 // 6649.571, 0.000
6650.571, 1.172 // 6651.809, 0.000 // 6678.612, 0.000 // 6679.612, 1.180 // 6680.849, 0.000
6707.486, 0.000 // 6708.486, 1.170 // 6709.639, 0.000 // 6736.297, 0.000 // 6737.297, 1.163
6738.651, 0.000 // 6765.289, 0.000 // 6766.289, 1.199 // 6767.476, 0.000 // 6794.245, 0.000
6795.245, 1.172 // 6796.454, 0.000 // 6823.198, 0.000 // 6824.198, 1.175 // 6825.417, 0.000
6852.070, 0.000 // 6853.070, 1.211 // 6854.316, 0.000 // 6880.949, 0.000 // 6881.949, 1.179
6883.133, 0.000 // 6909.853, 0.000 // 6910.853, 1.161 // 6912.024, 0.000 // 6938.643, 0.000
```

6939.643, 1.225 // 6940.851, 0.000 // 6967.468, 0.000 // 6968.468, 1.180 // 6969.649, 0.000
6996.360, 0.000 // 6997.360, 1.175 // 6998.550, 0.000 // 7025.191, 0.000 // 7026.191, 1.155
7027.397, 0.000 // 7054.132, 0.000 // 7055.132, 1.185 // 7056.471, 0.000 // 7083.057, 0.000
7084.057, 1.180 // 7085.255, 0.000 // 7111.887, 0.000 // 7112.887, 1.160 // 7114.087, 0.000
7140.740, 0.000 // 7141.740, 1.181 // 7142.973, 0.000 // 7169.737, 0.000 // 7170.737, 1.180
7171.932, 0.000 // 7198.602, 0.000 // 7199.602, 1.160 // 7200.824, 0.000 // 7227.634, 0.000
7228.634, 1.171 // 7229.818, 0.000 // 7256.481, 0.000 // 7257.481, 1.180 // 7258.664, 0.000
7285.352, 0.000 // 7286.352, 1.175 // 7287.543, 0.000 // 7314.214, 0.000 // 7315.214, 1.160
7316.402, 0.000 // 7343.285, 0.000 // 7344.285, 1.173 // 7345.504, 0.000 // 7372.207, 0.000
7373.207, 1.179 // 7374.393, 0.000 // 7401.037, 0.000 // 7402.037, 1.181 // 7403.228, 0.000
7429.905, 0.000 // 7430.905, 1.199 // 7432.118, 0.000 // 7458.683, 0.000 // 7459.683, 1.210
7460.864, 0.000 // 7487.603, 0.000 // 7488.603, 1.170 // 7489.804, 0.000 // 7516.424, 0.000
7517.424, 1.170 // 7518.647, 0.000 // 7545.273, 0.000 // 7546.273, 1.176 // 7547.463, 0.000
7574.312, 0.000 // 7575.312, 1.198 // 7576.536, 0.000 // 7603.389, 0.000 // 7604.389, 1.170
7605.571, 0.000 // 7632.330, 0.000 // 7633.330, 1.184 // 7634.548, 0.000 // 7661.233, 0.000
7662.233, 1.168 // 7663.426, 0.000 // 7689.973, 0.000 // 7690.973, 1.197 // 7692.145, 0.000
7718.774, 0.000 // 7719.774, 1.191 // 7720.971, 0.000 // 7747.549, 0.000 // 7748.549, 1.196
7749.695, 0.000 // 7776.308, 0.000 // 7777.308, 1.194 // 7778.547, 0.000 // 7805.125, 0.000
7806.125, 1.174 // 7807.354, 0.000 // 7834.016, 0.000 // 7835.016, 1.178 // 7836.206, 0.000
7862.905, 0.000 // 7863.905, 1.186 // 7865.085, 0.000 // 7891.812, 0.000 // 7892.812, 1.191
7894.037, 0.000 // 7920.822, 0.000 // 7921.822, 1.190 // 7923.003, 0.000 // 7949.735, 0.000
7950.735, 1.172 // 7951.928, 0.000 // 7978.546, 0.000 // 7979.546, 1.205 // 7980.687, 0.000
8007.401, 0.000 // 8008.401, 1.184 // 8009.602, 0.000 // 8036.235, 0.000 // 8037.235, 1.194
8038.392, 0.000 // 8065.166, 0.000 // 8066.166, 1.177 // 8067.398, 0.000 // 8094.140, 0.000
8095.140, 1.187 // 8096.332, 0.000 // 8123.111, 0.000 // 8124.111, 1.190 // 8125.253, 0.000
8151.856, 0.000 // 8152.856, 1.165 // 8154.059, 0.000 // 8180.769, 0.000 // 8181.769, 1.189
8182.941, 0.000 // 8209.616, 0.000 // 8210.616, 1.203 // 8211.874, 0.000 // 8238.553, 0.000
8239.553, 1.179 // 8240.732, 0.000 // 8267.428, 0.000 // 8268.428, 1.181 // 8269.684, 0.000
8296.315, 0.000 // 8297.315, 1.183 // 8298.512, 0.000 // 8325.242, 0.000 // 8326.242, 1.204
8327.543, 0.000 // 8354.247, 0.000 // 8355.247, 1.187 // 8356.442, 0.000 // 8383.191, 0.000
8384.191, 1.215 // 8385.356, 0.000 // 8412.106, 0.000 // 8413.106, 1.213 // 8414.253, 0.000
8440.978, 0.000 // 8441.978, 1.202 // 8443.159, 0.000 // 8469.862, 0.000 // 8470.862, 1.181
8472.140, 0.000 // 8498.871, 0.000 // 8499.871, 1.192 // 8501.070, 0.000 // 8527.798, 0.000
8528.798, 1.190 // 8529.954, 0.000 // 8556.681, 0.000 // 8557.681, 1.199 // 8558.948, 0.000
8585.760, 0.000 // 8586.760, 1.184 // 8587.988, 0.000 // 8614.789, 0.000 // 8615.789, 1.193
8617.028, 0.000 // 8643.730, 0.000 // 8644.730, 1.228 // 8645.932, 0.000 // 8672.613, 0.000
8673.613, 1.213 // 8674.777, 0.000 // 8701.474, 0.000 // 8702.474, 1.206 // 8703.718, 0.000
8730.329, 0.000 // 8731.329, 1.184 // 8732.464, 0.000 // 8759.134, 0.000 // 8760.134, 1.187
8761.333, 0.000 // 8787.943, 0.000 // 8788.943, 1.164 // 8790.141, 0.000 // 8816.831, 0.000
8817.831, 1.187 // 8819.032, 0.000 // 8845.664, 0.000 // 8846.664, 1.177 // 8847.847, 0.000
8874.448, 0.000 // 8875.448, 1.175 // 8876.664, 0.000 // 8903.270, 0.000 // 8904.270, 1.170
8905.469, 0.000 // 8931.980, 0.000 // 8932.980, 1.214 // 8934.185, 0.000 // 8960.912, 0.000
8961.912, 1.191 // 8963.123, 0.000 // 8989.855, 0.000 // 8990.855, 1.192 // 8992.136, 0.000
9018.870, 0.000 // 9019.870, 1.205 // 9021.063, 0.000 // 9047.780, 0.000 // 9048.780, 1.172
9050.031, 0.000 // 9076.729, 0.000 // 9077.729, 1.170 // 9078.944, 0.000 // 9105.663, 0.000
9106.663, 1.158 // 9107.828, 0.000 // 9134.543, 0.000 // 9135.543, 1.154 // 9136.734, 0.000
9163.380, 0.000 // 9164.380, 1.157 // 9165.569, 0.000 // 9192.220, 0.000 // 9193.220, 1.163
9194.402, 0.000 // 9221.101, 0.000 // 9222.101, 1.167 // 9223.343, 0.000 // 9250.036, 0.000
9251.036, 1.179 // 9252.208, 0.000 // 9278.978, 0.000 // 9279.978, 0.704 // 9281.945, 0.000
9308.582, 0.000 // 9309.582, 1.156 // 9310.789, 0.000 // 9337.477, 0.000 // 9338.477, 1.192
9339.676, 0.000 // 9366.337, 0.000 // 9367.337, 1.191 // 9368.528, 0.000 // 9395.282, 0.000
9396.282, 1.192 // 9397.485, 0.000 // 9424.197, 0.000 // 9425.197, 1.170 // 9426.381, 0.000
9453.091, 0.000 // 9454.091, 1.177 // 9455.317, 0.000 // 9481.998, 0.000 // 9482.998, 1.172
9484.161, 0.000 // 9510.772, 0.000 // 9511.772, 1.179 // 9512.995, 0.000 // 9539.674, 0.000
9540.674, 1.201 // 9541.876, 0.000 // 9568.473, 0.000 // 9569.473, 1.194 // 9570.662, 0.000
9597.331, 0.000 // 9598.331, 1.181 // 9599.523, 0.000 // 9626.202, 0.000 // 9627.202, 1.185
9628.428, 0.000 // 9655.202, 0.000 // 9656.202, 1.185 // 9657.383, 0.000 // 9684.104, 0.000
9685.104, 1.191 // 9686.378, 0.000 // 9713.104, 0.000 // 9714.104, 1.171 // 9715.284, 0.000
9741.948, 0.000 // 9742.948, 1.176 // 9744.233, 0.000 // 9771.005, 0.000 // 9772.005, 1.153
9773.220, 0.000 // 9799.888, 0.000 // 9800.888, 1.171 // 9802.082, 0.000 // 9828.649, 0.000
9829.649, 1.157 // 9830.792, 0.000 // 9857.518, 0.000 // 9858.518, 1.184 // 9859.814, 0.000
9886.503, 0.000 // 9887.503, 1.177 // 9888.693, 0.000 // 9915.316, 0.000 // 9916.316, 1.178
9917.612, 0.000 // 9944.332, 0.000 // 9945.332, 1.178 // 9946.496, 0.000 // 9973.281, 0.000

9974.281, 1.189 // 9975.498, 0.000 // 10002.182, 0.000 // 10003.182, 1.186 // 10004.413, 0.000
10031.092, 0.000 // 10032.092, 1.184 // 10033.283, 0.000 // 10060.073, 0.000 // 10061.073, 1.188
10062.204, 0.000 // 10088.838, 0.000 // 10089.838, 1.204 // 10091.024, 0.000 // 10117.768, 0.000
10118.768, 1.184 // 10119.992, 0.000 // 10146.665, 0.000 // 10147.665, 1.199 // 10148.829, 0.000
10175.446, 0.000 // 10176.446, 1.225 // 10177.628, 0.000 // 10204.340, 0.000 // 10205.340, 1.173
10206.543, 0.000 // 10233.263, 0.000 // 10234.263, 1.184 // 10235.493, 0.000 // 10262.208, 0.000
10263.208, 1.191 // 10264.363, 0.000 // 10291.119, 0.000 // 10292.119, 1.182 // 10293.291, 0.000
10320.084, 0.000 // 10321.084, 1.184 // 10322.322, 0.000 // 10349.049, 0.000 // 10350.049, 1.165
10351.264, 0.000 // 10378.024, 0.000 // 10379.024, 1.170 // 10380.224, 0.000 // 10406.999, 0.000
10407.999, 1.151 // 10409.291, 0.000 // 10436.035, 0.000 // 10437.035, 1.204 // 10438.187, 0.000
10464.853, 0.000 // 10465.853, 1.167 // 10467.025, 0.000 // 10493.808, 0.000 // 10494.808, 1.166
10496.178, 0.000 // 10522.829, 0.000 // 10523.829, 1.178 // 10525.022, 0.000 // 10551.709, 0.000
10552.709, 1.177 // 10553.856, 0.000 // 10580.482, 0.000 // 10581.482, 1.181 // 10582.666, 0.000
10609.341, 0.000 // 10610.341, 1.149 // 10611.519, 0.000 // 10638.230, 0.000 // 10639.230, 1.162
10640.408, 0.000 // 10667.019, 0.000 // 10668.019, 1.181 // 10669.180, 0.000 // 10695.877, 0.000
10696.877, 1.154 // 10698.112, 0.000 // 10724.856, 0.000 // 10725.856, 1.190 // 10727.090, 0.000
10753.865, 0.000 // 10754.865, 1.179 // 10756.120, 0.000 // 10782.899, 0.000 // 10783.899, 1.166
10785.195, 0.000 // 10811.856, 0.000 // 10812.856, 1.167 // 10814.023, 0.000 // 10840.744, 0.000
10841.744, 1.174 // 10842.938, 0.000 // 10869.571, 0.000 // 10870.571, 1.160 // 10871.721, 0.000
10898.502, 0.000 // 10899.502, 1.196 // 10900.708, 0.000 // 10927.341, 0.000 // 10928.341, 1.181
10929.549, 0.000 // 10956.152, 0.000 // 10957.152, 1.187 // 10958.345, 0.000 // 10985.166, 0.000
10986.166, 1.139 // 10987.350, 0.000 // 11013.936, 0.000 // 11014.936, 1.161 // 11016.131, 0.000
11042.731, 0.000 // 11043.731, 1.138 // 11044.920, 0.000 // 11071.728, 0.000 // 11072.728, 1.136
11073.952, 0.000 // 11100.727, 0.000 // 11101.727, 1.166 // 11102.861, 0.000 // 11129.513, 0.000
11130.513, 1.121 // 11131.690, 0.000 // 11158.366, 0.000 // 11159.366, 1.127 // 11160.497, 0.000
11187.295, 0.000 // 11188.295, 1.117 // 11189.596, 0.000 // 11216.371, 0.000 // 11217.371, 1.147
11218.562, 0.000 // 11245.273, 0.000 // 11246.273, 1.146 // 11247.486, 0.000 // 11274.179, 0.000
11275.179, 1.127 // 11276.360, 0.000 // 11303.032, 0.000 // 11304.032, 1.150 // 11305.207, 0.000
11331.899, 0.000 // 11332.899, 1.125 // 11334.154, 0.000 // 11360.861, 0.000 // 11361.861, 1.129
11363.024, 0.000 // 11389.783, 0.000 // 11390.783, 1.145 // 11392.025, 0.000 // 11418.563, 0.000
11419.563, 1.141 // 11420.731, 0.000 // 11447.393, 0.000 // 11448.393, 1.123 // 11449.611, 0.000
11476.461, 0.000 // 11477.461, 1.135 // 11478.659, 0.000 // 11505.285, 0.000 // 11506.285, 1.124
11507.494, 0.000 // 11534.212, 0.000 // 11535.212, 1.141 // 11536.414, 0.000 // 11563.192, 0.000
11564.192, 1.117 // 11565.396, 0.000 // 11592.049, 0.000 // 11593.049, 1.115 // 11594.222, 0.000
11620.828, 0.000 // 11621.828, 1.116 // 11623.016, 0.000 // 11649.753, 0.000 // 11650.753, 1.125
11651.945, 0.000 // 11678.726, 0.000 // 11679.726, 1.151 // 11680.939, 0.000 // 11707.625, 0.000
11708.625, 1.128 // 11709.975, 0.000 // 11736.697, 0.000 // 11737.697, 1.120 // 11738.882, 0.000
11765.603, 0.000 // 11766.603, 1.118 // 11767.797, 0.000 // 11794.414, 0.000 // 11795.414, 1.124
11796.614, 0.000 // 11823.403, 0.000 // 11824.403, 1.149 // 11825.628, 0.000 // 11852.283, 0.000
11853.283, 1.115 // 11854.424, 0.000 // 11881.215, 0.000 // 11882.215, 1.139 // 11883.378, 0.000
11910.080, 0.000 // 11911.080, 1.142 // 11912.328, 0.000 // 11939.035, 0.000 // 11940.035, 0.000
11941.160, 0.000 // 11967.793, 0.000 // 11968.793, 1.113 // 11970.026, 0.000 // 11996.808, 0.000
11997.808, 1.115 // 11999.030, 0.000 // 12025.778, 0.000 // 12026.778, 1.124 // 12027.944, 0.000
12054.622, 0.000 // 12055.622, 1.124 // 12056.860, 0.000 // 12083.671, 0.000 // 12084.671, 1.124
12085.875, 0.000 // 12112.527, 0.000 // 12113.527, 1.125 // 12114.683, 0.000 // 12141.476, 0.000
12142.476, 1.114 // 12143.652, 0.000 // 12170.251, 0.000 // 12171.251, 1.123 // 12172.383, 0.000
12199.017, 0.000 // 12200.017, 1.138 // 12201.184, 0.000 // 12227.829, 0.000 // 12228.829, 1.148
12230.072, 0.000 // 12256.882, 0.000 // 12257.882, 1.148 // 12259.076, 0.000 // 12285.756, 0.000
12286.756, 1.158 // 12287.942, 0.000 // 12314.515, 0.000 // 12315.515, 1.161 // 12316.718, 0.000
12343.349, 0.000 // 12344.349, 1.137 // 12345.526, 0.000 // 12372.160, 0.000 // 12373.160, 0.509
12375.407, 0.000 // 12402.160, 0.000 // 12403.160, 1.124 // 12404.402, 0.000 // 12431.044, 0.000
12432.044, 1.129 // 12433.412, 0.000 // 12460.123, 0.000 // 12461.123, 1.125 // 12462.327, 0.000
12489.008, 0.000 // 12490.008, 1.133 // 12491.242, 0.000 // 12517.881, 0.000 // 12518.881, 1.132
12520.052, 0.000 // 12546.752, 0.000 // 12547.752, 1.127 // 12548.904, 0.000 // 12575.499, 0.000
12576.499, 1.159 // 12577.668, 0.000 // 12604.324, 0.000 // 12605.324, 1.171 // 12606.509, 0.000
12633.131, 0.000 // 12634.131, 1.156 // 12635.317, 0.000 // 12662.007, 0.000 // 12663.007, 1.138
12664.179, 0.000 // 12690.935, 0.000 // 12691.935, 1.138 // 12693.111, 0.000 // 12719.905, 0.000
12720.905, 1.102 // 12722.124, 0.000 // 12748.786, 0.000 // 12749.786, 1.145 // 12750.967, 0.000
12777.586, 0.000 // 12778.586, 1.132 // 12779.781, 0.000 // 12806.469, 0.000 // 12807.469, 1.145
12808.642, 0.000 // 12835.343, 0.000 // 12836.343, 1.141 // 12837.574, 0.000 // 12864.264, 0.000
12865.264, 1.157 // 12866.508, 0.000 // 12893.099, 0.000 // 12894.099, 1.170 // 12895.293, 0.000
12921.880, 0.000 // 12922.880, 1.151 // 12924.054, 0.000 // 12950.913, 0.000 // 12951.913, 1.140
12953.100, 0.000 // 12979.771, 0.000 // 12980.771, 1.151 // 12981.997, 0.000 // 13008.783, 0.000

13009.783, 1.145 // 13010.969, 0.000 // 13037.710, 0.000 // 13038.710, 1.138 // 13039.892, 0.000
13066.659, 0.000 // 13067.659, 1.147 // 13068.864, 0.000 // 13095.523, 0.000 // 13096.523, 1.140
13097.691, 0.000 // 13124.447, 0.000 // 13125.447, 0.000 // 13126.559, 0.000 // 13153.174, 0.000
13154.174, 1.153 // 13155.348, 0.000 // 13182.020, 0.000 // 13183.020, 1.131 // 13184.201, 0.000
13210.924, 0.000 // 13211.924, 1.139 // 13213.130, 0.000 // 13239.874, 0.000 // 13240.874, 1.138
13242.072, 0.000 // 13268.762, 0.000 // 13269.762, 1.132 // 13270.978, 0.000 // 13297.647, 0.000
13298.647, 1.129 // 13299.893, 0.000 // 13326.557, 0.000 // 13327.557, 1.129 // 13328.808, 0.000
13355.553, 0.000 // 13356.553, 1.144 // 13357.730, 0.000 // 13384.327, 0.000 // 13385.327, 1.138
13386.501, 0.000 // 13413.188, 0.000 // 13414.188, 1.143 // 13415.364, 0.000 // 13442.127, 0.000
13443.127, 1.131 // 13444.399, 0.000 // 13471.163, 0.000 // 13472.163, 1.140 // 13473.403, 0.000
13500.176, 0.000 // 13501.176, 1.097 // 13502.362, 0.000 // 13529.309, 0.000 // 13530.309, 1.133
13531.519, 0.000 // 13558.279, 0.000 // 13559.279, 1.118 // 13560.435, 0.000 // 13587.192, 0.000
13588.192, 1.103 // 13589.386, 0.000 // 13616.108, 0.000 // 13617.108, 1.111 // 13618.391, 0.000
13645.088, 0.000 // 13646.088, 1.116 // 13647.254, 0.000 // 13673.959, 0.000 // 13674.959, 1.163
13676.170, 0.000 // 13702.913, 0.000 // 13703.913, 1.130 // 13705.093, 0.000 // 13731.744, 0.000
13732.744, 1.116 // 13733.928, 0.000 // 13760.621, 0.000 // 13761.621, 1.122 // 13762.834, 0.000
13789.362, 0.000 // 13790.362, 1.130 // 13791.574, 0.000 // 13818.444, 0.000 // 13819.444, 1.137
13820.668, 0.000 // 13847.358, 0.000 // 13848.358, 1.118 // 13849.601, 0.000 // 13876.189, 0.000
13877.189, 1.153 // 13878.372, 0.000 // 13905.071, 0.000 // 13906.071, 1.138 // 13907.269, 0.000
13934.067, 0.000 // 13935.067, 1.124 // 13936.242, 0.000 // 13962.966, 0.000 // 13963.966, 1.142
13965.154, 0.000 // 13991.877, 0.000 // 13992.877, 1.161 // 13994.065, 0.000 // 14020.780, 0.000
14021.780, 1.149 // 14022.956, 0.000 // 14049.634, 0.000 // 14050.634, 1.151 // 14051.871, 0.000
14078.498, 0.000 // 14079.498, 1.132 // 14080.871, 0.000 // 14107.497, 0.000 // 14108.497, 1.122
14109.723, 0.000 // 14136.326, 0.000 // 14137.326, 1.117 // 14138.537, 0.000 // 14165.301, 0.000
14166.301, 1.148 // 14167.693, 0.000 // 14194.343, 0.000 // 14195.343, 1.142 // 14196.521, 0.000
14223.208, 0.000 // 14224.208, 1.112 // 14225.395, 0.000 // 14252.103, 0.000 // 14253.103, 1.165
14254.416, 0.000 // 14281.190, 0.000 // 14282.190, 1.156 // 14283.394, 0.000 // 14310.225, 0.000
14311.225, 0.098 // 14312.335, 0.000 // 14339.117, 0.000 // 14340.117, 1.169 // 14341.277, 0.000
14368.029, 0.000 // 14369.029, 1.182 // 14370.261, 0.000 // 14397.009, 0.000 // 14398.009, 1.182
14399.235, 0.000 // 14425.891, 0.000 // 14426.891, 1.202 // 14428.087, 0.000 // 14454.768, 0.000
14455.768, 1.173 // 14456.921, 0.000 // 14483.547, 0.000 // 14484.547, 1.193 // 14485.739, 0.000
14512.377, 0.000 // 14513.377, 1.158 // 14514.618, 0.000 // 14541.403, 0.000 // 14542.403, 1.169
14543.604, 0.000 // 14570.324, 0.000 // 14571.324, 1.189 // 14572.599, 0.000 // 14599.430, 0.000
14600.430, 1.160 // 14601.644, 0.000 // 14628.436, 0.000 // 14629.436, 1.175 // 14630.644, 0.000
14657.354, 0.000 // 14658.354, 1.180 // 14659.577, 0.000 // 14686.380, 0.000 // 14687.380, 1.169
14688.545, 0.000 // 14715.154, 0.000 // 14716.154, 1.162 // 14717.334, 0.000 // 14744.004, 0.000
14745.004, 1.154 // 14746.237, 0.000 // 14772.878, 0.000 // 14773.878, 1.159 // 14775.051, 0.000
14801.675, 0.000 // 14802.675, 1.169 // 14803.831, 0.000 // 14830.433, 0.000 // 14831.433, 1.166
14832.603, 0.000 // 14859.245, 0.000 // 14860.245, 1.162 // 14861.429, 0.000 // 14888.124, 0.000
14889.124, 1.174 // 14890.324, 0.000 // 14917.032, 0.000 // 14918.032, 1.168 // 14919.239, 0.000
14945.929, 0.000 // 14946.929, 1.153 // 14948.089, 0.000 // 14974.804, 0.000 // 14975.804, 1.165
14976.994, 0.000 // 15003.644, 0.000 // 15004.644, 1.151 // 15005.814, 0.000 // 15032.657, 0.000
15033.657, 1.158 // 15034.872, 0.000 // 15061.455, 0.000 // 15062.455, 1.161 // 15063.662, 0.000
15090.346, 0.000 // 15091.346, 1.159 // 15092.604, 0.000 // 15119.414, 0.000 // 15120.414, 1.170
15121.600, 0.000 // 15148.316, 0.000 // 15149.316, 1.140 // 15150.571, 0.000 // 15177.234, 0.000
15178.234, 1.141 // 15179.465, 0.000 // 15206.245, 0.000 // 15207.245, 1.177 // 15208.427, 0.000
15235.084, 0.000 // 15236.084, 1.168 // 15237.284, 0.000 // 15263.981, 0.000 // 15264.981, 1.142
15266.181, 0.000 // 15292.869, 0.000 // 15293.869, 1.154 // 15295.033, 0.000 // 15321.615, 0.000
15322.615, 1.178 // 15324.341, 0.000 // 15351.045, 0.000 // 15352.045, 1.086 // 15353.346, 0.000
15380.084, 0.000 // 15381.084, 1.132 // 15382.281, 0.000 // 15409.024, 0.000 // 15410.024, 1.159
15411.285, 0.000 // 15437.939, 0.000 // 15438.939, 1.157 // 15440.125, 0.000 // 15466.861, 0.000
15467.861, 1.146 // 15469.053, 0.000 // 15495.766, 0.000 // 15496.766, 1.155 // 15498.014, 0.000
15524.765, 0.000 // 15525.765, 0.000 // 15526.908, 0.000 // 15553.611, 0.000 // 15554.611, 1.180
15555.779, 0.000 // 15582.422, 0.000 // 15583.422, 1.168 // 15584.613, 0.000 // 15611.345, 0.000
15612.345, 1.161 // 15613.567, 0.000 // 15640.294, 0.000 // 15641.294, 1.150 // 15642.474, 0.000
15669.087, 0.000 // 15670.087, 1.157 // 15671.250, 0.000 // 15697.972, 0.000 // 15698.972, 1.174
15700.200, 0.000 // 15726.926, 0.000 // 15727.926, 1.154 // 15729.151, 0.000 // 15755.825, 0.000
15756.825, 1.168 // 15758.033, 0.000 // 15784.735, 0.000 // 15785.735, 1.162 // 15786.942, 0.000
15813.668, 0.000 // 15814.668, 1.178 // 15815.888, 0.000 // 15842.464, 0.000 // 15843.464, 1.166
15844.659, 0.000 // 15871.326, 0.000 // 15872.326, 1.169 // 15873.503, 0.000 // 15900.118, 0.000
15901.118, 1.173 // 15902.284, 0.000 // 15928.908, 0.000 // 15929.908, 1.169 // 15931.104, 0.000
15957.779, 0.000 // 15958.779, 1.167 // 15959.920, 0.000 // 15986.496, 0.000 // 15987.496, 1.189
15988.734, 0.000 // 16015.518, 0.000 // 16016.518, 1.185 // 16017.704, 0.000 // 16044.298, 0.000

16045.298, 1.197 // 16046.471, 0.000 // 16073.115, 0.000 // 16074.115, 1.179 // 16075.326, 0.000
16102.020, 0.000 // 16103.020, 1.182 // 16104.286, 0.000 // 16131.038, 0.000 // 16132.038, 1.159
16133.308, 0.000 // 16160.117, 0.000 // 16161.117, 0.922 // 16162.904, 0.000 // 16189.623, 0.000
16190.623, 1.192 // 16191.817, 0.000 // 16218.553, 0.000 // 16219.553, 1.180 // 16220.786, 0.000
16247.592, 0.000 // 16248.592, 1.168 // 16249.823, 0.000 // 16276.547, 0.000 // 16277.547, 1.169
16278.747, 0.000 // 16305.523, 0.000 // 16306.523, 1.178 // 16307.805, 0.000 // 16334.568, 0.000
16335.568, 1.184 // 16336.738, 0.000 // 16363.480, 0.000 // 16364.480, 1.190 // 16365.680, 0.000
16392.426, 0.000 // 16393.426, 1.192 // 16394.665, 0.000 // 16421.237, 0.000 // 16422.237, 1.168
16423.413, 0.000 // 16450.031, 0.000 // 16451.031, 1.178 // 16452.242, 0.000 // 16478.898, 0.000
16479.898, 1.174 // 16481.125, 0.000 // 16507.861, 0.000 // 16508.861, 1.167 // 16510.120, 0.000
16536.881, 0.000 // 16537.881, 1.198 // 16539.051, 0.000 // 16565.656, 0.000 // 16566.656, 1.161
16567.839, 0.000 // 16594.676, 0.000 // 16595.676, 1.173 // 16596.868, 0.000 // 16623.688, 0.000
16624.688, 1.182 // 16625.872, 0.000 // 16652.575, 0.000 // 16653.575, 1.278 // 16654.763, 0.000
16681.434, 0.000 // 16682.434, 1.175 // 16683.655, 0.000 // 16710.559, 0.000 // 16711.559, 0.000
16712.810, 0.000 // 16739.626, 0.000 // 16740.626, 1.162 // 16741.872, 0.000 // 16768.634, 0.000
16769.634, 1.183 // 16770.805, 0.000 // 16797.563, 0.000 // 16798.563, 1.152 // 16799.760, 0.000
16826.430, 0.000 // 16827.430, 1.179 // 16828.633, 0.000 // 16855.331, 0.000 // 16856.331, 1.159
16857.485, 0.000 // 16884.184, 0.000 // 16885.184, 1.141 // 16886.381, 0.000 // 16912.987, 0.000
16913.987, 1.162 // 16915.228, 0.000 // 16941.926, 0.000 // 16942.926, 1.175 // 16944.128, 0.000
16970.826, 0.000 // 16971.826, 1.159 // 16973.025, 0.000 // 16999.754, 0.000 // 17000.754, 1.174
17001.943, 0.000 // 17028.639, 0.000 // 17029.639, 1.169 // 17030.839, 0.000 // 17057.504, 0.000
17058.504, 1.150 // 17059.709, 0.000 // 17086.412, 0.000 // 17087.412, 1.164 // 17088.575, 0.000
17115.293, 0.000 // 17116.293, 1.190 // 17117.454, 0.000 // 17144.103, 0.000 // 17145.103, 1.183
17146.293, 0.000 // 17172.988, 0.000 // 17173.988, 1.173 // 17175.248, 0.000 // 17202.010, 0.000
17203.010, 1.173 // 17204.163, 0.000 // 17230.929, 0.000 // 17231.929, 1.165 // 17233.076, 0.000
17259.803, 0.000 // 17260.803, 1.165 // 17261.948, 0.000 // 17288.682, 0.000 // 17289.682, 1.153
17290.854, 0.000 // 17317.644, 0.000 // 17318.644, 1.156 // 17319.852, 0.000 // 17346.530, 0.000
17347.530, 1.160 // 17348.691, 0.000 // 17375.450, 0.000 // 17376.450, 1.170 // 17377.619, 0.000
17404.376, 0.000 // 17405.376, 1.167 // 17406.539, 0.000 // 17433.238, 0.000 // 17434.238, 1.172
17435.432, 0.000 // 17462.194, 0.000 // 17463.194, 1.152 // 17464.408, 0.000 // 17491.144, 0.000
17492.144, 1.150 // 17493.358, 0.000 // 17520.119, 0.000 // 17521.119, 1.124 // 17522.300, 0.000
17549.054, 0.000 // 17550.054, 1.118 // 17551.275, 0.000 // 17577.897, 0.000 // 17578.897, 1.157
17580.063, 0.000 // 17606.722, 0.000 // 17607.722, 1.120 // 17608.951, 0.000 // 17635.687, 0.000
17636.687, 1.170 // 17637.842, 0.000 // 17664.680, 0.000 // 17665.680, 1.164 // 17666.976, 0.000
17693.648, 0.000 // 17694.648, 1.148 // 17695.861, 0.000 // 17722.575, 0.000 // 17723.575, 1.181
17724.724, 0.000 // 17751.507, 0.000 // 17752.507, 1.182 // 17753.817, 0.000 // 17780.692, 0.000
17781.692, 1.174 // 17782.871, 0.000 // 17809.589, 0.000 // 17810.589, 1.173 // 17811.778, 0.000
17838.538, 0.000 // 17839.538, 1.181 // 17840.735, 0.000 // 17867.335, 0.000 // 17868.335, 1.173
17869.511, 0.000 // 17896.279, 0.000 // 17897.279, 1.171 // 17898.514, 0.000 // 17925.318, 0.000
17926.318, 1.155 // 17927.545, 0.000 // 17954.241, 0.000 // 17955.241, 1.153 // 17956.416, 0.000
17983.128, 0.000 // 17984.128, 1.166 // 17985.352, 0.000 // 18011.957, 0.000 // 18012.957, 1.156
18014.143, 0.000 // 18040.897, 0.000 // 18041.897, 1.172 // 18043.112, 0.000 // 18069.807, 0.000
18070.807, 1.155 // 18071.973, 0.000 // 18098.673, 0.000 // 18099.673, 1.136 // 18100.848, 0.000
18127.617, 0.000 // 18128.617, 1.166 // 18129.802, 0.000 // 18156.535, 0.000 // 18157.535, 1.151
18158.762, 0.000 // 18185.473, 0.000 // 18186.473, 1.184 // 18187.650, 0.000 // 18214.307, 0.000
18215.307, 1.153 // 18216.482, 0.000 // 18243.219, 0.000 // 18244.219, 1.161 // 18245.385, 0.000
18272.198, 0.000 // 18273.198, 1.163 // 18274.363, 0.000 // 18300.989, 0.000 // 18301.989, 1.135
18303.192, 0.000 // 18329.814, 0.000 // 18330.814, 1.157 // 18332.055, 0.000 // 18358.863, 0.000
18359.863, 1.162 // 18361.050, 0.000 // 18387.847, 0.000 // 18388.847, 1.171 // 18390.045, 0.000
18416.802, 0.000 // 18417.802, 1.160 // 18418.980, 0.000 // 18445.708, 0.000 // 18446.708, 1.158
18448.015, 0.000 // 18474.780, 0.000 // 18475.780, 1.163 // 18476.953, 0.000 // 18503.600, 0.000
18504.600, 1.158 // 18505.787, 0.000 // 18532.407, 0.000 // 18533.407, 1.146 // 18534.616, 0.000
18561.254, 0.000 // 18562.254, 1.155 // 18563.443, 0.000 // 18590.076, 0.000 // 18591.076, 1.213
18592.334, 0.000 // 18619.027, 0.000 // 18620.027, 1.154 // 18621.231, 0.000 // 18647.858, 0.000
18648.858, 1.150 // 18650.047, 0.000 // 18676.711, 0.000 // 18677.711, 1.156 // 18678.935, 0.000
18705.688, 0.000 // 18706.688, 1.148 // 18707.895, 0.000 // 18734.615, 0.000 // 18735.615, 1.174
18736.858, 0.000 // 18763.533, 0.000 // 18764.533, 1.152 // 18765.695, 0.000 // 18792.382, 0.000
18793.382, 1.174 // 18794.565, 0.000 // 18821.230, 0.000 // 18822.230, 1.149 // 18823.436, 0.000
18850.257, 0.000 // 18851.257, 1.169 // 18852.421, 0.000 // 18879.138, 0.000 // 18880.138, 1.160
18881.288, 0.000 // 18908.051, 0.000 // 18909.051, 1.177 // 18910.250, 0.000 // 18936.903, 0.000
18937.903, 1.179 // 18939.046, 0.000 // 18965.712, 0.000 // 18966.712, 1.153 // 18967.867, 0.000
18994.480, 0.000 // 18995.480, 1.152 // 18996.701, 0.000 // 19023.318, 0.000 // 19024.318, 1.144
19025.501, 0.000 // 19052.180, 0.000 // 19053.180, 1.141 // 19054.341, 0.000 // 19081.053, 0.000

19082.053, 1.161 // 19083.265, 0.000 // 19109.958, 0.000 // 19110.958, 0.000 // 19112.060, 0.000
19138.757, 0.000 // 19139.757, 1.147 // 19140.926, 0.000 // 19167.627, 0.000 // 19168.627, 1.137
19169.814, 0.000 // 19196.655, 0.000 // 19197.655, 1.132 // 19198.862, 0.000 // 19225.585, 0.000
19226.585, 1.167 // 19227.750, 0.000 // 19254.455, 0.000 // 19255.455, 1.149 // 19256.621, 0.000
19283.219, 0.000 // 19284.219, 1.164 // 19285.437, 0.000 // 19312.047, 0.000 // 19313.047, 1.143
19314.230, 0.000 // 19340.966, 0.000 // 19341.966, 1.151 // 19343.172, 0.000 // 19369.786, 0.000
19370.786, 1.167 // 19371.961, 0.000 // 19398.650, 0.000 // 19399.650, 1.145 // 19400.867, 0.000
19427.568, 0.000 // 19428.568, 1.144 // 19429.776, 0.000 // 19456.441, 0.000 // 19457.441, 1.148
19458.633, 0.000 // 19485.390, 0.000 // 19486.390, 1.123 // 19487.564, 0.000 // 19514.295, 0.000
19515.295, 1.164 // 19516.541, 0.000 // 19543.221, 0.000 // 19544.221, 1.151 // 19545.421, 0.000
19572.127, 0.000 // 19573.127, 1.133 // 19574.335, 0.000 // 19601.021, 0.000 // 19602.021, 1.150
19603.154, 0.000 // 19629.766, 0.000 // 19630.766, 1.098 // 19632.046, 0.000 // 19658.783, 0.000
19659.783, 1.143 // 19660.979, 0.000 // 19687.737, 0.000 // 19688.737, 1.148 // 19689.918, 0.000
19716.588, 0.000 // 19717.588, 1.129 // 19718.797, 0.000 // 19745.458, 0.000 // 19746.458, 1.155
19747.659, 0.000 // 19774.384, 0.000 // 19775.384, 1.157 // 19776.700, 0.000 // 19803.463, 0.000
19804.463, 1.148 // 19805.660, 0.000 // 19832.355, 0.000 // 19833.355, 1.125 // 19834.572, 0.000
19861.285, 0.000 // 19862.285, 1.141 // 19863.485, 0.000 // 19890.150, 0.000 // 19891.150, 1.164
19892.326, 0.000 // 19919.106, 0.000 // 19920.106, 1.138 // 19921.295, 0.000 // 19948.117, 0.000
19949.117, 1.156 // 19950.364, 0.000 // 19977.042, 0.000 // 19978.042, 1.147 // 19979.270, 0.000
20005.861, 0.000 // 20006.861, 1.144 // 20008.051, 0.000 // 20034.773, 0.000 // 20035.773, 1.165
20036.960, 0.000 // 20063.795, 0.000 // 20064.795, 1.117 // 20066.029, 0.000 // 20092.735, 0.000
20093.735, 1.144 // 20094.943, 0.000 // 20121.664, 0.000 // 20122.664, 1.147 // 20123.820, 0.000
20150.690, 0.000 // 20151.690, 1.153 // 20152.904, 0.000 // 20179.731, 0.000 // 20180.731, 1.165
20181.971, 0.000 // 20208.769, 0.000 // 20209.769, 1.145 // 20210.913, 0.000 // 20237.579, 0.000
20238.579, 1.134 // 20239.783, 0.000 // 20266.524, 0.000 // 20267.524, 1.167 // 20268.689, 0.000
20295.376, 0.000 // 20296.376, 0.000 // 20297.524, 0.000 // 20324.268, 0.000 // 20325.268, 1.145
20326.466, 0.000 // 20353.202, 0.000 // 20354.202, 1.158 // 20355.398, 0.000 // 20382.045, 0.000
20383.045, 1.144 // 20384.313, 0.000 // 20411.146, 0.000 // 20412.146, 1.137 // 20413.343, 0.000
20439.975, 0.000 // 20440.975, 1.164 // 20442.129, 0.000 // 20468.951, 0.000 // 20469.951, 1.152
20471.097, 0.000 // 20497.728, 0.000 // 20498.728, 1.134 // 20499.896, 0.000 // 20526.660, 0.000
20527.660, 1.109 // 20528.857, 0.000 // 20555.524, 0.000 // 20556.524, 1.116 // 20557.721, 0.000
20584.403, 0.000 // 20585.403, 1.163 // 20586.609, 0.000 // 20613.308, 0.000 // 20614.308, 1.155
20615.532, 0.000 // 20642.213, 0.000 // 20643.213, 1.128 // 20644.402, 0.000 // 20671.139, 0.000
20672.139, 1.130 // 20673.337, 0.000 // 20699.962, 0.000 // 20700.962, 1.117 // 20702.145, 0.000
20728.796, 0.000 // 20729.796, 1.122 // 20730.988, 0.000 // 20757.789, 0.000 // 20758.789, 1.113
20759.965, 0.000 // 20786.708, 0.000 // 20787.708, 1.136 // 20788.897, 0.000 // 20815.601, 0.000
20816.601, 1.121 // 20817.775, 0.000 // 20844.438, 0.000 // 20845.438, 1.121 // 20846.663, 0.000
20873.322, 0.000 // 20874.322, 1.140 // 20875.513, 0.000 // 20902.193, 0.000 // 20903.193, 1.140
20904.375, 0.000 // 20931.137, 0.000 // 20932.137, 1.116 // 20933.343, 0.000 // 20960.063, 0.000
20961.063, 1.139 // 20962.262, 0.000 // 20988.947, 0.000 // 20989.947, 1.141 // 20991.122, 0.000
21017.758, 0.000 // 21018.758, 1.160 // 21019.983, 0.000 // 21046.666, 0.000 // 21047.666, 1.150
21048.853, 0.000 // 21075.520, 0.000 // 21076.520, 1.166 // 21077.741, 0.000 // 21104.548, 0.000
21105.548, 1.137 // 21106.728, 0.000 // 21133.399, 0.000 // 21134.399, 1.126 // 21135.571, 0.000
21162.206, 0.000 // 21163.206, 1.107 // 21164.401, 0.000 // 21191.176, 0.000 // 21192.176, 1.150
21193.379, 0.000 // 21220.041, 0.000 // 21221.041, 1.153 // 21222.285, 0.000 // 21249.040, 0.000
21250.040, 1.139 // 21251.253, 0.000 // 21277.874, 0.000 // 21278.874, 1.132 // 21280.065, 0.000
21306.797, 0.000 // 21307.797, 1.114 // 21308.970, 0.000 // 21335.695, 0.000 // 21336.695, 1.165
21337.887, 0.000 // 21364.615, 0.000 // 21365.615, 1.160 // 21366.819, 0.000 // 21393.615, 0.000
21394.615, 1.142 // 21395.777, 0.000 // 21422.506, 0.000 // 21423.506, 1.163 // 21424.664, 0.000
21451.278, 0.000 // 21452.278, 1.153 // 21453.471, 0.000 // 21480.209, 0.000 // 21481.209, 1.166
21482.443, 0.000 // 21509.283, 0.000 // 21510.283, 0.000 // 21511.412, 0.000 // 21538.184, 0.000
21539.184, 1.119 // 21540.384, 0.000 // 21567.084, 0.000 // 21568.084, 1.142 // 21569.331, 0.000
21596.086, 0.000 // 21597.086, 1.158 // 21598.264, 0.000 // 21625.071, 0.000 // 21626.071, 1.150
21627.304, 0.000 // 21654.142, 0.000 // 21655.142, 1.149 // 21656.281, 0.000 // 21683.001, 0.000
21684.001, 1.136 // 21685.160, 0.000 // 21711.829, 0.000 // 21712.829, 1.132 // 21714.004, 0.000
21740.763, 0.000 // 21741.763, 1.166 // 21743.017, 0.000 // 21769.753, 0.000 // 21770.753, 1.143
21771.923, 0.000 // 21798.640, 0.000 // 21799.640, 1.146 // 21800.864, 0.000 // 21827.541, 0.000
21828.541, 1.130 // 21829.751, 0.000 // 21856.447, 0.000 // 21857.447, 1.129 // 21858.688, 0.000
21885.607, 0.000 // 21886.607, 1.157 // 21887.963, 0.000 // 21914.795, 0.000 // 21915.795, 1.120
21916.967, 0.000 // 21943.696, 0.000 // 21944.696, 1.150 // 21945.905, 0.000 // 21972.648, 0.000
21973.648, 1.124 // 21974.849, 0.000 // 22001.510, 0.000 // 22002.510, 1.132 // 22003.729, 0.000
22030.476, 0.000 // 22031.476, 1.134 // 22032.641, 0.000 // 22059.281, 0.000 // 22060.281, 1.133
22061.486, 0.000 // 22088.393, 0.000 // 22089.393, 1.141 // 22090.588, 0.000 // 22117.479, 0.000

22118.479, 1.121 // 22119.628, 0.000 // 22146.284, 0.000 // 22147.284, 1.131 // 22148.587, 0.000
22175.400, 0.000 // 22176.400, 1.137 // 22177.645, 0.000 // 22204.441, 0.000 // 22205.441, 1.137
22206.684, 0.000 // 22233.511, 0.000 // 22234.511, 1.136 // 22235.671, 0.000 // 22262.427, 0.000
22263.427, 1.138 // 22264.634, 0.000 // 22291.477, 0.000 // 22292.477, 1.143 // 22293.665, 0.000
22320.445, 0.000 // 22321.445, 1.127 // 22322.652, 0.000 // 22349.460, 0.000 // 22350.460, 1.137
22351.683, 0.000 // 22378.416, 0.000 // 22379.416, 1.159 // 22380.688, 0.000 // 22407.312, 0.000
22408.312, 1.105 // 22409.523, 0.000 // 22436.219, 0.000 // 22437.219, 1.121 // 22438.421, 0.000
22465.243, 0.000 // 22466.243, 1.135 // 22467.470, 0.000 // 22494.117, 0.000 // 22495.117, 1.140
22496.273, 0.000 // 22522.934, 0.000 // 22523.934, 1.119 // 22525.134, 0.000 // 22551.947, 0.000
22552.947, 1.113 // 22554.113, 0.000 // 22580.795, 0.000 // 22581.795, 1.149 // 22582.992, 0.000
22609.687, 0.000 // 22610.687, 1.145 // 22611.880, 0.000 // 22638.674, 0.000 // 22639.674, 1.139
22640.848, 0.000 // 22667.649, 0.000 // 22668.649, 1.116 // 22669.883, 0.000 // 22696.682, 0.000
22697.682, 0.000 // 22698.825, 0.000 // 22725.500, 0.000 // 22726.500, 1.188 // 22727.683, 0.000
22754.338, 0.000 // 22755.338, 1.130 // 22756.553, 0.000 // 22783.334, 0.000 // 22784.334, 1.120
22785.525, 0.000 // 22812.223, 0.000 // 22813.223, 1.128 // 22814.386, 0.000 // 22841.073, 0.000
22842.073, 1.116 // 22843.229, 0.000 // 22869.871, 0.000 // 22870.871, 1.115 // 22872.046, 0.000
22898.667, 0.000 // 22899.667, 1.123 // 22900.853, 0.000 // 22927.595, 0.000 // 22928.595, 1.129
22929.754, 0.000 // 22956.487, 0.000 // 22957.487, 1.137 // 22958.704, 0.000 // 22985.375, 0.000
22986.375, 1.120 // 22987.533, 0.000 // 23014.316, 0.000 // 23015.316, 1.141 // 23016.548, 0.000
23043.403, 0.000 // 23044.403, 0.801 // 23046.205, 0.000 // 23072.911, 0.000 // 23073.911, 1.159
23075.103, 0.000 // 23101.911, 0.000 // 23102.911, 1.150 // 23104.080, 0.000 // 23130.716, 0.000
23131.716, 1.146 // 23132.901, 0.000 // 23159.519, 0.000 // 23160.519, 1.120 // 23161.711, 0.000
23188.406, 0.000 // 23189.406, 1.128 // 23190.575, 0.000 // 23217.253, 0.000 // 23218.253, 1.134
23219.429, 0.000 // 23246.146, 0.000 // 23247.146, 1.152 // 23248.334, 0.000 // 23274.949, 0.000
23275.949, 1.134 // 23277.144, 0.000 // 23303.839, 0.000 // 23304.839, 1.148 // 23306.041, 0.000
23332.804, 0.000 // 23333.804, 1.106 // 23335.019, 0.000 // 23361.869, 0.000 // 23362.869, 1.133
23364.112, 0.000 // 23390.881, 0.000 // 23391.881, 1.113 // 23393.071, 0.000 // 23419.774, 0.000
23420.774, 1.148 // 23421.934, 0.000 // 23448.800, 0.000 // 23449.800, 1.127 // 23450.942, 0.000
23477.680, 0.000 // 23478.680, 1.101 // 23479.873, 0.000 // 23506.574, 0.000 // 23507.574, 1.136
23508.778, 0.000 // 23535.563, 0.000 // 23536.563, 1.120 // 23537.774, 0.000 // 23564.556, 0.000
23565.556, 1.113 // 23566.734, 0.000 // 23593.399, 0.000 // 23594.399, 1.121 // 23595.613, 0.000
23622.350, 0.000 // 23623.350, 1.130 // 23624.606, 0.000 // 23651.358, 0.000 // 23652.358, 1.126
23653.584, 0.000 // 23680.319, 0.000 // 23681.319, 1.133 // 23682.517, 0.000 // 23709.244, 0.000
23710.244, 1.121 // 23711.437, 0.000 // 23738.152, 0.000 // 23739.152, 1.127 // 23740.307, 0.000
23767.212, 0.000 // 23768.212, 1.122 // 23769.446, 0.000 // 23796.039, 0.000 // 23797.039, 1.133
23798.246, 0.000 // 23824.950, 0.000 // 23825.950, 1.120 // 23827.144, 0.000 // 23853.907, 0.000
23854.907, 1.112 // 23856.121, 0.000 // 23882.971, 0.000 // 23883.971, 1.120 // 23885.179, 0.000
23911.927, 0.000 // 23912.927, 0.000 // 23914.014, 0.000 // 23940.647, 0.000 // 23941.647, 1.139
23942.804, 0.000 // 23969.733, 0.000 // 23970.733, 1.126 // 23971.951, 0.000 // 23998.703, 0.000
23999.703, 1.137 // 24000.902, 0.000 // 24027.688, 0.000 // 24028.688, 1.153 // 24029.900, 0.000
24056.622, 0.000 // 24057.622, 1.121 // 24058.924, 0.000 // 24085.701, 0.000 // 24086.701, 1.137
24087.913, 0.000 // 24114.671, 0.000 // 24115.671, 1.138 // 24116.918, 0.000 // 24143.605, 0.000
24144.605, 1.147 // 24145.813, 0.000 // 24172.464, 0.000 // 24173.464, 1.148 // 24174.647, 0.000
24201.423, 0.000 // 24202.423, 1.143 // 24203.629, 0.000 // 24230.249, 0.000 // 24231.249, 1.121
24232.511, 0.000 // 24259.221, 0.000 // 24260.221, 1.133 // 24261.418, 0.000 // 24288.127, 0.000
24289.127, 1.125 // 24290.324, 0.000 // 24317.063, 0.000 // 24318.063, 1.102 // 24319.239, 0.000
24346.020, 0.000 // 24347.020, 1.139 // 24348.183, 0.000 // 24374.917, 0.000 // 24375.917, 1.163
24377.134, 0.000 // 24403.823, 0.000 // 24404.823, 1.125 // 24406.013, 0.000 // 24432.660, 0.000
24433.660, 1.161 // 24434.885, 0.000 // 24461.581, 0.000 // 24462.581, 1.135 // 24463.739, 0.000
24490.522, 0.000 // 24491.522, 1.148 // 24492.768, 0.000 // 24519.433, 0.000 // 24520.433, 1.125
24521.604, 0.000 // 24548.252, 0.000 // 24549.252, 1.149 // 24550.469, 0.000 // 24577.268, 0.000
24578.268, 1.148 // 24579.464, 0.000 // 24606.145, 0.000 // 24607.145, 1.106 // 24608.370, 0.000
24635.189, 0.000 // 24636.189, 1.145 // 24637.365, 0.000 // 24664.115, 0.000 // 24665.115, 1.116
24666.307, 0.000 // 24692.979, 0.000 // 24693.979, 1.084 // 24695.194, 0.000 // 24722.018, 0.000
24723.018, 1.109 // 24724.191, 0.000 // 24750.837, 0.000 // 24751.837, 1.088 // 24753.004, 0.000
24779.689, 0.000 // 24780.689, 1.094 // 24781.907, 0.000 // 24808.633, 0.000 // 24809.633, 1.111
24810.814, 0.000 // 24837.492, 0.000 // 24838.492, 1.089 // 24839.720, 0.000 // 24866.404, 0.000
24867.404, 1.115 // 24868.644, 0.000 // 24895.359, 0.000 // 24896.359, 1.148 // 24897.534, 0.000
24924.223, 0.000 // 24925.223, 1.109 // 24926.422, 0.000 // 24953.118, 0.000 // 24954.118, 1.102
24955.272, 0.000 // 24981.944, 0.000 // 24982.944, 1.109 // 24984.138, 0.000 // 25010.858, 0.000
25011.858, 1.119 // 25013.022, 0.000 // 25039.702, 0.000 // 25040.702, 1.124 // 25041.856, 0.000
25068.678, 0.000 // 25069.678, 1.127 // 25071.013, 0.000 // 25097.856, 0.000 // 25098.856, 0.000
25100.044, 0.000 // 25126.871, 0.000 // 25127.871, 1.131 // 25129.271, 0.000 // 25156.035, 0.000

25157.035, 1.019 // 25158.095, 0.000 // 25184.793, 0.000 // 25185.793, 1.144 // 25186.966, 0.000
25213.686, 0.000 // 25214.686, 1.133 // 25215.881, 0.000 // 25242.566, 0.000 // 25243.566, 1.163
25244.777, 0.000 // 25271.518, 0.000 // 25272.518, 1.144 // 25273.691, 0.000 // 25300.462, 0.000
25301.462, 1.097 // 25302.669, 0.000 // 25329.293, 0.000 // 25330.293, 1.159 // 25331.493, 0.000
25358.178, 0.000 // 25359.178, 1.131 // 25360.365, 0.000 // 25387.085, 0.000 // 25388.085, 1.144
25389.238, 0.000 // 25415.940, 0.000 // 25416.940, 1.126 // 25418.145, 0.000 // 25444.844, 0.000
25445.844, 1.135 // 25447.015, 0.000 // 25473.765, 0.000 // 25474.765, 1.123 // 25475.894, 0.000
25502.570, 0.000 // 25503.570, 1.118 // 25504.767, 0.000 // 25531.365, 0.000 // 25532.365, 1.116
25533.564, 0.000 // 25560.237, 0.000 // 25561.237, 1.154 // 25562.444, 0.000 // 25589.234, 0.000
25590.234, 1.121 // 25591.468, 0.000 // 25618.264, 0.000 // 25619.264, 1.127 // 25620.491, 0.000
25647.251, 0.000 // 25648.251, 1.101 // 25649.419, 0.000 // 25676.081, 0.000 // 25677.081, 1.131
25678.271, 0.000 // 25704.985, 0.000 // 25705.985, 1.133 // 25707.167, 0.000 // 25733.956, 0.000
25734.956, 1.104 // 25736.181, 0.000 // 25762.891, 0.000 // 25763.891, 1.140 // 25765.257, 0.000
25791.982, 0.000 // 25792.982, 1.115 // 25794.136, 0.000 // 25820.808, 0.000 // 25821.808, 1.133
25823.024, 0.000 // 25849.689, 0.000 // 25850.689, 1.103 // 25851.875, 0.000 // 25878.601, 0.000
25879.601, 1.128 // 25880.781, 0.000 // 25907.535, 0.000 // 25908.535, 1.096 // 25909.761, 0.000
25936.501, 0.000 // 25937.501, 1.104 // 25938.681, 0.000 // 25965.452, 0.000 // 25966.452, 1.116
25967.623, 0.000 // 25994.267, 0.000 // 25995.267, 1.117 // 25996.484, 0.000 // 26023.274, 0.000
26024.274, 1.114 // 26025.507, 0.000 // 26052.235, 0.000 // 26053.235, 1.125 // 26054.412, 0.000
26081.131, 0.000 // 26082.131, 1.116 // 26083.324, 0.000 // 26110.025, 0.000 // 26111.025, 1.110
26112.189, 0.000 // 26138.882, 0.000 // 26139.882, 1.119 // 26141.032, 0.000 // 26167.769, 0.000
26168.769, 1.111 // 26169.930, 0.000 // 26196.620, 0.000 // 26197.620, 1.112 // 26198.790, 0.000
26225.549, 0.000 // 26226.549, 0.413 // 26228.965, 0.000 // 26255.736, 0.000 // 26256.736, 1.128
26257.934, 0.000 // 26284.633, 0.000 // 26285.633, 1.118 // 26286.824, 0.000 // 26313.638, 0.000
26314.638, 0.000 // 26315.723, 0.000 // 26342.476, 0.000 // 26343.476, 1.100 // 26344.664, 0.000
26371.404, 0.000 // 26372.404, 1.090 // 26373.598, 0.000 // 26400.305, 0.000 // 26401.305, 1.134
26402.512, 0.000 // 26429.186, 0.000 // 26430.186, 1.133 // 26431.338, 0.000 // 26458.021, 0.000
26459.021, 1.120 // 26460.195, 0.000 // 26486.848, 0.000 // 26487.848, 1.108 // 26489.069, 0.000
26515.750, 0.000 // 26516.750, 1.110 // 26517.925, 0.000 // 26544.695, 0.000 // 26545.695, 1.128
26546.885, 0.000 // 26573.651, 0.000 // 26574.651, 1.100 // 26575.818, 0.000 // 26602.592, 0.000
26603.592, 1.116 // 26604.796, 0.000 // 26631.601, 0.000 // 26632.601, 1.125 // 26633.778, 0.000
26660.654, 0.000 // 26661.654, 1.118 // 26662.870, 0.000 // 26689.601, 0.000 // 26690.601, 1.099
26691.778, 0.000 // 26718.376, 0.000 // 26719.376, 1.101 // 26720.532, 0.000 // 26747.241, 0.000
26748.241, 1.068 // 26749.455, 0.000 // 26776.129, 0.000 // 26777.129, 1.116 // 26778.293, 0.000
26804.986, 0.000 // 26805.986, 1.114 // 26807.162, 0.000 // 26833.899, 0.000 // 26834.899, 1.124
26836.095, 0.000 // 26862.733, 0.000 // 26863.733, 1.110 // 26864.929, 0.000 // 26891.764, 0.000
26892.764, 1.099 // 26893.934, 0.000 // 26920.549, 0.000 // 26921.549, 1.079 // 26922.774, 0.000
26949.490, 0.000 // 26950.490, 1.115 // 26951.653, 0.000 // 26978.496, 0.000 // 26979.496, 1.107
26980.702, 0.000 // 27007.418, 0.000 // 27008.418, 1.108 // 27009.618, 0.000 // 27036.293, 0.000
27037.293, 1.129 // 27038.480, 0.000 // 27065.142, 0.000 // 27066.142, 1.114 // 27067.345, 0.000
27094.179, 0.000 // 27095.179, 1.106 // 27096.359, 0.000 // 27123.013, 0.000 // 27124.013, 1.095
27125.196, 0.000 // 27151.906, 0.000 // 27152.906, 1.100 // 27154.095, 0.000 // 27180.814, 0.000
27181.814, 1.100 // 27183.019, 0.000 // 27209.761, 0.000 // 27210.761, 1.116 // 27211.947, 0.000
27238.718, 0.000 // 27239.718, 1.093 // 27240.951, 0.000 // 27267.627, 0.000 // 27268.627, 1.103
27269.786, 0.000 // 27296.482, 0.000 // 27297.482, 1.122 // 27298.650, 0.000 // 27325.374, 0.000
27326.374, 1.093 // 27327.537, 0.000 // 27354.300, 0.000 // 27355.300, 1.087 // 27356.494, 0.000
27383.306, 0.000 // 27384.306, 1.114 // 27385.462, 0.000 // 27412.186, 0.000 // 27413.186, 1.106
27414.414, 0.000 // 27441.135, 0.000 // 27442.135, 1.118 // 27443.324, 0.000 // 27470.025, 0.000
27471.025, 1.132 // 27472.275, 0.000 // 27499.092, 0.000 // 27500.092, 0.000 // 27501.228, 0.000
27527.945, 0.000 // 27528.945, 1.113 // 27530.281, 0.000 // 27556.954, 0.000 // 27557.954, 1.111
27559.124, 0.000 // 27585.856, 0.000 // 27586.856, 1.121 // 27588.039, 0.000 // 27614.815, 0.000
27615.815, 1.121 // 27617.007, 0.000 // 27643.647, 0.000 // 27644.647, 1.103 // 27645.842, 0.000
27672.526, 0.000 // 27673.526, 1.125 // 27674.688, 0.000 // 27701.440, 0.000 // 27702.440, 1.117
27703.711, 0.000 // 27730.426, 0.000 // 27731.426, 1.132 // 27732.641, 0.000 // 27759.369, 0.000
27760.369, 1.104 // 27761.582, 0.000 // 27788.248, 0.000 // 27789.248, 1.146 // 27790.414, 0.000
27817.117, 0.000 // 27818.117, 1.123 // 27819.302, 0.000 // 27845.969, 0.000 // 27846.969, 1.101
27848.123, 0.000 // 27874.811, 0.000 // 27875.811, 1.125 // 27876.943, 0.000 // 27903.602, 0.000
27904.602, 1.105 // 27905.763, 0.000 // 27932.444, 0.000 // 27933.444, 1.108 // 27934.627, 0.000
27961.382, 0.000 // 27962.382, 1.109 // 27963.532, 0.000 // 27990.293, 0.000 // 27991.293, 1.103
27992.506, 0.000 // 28019.146, 0.000 // 28020.146, 1.126 // 28021.331, 0.000 // 28048.009, 0.000
28049.009, 1.111 // 28050.184, 0.000 // 28076.872, 0.000 // 28077.872, 1.131 // 28079.098, 0.000
28105.817, 0.000 // 28106.817, 1.115 // 28107.987, 0.000 // 28134.708, 0.000 // 28135.708, 1.131
28136.945, 0.000 // 28163.634, 0.000 // 28164.634, 1.127 // 28165.939, 0.000 // 28192.812, 0.000

28193.812, 1.104 // 28195.221, 0.000 // 28221.988, 0.000 // 28222.988, 1.093 // 28224.185, 0.000
28250.917, 0.000 // 28251.917, 1.099 // 28253.188, 0.000 // 28279.985, 0.000 // 28280.985, 1.124
28282.213, 0.000 // 28308.972, 0.000 // 28309.972, 1.105 // 28311.173, 0.000 // 28337.952, 0.000
28338.952, 1.117 // 28340.122, 0.000 // 28366.802, 0.000 // 28367.802, 1.111 // 28368.966, 0.000
28395.624, 0.000 // 28396.624, 1.139 // 28397.818, 0.000 // 28424.668, 0.000 // 28425.668, 1.095
28426.849, 0.000 // 28453.691, 0.000 // 28454.691, 1.118 // 28455.899, 0.000 // 28482.572, 0.000
28483.572, 1.113 // 28484.733, 0.000 // 28511.389, 0.000 // 28512.389, 1.110 // 28513.541, 0.000
28540.270, 0.000 // 28541.270, 1.094 // 28542.482, 0.000 // 28569.117, 0.000 // 28570.117, 1.090
28571.289, 0.000 // 28597.991, 0.000 // 28598.991, 1.083 // 28600.159, 0.000 // 28626.887, 0.000
28627.887, 1.094 // 28629.066, 0.000 // 28655.823, 0.000 // 28656.823, 1.058 // 28658.017, 0.000
28684.795, 0.000 // 28685.795, 1.108 // 28686.993, 0.000 // 28713.800, 0.000 // 28714.800, 0.000
28715.849, 0.000 // 28742.599, 0.000 // 28743.599, 1.075 // 28744.776, 0.000 // 28771.589, 0.000
28772.589, 1.066 // 28773.843, 0.000 // 28800.552, 0.000 // 28801.552, 1.094 // 28802.749, 0.000
28829.410, 0.000 // 28830.410, 1.118 // 28831.631, 0.000 // 28858.285, 0.000 // 28859.285, 1.097
28860.501, 0.000 // 28887.172, 0.000 // 28888.172, 1.105 // 28889.435, 0.000 // 28916.307, 0.000
28917.307, 1.079 // 28918.510, 0.000 // 28945.242, 0.000 // 28946.242, 1.108 // 28947.428, 0.000
28974.182, 0.000 // 28975.182, 1.105 // 28976.357, 0.000 // 29003.093, 0.000 // 29004.093, 1.122
29005.272, 0.000 // 29031.959, 0.000 // 29032.959, 1.087 // 29034.107, 0.000 // 29060.724, 0.000
29061.724, 1.114 // 29063.033, 0.000 // 29089.679, 0.000 // 29090.679, 1.085 // 29091.892, 0.000
29118.683, 0.000 // 29119.683, 1.087 // 29120.825, 0.000 // 29147.484, 0.000 // 29148.484, 1.062
29149.646, 0.000 // 29176.379, 0.000 // 29177.379, 1.098 // 29178.561, 0.000 // 29205.287, 0.000
29206.287, 1.079 // 29207.493, 0.000 // 29234.282, 0.000 // 29235.282, 1.076 // 29236.460, 0.000
29263.109, 0.000 // 29264.109, 1.075 // 29265.286, 0.000 // 29292.073, 0.000 // 29293.073, 1.080
29294.258, 0.000 // 29321.005, 0.000 // 29322.005, 1.108 // 29323.191, 0.000 // 29349.999, 0.000
29350.999, 1.073 // 29352.194, 0.000 // 29378.977, 0.000 // 29379.977, 1.098 // 29381.130, 0.000
29407.876, 0.000 // 29408.876, 1.091 // 29410.097, 0.000 // 29436.953, 0.000 // 29437.953, 1.089
29439.164, 0.000 // 29466.024, 0.000 // 29467.024, 1.090 // 29468.195, 0.000 // 29494.976, 0.000
29495.976, 1.070 // 29497.190, 0.000 // 29523.807, 0.000 // 29524.807, 1.076 // 29526.003, 0.000
29552.766, 0.000 // 29553.766, 1.072 // 29554.962, 0.000 // 29581.730, 0.000 // 29582.730, 1.075
29584.064, 0.000 // 29610.761, 0.000 // 29611.761, 1.096 // 29612.945, 0.000 // 29639.874, 0.000
29640.874, 1.093 // 29642.066, 0.000 // 29668.853, 0.000 // 29669.853, 1.107 // 29671.251, 0.000
29698.031, 0.000 // 29699.031, 1.056 // 29700.191, 0.000 // 29727.026, 0.000 // 29728.026, 1.086
29729.255, 0.000 // 29756.055, 0.000 // 29757.055, 0.804 // 29758.867, 0.000 // 29785.594, 0.000
29786.594, 1.100 // 29787.782, 0.000 // 29814.580, 0.000 // 29815.580, 1.103 // 29816.805, 0.000
29843.619, 0.000 // 29844.619, 1.097 // 29845.889, 0.000 // 29872.592, 0.000 // 29873.592, 1.114
29874.807, 0.000 // 29901.679, 0.000 // 29902.679, 0.000 // 29903.757, 0.000 // 29930.649, 0.000
29931.649, 0.000 // 29932.726, 0.000 // 29959.557, 0.000 // 29960.557, 0.000 // 29961.681, 0.000
29988.498, 0.000 // 29989.498, 1.089 // 29990.660, 0.000 // 30017.345, 0.000 // 30018.345, 1.073
30019.558, 0.000 // 30046.313, 0.000 // 30047.313, 1.103 // 30048.553, 0.000 // 30075.402, 0.000
30076.402, 1.099 // 30077.584, 0.000 // 30104.294, 0.000 // 30105.294, 1.090 // 30106.472, 0.000
30133.185, 0.000 // 30134.185, 1.082 // 30135.312, 0.000 // 30162.096, 0.000 // 30163.096, 1.065
30164.303, 0.000 // 30191.071, 0.000 // 30192.071, 1.078 // 30193.254, 0.000 // 30219.947, 0.000
30220.947, 1.085 // 30222.173, 0.000 // 30249.067, 0.000 // 30250.067, 1.066 // 30251.275, 0.000
30278.002, 0.000 // 30279.002, 1.092 // 30280.165, 0.000 // 30306.909, 0.000 // 30307.909, 1.098
30309.091, 0.000 // 30335.858, 0.000 // 30336.858, 1.069 // 30338.042, 0.000 // 30364.667, 0.000
30365.667, 1.082 // 30366.844, 0.000 // 30393.637, 0.000 // 30394.637, 1.079 // 30395.844, 0.000
30422.608, 0.000 // 30423.608, 1.078 // 30424.787, 0.000 // 30451.420, 0.000 // 30452.420, 1.083
30453.604, 0.000 // 30480.315, 0.000 // 30481.315, 1.076 // 30482.496, 0.000 // 30509.135, 0.000
30510.135, 1.066 // 30511.307, 0.000 // 30538.059, 0.000 // 30539.059, 1.077 // 30540.327, 0.000
30567.137, 0.000 // 30568.137, 1.091 // 30569.340, 0.000 // 30596.077, 0.000 // 30597.077, 1.078
30598.237, 0.000 // 30625.042, 0.000 // 30626.042, 1.117 // 30627.224, 0.000 // 30654.001, 0.000
30655.001, 1.071 // 30656.156, 0.000 // 30682.849, 0.000 // 30683.849, 1.078 // 30685.060, 0.000
30711.728, 0.000 // 30712.728, 1.076 // 30714.047, 0.000 // 30740.750, 0.000 // 30741.750, 1.083
30742.902, 0.000 // 30769.571, 0.000 // 30770.571, 1.098 // 30771.744, 0.000 // 30798.397, 0.000
30799.397, 1.089 // 30800.621, 0.000 // 30827.378, 0.000 // 30828.378, 1.098 // 30829.562, 0.000
30856.389, 0.000 // 30857.389, 1.103 // 30858.541, 0.000 // 30885.353, 0.000 // 30886.353, 1.105
30887.504, 0.000 // 30914.278, 0.000 // 30915.278, 1.058 // 30916.419, 0.000 // 30943.213, 0.000
30944.213, 1.077 // 30945.405, 0.000 // 30972.156, 0.000 // 30973.156, 1.087 // 30974.347, 0.000
31001.026, 0.000 // 31002.026, 1.085 // 31003.272, 0.000 // 31030.007, 0.000 // 31031.007, 1.079
31032.210, 0.000 // 31058.907, 0.000 // 31059.907, 1.104 // 31061.061, 0.000 // 31087.801, 0.000
31088.801, 1.092 // 31089.955, 0.000 // 31116.724, 0.000 // 31117.724, 0.000 // 31118.810, 0.000
31145.497, 0.000 // 31146.497, 1.090 // 31147.685, 0.000 // 31174.351, 0.000 // 31175.351, 1.092
31176.539, 0.000 // 31203.125, 0.000 // 31204.125, 1.064 // 31205.388, 0.000 // 31232.043, 0.000

31233.043, 1.053 // 31234.213, 0.000 // 31260.903, 0.000 // 31261.903, 1.048 // 31263.096, 0.000
31289.864, 0.000 // 31290.864, 1.065 // 31292.017, 0.000 // 31318.685, 0.000 // 31319.685, 1.073
31320.885, 0.000 // 31347.609, 0.000 // 31348.609, 1.053 // 31349.803, 0.000 // 31376.568, 0.000
31377.568, 1.054 // 31378.753, 0.000 // 31405.532, 0.000 // 31406.532, 1.031 // 31407.747, 0.000
31434.426, 0.000 // 31435.426, 1.051 // 31436.641, 0.000 // 31463.402, 0.000 // 31464.402, 1.046
31465.620, 0.000 // 31492.314, 0.000 // 31493.314, 1.023 // 31494.490, 0.000 // 31521.372, 0.000
31522.372, 1.039 // 31523.568, 0.000 // 31550.188, 0.000 // 31551.188, 1.046 // 31552.334, 0.000
31579.005, 0.000 // 31580.005, 1.026 // 31581.168, 0.000 // 31608.013, 0.000 // 31609.013, 1.046
31610.191, 0.000 // 31637.029, 0.000 // 31638.029, 1.044 // 31639.257, 0.000 // 31665.915, 0.000
31666.915, 1.063 // 31668.103, 0.000 // 31694.771, 0.000 // 31695.771, 1.054 // 31696.968, 0.000
31723.674, 0.000 // 31724.674, 1.077 // 31725.847, 0.000 // 31752.560, 0.000 // 31753.560, 1.064
31754.737, 0.000 // 31781.547, 0.000 // 31782.547, 1.055 // 31783.743, 0.000 // 31810.474, 0.000
31811.474, 1.084 // 31812.676, 0.000 // 31839.320, 0.000 // 31840.320, 1.065 // 31841.503, 0.000
31868.259, 0.000 // 31869.259, 1.045 // 31870.454, 0.000 // 31897.167, 0.000 // 31898.167, 1.051
31899.337, 0.000 // 31926.063, 0.000 // 31927.063, 1.047 // 31928.243, 0.000 // 31954.899, 0.000
31955.899, 1.072 // 31957.104, 0.000 // 31983.840, 0.000 // 31984.840, 1.042 // 31986.063, 0.000
32012.791, 0.000 // 32013.791, 1.041 // 32014.964, 0.000 // 32041.689, 0.000 // 32042.689, 1.044
32043.847, 0.000 // 32070.523, 0.000 // 32071.523, 1.051 // 32072.703, 0.000 // 32099.408, 0.000
32100.408, 1.045 // 32101.583, 0.000 // 32128.426, 0.000 // 32129.426, 1.037 // 32130.587, 0.000
32157.271, 0.000 // 32158.271, 1.048 // 32159.466, 0.000 // 32186.170, 0.000 // 32187.170, 1.052
32188.336, 0.000 // 32215.174, 0.000 // 32216.174, 1.046 // 32217.394, 0.000 // 32244.222, 0.000
32245.222, 1.057 // 32246.403, 0.000 // 32273.153, 0.000 // 32274.153, 1.051 // 32275.301, 0.000
32302.225, 0.000 // 32303.225, 0.000 // 32304.322, 0.000 // 32331.001, 0.000 // 32332.001, 1.045
32333.246, 0.000 // 32360.042, 0.000 // 32361.042, 1.113 // 32362.211, 0.000 // 32389.025, 0.000
32390.025, 1.048 // 32391.224, 0.000 // 32418.051, 0.000 // 32419.051, 1.050 // 32420.251, 0.000
32447.116, 0.000 // 32448.116, 1.053 // 32449.320, 0.000 // 32475.978, 0.000 // 32476.978, 1.058
32478.179, 0.000 // 32504.961, 0.000 // 32505.961, 1.048 // 32507.113, 0.000 // 32533.795, 0.000
32534.795, 1.061 // 32535.973, 0.000 // 32562.641, 0.000 // 32563.641, 1.058 // 32564.838, 0.000
32591.595, 0.000 // 32592.595, 1.043 // 32593.771, 0.000 // 32620.511, 0.000 // 32621.511, 1.058
32622.713, 0.000 // 32649.474, 0.000 // 32650.474, 1.052 // 32651.652, 0.000 // 32678.256, 0.000
32679.256, 1.070 // 32680.417, 0.000 // 32707.142, 0.000 // 32708.142, 1.044 // 32709.349, 0.000
32736.183, 0.000 // 32737.183, 1.043 // 32738.335, 0.000 // 32765.050, 0.000 // 32766.050, 1.034
32767.225, 0.000 // 32794.003, 0.000 // 32795.003, 1.051 // 32796.178, 0.000 // 32823.007, 0.000
32824.007, 0.999 // 32825.317, 0.000 // 32852.035, 0.000 // 32853.035, 1.043 // 32854.213, 0.000
32880.932, 0.000 // 32881.932, 1.045 // 32883.089, 0.000 // 32909.790, 0.000 // 32910.790, 1.027
32911.990, 0.000 // 32938.680, 0.000 // 32939.680, 1.063 // 32940.874, 0.000 // 32967.545, 0.000
32968.545, 1.034 // 32969.712, 0.000 // 32996.566, 0.000 // 32997.566, 1.057 // 32998.769, 0.000
33025.491, 0.000 // 33026.491, 1.036 // 33027.724, 0.000 // 33054.422, 0.000 // 33055.422, 1.064
33056.592, 0.000 // 33083.400, 0.000 // 33084.400, 1.011 // 33085.701, 0.000 // 33112.534, 0.000
33113.534, 1.026 // 33114.714, 0.000 // 33141.444, 0.000 // 33142.444, 1.021 // 33143.617, 0.000
33170.374, 0.000 // 33171.374, 1.019 // 33172.618, 0.000 // 33199.339, 0.000 // 33200.339, 1.028
33201.539, 0.000 // 33228.273, 0.000 // 33229.273, 1.046 // 33230.439, 0.000 // 33257.162, 0.000
33258.162, 1.023 // 33259.345, 0.000 // 33286.044, 0.000 // 33287.044, 1.036 // 33288.292, 0.000
33315.139, 0.000 // 33316.139, 1.034 // 33317.349, 0.000 // 33344.122, 0.000 // 33345.122, 1.034
33346.308, 0.000 // 33373.070, 0.000 // 33374.070, 1.017 // 33375.268, 0.000 // 33402.128, 0.000
33403.128, 1.027 // 33405.013, 0.000 // 33431.879, 0.000 // 33432.879, 1.023 // 33434.066, 0.000
33460.813, 0.000 // 33461.813, 1.051 // 33462.992, 0.000 // 33489.820, 0.000 // 33490.820, 0.000
33491.965, 0.000 // 33518.667, 0.000 // 33519.667, 1.023 // 33520.837, 0.000 // 33547.662, 0.000
33548.662, 1.044 // 33549.835, 0.000 // 33576.494, 0.000 // 33577.494, 1.032 // 33578.635, 0.000
33605.415, 0.000 // 33606.415, 1.017 // 33607.629, 0.000 // 33634.350, 0.000 // 33635.350, 1.031
33636.517, 0.000 // 33663.445, 0.000 // 33664.445, 1.037 // 33665.602, 0.000 // 33692.280, 0.000
33693.280, 1.029 // 33694.472, 0.000 // 33721.245, 0.000 // 33722.245, 1.023 // 33723.404, 0.000
33750.349, 0.000 // 33751.349, 1.037 // 33752.508, 0.000 // 33779.439, 0.000 // 33780.439, 1.032
33781.634, 0.000 // 33808.371, 0.000 // 33809.371, 1.034 // 33810.553, 0.000 // 33837.281, 0.000
33838.281, 1.023 // 33839.441, 0.000 // 33866.116, 0.000 // 33867.116, 1.016 // 33868.276, 0.000
33894.994, 0.000 // 33895.994, 1.014 // 33897.217, 0.000 // 33923.915, 0.000 // 33924.915, 1.043
33926.132, 0.000 // 33952.913, 0.000 // 33953.913, 1.022 // 33955.098, 0.000 // 33981.810, 0.000
33982.810, 1.024 // 33983.969, 0.000 // 34010.692, 0.000 // 34011.692, 1.043 // 34012.874, 0.000
34039.571, 0.000 // 34040.571, 1.041 // 34041.753, 0.000 // 34068.423, 0.000 // 34069.423, 1.040
34070.587, 0.000 // 34097.407, 0.000 // 34098.407, 1.019 // 34099.747, 0.000 // 34126.493, 0.000
34127.493, 1.008 // 34128.715, 0.000 // 34156.032, 0.000 // 34157.032, 0.663 // 34157.670, 0.000
34184.367, 0.000 // 34185.367, 1.053 // 34186.558, 0.000 // 34213.251, 0.000 // 34214.251, 1.053
34215.421, 0.000 // 34242.119, 0.000 // 34243.119, 1.050 // 34244.352, 0.000 // 34271.192, 0.000

34272.192, 1.018 // 34273.508, 0.000 // 34300.328, 0.000 // 34301.328, 1.024 // 34302.478, 0.000
34329.245, 0.000 // 34330.245, 1.036 // 34331.410, 0.000 // 34358.106, 0.000 // 34359.106, 1.030
34360.319, 0.000 // 34387.146, 0.000 // 34388.146, 1.029 // 34389.325, 0.000 // 34416.256, 0.000
34417.256, 1.009 // 34418.427, 0.000 // 34445.306, 0.000 // 34446.306, 1.024 // 34447.538, 0.000
34474.330, 0.000 // 34475.330, 1.007 // 34476.531, 0.000 // 34503.287, 0.000 // 34504.287, 1.010
34505.525, 0.000 // 34532.288, 0.000 // 34533.288, 1.034 // 34534.485, 0.000 // 34561.231, 0.000
34562.231, 0.968 // 34563.427, 0.000 // 34590.149, 0.000 // 34591.149, 1.013 // 34592.375, 0.000
34619.100, 0.000 // 34620.100, 1.008 // 34621.325, 0.000 // 34648.014, 0.000 // 34649.014, 0.988
34650.216, 0.000 // 34677.054, 0.000 // 34678.054, 1.002 // 34679.282, 0.000 // 34706.159, 0.000
34707.159, 0.000 // 34708.242, 0.000 // 34735.076, 0.000 // 34736.076, 0.975 // 34737.273, 0.000
34764.189, 0.000 // 34765.189, 1.013 // 34766.384, 0.000 // 34793.182, 0.000 // 34794.182, 1.004
34795.398, 0.000 // 34822.221, 0.000 // 34823.221, 1.007 // 34824.384, 0.000 // 34851.266, 0.000
34852.266, 1.042 // 34853.496, 0.000 // 34880.347, 0.000 // 34881.347, 1.017 // 34882.492, 0.000
34909.301, 0.000 // 34910.301, 1.010 // 34911.532, 0.000 // 34938.280, 0.000 // 34939.280, 1.018
34940.440, 0.000 // 34967.175, 0.000 // 34968.175, 1.029 // 34969.354, 0.000 // 34996.115, 0.000
34997.115, 1.015 // 34998.278, 0.000 // 35025.043, 0.000 // 35026.043, 1.004 // 35027.212, 0.000
35053.953, 0.000 // 35054.953, 1.036 // 35056.189, 0.000 // 35082.890, 0.000 // 35083.890, 1.104
35085.059, 0.000 // 35111.872, 0.000 // 35112.872, 1.016 // 35114.153, 0.000 // 35140.966, 0.000
35141.966, 1.033 // 35143.219, 0.000 // 35170.168, 0.000 // 35171.168, 1.023 // 35172.330, 0.000
35199.172, 0.000 // 35200.172, 1.012 // 35201.366, 0.000 // 35228.082, 0.000 // 35229.082, 1.014
35230.321, 0.000 // 35257.061, 0.000 // 35258.061, 1.010 // 35259.263, 0.000 // 35286.094, 0.000
35287.094, 1.039 // 35288.272, 0.000 // 35315.169, 0.000 // 35316.169, 1.054 // 35317.366, 0.000
35344.109, 0.000 // 35345.109, 1.002 // 35346.305, 0.000 // 35373.010, 0.000 // 35374.010, 1.032
35375.194, 0.000 // 35401.834, 0.000 // 35402.834, 1.016 // 35404.036, 0.000 // 35430.775, 0.000
35431.775, 1.011 // 35432.987, 0.000 // 35459.753, 0.000 // 35460.753, 1.019 // 35461.920, 0.000
35488.787, 0.000 // 35489.787, 1.003 // 35490.987, 0.000 // 35517.797, 0.000 // 35518.797, 0.998
35520.047, 0.000 // 35546.771, 0.000 // 35547.771, 1.022 // 35548.965, 0.000 // 35575.756, 0.000
35576.756, 1.008 // 35577.978, 0.000 // 35604.780, 0.000 // 35605.780, 1.017 // 35607.019, 0.000
35633.786, 0.000 // 35634.786, 0.994 // 35635.978, 0.000 // 35662.750, 0.000 // 35663.750, 1.038
35664.952, 0.000 // 35691.648, 0.000 // 35692.648, 0.995 // 35693.840, 0.000 // 35720.605, 0.000
35721.605, 0.994 // 35722.794, 0.000 // 35749.697, 0.000 // 35750.697, 1.000 // 35751.950, 0.000
35778.883, 0.000 // 35779.883, 1.018 // 35781.080, 0.000 // 35807.860, 0.000 // 35808.860, 1.011
35810.011, 0.000 // 35836.700, 0.000 // 35837.700, 0.995 // 35838.828, 0.000 // 35865.579, 0.000
35866.579, 0.000 // 35867.665, 0.000 // 35894.471, 0.000 // 35895.471, 1.018 // 35896.675, 0.000
35923.437, 0.000 // 35924.437, 1.014 // 35925.628, 0.000 // 35952.368, 0.000 // 35953.368, 1.012
35954.544, 0.000 // 35981.392, 0.000 // 35982.392, 1.015 // 35983.583, 0.000 // 36010.411, 0.000
36011.411, 1.036 // 36012.592, 0.000 // 36039.496, 0.000 // 36040.496, 0.983 // 36041.739, 0.000
36068.520, 0.000 // 36069.520, 1.034 // 36070.734, 0.000 // 36097.455, 0.000 // 36098.455, 1.009
36099.801, 0.000 // 36126.489, 0.000 // 36127.489, 1.032 // 36128.698, 0.000 // 36155.518, 0.000
36156.518, 1.028 // 36157.711, 0.000 // 36184.463, 0.000 // 36185.463, 1.030 // 36186.617, 0.000
36213.445, 0.000 // 36214.445, 1.031 // 36215.608, 0.000 // 36242.437, 0.000 // 36243.437, 0.998
36244.618, 0.000 // 36271.510, 0.000 // 36272.510, 1.024 // 36273.796, 0.000 // 36300.674, 0.000
36301.674, 1.027 // 36302.863, 0.000 // 36329.583, 0.000 // 36330.583, 1.049 // 36331.760, 0.000
36358.589, 0.000 // 36359.589, 1.106 // 36360.747, 0.000 // 36387.510, 0.000 // 36388.510, 1.029
36389.680, 0.000 // 36416.443, 0.000 // 36417.443, 1.040 // 36418.650, 0.000 // 36445.371, 0.000
36446.371, 1.020 // 36447.628, 0.000 // 36474.360, 0.000 // 36475.360, 1.027 // 36476.515, 0.000
36503.248, 0.000 // 36504.248, 1.037 // 36505.413, 0.000 // 36532.172, 0.000 // 36533.172, 1.048
36534.372, 0.000 // 36561.089, 0.000 // 36562.089, 1.065 // 36563.322, 0.000 // 36590.078, 0.000
36591.078, 0.755 // 36593.549, 0.000 // 36620.371, 0.000 // 36621.371, 1.019 // 36622.581, 0.000
36649.327, 0.000 // 36650.327, 1.019 // 36651.592, 0.000 // 36678.425, 0.000 // 36679.425, 1.028
36680.605, 0.000 // 36707.473, 0.000 // 36708.473, 1.032 // 36709.625, 0.000 // 36736.415, 0.000
36737.415, 0.973 // 36738.617, 0.000 // 36765.352, 0.000 // 36766.352, 1.018 // 36767.550, 0.000
36794.304, 0.000 // 36795.304, 1.019 // 36796.492, 0.000 // 36823.200, 0.000 // 36824.200, 1.020
36825.415, 0.000 // 36852.155, 0.000 // 36853.155, 0.985 // 36854.339, 0.000 // 36880.982, 0.000
36881.982, 0.997 // 36883.191, 0.000 // 36909.926, 0.000 // 36910.926, 0.999 // 36912.100, 0.000
36938.908, 0.000 // 36939.908, 1.014 // 36941.065, 0.000 // 36967.761, 0.000 // 36968.761, 1.024
36969.908, 0.000 // 36996.732, 0.000 // 36997.732, 1.031 // 36998.984, 0.000 // 37025.671, 0.000
37026.671, 1.005 // 37027.833, 0.000 // 37054.515, 0.000 // 37055.515, 1.009 // 37056.699, 0.000
37083.525, 0.000 // 37084.525, 1.030 // 37085.848, 0.000 // 37112.695, 0.000 // 37113.695, 1.049
37114.933, 0.000 // 37141.708, 0.000 // 37142.708, 1.019 // 37143.874, 0.000 // 37170.621, 0.000
37171.621, 1.050 // 37172.812, 0.000 // 37199.753, 0.000 // 37200.753, 1.025 // 37201.915, 0.000
37228.816, 0.000 // 37229.816, 0.000 // 37230.945, 0.000 // 37257.724, 0.000 // 37258.724, 1.042
37259.914, 0.000 // 37286.693, 0.000 // 37287.693, 1.036 // 37288.887, 0.000 // 37315.617, 0.000

37316.617, 1.029 // 37317.984, 0.000 // 37344.801, 0.000 // 37345.801, 1.009 // 37347.029, 0.000
37373.804, 0.000 // 37374.804, 1.032 // 37375.997, 0.000 // 37402.775, 0.000 // 37403.775, 1.046
37404.954, 0.000 // 37431.689, 0.000 // 37432.689, 1.014 // 37433.851, 0.000 // 37460.746, 0.000
37461.746, 1.022 // 37462.959, 0.000 // 37489.716, 0.000 // 37490.716, 1.013 // 37491.910, 0.000
37518.656, 0.000 // 37519.656, 1.038 // 37520.807, 0.000 // 37547.564, 0.000 // 37548.564, 1.008
37549.766, 0.000 // 37576.737, 0.000 // 37577.737, 1.036 // 37578.932, 0.000 // 37605.704, 0.000
37606.704, 1.036 // 37607.908, 0.000 // 37634.713, 0.000 // 37635.713, 1.028 // 37636.902, 0.000
37663.620, 0.000 // 37664.620, 1.024 // 37665.906, 0.000 // 37692.631, 0.000 // 37693.631, 1.016
37694.864, 0.000 // 37721.669, 0.000 // 37722.669, 1.023 // 37723.922, 0.000 // 37750.779, 0.000
37751.779, 1.025 // 37753.070, 0.000 // 37779.833, 0.000 // 37780.833, 1.013 // 37782.029, 0.000
37808.852, 0.000 // 37809.852, 1.041 // 37811.114, 0.000 // 37837.975, 0.000 // 37838.975, 0.982
37840.192, 0.000 // 37867.047, 0.000 // 37868.047, 0.986 // 37869.283, 0.000 // 37896.065, 0.000
37897.065, 1.021 // 37898.268, 0.000 // 37924.993, 0.000 // 37925.993, 1.018 // 37927.218, 0.000
37954.052, 0.000 // 37955.052, 1.034 // 37956.321, 0.000 // 37983.141, 0.000 // 37984.141, 1.032
37985.451, 0.000 // 38012.145, 0.000 // 38013.145, 1.000 // 38014.356, 0.000 // 38041.144, 0.000
38042.144, 1.004 // 38043.352, 0.000 // 38070.162, 0.000 // 38071.162, 1.018 // 38072.375, 0.000
38099.097, 0.000 // 38100.097, 1.037 // 38101.267, 0.000 // 38128.083, 0.000 // 38129.083, 1.019
38130.289, 0.000 // 38157.061, 0.000 // 38158.061, 1.036 // 38159.284, 0.000 // 38186.113, 0.000
38187.113, 1.041 // 38188.314, 0.000 // 38215.173, 0.000 // 38216.173, 1.003 // 38217.338, 0.000
38244.072, 0.000 // 38245.072, 1.013 // 38246.244, 0.000 // 38273.044, 0.000 // 38274.044, 0.991
38275.204, 0.000 // 38301.939, 0.000 // 38302.939, 1.009 // 38304.137, 0.000 // 38330.949, 0.000
38331.949, 1.009 // 38333.124, 0.000 // 38360.039, 0.000 // 38361.039, 0.999 // 38362.252, 0.000
38389.026, 0.000 // 38390.026, 1.003 // 38391.305, 0.000 // 38418.111, 0.000 // 38419.111, 1.001
38420.301, 0.000 // 38447.000, 0.000 // 38448.000, 0.973 // 38449.313, 0.000 // 38476.132, 0.000
38477.132, 1.015 // 38478.317, 0.000 // 38505.289, 0.000 // 38506.289, 1.027 // 38507.531, 0.000
38534.310, 0.000 // 38535.310, 1.084 // 38536.553, 0.000 // 38563.479, 0.000 // 38564.479, 1.016
38565.674, 0.000 // 38592.547, 0.000 // 38593.547, 1.001 // 38594.751, 0.000 // 38621.507, 0.000
38622.507, 1.018 // 38623.666, 0.000 // 38650.524, 0.000 // 38651.524, 1.006 // 38652.687, 0.000
38679.465, 0.000 // 38680.465, 1.006 // 38681.633, 0.000 // 38708.367, 0.000 // 38709.367, 1.006
38710.539, 0.000 // 38737.268, 0.000 // 38738.268, 0.999 // 38739.538, 0.000 // 38766.413, 0.000
38767.413, 0.993 // 38768.593, 0.000 // 38795.433, 0.000 // 38796.433, 1.017 // 38797.723, 0.000
38824.500, 0.000 // 38825.500, 0.985 // 38826.682, 0.000 // 38853.460, 0.000 // 38854.460, 0.998
38855.675, 0.000 // 38882.415, 0.000 // 38883.415, 1.015 // 38884.586, 0.000 // 38911.520, 0.000
38912.520, 0.985 // 38913.717, 0.000 // 38940.485, 0.000 // 38941.485, 1.024 // 38942.697, 0.000
38969.429, 0.000 // 38970.429, 1.024 // 38971.647, 0.000 // 38998.348, 0.000 // 38999.348, 1.010
39000.503, 0.000 // 39027.221, 0.000 // 39028.221, 0.999 // 39029.400, 0.000 // 39056.298, 0.000
39057.298, 1.002 // 39058.479, 0.000 // 39085.152, 0.000 // 39086.152, 0.989 // 39087.322, 0.000
39114.091, 0.000 // 39115.091, 1.014 // 39116.348, 0.000 // 39143.289, 0.000 // 39144.289, 0.987
39145.523, 0.000 // 39172.293, 0.000 // 39173.293, 1.019 // 39174.541, 0.000 // 39201.257, 0.000
39202.257, 0.987 // 39203.428, 0.000 // 39230.326, 0.000 // 39231.326, 0.979 // 39232.498, 0.000
39259.424, 0.000 // 39260.424, 1.028 // 39261.701, 0.000 // 39288.439, 0.000 // 39289.439, 0.997
39290.616, 0.000 // 39317.364, 0.000 // 39318.364, 1.000 // 39319.513, 0.000 // 39346.174, 0.000
39347.174, 0.988 // 39348.366, 0.000 // 39375.163, 0.000 // 39376.163, 0.994 // 39377.446, 0.000
39404.322, 0.000 // 39405.322, 0.980 // 39406.482, 0.000 // 39433.206, 0.000 // 39434.206, 1.005
39435.379, 0.000 // 39462.044, 0.000 // 39463.044, 0.988 // 39464.218, 0.000 // 39490.925, 0.000
39491.925, 1.002 // 39493.085, 0.000 // 39519.820, 0.000 // 39520.820, 1.022 // 39522.034, 0.000
39548.975, 0.000 // 39549.975, 0.000 // 39551.057, 0.000 // 39577.765, 0.000 // 39578.765, 1.012
39579.906, 0.000 // 39606.715, 0.000 // 39607.715, 0.989 // 39608.906, 0.000 // 39635.680, 0.000
39636.680, 0.959 // 39637.896, 0.000 // 39664.704, 0.000 // 39665.704, 0.984 // 39666.856, 0.000
39693.531, 0.000 // 39694.531, 0.995 // 39695.730, 0.000 // 39722.514, 0.000 // 39723.514, 1.007
39724.699, 0.000 // 39751.473, 0.000 // 39752.473, 1.003 // 39753.658, 0.000 // 39780.447, 0.000
39781.447, 0.980 // 39782.672, 0.000 // 39809.455, 0.000 // 39810.455, 1.007 // 39811.712, 0.000
39838.643, 0.000 // 39839.643, 1.010 // 39840.808, 0.000 // 39867.658, 0.000 // 39868.658, 1.002
39869.892, 0.000 // 39896.734, 0.000 // 39897.734, 1.026 // 39898.957, 0.000 // 39925.802, 0.000
39926.802, 0.994 // 39928.006, 0.000 // 39954.801, 0.000 // 39955.801, 1.018 // 39956.966, 0.000
39983.716, 0.000 // 39984.716, 1.002 // 39986.016, 0.000 // 40012.844, 0.000 // 40013.844, 1.024
40015.012, 0.000 // 40041.785, 0.000 // 40042.785, 0.993 // 40043.963, 0.000 // 40070.710, 0.000
40071.710, 0.995 // 40072.843, 0.000 // 40099.574, 0.000 // 40100.574, 0.994 // 40101.820, 0.000
40128.634, 0.000 // 40129.634, 1.006 // 40130.821, 0.000 // 40157.568, 0.000 // 40158.568, 1.104
40159.745, 0.000 // 40186.528, 0.000 // 40187.528, 1.007 // 40188.719, 0.000 // 40215.679, 0.000
40216.679, 1.012 // 40217.965, 0.000 // 40244.817, 0.000 // 40245.817, 1.049 // 40247.014, 0.000
40273.928, 0.000 // 40274.928, 1.004 // 40276.122, 0.000 // 40303.106, 0.000 // 40304.106, 1.013
40305.289, 0.000 // 40332.101, 0.000 // 40333.101, 1.007 // 40334.254, 0.000 // 40361.191, 0.000

40362.191, 1.005 // 40363.389, 0.000 // 40390.247, 0.000 // 40391.247, 1.011 // 40392.418, 0.000
40419.185, 0.000 // 40420.185, 1.006 // 40421.360, 0.000 // 40448.194, 0.000 // 40449.194, 0.984
40450.400, 0.000 // 40477.237, 0.000 // 40478.237, 0.997 // 40479.602, 0.000 // 40506.403, 0.000
40507.403, 1.003 // 40508.698, 0.000 // 40535.548, 0.000 // 40536.548, 1.005 // 40537.724, 0.000
40564.432, 0.000 // 40565.432, 1.003 // 40566.645, 0.000 // 40593.483, 0.000 // 40594.483, 0.981
40595.694, 0.000 // 40622.552, 0.000 // 40623.552, 0.997 // 40624.770, 0.000 // 40651.663, 0.000
40652.663, 0.991 // 40653.900, 0.000 // 40680.648, 0.000 // 40681.648, 0.993 // 40682.841, 0.000
40709.644, 0.000 // 40710.644, 0.981 // 40711.846, 0.000 // 40738.741, 0.000 // 40739.741, 0.982
40740.924, 0.000 // 40767.721, 0.000 // 40768.721, 0.967 // 40770.009, 0.000 // 40796.690, 0.000
40797.690, 0.994 // 40798.969, 0.000 // 40825.904, 0.000 // 40826.904, 0.973 // 40828.113, 0.000
40854.828, 0.000 // 40855.828, 1.003 // 40857.014, 0.000 // 40883.767, 0.000 // 40884.767, 0.984
40885.946, 0.000 // 40912.708, 0.000 // 40913.708, 0.974 // 40914.976, 0.000 // 40941.906, 0.000
40942.906, 0.981 // 40944.087, 0.000 // 40970.756, 0.000 // 40971.756, 0.982 // 40972.972, 0.000
40999.686, 0.000 // 41000.686, 0.953 // 41001.808, 0.000 // 41028.499, 0.000 // 41029.499, 0.981
41030.713, 0.000 // 41057.587, 0.000 // 41058.587, 0.981 // 41059.744, 0.000 // 41086.442, 0.000
41087.442, 0.979 // 41088.651, 0.000 // 41115.406, 0.000 // 41116.406, 1.000 // 41117.593, 0.000
41144.467, 0.000 // 41145.467, 0.968 // 41146.651, 0.000 // 41173.469, 0.000 // 41174.469, 1.032
41175.691, 0.000 // 41202.413, 0.000 // 41203.413, 0.948 // 41204.633, 0.000 // 41231.411, 0.000
41232.411, 1.025 // 41233.698, 0.000 // 41260.425, 0.000 // 41261.425, 0.985 // 41262.606, 0.000
41289.530, 0.000 // 41290.530, 0.984 // 41291.750, 0.000 // 41318.520, 0.000 // 41319.520, 0.989
41320.657, 0.000 // 41347.356, 0.000 // 41348.356, 0.972 // 41349.620, 0.000 // 41376.560, 0.000
41377.560, 1.004 // 41378.848, 0.000 // 41405.734, 0.000 // 41406.734, 0.993 // 41407.942, 0.000
41434.754, 0.000 // 41435.754, 0.990 // 41436.955, 0.000 // 41463.788, 0.000 // 41464.788, 0.999
41465.977, 0.000 // 41492.756, 0.000 // 41493.756, 0.979 // 41495.053, 0.000 // 41521.878, 0.000
41522.878, 0.998 // 41524.084, 0.000 // 41550.946, 0.000 // 41551.946, 0.987 // 41553.226, 0.000
41580.132, 0.000 // 41581.132, 0.956 // 41582.436, 0.000 // 41609.436, 0.000 // 41610.436, 0.947
41611.691, 0.000 // 41638.465, 0.000 // 41639.465, 0.998 // 41640.642, 0.000 // 41667.372, 0.000
41668.372, 1.011 // 41669.557, 0.000 // 41696.301, 0.000 // 41697.301, 1.012 // 41698.517, 0.000
41725.318, 0.000 // 41726.318, 0.969 // 41727.539, 0.000 // 41754.456, 0.000 // 41755.456, 0.966
41756.695, 0.000 // 41783.778, 0.000 // 41784.778, 1.002 // 41786.004, 0.000 // 41813.129, 0.000
41814.129, 0.000 // 41815.223, 0.000 // 41842.066, 0.000 // 41843.066, 0.948 // 41844.341, 0.000
41871.218, 0.000 // 41872.218, 0.956 // 41873.416, 0.000 // 41900.409, 0.000 // 41901.409, 0.956
41902.589, 0.000 // 41929.454, 0.000 // 41930.454, 0.994 // 41931.709, 0.000 // 41958.547, 0.000
41959.547, 0.961 // 41960.749, 0.000 // 41987.595, 0.000 // 41988.595, 0.971 // 41989.758, 0.000
42016.570, 0.000 // 42017.570, 0.949 // 42018.821, 0.000 // 42045.851, 0.000 // 42046.851, 0.961
42048.027, 0.000 // 42075.019, 0.000 // 42076.019, 0.971 // 42077.227, 0.000 // 42103.937, 0.000
42104.937, 0.948 // 42106.213, 0.000 // 42133.051, 0.000 // 42134.051, 0.961 // 42135.231, 0.000
42162.177, 0.000 // 42163.177, 0.975 // 42164.364, 0.000 // 42191.148, 0.000 // 42192.148, 0.952
42193.351, 0.000 // 42220.225, 0.000 // 42221.225, 0.983 // 42222.408, 0.000 // 42249.271, 0.000
42250.271, 0.976 // 42251.502, 0.000 // 42278.475, 0.000 // 42279.475, 0.970 // 42280.649, 0.000
42307.386, 0.000 // 42308.386, 0.980 // 42309.563, 0.000 // 42336.382, 0.000 // 42337.382, 0.970
42338.536, 0.000 // 42365.410, 0.000 // 42366.410, 0.978 // 42367.596, 0.000 // 42394.404, 0.000
42395.404, 0.975 // 42396.582, 0.000 // 42423.341, 0.000 // 42424.341, 0.964 // 42425.589, 0.000
42452.471, 0.000 // 42453.471, 0.972 // 42455.236, 0.000 // 42482.024, 0.000 // 42483.024, 0.944
42484.264, 0.000 // 42511.106, 0.000 // 42512.106, 0.967 // 42513.363, 0.000 // 42540.250, 0.000
42541.250, 0.974 // 42542.467, 0.000 // 42569.316, 0.000 // 42570.316, 0.960 // 42571.578, 0.000
42598.442, 0.000 // 42599.442, 0.962 // 42600.667, 0.000 // 42627.437, 0.000 // 42628.437, 0.959
42629.667, 0.000 // 42656.511, 0.000 // 42657.511, 0.975 // 42658.715, 0.000 // 42685.575, 0.000
42686.575, 1.018 // 42687.761, 0.000 // 42714.557, 0.000 // 42715.557, 0.984 // 42716.756, 0.000
42743.620, 0.000 // 42744.620, 1.002 // 42745.873, 0.000 // 42772.845, 0.000 // 42773.845, 0.965
42775.029, 0.000 // 42801.823, 0.000 // 42802.823, 0.959 // 42804.002, 0.000 // 42830.898, 0.000
42831.898, 0.979 // 42833.192, 0.000 // 42860.209, 0.000 // 42861.209, 0.975 // 42862.429, 0.000
42889.248, 0.000 // 42890.248, 0.973 // 42891.414, 0.000 // 42918.199, 0.000 // 42919.199, 0.982
42920.383, 0.000 // 42947.224, 0.000 // 42948.224, 0.934 // 42949.434, 0.000 // 42976.287, 0.000
42977.287, 0.955 // 42978.465, 0.000 // 43005.158, 0.000 // 43006.158, 0.967 // 43007.331, 0.000
43034.152, 0.000 // 43035.152, 0.977 // 43036.333, 0.000 // 43063.230, 0.000 // 43064.230, 0.977
43065.495, 0.000 // 43092.474, 0.000 // 43093.474, 0.963 // 43094.695, 0.000 // 43121.428, 0.000
43122.428, 1.009 // 43123.603, 0.000 // 43150.368, 0.000 // 43151.368, 0.981 // 43152.558, 0.000
43179.338, 0.000 // 43180.338, 0.986 // 43181.622, 0.000 // 43208.435, 0.000 // 43209.435, 0.973
43210.595, 0.000 // 43237.405, 0.000 // 43238.405, 0.743 // 43240.341, 0.000 // 43267.080, 0.000
43268.080, 1.001 // 43269.313, 0.000 // 43296.140, 0.000 // 43297.140, 0.985 // 43298.300, 0.000
43325.121, 0.000 // 43326.121, 0.987 // 43327.367, 0.000 // 43354.129, 0.000 // 43355.129, 1.031
43356.325, 0.000 // 43383.068, 0.000 // 43384.068, 1.008 // 43385.275, 0.000 // 43412.217, 0.000

```
43413.217, 0.999 // 43414.448, 0.000 // 43441.350, 0.000 // 43442.350, 1.012 // 43443.640, 0.000
43470.573, 0.000 // 43471.573, 1.005 // 43472.764, 0.000 // 43499.544, 0.000 // 43500.544, 0.999
43501.776, 0.000 // 43528.506, 0.000 // 43529.506, 1.004 // 43530.697, 0.000 // 43557.533, 0.000
43558.533, 1.018 // 43559.728, 0.000 // 43586.697, 0.000 // 43587.697, 1.005 // 43588.867, 0.000
43615.877, 0.000 // 43616.877, 0.970 // 43618.094, 0.000 // 43644.957, 0.000 // 43645.957, 0.000
43647.043, 0.000 // 43673.739, 0.000 // 43674.739, 1.002 // 43675.947, 0.000 // 43702.657, 0.000
43703.657, 0.993 // 43704.881, 0.000 // 43731.635, 0.000 // 43732.635, 0.993 // 43733.840, 0.000
43760.789, 0.000 // 43761.789, 0.995 // 43763.032, 0.000 // 43789.717, 0.000 // 43790.717, 1.012
43792.012, 0.000 // 43818.838, 0.000 // 43819.838, 0.974 // 43821.050, 0.000 // 43847.848, 0.000
43848.848, 0.992 // 43850.012, 0.000 // 43876.816, 0.000 // 43877.816, 0.999 // 43878.999, 0.000
43905.748, 0.000 // 43906.748, 0.973 // 43907.967, 0.000 // 43934.876, 0.000 // 43935.876, 1.016
43937.196, 0.000 // 43964.174, 0.000 // 43965.174, 0.969 // 43966.532, 0.000 // 43993.407, 0.000
43994.407, 0.985 // 43995.603, 0.000 // 44022.510, 0.000 // 44023.510, 0.996 // 44024.852, 0.000
44051.630, 0.000 // 44052.630, 1.001 // 44053.824, 0.000 // 44080.790, 0.000 // 44081.790, 0.966
44083.036, 0.000 // 44109.753, 0.000 // 44110.753, 0.989 // 44111.915, 0.000 // 44138.633, 0.000
44139.633, 0.984 // 44140.824, 0.000 // 44167.559, 0.000 // 44168.559, 0.984 // 44169.828, 0.000
44196.671, 0.000 // 44197.671, 0.986 // 44198.849, 0.000 // 44225.650, 0.000 // 44226.650, 0.989
44227.829, 0.000 // 44254.692, 0.000 // 44255.692, 0.961 // 44256.892, 0.000 // 44283.597, 0.000
44284.597, 0.973 // 44285.780, 0.000 // 44312.528, 0.000 // 44313.528, 0.955 // 44314.721, 0.000
44341.499, 0.000 // 44342.499, 0.999 // 44343.726, 0.000 // 44370.502, 0.000 // 44371.502, 0.976
44372.694, 0.000 // 44399.415, 0.000 // 44400.415, 0.987 // 44401.635, 0.000 // 44428.374, 0.000
44429.374, 1.010 // 44430.559, 0.000 // 44457.414, 0.000 // 44458.414, 0.980 // 44459.634, 0.000
44486.555, 0.000 // 44487.555, 0.999 // 44488.768, 0.000 // 44515.564, 0.000 // 44516.564, 0.976
44517.807, 0.000 // 44544.744, 0.000 // 44545.744, 1.048 // 44546.972, 0.000 // 44573.858, 0.000
44574.858, 0.999 // 44576.100, 0.000 // 44603.067, 0.000 // 44604.067, 1.013 // 44605.310, 0.000
44632.267, 0.000 // 44633.267, 1.026 // 44634.507, 0.000 // 44661.494, 0.000 // 44662.494, 1.055
44663.683, 0.000 // 44690.693, 0.000 // 44691.693, 1.050 // 44692.878, 0.000 // 44719.613, 0.000
44720.613, 1.020 // 44721.837, 0.000 // 44748.596, 0.000 // 44749.596, 1.024 // 44750.823, 0.000
44777.639, 0.000 // 44778.639, 1.043 // 44779.836, 0.000 // 44806.740, 0.000 // 44807.740, 1.065
44808.939, 0.000 // 44835.905, 0.000 // 44836.905, 1.039 // 44838.121, 0.000 // 44864.857, 0.000
44865.857, 1.035 // 44867.062, 0.000 // 44893.973, 0.000 // 44894.973, 1.038 // 44896.203, 0.000
44922.871, 0.000 // 44923.871, 1.054 // 44925.051, 0.000 // 44951.889, 0.000 // 44952.889, 1.065
44954.101, 0.000 // 44980.917, 0.000 // 44981.917, 1.036 // 44983.105, 0.000 // 45009.895, 0.000
45010.895, 1.044 // 45012.044, 0.000 // 45038.838, 0.000 // 45039.838, 1.023 // 45041.014, 0.000
45067.962, 0.000 // 45068.962, 1.039 // 45070.161, 0.000 // 45097.079, 0.000 // 45098.079, 1.053
45099.283, 0.000 // 45126.163, 0.000 // 45127.163, 1.043 // 45128.337, 0.000 // 45155.177, 0.000
45156.177, 1.039 // 45157.359, 0.000 // 45184.220, 0.000 // 45185.220, 1.033 // 45186.452, 0.000
45213.340, 0.000 // 45214.340, 1.035 // 45215.622, 0.000 // 45242.372, 0.000 // 45243.372, 1.036
45244.697, 0.000 // 45271.529, 0.000 // 45272.529, 1.022 // 45273.723, 0.000 // 45300.565, 0.000
45301.565, 1.038 // 45302.792, 0.000 // 45329.496, 0.000 // 45330.496, 1.013 // 45331.716, 0.000
45358.577, 0.000 // 45359.577, 1.035 // 45360.760, 0.000 // 45387.484, 0.000 // 45388.484, 1.053
45389.643, 0.000 // 45416.510, 0.000 // 45417.510, 1.048 // 45418.732, 0.000 // 45445.578, 0.000
45446.578, 1.082 // 45447.804, 0.000 // 45474.624, 0.000 // 45475.624, 1.043 // 45476.826, 0.000
45503.688, 0.000 // 45504.688, 1.054 // 45505.884, 0.000 // 45532.834, 0.000 // 45533.834, 1.015
45535.026, 0.000 // 45561.787, 0.000 // 45562.787, 1.017 // 45563.950, 0.000 // 45590.847, 0.000
45591.847, 1.032 // 45593.066, 0.000 // 45619.859, 0.000 // 45620.859, 1.038 // 45622.079, 0.000
45649.013, 0.000 // 45650.013, 1.001 // 45651.155, 0.000 // 45677.910, 0.000 // 45678.910, 1.061
45680.097, 0.000 // 45706.928, 0.000 // 45707.928, 1.006 // 45709.121, 0.000 // 45736.009, 0.000
45737.009, 0.000 // 45738.081, 0.000 // 45764.893, 0.000 // 45765.893, 1.038 // 45767.108, 0.000
45793.925, 0.000 // 45794.925, 1.013 // 45796.119, 0.000 // 45822.885, 0.000 // 45823.885, 1.032
45825.096, 0.000 // 45851.882, 0.000 // 45852.882, 1.022 // 45854.090, 0.000 // 45881.017, 0.000
45882.017, 1.042 // 45883.192, 0.000 // 45909.998, 0.000 // 45910.998, 1.025 // 45912.178, 0.000
45939.254, 0.000 // 45940.254, 1.027 // 45941.481, 0.000 // 45968.322, 0.000 // 45969.322, 1.022
45970.548, 0.000 // 45997.436, 0.000 // 45998.436, 1.018 // 45999.668, 0.000 // 46026.473, 0.000
46027.473, 1.026 // 46028.676, 0.000 // 46055.421, 0.000 // 46056.421, 1.034 // 46057.617, 0.000
46084.500, 0.000 // 46085.500, 1.003 // 46086.756, 0.000 // 46113.583, 0.000 // 46114.583, 1.036
46115.720, 0.000 // 46142.568, 0.000 // 46143.568, 1.010 // 46144.732, 0.000 // 46171.518, 0.000
46172.518, 1.019 // 46173.701, 0.000 // 46200.516, 0.000 // 46201.516, 1.017 // 46202.704, 0.000
46229.428, 0.000 // 46230.428, 1.043 // 46231.591, 0.000 // 46258.400, 0.000 // 46259.400, 1.074
46260.593, 0.000 // 46287.428, 0.000 // 46288.428, 1.030 // 46289.672, 0.000 // 46316.567, 0.000
46317.567, 1.022 // 46318.754, 0.000 // 46345.501, 0.000 // 46346.501, 1.044 // 46347.689, 0.000
46374.433, 0.000 // 46375.433, 1.039 // 46376.655, 0.000 // 46403.436, 0.000 // 46404.436, 1.029
46405.616, 0.000 // 46432.582, 0.000 // 46433.582, 1.012 // 46434.781, 0.000 // 46461.571, 0.000
```

46462.571, 1.003 // 46463.817, 0.000 // 46490.801, 0.000 // 46491.801, 1.010 // 46493.027, 0.000
46519.937, 0.000 // 46520.937, 1.029 // 46522.201, 0.000 // 46549.006, 0.000 // 46550.006, 1.037
46551.233, 0.000 // 46578.054, 0.000 // 46579.054, 1.058 // 46580.176, 0.000 // 46607.034, 0.000
46608.034, 1.023 // 46609.250, 0.000 // 46636.177, 0.000 // 46637.177, 1.037 // 46638.334, 0.000
46665.141, 0.000 // 46666.141, 1.033 // 46667.365, 0.000 // 46694.228, 0.000 // 46695.228, 1.030
46696.432, 0.000 // 46723.208, 0.000 // 46724.208, 1.040 // 46725.436, 0.000 // 46752.224, 0.000
46753.224, 1.024 // 46754.406, 0.000 // 46781.211, 0.000 // 46782.211, 1.016 // 46783.393, 0.000
46810.160, 0.000 // 46811.160, 1.003 // 46812.370, 0.000 // 46839.143, 0.000 // 46840.143, 1.009
46841.321, 0.000 // 46868.073, 0.000 // 46869.073, 0.997 // 46870.268, 0.000 // 46896.990, 0.000
46897.990, 1.012 // 46899.177, 0.000 // 46925.878, 0.000 // 46926.878, 1.006 // 46928.045, 0.000
46954.742, 0.000 // 46955.742, 0.772 // 46957.725, 0.000 // 46984.487, 0.000 // 46985.487, 1.030
46986.702, 0.000 // 47013.490, 0.000 // 47014.490, 1.023 // 47015.679, 0.000 // 47042.438, 0.000
47043.438, 1.000 // 47044.665, 0.000 // 47071.636, 0.000 // 47072.636, 1.006 // 47073.830, 0.000
47100.669, 0.000 // 47101.669, 1.040 // 47102.834, 0.000 // 47129.571, 0.000 // 47130.571, 1.028
47131.744, 0.000 // 47158.583, 0.000 // 47159.583, 1.041 // 47160.749, 0.000 // 47187.589, 0.000
47188.589, 1.012 // 47189.762, 0.000 // 47216.519, 0.000 // 47217.519, 1.025 // 47218.712, 0.000
47245.555, 0.000 // 47246.555, 1.018 // 47247.755, 0.000 // 47274.587, 0.000 // 47275.587, 1.032
47276.831, 0.000 // 47303.567, 0.000 // 47304.567, 0.994 // 47305.786, 0.000 // 47332.516, 0.000
47333.516, 1.017 // 47334.772, 0.000 // 47361.538, 0.000 // 47362.538, 1.005 // 47363.751, 0.000
47390.521, 0.000 // 47391.521, 1.016 // 47392.711, 0.000 // 47419.396, 0.000 // 47420.396, 1.026
47421.590, 0.000 // 47448.474, 0.000 // 47449.474, 1.035 // 47450.657, 0.000 // 47477.454, 0.000
47478.454, 1.018 // 47479.652, 0.000 // 47506.432, 0.000 // 47507.432, 1.020 // 47508.637, 0.000
47535.475, 0.000 // 47536.475, 1.010 // 47537.672, 0.000 // 47564.420, 0.000 // 47565.420, 1.006
47566.578, 0.000 // 47593.330, 0.000 // 47594.330, 0.988 // 47595.528, 0.000 // 47622.345, 0.000
47623.345, 1.028 // 47624.496, 0.000 // 47651.435, 0.000 // 47652.435, 1.002 // 47653.598, 0.000
47680.358, 0.000 // 47681.358, 1.027 // 47682.542, 0.000 // 47709.490, 0.000 // 47710.490, 1.025
47711.700, 0.000 // 47738.550, 0.000 // 47739.550, 1.023 // 47740.744, 0.000 // 47767.657, 0.000
47768.657, 1.015 // 47769.878, 0.000 // 47796.691, 0.000 // 47797.691, 1.002 // 47798.945, 0.000
47825.812, 0.000 // 47826.812, 1.023 // 47828.038, 0.000 // 47854.862, 0.000 // 47855.862, 1.015
47857.051, 0.000 // 47883.993, 0.000 // 47884.993, 0.000 // 47886.098, 0.000 // 47912.986, 0.000
47913.986, 1.021 // 47915.200, 0.000 // 47941.983, 0.000 // 47942.983, 1.016 // 47944.159, 0.000
47970.937, 0.000 // 47971.937, 1.007 // 47973.137, 0.000 // 47999.894, 0.000 // 48000.894, 1.011
48002.069, 0.000 // 48028.834, 0.000 // 48029.834, 1.007 // 48031.017, 0.000 // 48057.765, 0.000
48058.765, 1.016 // 48060.009, 0.000 // 48086.844, 0.000 // 48087.844, 1.007 // 48089.125, 0.000
48115.878, 0.000 // 48116.878, 1.016 // 48118.068, 0.000 // 48144.824, 0.000 // 48145.824, 1.005
48146.999, 0.000 // 48173.857, 0.000 // 48174.857, 0.995 // 48176.080, 0.000 // 48203.036, 0.000
48204.036, 0.982 // 48205.471, 0.000 // 48232.196, 0.000 // 48233.196, 0.997 // 48234.332, 0.000
48261.271, 0.000 // 48262.271, 1.006 // 48263.436, 0.000 // 48290.314, 0.000 // 48291.314, 1.003
48292.515, 0.000 // 48319.312, 0.000 // 48320.312, 0.983 // 48321.502, 0.000 // 48348.363, 0.000
48349.363, 0.996 // 48350.586, 0.000 // 48377.585, 0.000 // 48378.585, 1.002 // 48379.773, 0.000
48406.608, 0.000 // 48407.608, 0.989 // 48408.857, 0.000 // 48435.660, 0.000 // 48436.660, 1.022
48437.870, 0.000 // 48464.700, 0.000 // 48465.700, 0.995 // 48466.874, 0.000 // 48493.733, 0.000
48494.733, 1.007 // 48495.903, 0.000 // 48522.686, 0.000 // 48523.686, 0.986 // 48524.916, 0.000
48551.760, 0.000 // 48552.760, 0.999 // 48554.125, 0.000 // 48580.953, 0.000 // 48581.953, 0.995
48583.233, 0.000 // 48610.077, 0.000 // 48611.077, 0.968 // 48612.304, 0.000 // 48639.047, 0.000
48640.047, 0.958 // 48641.227, 0.000 // 48668.081, 0.000 // 48669.081, 0.979 // 48670.280, 0.000
48697.230, 0.000 // 48698.230, 0.963 // 48699.460, 0.000 // 48726.316, 0.000 // 48727.316, 0.974
48728.534, 0.000 // 48755.442, 0.000 // 48756.442, 0.992 // 48757.677, 0.000 // 48784.461, 0.000
48785.461, 1.004 // 48786.709, 0.000 // 48813.558, 0.000 // 48814.558, 0.999 // 48815.796, 0.000
48842.562, 0.000 // 48843.562, 0.978 // 48844.812, 0.000 // 48871.569, 0.000 // 48872.569, 0.976
48873.753, 0.000 // 48900.450, 0.000 // 48901.450, 0.993 // 48902.641, 0.000 // 48929.503, 0.000
48930.503, 0.989 // 48931.710, 0.000 // 48958.559, 0.000 // 48959.559, 0.982 // 48960.692, 0.000
48987.450, 0.000 // 48988.450, 0.995 // 48989.666, 0.000 // 49016.505, 0.000 // 49017.505, 0.970
49018.803, 0.000 // 49045.753, 0.000 // 49046.753, 1.007 // 49047.993, 0.000 // 49074.890, 0.000
49075.890, 1.031 // 49077.095, 0.000 // 49104.049, 0.000 // 49105.049, 0.991 // 49106.242, 0.000
49133.101, 0.000 // 49134.101, 0.994 // 49135.390, 0.000 // 49162.203, 0.000 // 49163.203, 0.979
49164.431, 0.000 // 49191.434, 0.000 // 49192.434, 0.974 // 49193.650, 0.000 // 49220.456, 0.000
49221.456, 0.989 // 49222.662, 0.000 // 49249.648, 0.000 // 49250.648, 0.988 // 49251.835, 0.000
49278.681, 0.000 // 49279.681, 0.981 // 49280.849, 0.000 // 49307.623, 0.000 // 49308.623, 0.991
49309.936, 0.000 // 49336.673, 0.000 // 49337.673, 1.033 // 49338.859, 0.000 // 49365.667, 0.000
49366.667, 1.003 // 49367.864, 0.000 // 49394.618, 0.000 // 49395.618, 0.980 // 49396.966, 0.000
49423.701, 0.000 // 49424.701, 0.967 // 49425.931, 0.000 // 49452.675, 0.000 // 49453.675, 0.972
49454.907, 0.000 // 49481.892, 0.000 // 49482.892, 1.000 // 49484.082, 0.000 // 49511.060, 0.000

```
49512.060, 1.002 // 49513.282, 0.000 // 49540.169, 0.000 // 49541.169, 0.971 // 49542.391, 0.000
49569.215, 0.000 // 49570.215, 0.995 // 49571.496, 0.000 // 49598.391, 0.000 // 49599.391, 0.996
49600.563, 0.000 // 49627.603, 0.000 // 49628.603, 0.979 // 49629.902, 0.000 // 49656.632, 0.000
49657.632, 0.991 // 49658.835, 0.000 // 49685.657, 0.000 // 49686.657, 0.994 // 49687.844, 0.000
49714.738, 0.000 // 49715.738, 0.998 // 49716.911, 0.000 // 49743.746, 0.000 // 49744.746, 0.965
49745.924, 0.000 // 49772.713, 0.000 // 49773.713, 0.967 // 49774.912, 0.000 // 49801.688, 0.000
49802.688, 0.962 // 49803.907, 0.000 // 49830.744, 0.000 // 49831.744, 0.979 // 49832.908, 0.000
49859.757, 0.000 // 49860.757, 1.005 // 49861.984, 0.000 // 49888.946, 0.000 // 49889.946, 0.963
49891.123, 0.000 // 49917.948, 0.000 // 49918.948, 0.993 // 49920.208, 0.000 // 49946.942, 0.000
49947.942, 0.997 // 49949.135, 0.000 // 49975.844, 0.000 // 49976.844, 0.994 // 49978.031, 0.000
50005.004, 0.000 // 50006.004, 1.007 // 50007.242, 0.000 // 50034.182, 0.000 // 50035.182, 0.987
50036.345, 0.000 // 50063.107, 0.000 // 50064.107, 0.989 // 50065.295, 0.000 // 50092.214, 0.000
50093.214, 0.000 // 50094.332, 0.000 // 50121.212, 0.000 // 50122.212, 0.996 // 50123.381, 0.000
50150.161, 0.000 // 50151.161, 0.989 // 50152.438, 0.000 // 50179.278, 0.000 // 50180.278, 0.992
50181.461, 0.000 // 50208.276, 0.000 // 50209.276, 1.003 // 50210.465, 0.000 // 50237.222, 0.000
50238.222, 0.963 // 50239.397, 0.000 // 50266.273, 0.000 // 50267.273, 0.972 // 50268.446, 0.000
50295.233, 0.000 // 50296.233, 0.991 // 50297.428, 0.000 // 50324.241, 0.000 // 50325.241, 0.652
50327.112, 0.000 // 50354.012, 0.000 // 50355.012, 0.987 // 50356.233, 0.000 // 50383.175, 0.000
50384.175, 0.972 // 50385.371, 0.000 // 50412.211, 0.000 // 50413.211, 0.993 // 50414.404, 0.000
50441.137, 0.000 // 50442.137, 0.983 // 50443.383, 0.000 // 50470.265, 0.000 // 50471.265, 1.001
50472.577, 0.000 // 50499.532, 0.000 // 50500.532, 0.979 // 50501.706, 0.000 // 50528.729, 0.000
50529.729, 0.996 // 50531.030, 0.000 // 50558.010, 0.000 // 50559.010, 0.983 // 50560.330, 0.000
50587.250, 0.000 // 50588.250, 0.997 // 50589.452, 0.000 // 50616.293, 0.000 // 50617.293, 1.000
50618.492, 0.000 // 50645.391, 0.000 // 50646.391, 0.979 // 50647.755, 0.000 // 50674.597, 0.000
50675.597, 0.976 // 50676.822, 0.000 // 50703.674, 0.000 // 50704.674, 0.973 // 50705.890, 0.000
50732.783, 0.000 // 50733.783, 0.994 // 50735.136, 0.000 // 50762.012, 0.000 // 50763.012, 1.022
50764.207, 0.000 // 50791.075, 0.000 // 50792.075, 0.969 // 50793.393, 0.000 // 50820.264, 0.000
50821.264, 0.985 // 50822.478, 0.000 // 50849.416, 0.000 // 50850.416, 0.991 // 50851.637, 0.000
50878.502, 0.000 // 50879.502, 0.976 // 50880.705, 0.000 // 50907.428, 0.000 // 50908.428, 1.031
50909.624, 0.000 // 50936.380, 0.000 // 50937.380, 0.975 // 50938.584, 0.000 // 50965.448, 0.000
50966.448, 1.003 // 50967.633, 0.000 // 50994.596, 0.000 // 50995.596, 0.991 // 50996.796, 0.000
51023.540, 0.000 // 51024.540, 1.014 // 51025.703, 0.000 // 51052.726, 0.000 // 51053.726, 0.997
51054.858, 0.000 // 51081.870, 0.000 // 51082.870, 1.023 // 51084.042, 0.000 // 51110.784, 0.000
51111.784, 0.995 // 51112.992, 0.000 // 51139.748, 0.000 // 51140.748, 0.986 // 51141.949, 0.000
51168.711, 0.000 // 51169.711, 1.023 // 51171.006, 0.000 // 51197.930, 0.000 // 51198.930, 1.014
51200.873, 0.000 // 51227.741, 0.000 // 51228.741, 0.979 // 51229.975, 0.000 // 51256.744, 0.000
51257.744, 1.018 // 51258.926, 0.000 // 51285.642, 0.000 // 51286.642, 0.977 // 51287.842, 0.000
51314.749, 0.000 // 51315.749, 1.009 // 51316.944, 0.000 // 51343.709, 0.000 // 51344.709, 1.007
51345.896, 0.000 // 51372.778, 0.000 // 51373.778, 1.013 // 51374.980, 0.000 // 51401.782, 0.000
51402.782, 0.926 // 51404.047, 0.000 // 51430.863, 0.000 // 51431.863, 0.919 // 51433.024, 0.000
51459.941, 0.000 // 51460.941, 0.949 // 51462.215, 0.000 // 51489.061, 0.000 // 51490.061, 0.954
51491.216, 0.000 // 51518.186, 0.000 // 51519.186, 0.962 // 51520.433, 0.000 // 51547.340, 0.000
51548.340, 0.926 // 51549.554, 0.000 // 51576.597, 0.000 // 51577.597, 0.999 // 51578.808, 0.000
51605.662, 0.000 // 51606.662, 1.004 // 51607.878, 0.000 // 51634.733, 0.000 // 51635.733, 0.997
51636.918, 0.000 // 51663.940, 0.000 // 51664.940, 1.000 // 51666.225, 0.000 // 51693.378, 0.000
51694.378, 0.972 // 51695.577, 0.000 // 51722.488, 0.000 // 51723.488, 0.987 // 51724.706, 0.000
51751.601, 0.000 // 51752.601, 0.998 // 51753.789, 0.000 // 51780.702, 0.000 // 51781.702, 1.005
51782.883, 0.000 // 51809.717, 0.000 // 51810.717, 0.996 // 51811.932, 0.000 // 51838.839, 0.000
51839.839, 1.019 // 51841.076, 0.000 // 51867.847, 0.000 // 51868.847, 0.951 // 51870.008, 0.000
51896.806, 0.000 // 51897.806, 0.991 // 51899.093, 0.000 // 51925.945, 0.000 // 51926.945, 0.972
51928.168, 0.000 // 51955.055, 0.000 // 51956.055, 0.972 // 51957.234, 0.000 // 51984.036, 0.000
51985.036, 0.991 // 51986.250, 0.000 // 52013.122, 0.000 // 52014.122, 0.980 // 52015.376, 0.000
52042.217, 0.000 // 52043.217, 0.982 // 52044.371, 0.000 // 52071.248, 0.000 // 52072.248, 0.986
52073.463, 0.000 // 52100.554, 0.000 // 52101.554, 0.961 // 52102.867, 0.000 // 52129.714, 0.000
52130.714, 0.987 // 52131.861, 0.000 // 52158.632, 0.000 // 52159.632, 0.981 // 52160.814, 0.000
52187.693, 0.000 // 52188.693, 0.970 // 52189.907, 0.000 // 52216.869, 0.000 // 52217.869, 0.966
52219.088, 0.000 // 52245.921, 0.000 // 52246.921, 0.983 // 52248.136, 0.000 // 52275.173, 0.000
52276.173, 0.978 // 52277.381, 0.000 // 52304.242, 0.000 // 52305.242, 0.952 // 52306.446, 0.000
52333.246, 0.000 // 52334.246, 0.973 // 52335.432, 0.000 // 52362.238, 0.000 // 52363.238, 0.964
52364.419, 0.000 // 52391.257, 0.000 // 52392.257, 0.951 // 52393.474, 0.000 // 52420.229, 0.000
52421.229, 0.965 // 52422.441, 0.000 // 52449.332, 0.000 // 52450.332, 0.944 // 52451.457, 0.000
52478.249, 0.000 // 52479.249, 0.982 // 52480.574, 0.000 // 52507.361, 0.000 // 52508.361, 0.930
52509.596, 0.000 // 52536.369, 0.000 // 52537.369, 0.959 // 52538.564, 0.000 // 52565.355, 0.000
```

52566.355, 0.916 // 52567.568, 0.000 // 52594.357, 0.000 // 52595.357, 0.954 // 52596.548, 0.000
52623.477, 0.000 // 52624.477, 0.931 // 52625.724, 0.000 // 52652.493, 0.000 // 52653.493, 0.932
52654.684, 0.000 // 52681.522, 0.000 // 52682.522, 0.997 // 52683.777, 0.000 // 52710.703, 0.000
52711.703, 0.969 // 52712.889, 0.000 // 52739.631, 0.000 // 52740.631, 0.966 // 52741.902, 0.000
52768.759, 0.000 // 52769.759, 0.980 // 52770.929, 0.000 // 52797.775, 0.000 // 52798.775, 0.971
52799.984, 0.000 // 52826.836, 0.000 // 52827.836, 0.944 // 52829.018, 0.000 // 52855.821, 0.000
52856.821, 0.950 // 52858.031, 0.000 // 52884.796, 0.000 // 52885.796, 0.924 // 52887.054, 0.000
52914.013, 0.000 // 52915.013, 0.965 // 52916.236, 0.000 // 52943.045, 0.000 // 52944.045, 0.952
52945.231, 0.000 // 52972.073, 0.000 // 52973.073, 0.000 // 52974.220, 0.000 // 53001.052, 0.000
53002.052, 0.948 // 53003.229, 0.000 // 53030.056, 0.000 // 53031.056, 0.944 // 53032.257, 0.000
53059.109, 0.000 // 53060.109, 0.951 // 53061.284, 0.000 // 53088.070, 0.000 // 53089.070, 0.941
53090.288, 0.000 // 53117.161, 0.000 // 53118.161, 0.945 // 53119.387, 0.000 // 53146.250, 0.000
53147.250, 0.960 // 53148.580, 0.000 // 53175.436, 0.000 // 53176.436, 0.965 // 53177.676, 0.000
53204.604, 0.000 // 53205.604, 0.977 // 53206.841, 0.000 // 53233.854, 0.000 // 53234.854, 0.945
53236.079, 0.000 // 53262.972, 0.000 // 53263.972, 0.965 // 53265.199, 0.000 // 53291.960, 0.000
53292.960, 0.933 // 53294.122, 0.000 // 53320.907, 0.000 // 53321.907, 0.982 // 53323.132, 0.000
53350.022, 0.000 // 53351.022, 0.958 // 53352.244, 0.000 // 53379.144, 0.000 // 53380.144, 0.965
53381.328, 0.000 // 53408.359, 0.000 // 53409.359, 0.963 // 53410.636, 0.000 // 53437.476, 0.000
53438.476, 0.959 // 53439.694, 0.000 // 53466.506, 0.000 // 53467.506, 0.955 // 53468.712, 0.000
53495.590, 0.000 // 53496.590, 0.964 // 53497.796, 0.000 // 53524.744, 0.000 // 53525.744, 0.936
53526.943, 0.000 // 53553.840, 0.000 // 53554.840, 0.942 // 53556.045, 0.000 // 53582.959, 0.000
53583.959, 0.949 // 53585.195, 0.000 // 53612.023, 0.000 // 53613.023, 0.961 // 53614.261, 0.000
53641.085, 0.000 // 53642.085, 1.001 // 53643.283, 0.000 // 53670.075, 0.000 // 53671.075, 0.942
53672.300, 0.000 // 53699.144, 0.000 // 53700.144, 0.944 // 53701.389, 0.000 // 53728.207, 0.000
53729.207, 0.939 // 53730.429, 0.000 // 53757.159, 0.000 // 53758.159, 0.941 // 53759.371, 0.000
53786.109, 0.000 // 53787.109, 0.969 // 53788.346, 0.000 // 53815.100, 0.000 // 53816.100, 0.972
53817.319, 0.000 // 53844.128, 0.000 // 53845.128, 0.977 // 53846.346, 0.000 // 53873.121, 0.000
53874.121, 0.998 // 53875.362, 0.000 // 53902.139, 0.000 // 53903.139, 0.974 // 53904.332, 0.000
53931.127, 0.000 // 53932.127, 0.979 // 53933.363, 0.000 // 53960.149, 0.000 // 53961.149, 0.971
53962.353, 0.000 // 53989.148, 0.000 // 53990.148, 0.972 // 53991.325, 0.000 // 54018.045, 0.000
54019.045, 0.967 // 54020.218, 0.000 // 54047.097, 0.000 // 54048.097, 0.968 // 54049.347, 0.000
54076.293, 0.000 // 54077.293, 1.016 // 54078.486, 0.000 // 54105.213, 0.000 // 54106.213, 0.969
54107.368, 0.000 // 54134.137, 0.000 // 54135.137, 0.956 // 54136.372, 0.000 // 54163.126, 0.000
54164.126, 1.020 // 54165.321, 0.000 // 54192.128, 0.000 // 54193.128, 0.994 // 54194.307, 0.000
54221.100, 0.000 // 54222.100, 0.974 // 54223.295, 0.000 // 54249.982, 0.000 // 54250.982, 0.984
54252.165, 0.000 // 54278.977, 0.000 // 54279.977, 0.998 // 54281.245, 0.000 // 54308.058, 0.000
54309.058, 0.970 // 54310.357, 0.000 // 54337.242, 0.000 // 54338.242, 0.958 // 54339.439, 0.000
54366.201, 0.000 // 54367.201, 0.945 // 54368.381, 0.000 // 54395.307, 0.000 // 54396.307, 0.972
54397.554, 0.000 // 54424.445, 0.000 // 54425.445, 0.965 // 54426.657, 0.000 // 54453.534, 0.000
54454.534, 0.961 // 54455.733, 0.000 // 54482.604, 0.000 // 54483.604, 0.984 // 54484.808, 0.000
54511.672, 0.000 // 54512.672, 0.960 // 54513.872, 0.000 // 54540.678, 0.000 // 54541.678, 0.989
54542.923, 0.000 // 54569.748, 0.000 // 54570.748, 0.957 // 54571.912, 0.000 // 54598.680, 0.000
54599.680, 0.963 // 54600.865, 0.000 // 54627.640, 0.000 // 54628.640, 0.959 // 54629.823, 0.000
54656.668, 0.000 // 54657.668, 0.970 // 54658.895, 0.000 // 54685.724, 0.000 // 54686.724, 0.964
54687.962, 0.000 // 54714.919, 0.000 // 54715.919, 0.968 // 54717.104, 0.000 // 54744.036, 0.000
54745.036, 0.955 // 54746.233, 0.000 // 54772.999, 0.000 // 54773.999, 0.915 // 54775.197, 0.000
54802.048, 0.000 // 54803.048, 0.944 // 54804.225, 0.000 // 54831.077, 0.000 // 54832.077, 1.006
54833.242, 0.000 // 54860.003, 0.000 // 54861.003, 0.976 // 54862.183, 0.000 // 54889.050, 0.000
54890.050, 0.955 // 54891.223, 0.000 // 54918.042, 0.000 // 54919.042, 0.958 // 54920.254, 0.000
54947.048, 0.000 // 54948.048, 0.953 // 54949.230, 0.000 // 54976.049, 0.000 // 54977.049, 0.944
54978.216, 0.000 // 55005.038, 0.000 // 55006.038, 0.956 // 55007.229, 0.000 // 55033.991, 0.000
55034.991, 0.922 // 55036.170, 0.000 // 55062.961, 0.000 // 55063.961, 0.992 // 55065.107, 0.000
55092.011, 0.000 // 55093.011, 0.108 // 55094.194, 0.000 // 55121.138, 0.000 // 55122.138, 0.000
55123.228, 0.000 // 55150.030, 0.000 // 55151.030, 0.966 // 55152.230, 0.000 // 55179.078, 0.000
55180.078, 0.960 // 55181.305, 0.000 // 55208.142, 0.000 // 55209.142, 0.968 // 55210.354, 0.000
55237.186, 0.000 // 55238.186, 0.948 // 55239.367, 0.000 // 55266.282, 0.000 // 55267.282, 0.964
55268.478, 0.000 // 55295.209, 0.000 // 55296.209, 0.924 // 55297.402, 0.000 // 55324.399, 0.000
55325.399, 0.953 // 55326.579, 0.000 // 55353.319, 0.000 // 55354.319, 0.969 // 55355.503, 0.000
55382.352, 0.000 // 55383.352, 0.937 // 55384.529, 0.000 // 55411.358, 0.000 // 55412.358, 0.938
55413.568, 0.000 // 55440.401, 0.000 // 55441.401, 0.962 // 55442.592, 0.000 // 55469.482, 0.000
55470.482, 0.958 // 55471.685, 0.000 // 55498.580, 0.000 // 55499.580, 0.957 // 55500.734, 0.000
55527.557, 0.000 // 55528.557, 0.983 // 55529.756, 0.000 // 55556.517, 0.000 // 55557.517, 0.968
55558.708, 0.000 // 55585.560, 0.000 // 55586.560, 0.966 // 55587.796, 0.000 // 55614.747, 0.000

55615.747, 0.932 // 55617.005, 0.000 // 55643.930, 0.000 // 55644.930, 0.953 // 55646.162, 0.000
55673.114, 0.000 // 55674.114, 0.938 // 55675.327, 0.000 // 55702.311, 0.000 // 55703.311, 0.916
55704.524, 0.000 // 55731.375, 0.000 // 55732.375, 0.950 // 55733.626, 0.000 // 55760.600, 0.000
55761.600, 0.943 // 55762.791, 0.000 // 55789.513, 0.000 // 55790.513, 0.957 // 55791.688, 0.000
55818.457, 0.000 // 55819.457, 0.935 // 55820.626, 0.000 // 55847.649, 0.000 // 55848.649, 0.956
55849.889, 0.000 // 55876.717, 0.000 // 55877.717, 0.932 // 55878.949, 0.000 // 55905.742, 0.000
55906.742, 0.959 // 55907.945, 0.000 // 55934.856, 0.000 // 55935.856, 0.951 // 55937.034, 0.000
55963.897, 0.000 // 55964.897, 0.939 // 55966.136, 0.000 // 55992.954, 0.000 // 55993.954, 0.997
55995.240, 0.000 // 56022.052, 0.000 // 56023.052, 0.933 // 56024.244, 0.000 // 56051.166, 0.000
56052.166, 0.996 // 56053.346, 0.000 // 56080.277, 0.000 // 56081.277, 0.934 // 56082.457, 0.000
56109.281, 0.000 // 56110.281, 0.918 // 56111.526, 0.000 // 56138.502, 0.000 // 56139.502, 0.980
56140.701, 0.000 // 56167.658, 0.000 // 56168.658, 0.994 // 56169.856, 0.000 // 56196.780, 0.000
56197.780, 0.982 // 56199.005, 0.000 // 56225.852, 0.000 // 56226.852, 0.964 // 56228.090, 0.000
56255.032, 0.000 // 56256.032, 0.965 // 56257.326, 0.000 // 56284.136, 0.000 // 56285.136, 0.936
56286.313, 0.000 // 56313.212, 0.000 // 56314.212, 0.977 // 56315.453, 0.000 // 56342.476, 0.000
56343.476, 0.972 // 56344.806, 0.000 // 56371.770, 0.000 // 56372.770, 0.963 // 56374.015, 0.000
56400.840, 0.000 // 56401.840, 0.950 // 56403.010, 0.000 // 56429.787, 0.000 // 56430.787, 0.957
56432.015, 0.000 // 56458.884, 0.000 // 56459.884, 0.940 // 56461.141, 0.000 // 56488.119, 0.000
56489.119, 0.975 // 56490.336, 0.000 // 56517.190, 0.000 // 56518.190, 0.964 // 56519.462, 0.000
56546.198, 0.000 // 56547.198, 0.977 // 56548.395, 0.000 // 56575.307, 0.000 // 56576.307, 0.942
56577.509, 0.000 // 56604.334, 0.000 // 56605.334, 0.933 // 56606.638, 0.000 // 56633.474, 0.000
56634.474, 0.946 // 56635.649, 0.000 // 56662.712, 0.000 // 56663.712, 0.943 // 56664.889, 0.000
56691.724, 0.000 // 56692.724, 0.969 // 56693.951, 0.000 // 56720.798, 0.000 // 56721.798, 0.959
56723.065, 0.000 // 56749.956, 0.000 // 56750.956, 0.943 // 56752.138, 0.000 // 56778.858, 0.000
56779.858, 0.939 // 56781.017, 0.000 // 56808.010, 0.000 // 56809.010, 0.949 // 56810.397, 0.000
56837.397, 0.000 // 56838.397, 0.946 // 56839.624, 0.000 // 56866.410, 0.000 // 56867.410, 0.937
56868.602, 0.000 // 56895.478, 0.000 // 56896.478, 0.959 // 56897.695, 0.000 // 56924.517, 0.000
56925.517, 0.950 // 56926.702, 0.000 // 56953.588, 0.000 // 56954.588, 0.970 // 56955.832, 0.000
56982.631, 0.000 // 56983.631, 0.957 // 56984.809, 0.000 // 57011.695, 0.000 // 57012.695, 0.942
57013.861, 0.000 // 57040.812, 0.000 // 57041.812, 0.979 // 57043.029, 0.000 // 57070.067, 0.000
57071.067, 0.934 // 57072.274, 0.000 // 57099.196, 0.000 // 57100.196, 0.940 // 57101.403, 0.000
57128.589, 0.000 // 57129.589, 0.936 // 57130.792, 0.000 // 57157.857, 0.000 // 57158.857, 0.928
57160.100, 0.000 // 57187.099, 0.000 // 57188.099, 0.945 // 57189.363, 0.000 // 57216.419, 0.000
57217.419, 0.961 // 57218.610, 0.000 // 57245.523, 0.000 // 57246.523, 0.943 // 57247.686, 0.000
57274.463, 0.000 // 57275.463, 0.946 // 57276.663, 0.000 // 57303.783, 0.000 // 57304.783, 0.794
57306.516, 0.000 // 57333.272, 0.000 // 57334.272, 0.921 // 57335.503, 0.000 // 57362.314, 0.000
57363.314, 0.922 // 57364.506, 0.000 // 57391.313, 0.000 // 57392.313, 0.953 // 57393.482, 0.000
57420.335, 0.000 // 57421.335, 0.930 // 57422.531, 0.000 // 57449.443, 0.000 // 57450.443, 0.934
57451.737, 0.000 // 57478.819, 0.000 // 57479.819, 0.964 // 57481.057, 0.000 // 57507.873, 0.000
57508.873, 0.968 // 57510.073, 0.000 // 57537.019, 0.000 // 57538.019, 0.947 // 57539.209, 0.000
57565.953, 0.000 // 57566.953, 0.945 // 57568.230, 0.000 // 57595.128, 0.000 // 57596.128, 0.938
57597.404, 0.000 // 57624.366, 0.000 // 57625.366, 1.007 // 57626.596, 0.000 // 57653.672, 0.000
57654.672, 0.972 // 57655.859, 0.000 // 57682.876, 0.000 // 57683.876, 0.935 // 57685.122, 0.000
57712.097, 0.000 // 57713.097, 0.927 // 57714.323, 0.000 // 57741.154, 0.000 // 57742.154, 0.936
57743.363, 0.000 // 57770.287, 0.000 // 57771.287, 0.926 // 57772.494, 0.000 // 57799.500, 0.000
57800.500, 0.933 // 57801.774, 0.000 // 57828.680, 0.000 // 57829.680, 0.157 // 57830.895, 0.000
57857.866, 0.000 // 57858.866, 0.000 // 57860.076, 0.000 // 57887.118, 0.000 // 57888.118, 0.000
57889.264, 0.000 // 57916.234, 0.000 // 57917.234, 1.026 // 57918.393, 0.000 // 57945.341, 0.000
57946.341, 1.028 // 57947.594, 0.000 // 57974.446, 0.000 // 57975.446, 1.051 // 57976.625, 0.000
58003.512, 0.000 // 58004.512, 1.032 // 58005.737, 0.000 // 58032.617, 0.000 // 58033.617, 1.053
58034.823, 0.000 // 58061.698, 0.000 // 58062.698, 0.000 // 58063.872, 0.000 // 58090.702, 0.000
58091.702, 1.037 // 58092.885, 0.000 // 58119.690, 0.000 // 58120.690, 1.029 // 58121.909, 0.000
58148.754, 0.000 // 58149.754, 1.064 // 58151.177, 0.000 // 58178.152, 0.000 // 58179.152, 1.018
58180.347, 0.000 // 58207.389, 0.000 // 58208.389, 1.029 // 58209.574, 0.000 // 58236.620, 0.000
58237.620, 1.033 // 58238.847, 0.000 // 58265.731, 0.000 // 58266.731, 1.047 // 58267.935, 0.000
58294.789, 0.000 // 58295.789, 1.010 // 58297.023, 0.000 // 58323.965, 0.000 // 58324.965, 1.042
58326.153, 0.000 // 58353.023, 0.000 // 58354.023, 1.044 // 58355.193, 0.000 // 58382.163, 0.000
58383.163, 1.044 // 58384.377, 0.000 // 58411.185, 0.000 // 58412.185, 1.051 // 58413.375, 0.000
58440.321, 0.000 // 58441.321, 1.064 // 58442.532, 0.000 // 58469.338, 0.000 // 58470.338, 1.061
58471.540, 0.000 // 58498.334, 0.000 // 58499.334, 1.045 // 58500.568, 0.000 // 58527.589, 0.000
58528.589, 1.010 // 58529.929, 0.000 // 58556.865, 0.000 // 58557.865, 1.033 // 58559.030, 0.000
58585.896, 0.000 // 58586.896, 1.023 // 58588.166, 0.000 // 58614.985, 0.000 // 58615.985, 1.065
58617.215, 0.000 // 58644.069, 0.000 // 58645.069, 1.025 // 58646.246, 0.000 // 58673.130, 0.000

```
58674.130, 1.055 // 58675.313, 0.000 // 58702.225, 0.000 // 58703.225, 1.037 // 58704.444, 0.000
58731.380, 0.000 // 58732.380, 1.032 // 58733.534, 0.000 // 58760.332, 0.000 // 58761.332, 1.036
58762.528, 0.000 // 58789.299, 0.000 // 58790.299, 1.039 // 58791.510, 0.000 // 58818.332, 0.000
58819.332, 1.052 // 58820.507, 0.000 // 58847.294, 0.000 // 58848.294, 1.101 // 58849.494, 0.000
58876.438, 0.000 // 58877.438, 1.035 // 58878.624, 0.000 // 58905.568, 0.000 // 58906.568, 1.024
58907.771, 0.000 // 58934.608, 0.000 // 58935.608, 1.034 // 58936.945, 0.000 // 58963.829, 0.000
58964.829, 1.055 // 58966.064, 0.000 // 58993.095, 0.000 // 58994.095, 1.030 // 58995.389, 0.000
59022.417, 0.000 // 59023.417, 1.065 // 59024.679, 0.000 // 59051.531, 0.000 // 59052.531, 1.009
59053.737, 0.000 // 59080.647, 0.000 // 59081.647, 1.033 // 59082.940, 0.000 // 59109.744, 0.000
59110.744, 1.007 // 59111.980, 0.000 // 59138.741, 0.000 // 59139.741, 0.984 // 59140.948, 0.000
59167.765, 0.000 // 59168.765, 0.661 // 59170.676, 0.000 // 59197.591, 0.000 // 59198.591, 1.014
59199.805, 0.000 // 59226.759, 0.000 // 59227.759, 0.990 // 59228.962, 0.000 // 59255.905, 0.000
59256.905, 1.030 // 59258.148, 0.000 // 59285.020, 0.000 // 59286.020, 1.005 // 59287.211, 0.000
59313.949, 0.000 // 59314.949, 1.028 // 59316.132, 0.000 // 59342.944, 0.000 // 59343.944, 1.039
59345.199, 0.000 // 59372.238, 0.000 // 59373.238, 1.034 // 59374.498, 0.000 // 59401.393, 0.000
59402.393, 1.050 // 59403.623, 0.000 // 59430.436, 0.000 // 59431.436, 1.054 // 59432.628, 0.000
59459.530, 0.000 // 59460.530, 1.083 // 59461.707, 0.000 // 59488.692, 0.000 // 59489.692, 1.070
59490.890, 0.000 // 59517.737, 0.000 // 59518.737, 1.075 // 59519.947, 0.000 // 59547.017, 0.000
59548.017, 1.099 // 59549.226, 0.000 // 59576.125, 0.000 // 59577.125, 1.078 // 59578.372, 0.000
59605.342, 0.000 // 59606.342, 1.039 // 59607.556, 0.000 // 59634.385, 0.000 // 59635.385, 1.063
59636.567, 0.000 // 59663.557, 0.000 // 59664.557, 1.053 // 59665.735, 0.000 // 59692.605, 0.000
59693.605, 1.044 // 59694.927, 0.000 // 59721.749, 0.000 // 59722.749, 1.041 // 59723.970, 0.000
59750.894, 0.000 // 59751.894, 1.047 // 59753.073, 0.000 // 59779.986, 0.000 // 59780.986, 1.046
59782.201, 0.000 // 59809.043, 0.000 // 59810.043, 1.045 // 59811.271, 0.000 // 59838.216, 0.000
59839.216, 1.037 // 59840.477, 0.000 // 59867.402, 0.000 // 59868.402, 1.022 // 59869.627, 0.000
59896.412, 0.000 // 59897.412, 1.037 // 59898.595, 0.000 // 59925.456, 0.000 // 59926.456, 1.025
59927.841, 0.000 // 59954.679, 0.000 // 59955.679, 1.014 // 59956.899, 0.000 // 59983.883, 0.000
59984.883, 1.012 // 59986.128, 0.000 // 60013.247, 0.000 // 60014.247, 0.989 // 60015.481, 0.000
60042.505, 0.000 // 60043.505, 0.986 // 60044.700, 0.000 // 60071.507, 0.000 // 60072.507, 0.987
60073.713, 0.000 // 60100.529, 0.000 // 60101.529, 1.002 // 60102.771, 0.000 // 60129.763, 0.000
60130.763, 0.994 // 60131.960, 0.000 // 60158.908, 0.000 // 60159.908, 0.980 // 60161.144, 0.000
60188.220, 0.000 // 60189.220, 0.000 // 60190.374, 0.000 // 60217.188, 0.000 // 60218.188, 0.980
60219.405, 0.000 // 60246.554, 0.000 // 60247.554, 0.963 // 60248.724, 0.000 // 60275.586, 0.000
60276.586, 1.036 // 60277.796, 0.000 // 60304.674, 0.000 // 60305.674, 0.970 // 60306.880, 0.000
60333.789, 0.000 // 60334.789, 1.012 // 60335.965, 0.000 // 60362.771, 0.000 // 60363.771, 0.978
60364.969, 0.000 // 60391.903, 0.000 // 60392.903, 1.032 // 60394.116, 0.000 // 60421.000, 0.000
60422.000, 0.994 // 60423.201, 0.000 // 60450.170, 0.000 // 60451.170, 0.995 // 60452.402, 0.000
60479.384, 0.000 // 60480.384, 1.014 // 60481.580, 0.000 // 60508.447, 0.000 // 60509.447, 1.017
60510.632, 0.000 // 60537.531, 0.000 // 60538.531, 1.029 // 60539.726, 0.000 // 60566.519, 0.000
60567.519, 1.035 // 60568.722, 0.000 // 60595.786, 0.000 // 60596.786, 0.981 // 60598.057, 0.000
60625.161, 0.000 // 60626.161, 1.029 // 60627.365, 0.000 // 60654.216, 0.000 // 60655.216, 1.000
60656.424, 0.000 // 60683.231, 0.000 // 60684.231, 0.987 // 60685.446, 0.000 // 60712.244, 0.000
60713.244, 1.028 // 60714.429, 0.000 // 60741.383, 0.000 // 60742.383, 1.023 // 60744.014, 0.000
60771.136, 0.000 // 60772.136, 1.012 // 60773.334, 0.000 // 60800.216, 0.000 // 60801.216, 1.020
60802.447, 0.000 // 60829.252, 0.000 // 60830.252, 1.026 // 60831.453, 0.000 // 60858.261, 0.000
60859.261, 1.031 // 60860.436, 0.000 // 60887.278, 0.000 // 60888.278, 1.006 // 60889.523, 0.000
60916.646, 0.000 // 60917.646, 1.033 // 60918.903, 0.000 // 60945.779, 0.000 // 60946.779, 1.022
60947.946, 0.000 // 60974.933, 0.000 // 60975.933, 0.000 // 60977.048, 0.000 // 61004.065, 0.000
61005.065, 0.000 // 61006.178, 0.000 // 61033.074, 0.000 // 61034.074, 0.000 // 61035.182, 0.000
61062.251, 0.000 // 61063.251, 0.000 // 61064.321, 0.000 // 61091.323, 0.000 // 61092.323, 0.000
61093.414, 0.000 // 61120.519, 0.000 // 61121.519, 0.000 // 61122.723, 0.000 // 61149.833, 0.000
61150.833, 0.000 // 61151.962, 0.000 // 61178.849, 0.000 // 61179.849, 0.000 // 61180.976, 0.000
61207.851, 0.000 // 61208.851, 0.028 // 61209.980, 0.000 // 61236.905, 0.000 // 61237.905, 0.000
61239.082, 0.000 // 61265.975, 0.000 // 61266.975, 0.000 // 61268.158, 0.000 // 61295.181, 0.000
61296.181, 0.000 // 61297.315, 0.000 // 61324.365, 0.000 // 61325.365, 0.000 // 61326.502, 0.000
61353.684, 0.000 // 61354.684, 0.000 // 61355.811, 0.000 // 61382.834, 0.000 // 61383.834, 0.000
61385.003, 0.000 // 61412.159, 0.000 // 61413.159, 0.000 // 61414.301, 0.000 // 61441.282, 0.000
61442.282, 0.000 // 61443.359, 0.000 // 61470.391, 0.000 // 61471.391, 0.000 // 61472.488, 0.000
61499.612, 0.000 // 61500.612, 0.000 // 61501.719, 0.000 // 61528.739, 0.000 // 61529.739, 0.000
61530.884, 0.000 // 61557.876, 0.000 // 61558.876, 0.000 // 61559.959, 0.000 // 61587.059, 0.000
61588.059, 0.000 // 61589.142, 0.000 // 61616.130, 0.000 // 61617.130, 0.000 // 61618.250, 0.000
61645.273, 0.000 // 61646.273, 0.000 // 61647.442, 0.000 // 61674.424, 0.000 // 61675.424, 0.000
61676.518, 0.000 // 61703.526, 0.000 // 61704.526, 0.000 // 61705.639, 0.000 // 61732.711, 0.000
```

61733.711, 0.000 // 61734.813, 0.000 // 61761.815, 0.000 // 61762.815, 0.000 // 61763.928, 0.000
61790.978, 0.000 // 61791.978, 0.000 // 61793.111, 0.000 // 61820.145, 0.000 // 61821.145, 0.000
61822.242, 0.000 // 61849.213, 0.000 // 61850.213, 0.000 // 61851.349, 0.000 // 61878.351, 0.000
61879.351, 0.000 // 61880.442, 0.000 // 61907.370, 0.000 // 61908.370, 0.000 // 61909.477, 0.000
61936.598, 0.000 // 61937.598, 0.000 // 61938.678, 0.000 // 61965.731, 0.000 // 61966.731, 0.000
61967.843, 0.000 // 61994.991, 0.000 // 61995.991, 0.060 // 61997.120, 0.000 // 62024.301, 0.000
62025.301, 0.000 // 62026.397, 0.000 // 62053.694, 0.000 // 62054.694, 0.000 // 62055.828, 0.000
62082.938, 0.000 // 62083.938, 0.000 // 62085.043, 0.000 // 62112.047, 0.000 // 62113.047, 0.000
62114.242, 0.000 // 62141.416, 0.000 // 62142.416, 0.000 // 62143.530, 0.000 // 62170.635, 0.000
62171.635, 0.000 // 62172.747, 0.000 // 62199.706, 0.000 // 62200.706, 0.000 // 62201.819, 0.000
62228.761, 0.000 // 62229.761, 0.000 // 62230.880, 0.000 // 62257.927, 0.000 // 62258.927, 0.000
62260.038, 0.000 // 62287.048, 0.000 // 62288.048, 0.000 // 62289.150, 0.000 // 62316.075, 0.000
62317.075, 0.000 // 62318.176, 0.000 // 62345.083, 0.000 // 62346.083, 0.000 // 62347.192, 0.000
62373.968, 0.000 // 62374.968, 0.000 // 62376.071, 0.000 // 62402.903, 0.000 // 62403.903, 0.986
62405.090, 0.000 // 62432.001, 0.000 // 62433.001, 0.957 // 62434.210, 0.000 // 62461.202, 0.000
62462.202, 0.929 // 62463.485, 0.000 // 62490.408, 0.000 // 62491.408, 0.956 // 62492.655, 0.000
62519.498, 0.000 // 62520.498, 1.039 // 62521.658, 0.000 // 62548.666, 0.000 // 62549.666, 1.012
62550.881, 0.000 // 62577.949, 0.000 // 62578.949, 0.962 // 62580.178, 0.000 // 62607.140, 0.000
62608.140, 0.923 // 62609.368, 0.000 // 62636.384, 0.000 // 62637.384, 0.969 // 62638.570, 0.000
62665.397, 0.000 // 62666.397, 0.968 // 62667.664, 0.000 // 62694.594, 0.000 // 62695.594, 0.989
62696.945, 0.000 // 62724.022, 0.000 // 62725.022, 1.045 // 62726.236, 0.000 // 62753.134, 0.000
62754.134, 0.976 // 62755.321, 0.000 // 62782.117, 0.000 // 62783.117, 0.980 // 62784.284, 0.000
62811.072, 0.000 // 62812.072, 0.990 // 62813.278, 0.000 // 62840.087, 0.000 // 62841.087, 0.984
62842.284, 0.000 // 62869.154, 0.000 // 62870.154, 0.989 // 62871.347, 0.000 // 62898.375, 0.000
62899.375, 0.983 // 62900.593, 0.000 // 62927.423, 0.000 // 62928.423, 0.976 // 62929.759, 0.000
62956.721, 0.000 // 62957.721, 0.982 // 62959.048, 0.000 // 62985.818, 0.000 // 62986.818, 0.973
62988.056, 0.000 // 63014.817, 0.000 // 63015.817, 0.991 // 63017.007, 0.000 // 63043.812, 0.000
63044.812, 0.953 // 63046.024, 0.000 // 63072.807, 0.000 // 63073.807, 0.958 // 63075.008, 0.000
63101.814, 0.000 // 63102.814, 0.983 // 63104.050, 0.000 // 63130.808, 0.000 // 63131.808, 0.958
63133.028, 0.000 // 63159.880, 0.000 // 63160.880, 0.966 // 63162.088, 0.000 // 63188.926, 0.000
63189.926, 0.975 // 63191.130, 0.000 // 63217.915, 0.000 // 63218.915, 0.966 // 63220.105, 0.000
63247.009, 0.000 // 63248.009, 1.002 // 63249.158, 0.000 // 63275.897, 0.000 // 63276.897, 0.979
63278.109, 0.000 // 63304.948, 0.000 // 63305.948, 0.946 // 63307.337, 0.000 // 63334.251, 0.000
63335.251, 0.974 // 63336.467, 0.000 // 63363.387, 0.000 // 63364.387, 0.954 // 63365.587, 0.000
63392.437, 0.000 // 63393.437, 0.994 // 63394.618, 0.000 // 63421.458, 0.000 // 63422.458, 1.005
63423.684, 0.000 // 63450.460, 0.000 // 63451.460, 0.992 // 63452.646, 0.000 // 63479.675, 0.000
63480.675, 1.006 // 63481.874, 0.000 // 63508.735, 0.000 // 63509.735, 1.036 // 63510.918, 0.000
63537.768, 0.000 // 63538.768, 1.014 // 63539.994, 0.000 // 63566.845, 0.000 // 63567.845, 1.016
63568.965, 0.000 // 63595.898, 0.000 // 63596.898, 0.993 // 63598.106, 0.000 // 63625.069, 0.000
63626.069, 1.018 // 63627.243, 0.000 // 63654.143, 0.000 // 63655.143, 1.041 // 63656.338, 0.000
63683.234, 0.000 // 63684.234, 1.009 // 63685.402, 0.000 // 63712.354, 0.000 // 63713.354, 1.010
63714.590, 0.000 // 63741.510, 0.000 // 63742.510, 1.039 // 63743.758, 0.000 // 63770.761, 0.000
63771.761, 1.022 // 63772.982, 0.000 // 63799.768, 0.000 // 63800.768, 1.011 // 63801.960, 0.000
63828.750, 0.000 // 63829.750, 1.007 // 63830.944, 0.000 // 63857.810, 0.000 // 63858.810, 1.022
63860.022, 0.000 // 63887.049, 0.000 // 63888.049, 1.036 // 63889.230, 0.000 // 63916.030, 0.000
63917.030, 1.025 // 63918.262, 0.000 // 63945.116, 0.000 // 63946.116, 1.050 // 63947.320, 0.000
63974.101, 0.000 // 63975.101, 1.024 // 63976.406, 0.000 // 64003.311, 0.000 // 64004.311, 1.035
64005.527, 0.000 // 64032.448, 0.000 // 64033.448, 1.010 // 64034.641, 0.000 // 64061.535, 0.000
64062.535, 1.018 // 64063.753, 0.000 // 64090.577, 0.000 // 64091.577, 1.034 // 64092.744, 0.000
64119.562, 0.000 // 64120.562, 1.022 // 64121.762, 0.000 // 64148.586, 0.000 // 64149.586, 1.004
64150.776, 0.000 // 64177.766, 0.000 // 64178.766, 1.005 // 64179.978, 0.000 // 64206.763, 0.000
64207.763, 1.039 // 64208.979, 0.000 // 64235.990, 0.000 // 64236.990, 0.000 // 64237.999, 0.000
64264.842, 0.000 // 64265.842, 1.013 // 64267.648, 0.000 // 64294.429, 0.000 // 64295.429, 0.997
64296.607, 0.000 // 64323.412, 0.000 // 64324.412, 1.000 // 64325.585, 0.000 // 64352.784, 0.000
64353.784, 1.015 // 64354.966, 0.000 // 64381.946, 0.000 // 64382.946, 0.990 // 64384.131, 0.000
64411.078, 0.000 // 64412.078, 0.972 // 64413.358, 0.000 // 64440.208, 0.000 // 64441.208, 0.994
64442.394, 0.000 // 64469.301, 0.000 // 64470.301, 1.001 // 64471.496, 0.000 // 64498.299, 0.000
64499.299, 0.989 // 64500.509, 0.000 // 64527.365, 0.000 // 64528.365, 0.992 // 64529.558, 0.000
64556.395, 0.000 // 64557.395, 0.998 // 64558.611, 0.000 // 64585.714, 0.000 // 64586.714, 0.997
64588.018, 0.000 // 64614.961, 0.000 // 64615.961, 0.991 // 64617.116, 0.000 // 64643.955, 0.000
64644.955, 0.981 // 64646.160, 0.000 // 64673.011, 0.000 // 64674.011, 0.975 // 64675.187, 0.000
64702.083, 0.000 // 64703.083, 1.019 // 64704.307, 0.000 // 64731.298, 0.000 // 64732.298, 0.970
64733.603, 0.000 // 64760.551, 0.000 // 64761.551, 0.992 // 64762.767, 0.000 // 64789.669, 0.000

64790.669, 0.972 // 64791.903, 0.000 // 64818.876, 0.000 // 64819.876, 1.017 // 64821.123, 0.000
64847.981, 0.000 // 64848.981, 0.999 // 64850.241, 0.000 // 64877.164, 0.000 // 64878.164, 1.009
64879.385, 0.000 // 64906.136, 0.000 // 64907.136, 0.986 // 64908.380, 0.000 // 64935.469, 0.000
64936.469, 0.993 // 64937.661, 0.000 // 64964.692, 0.000 // 64965.692, 1.018 // 64966.946, 0.000
64994.103, 0.000 // 64995.103, 0.998 // 64996.360, 0.000 // 65023.334, 0.000 // 65024.334, 1.020
65025.648, 0.000 // 65052.544, 0.000 // 65053.544, 1.012 // 65054.749, 0.000 // 65081.627, 0.000
65082.627, 0.998 // 65083.893, 0.000 // 65110.942, 0.000 // 65111.942, 1.043 // 65113.166, 0.000
65140.088, 0.000 // 65141.088, 1.039 // 65142.355, 0.000 // 65169.281, 0.000 // 65170.281, 0.987
65172.163, 0.000 // 65198.983, 0.000 // 65199.983, 0.980 // 65201.187, 0.000 // 65228.054, 0.000
65229.054, 1.035 // 65230.225, 0.000 // 65257.137, 0.000 // 65258.137, 0.973 // 65259.336, 0.000
65286.169, 0.000 // 65287.169, 0.993 // 65288.403, 0.000 // 65315.179, 0.000 // 65316.179, 0.953
65317.314, 0.000 // 65344.171, 0.000 // 65345.171, 0.988 // 65346.351, 0.000 // 65373.133, 0.000
65374.133, 1.011 // 65375.306, 0.000 // 65402.249, 0.000 // 65403.249, 0.965 // 65404.433, 0.000
65431.316, 0.000 // 65432.316, 0.993 // 65433.536, 0.000 // 65460.386, 0.000 // 65461.386, 0.983
65462.576, 0.000 // 65489.444, 0.000 // 65490.444, 1.015 // 65491.652, 0.000 // 65518.447, 0.000
65519.447, 1.013 // 65520.626, 0.000 // 65547.440, 0.000 // 65548.440, 0.972 // 65549.638, 0.000
65576.439, 0.000 // 65577.439, 0.947 // 65578.673, 0.000 // 65605.544, 0.000 // 65606.544, 0.937
65607.713, 0.000 // 65634.558, 0.000 // 65635.558, 0.938 // 65636.816, 0.000 // 65663.793, 0.000
65664.793, 0.958 // 65666.089, 0.000 // 65692.982, 0.000 // 65693.982, 0.977 // 65695.218, 0.000
65722.088, 0.000 // 65723.088, 0.946 // 65724.383, 0.000 // 65751.297, 0.000 // 65752.297, 0.963
65753.533, 0.000 // 65780.393, 0.000 // 65781.393, 0.961 // 65782.600, 0.000 // 65809.503, 0.000
65810.503, 0.957 // 65811.703, 0.000 // 65838.655, 0.000 // 65839.655, 0.951 // 65840.944, 0.000
65867.822, 0.000 // 65868.822, 0.950 // 65870.021, 0.000 // 65896.875, 0.000 // 65897.875, 0.934
65899.112, 0.000 // 65926.136, 0.000 // 65927.136, 0.950 // 65928.340, 0.000 // 65955.167, 0.000
65956.167, 0.942 // 65957.377, 0.000 // 65984.274, 0.000 // 65985.274, 0.959 // 65986.471, 0.000
66013.253, 0.000 // 66014.253, 0.952 // 66015.506, 0.000 // 66042.356, 0.000 // 66043.356, 0.963
66044.581, 0.000 // 66071.446, 0.000 // 66072.446, 0.950 // 66073.640, 0.000 // 66100.446, 0.000
66101.446, 0.969 // 66102.617, 0.000 // 66129.514, 0.000 // 66130.514, 0.934 // 66131.700, 0.000
66158.627, 0.000 // 66159.627, 0.962 // 66160.831, 0.000 // 66187.760, 0.000 // 66188.760, 0.927
66189.996, 0.000 // 66217.109, 0.000 // 66218.109, 0.985 // 66219.295, 0.000 // 66246.163, 0.000
66247.163, 0.943 // 66248.415, 0.000 // 66275.436, 0.000 // 66276.436, 0.961 // 66277.640, 0.000
66304.479, 0.000 // 66305.479, 0.936 // 66306.663, 0.000 // 66333.715, 0.000 // 66334.715, 0.952
66335.891, 0.000 // 66362.964, 0.000 // 66363.964, 0.985 // 66365.137, 0.000 // 66392.318, 0.000
66393.318, 0.945 // 66394.592, 0.000 // 66421.393, 0.000 // 66422.393, 0.971 // 66423.650, 0.000
66450.547, 0.000 // 66451.547, 1.002 // 66452.728, 0.000 // 66479.561, 0.000 // 66480.561, 0.950
66481.785, 0.000 // 66508.669, 0.000 // 66509.669, 0.988 // 66510.906, 0.000 // 66537.972, 0.000
66538.972, 0.959 // 66540.152, 0.000 // 66567.066, 0.000 // 66568.066, 0.970 // 66569.317, 0.000
66596.153, 0.000 // 66597.153, 0.952 // 66598.384, 0.000 // 66625.247, 0.000 // 66626.247, 0.958
66627.446, 0.000 // 66654.565, 0.000 // 66655.565, 0.966 // 66656.805, 0.000 // 66683.629, 0.000
66684.629, 0.975 // 66685.871, 0.000 // 66712.892, 0.000 // 66713.892, 1.015 // 66715.179, 0.000
66742.179, 0.000 // 66743.179, 1.020 // 66744.361, 0.000 // 66771.567, 0.000 // 66772.567, 1.002
66773.785, 0.000 // 66800.645, 0.000 // 66801.645, 1.000 // 66802.843, 0.000 // 66829.837, 0.000
66830.837, 1.002 // 66832.045, 0.000 // 66859.131, 0.000 // 66860.131, 1.003 // 66861.327, 0.000
66888.282, 0.000 // 66889.282, 1.018 // 66890.490, 0.000 // 66917.449, 0.000 // 66918.449, 1.001
66919.650, 0.000 // 66946.563, 0.000 // 66947.563, 0.993 // 66948.753, 0.000 // 66975.749, 0.000
66976.749, 0.991 // 66977.927, 0.000 // 67004.829, 0.000 // 67005.829, 0.996 // 67007.000, 0.000
67033.994, 0.000 // 67034.994, 1.030 // 67036.219, 0.000 // 67063.054, 0.000 // 67064.054, 1.013
67065.252, 0.000 // 67092.321, 0.000 // 67093.321, 1.000 // 67094.499, 0.000 // 67121.374, 0.000
67122.374, 1.018 // 67123.647, 0.000 // 67150.626, 0.000 // 67151.626, 1.014 // 67152.816, 0.000
67179.634, 0.000 // 67180.634, 1.036 // 67181.968, 0.000 // 67208.848, 0.000 // 67209.848, 0.978
67211.035, 0.000 // 67238.007, 0.000 // 67239.007, 0.964 // 67240.483, 0.000 // 67267.640, 0.000
67268.640, 1.004 // 67269.831, 0.000 // 67296.878, 0.000 // 67297.878, 1.059 // 67299.028, 0.000
67325.977, 0.000 // 67326.977, 1.039 // 67328.169, 0.000 // 67355.264, 0.000 // 67356.264, 0.993
67357.468, 0.000 // 67384.433, 0.000 // 67385.433, 0.976 // 67386.607, 0.000 // 67413.499, 0.000
67414.499, 1.000 // 67415.684, 0.000 // 67442.603, 0.000 // 67443.603, 0.960 // 67444.804, 0.000
67471.960, 0.000 // 67472.960, 1.004 // 67474.363, 0.000 // 67501.260, 0.000 // 67502.260, 1.001
67503.442, 0.000 // 67530.430, 0.000 // 67531.430, 0.998 // 67532.602, 0.000 // 67559.357, 0.000
67560.357, 0.995 // 67561.691, 0.000 // 67588.654, 0.000 // 67589.654, 0.980 // 67590.859, 0.000
67617.839, 0.000 // 67618.839, 0.990 // 67620.058, 0.000 // 67647.030, 0.000 // 67648.030, 1.000
67649.224, 0.000 // 67676.136, 0.000 // 67677.136, 0.998 // 67678.317, 0.000 // 67705.289, 0.000
67706.289, 0.987 // 67707.501, 0.000 // 67734.617, 0.000 // 67735.617, 0.998 // 67736.813, 0.000
67763.784, 0.000 // 67764.784, 1.004 // 67766.059, 0.000 // 67793.085, 0.000 // 67794.085, 1.005
67795.333, 0.000 // 67822.360, 0.000 // 67823.360, 0.982 // 67824.579, 0.000 // 67851.480, 0.000

67852.480, 1.027 // 67853.706, 0.000 // 67880.645, 0.000 // 67881.645, 1.014 // 67883.358, 0.000
67910.211, 0.000 // 67911.211, 0.991 // 67912.387, 0.000 // 67939.325, 0.000 // 67940.325, 0.994
67941.541, 0.000 // 67968.498, 0.000 // 67969.498, 0.965 // 67970.688, 0.000 // 67997.757, 0.000
67998.757, 0.999 // 67999.970, 0.000 // 68026.840, 0.000 // 68027.840, 1.012 // 68029.056, 0.000
68055.975, 0.000 // 68056.975, 0.995 // 68058.197, 0.000 // 68085.091, 0.000 // 68086.091, 0.987
68087.315, 0.000 // 68114.391, 0.000 // 68115.391, 0.972 // 68116.581, 0.000 // 68143.361, 0.000
68144.361, 1.000 // 68145.550, 0.000 // 68172.506, 0.000 // 68173.506, 0.999 // 68174.724, 0.000
68201.577, 0.000 // 68202.577, 0.996 // 68203.782, 0.000 // 68230.866, 0.000 // 68231.866, 1.010
68233.045, 0.000 // 68259.876, 0.000 // 68260.876, 1.030 // 68262.034, 0.000 // 68289.150, 0.000
68290.150, 1.004 // 68291.327, 0.000 // 68318.306, 0.000 // 68319.306, 1.015 // 68320.485, 0.000
68347.381, 0.000 // 68348.381, 1.019 // 68349.589, 0.000 // 68376.439, 0.000 // 68377.439, 1.033
68378.708, 0.000 // 68405.898, 0.000 // 68406.898, 0.985 // 68408.114, 0.000 // 68435.006, 0.000
68436.006, 0.995 // 68437.199, 0.000 // 68464.188, 0.000 // 68465.188, 0.998 // 68466.436, 0.000
68493.499, 0.000 // 68494.499, 1.014 // 68495.744, 0.000 // 68522.646, 0.000 // 68523.646, 1.034
68524.910, 0.000 // 68551.884, 0.000 // 68552.884, 0.986 // 68554.069, 0.000 // 68580.867, 0.000
68581.867, 1.013 // 68583.028, 0.000 // 68609.859, 0.000 // 68610.859, 1.004 // 68612.006, 0.000
68638.901, 0.000 // 68639.901, 1.000 // 68641.082, 0.000 // 68667.955, 0.000 // 68668.955, 0.988
68670.167, 0.000 // 68697.251, 0.000 // 68698.251, 0.980 // 68699.497, 0.000 // 68726.429, 0.000
68727.429, 1.041 // 68728.618, 0.000 // 68755.666, 0.000 // 68756.666, 0.986 // 68757.873, 0.000
68784.830, 0.000 // 68785.830, 1.009 // 68787.048, 0.000 // 68814.006, 0.000 // 68815.006, 0.979
68816.168, 0.000 // 68843.161, 0.000 // 68844.161, 0.958 // 68845.372, 0.000 // 68872.194, 0.000
68873.194, 0.990 // 68874.436, 0.000 // 68901.402, 0.000 // 68902.402, 0.983 // 68903.576, 0.000
68930.658, 0.000 // 68931.658, 0.986 // 68932.911, 0.000 // 68959.783, 0.000 // 68960.783, 1.011
68961.960, 0.000 // 68988.971, 0.000 // 68989.971, 0.987 // 68991.143, 0.000 // 69017.957, 0.000
69018.957, 0.993 // 69020.133, 0.000 // 69046.991, 0.000 // 69047.991, 1.023 // 69049.170, 0.000
69075.949, 0.000 // 69076.949, 1.001 // 69078.123, 0.000 // 69104.968, 0.000 // 69105.968, 0.989
69107.134, 0.000 // 69134.063, 0.000 // 69135.063, 1.003 // 69136.282, 0.000 // 69163.284, 0.000
69164.284, 0.978 // 69165.616, 0.000 // 69192.561, 0.000 // 69193.561, 0.988 // 69194.790, 0.000
69221.616, 0.000 // 69222.616, 0.980 // 69223.774, 0.000 // 69250.875, 0.000 // 69251.875, 0.993
69253.039, 0.000 // 69280.054, 0.000 // 69281.054, 0.986 // 69282.267, 0.000 // 69309.158, 0.000
69310.158, 0.989 // 69311.422, 0.000 // 69338.195, 0.000 // 69339.195, 1.015 // 69340.372, 0.000
69367.273, 0.000 // 69368.273, 0.972 // 69369.485, 0.000 // 69396.588, 0.000 // 69397.588, 1.010
69398.819, 0.000 // 69425.685, 0.000 // 69426.685, 0.952 // 69427.860, 0.000 // 69454.596, 0.000
69455.596, 0.998 // 69456.777, 0.000 // 69483.620, 0.000 // 69484.620, 0.964 // 69485.823, 0.000
69512.780, 0.000 // 69513.780, 0.959 // 69514.970, 0.000 // 69541.790, 0.000 // 69542.790, 0.979
69544.046, 0.000 // 69570.851, 0.000 // 69571.851, 0.963 // 69573.024, 0.000 // 69599.813, 0.000
69600.813, 0.957 // 69602.017, 0.000 // 69628.980, 0.000 // 69629.980, 0.000 // 69631.033, 0.000
69657.879, 0.000 // 69658.879, 0.962 // 69660.074, 0.000 // 69686.875, 0.000 // 69687.875, 0.983
69689.127, 0.000 // 69715.944, 0.000 // 69716.944, 0.986 // 69718.141, 0.000 // 69745.061, 0.000
69746.061, 0.952 // 69747.262, 0.000 // 69774.031, 0.000 // 69775.031, 0.971 // 69776.220, 0.000
69803.188, 0.000 // 69804.188, 0.961 // 69805.368, 0.000 // 69832.281, 0.000 // 69833.281, 0.974
69834.489, 0.000 // 69861.369, 0.000 // 69862.369, 0.982 // 69863.574, 0.000 // 69890.470, 0.000
69891.470, 0.965 // 69892.645, 0.000 // 69919.565, 0.000 // 69920.565, 0.986 // 69921.855, 0.000
69948.682, 0.000 // 69949.682, 0.978 // 69950.877, 0.000 // 69978.024, 0.000 // 69979.024, 0.987
69980.338, 0.000 // 70007.446, 0.000 // 70008.446, 0.980 // 70009.610, 0.000 // 70036.468, 0.000
70037.468, 0.977 // 70038.650, 0.000 // 70065.512, 0.000 // 70066.512, 0.975 // 70067.707, 0.000
70094.534, 0.000 // 70095.534, 0.971 // 70096.685, 0.000 // 70123.651, 0.000 // 70124.651, 0.970
70125.885, 0.000 // 70152.917, 0.000 // 70153.917, 0.965 // 70155.104, 0.000 // 70182.015, 0.000
70183.015, 0.953 // 70184.236, 0.000 // 70211.342, 0.000 // 70212.342, 0.955 // 70213.750, 0.000
70240.851, 0.000 // 70241.851, 0.940 // 70243.032, 0.000 // 70269.891, 0.000 // 70270.891, 0.982
70272.107, 0.000 // 70299.203, 0.000 // 70300.203, 0.977 // 70301.407, 0.000 // 70328.345, 0.000
70329.345, 0.977 // 70330.540, 0.000 // 70357.783, 0.000 // 70358.783, 1.024 // 70360.031, 0.000
70386.993, 0.000 // 70387.993, 0.979 // 70389.214, 0.000 // 70416.368, 0.000 // 70417.368, 0.968
70418.591, 0.000 // 70445.491, 0.000 // 70446.491, 1.011 // 70447.684, 0.000 // 70474.725, 0.000
70475.725, 0.967 // 70476.935, 0.000 // 70503.776, 0.000 // 70504.776, 0.948 // 70506.065, 0.000
70533.121, 0.000 // 70534.121, 0.954 // 70535.320, 0.000 // 70562.285, 0.000 // 70563.285, 0.958
70564.486, 0.000 // 70591.529, 0.000 // 70592.529, 0.971 // 70593.696, 0.000 // 70620.562, 0.000
70621.562, 1.006 // 70622.838, 0.000 // 70649.793, 0.000 // 70650.793, 0.963 // 70651.982, 0.000
70679.037, 0.000 // 70680.037, 0.982 // 70681.248, 0.000 // 70708.176, 0.000 // 70709.176, 0.978
70710.379, 0.000 // 70737.300, 0.000 // 70738.300, 0.975 // 70739.473, 0.000 // 70766.407, 0.000
70767.407, 0.996 // 70768.631, 0.000 // 70795.634, 0.000 // 70796.634, 0.973 // 70797.805, 0.000
70824.853, 0.000 // 70825.853, 0.986 // 70827.060, 0.000 // 70854.030, 0.000 // 70855.030, 0.998
70856.208, 0.000 // 70883.327, 0.000 // 70884.327, 0.979 // 70885.552, 0.000 // 70912.426, 0.000

70913.426, 0.980 // 70914.625, 0.000 // 70941.703, 0.000 // 70942.703, 0.968 // 70943.977, 0.000
70970.938, 0.000 // 70971.938, 0.972 // 70973.189, 0.000 // 71000.042, 0.000 // 71001.042, 0.975
71002.226, 0.000 // 71029.105, 0.000 // 71030.105, 0.974 // 71031.274, 0.000 // 71058.175, 0.000
71059.175, 0.956 // 71060.396, 0.000 // 71087.376, 0.000 // 71088.376, 0.961 // 71089.584, 0.000
71116.429, 0.000 // 71117.429, 0.974 // 71118.615, 0.000 // 71145.552, 0.000 // 71146.552, 0.970
71147.731, 0.000 // 71174.653, 0.000 // 71175.653, 0.964 // 71176.836, 0.000 // 71203.876, 0.000
71204.876, 0.956 // 71206.145, 0.000 // 71233.100, 0.000 // 71234.100, 0.944 // 71235.338, 0.000
71262.309, 0.000 // 71263.309, 0.963 // 71264.515, 0.000 // 71291.355, 0.000 // 71292.355, 0.955
71293.533, 0.000 // 71320.473, 0.000 // 71321.473, 0.976 // 71322.670, 0.000 // 71349.541, 0.000
71350.541, 0.997 // 71351.729, 0.000 // 71378.659, 0.000 // 71379.659, 0.957 // 71380.847, 0.000
71407.763, 0.000 // 71408.763, 0.960 // 71411.125, 0.000 // 71438.198, 0.000 // 71439.198, 0.921
71440.456, 0.000 // 71467.256, 0.000 // 71468.256, 0.978 // 71469.551, 0.000 // 71496.467, 0.000
71497.467, 0.941 // 71498.671, 0.000 // 71525.621, 0.000 // 71526.621, 0.931 // 71527.834, 0.000
71554.819, 0.000 // 71555.819, 0.937 // 71557.047, 0.000 // 71584.074, 0.000 // 71585.074, 0.916
71586.286, 0.000 // 71613.244, 0.000 // 71614.244, 0.028 // 71615.317, 0.000 // 71642.180, 0.000
71643.180, 0.919 // 71644.382, 0.000 // 71671.264, 0.000 // 71672.264, 0.937 // 71673.434, 0.000
71700.380, 0.000 // 71701.380, 0.980 // 71702.662, 0.000 // 71729.559, 0.000 // 71730.559, 0.964
71731.747, 0.000 // 71758.624, 0.000 // 71759.624, 0.934 // 71760.818, 0.000 // 71787.652, 0.000
71788.652, 0.959 // 71789.876, 0.000 // 71816.836, 0.000 // 71817.836, 0.950 // 71819.024, 0.000
71845.925, 0.000 // 71846.925, 0.961 // 71848.153, 0.000 // 71875.050, 0.000 // 71876.050, 0.947
71877.283, 0.000 // 71904.168, 0.000 // 71905.168, 0.941 // 71906.386, 0.000 // 71933.523, 0.000
71934.523, 0.946 // 71935.715, 0.000 // 71962.573, 0.000 // 71963.573, 0.947 // 71964.756, 0.000
71991.631, 0.000 // 71992.631, 0.971 // 71993.855, 0.000 // 72020.834, 0.000 // 72021.834, 0.957
72022.984, 0.000 // 72049.868, 0.000 // 72050.868, 0.946 // 72052.105, 0.000 // 72079.172, 0.000
72080.172, 0.950 // 72081.369, 0.000 // 72108.160, 0.000 // 72109.160, 0.973 // 72110.356, 0.000
72137.266, 0.000 // 72138.266, 0.930 // 72139.466, 0.000 // 72166.440, 0.000 // 72167.440, 0.943
72168.632, 0.000 // 72195.483, 0.000 // 72196.483, 0.944 // 72197.664, 0.000 // 72224.536, 0.000
72225.536, 0.955 // 72226.690, 0.000 // 72253.619, 0.000 // 72254.619, 1.002 // 72255.793, 0.000
72282.757, 0.000 // 72283.757, 0.955 // 72285.031, 0.000 // 72312.182, 0.000 // 72313.182, 0.937
72314.402, 0.000 // 72341.269, 0.000 // 72342.269, 0.952 // 72343.443, 0.000 // 72370.249, 0.000
72371.249, 0.947 // 72372.621, 0.000 // 72399.389, 0.000 // 72400.389, 0.933 // 72401.590, 0.000
72428.672, 0.000 // 72429.672, 0.953 // 72430.953, 0.000 // 72457.819, 0.000 // 72458.819, 0.949
72460.002, 0.000 // 72486.754, 0.000 // 72487.754, 0.953 // 72488.929, 0.000 // 72516.108, 0.000
72517.108, 0.919 // 72518.315, 0.000 // 72545.156, 0.000 // 72546.156, 0.938 // 72547.337, 0.000
72574.271, 0.000 // 72575.271, 0.945 // 72576.428, 0.000 // 72603.262, 0.000 // 72604.262, 0.973
72605.433, 0.000 // 72632.314, 0.000 // 72633.314, 0.971 // 72634.536, 0.000 // 72661.675, 0.000
72662.675, 0.965 // 72663.877, 0.000 // 72690.854, 0.000 // 72691.854, 0.934 // 72693.142, 0.000
72720.046, 0.000 // 72721.046, 0.935 // 72722.273, 0.000 // 72749.112, 0.000 // 72750.112, 0.940
72751.277, 0.000 // 72778.093, 0.000 // 72779.093, 0.933 // 72780.282, 0.000 // 72807.143, 0.000
72808.143, 0.948 // 72809.299, 0.000 // 72836.231, 0.000 // 72837.231, 0.961 // 72838.460, 0.000
72865.471, 0.000 // 72866.471, 0.976 // 72867.763, 0.000 // 72894.667, 0.000 // 72895.667, 0.954
72896.925, 0.000 // 72923.941, 0.000 // 72924.941, 0.941 // 72926.261, 0.000 // 72953.189, 0.000
72954.189, 0.965 // 72955.355, 0.000 // 72982.258, 0.000 // 72983.258, 0.919 // 72984.470, 0.000
73011.408, 0.000 // 73012.408, 0.972 // 73013.625, 0.000 // 73040.418, 0.000 // 73041.418, 0.941
73042.650, 0.000 // 73069.642, 0.000 // 73070.642, 0.913 // 73071.832, 0.000 // 73098.813, 0.000
73099.813, 0.887 // 73101.013, 0.000 // 73127.962, 0.000 // 73128.962, 0.939 // 73130.160, 0.000
73157.080, 0.000 // 73158.080, 0.993 // 73159.243, 0.000 // 73186.082, 0.000 // 73187.082, 0.923
73188.255, 0.000 // 73215.267, 0.000 // 73216.267, 0.927 // 73217.453, 0.000 // 73244.444, 0.000
73245.444, 0.928 // 73246.649, 0.000 // 73273.458, 0.000 // 73274.458, 0.938 // 73275.660, 0.000
73302.571, 0.000 // 73303.571, 0.907 // 73304.767, 0.000 // 73331.606, 0.000 // 73332.606, 0.913
73333.867, 0.000 // 73360.724, 0.000 // 73361.724, 0.937 // 73362.970, 0.000 // 73389.789, 0.000
73390.789, 0.943 // 73392.000, 0.000 // 73418.949, 0.000 // 73419.949, 0.957 // 73421.187, 0.000
73448.258, 0.000 // 73449.258, 0.943 // 73450.460, 0.000 // 73477.579, 0.000 // 73478.579, 0.907
73479.763, 0.000 // 73506.671, 0.000 // 73507.671, 0.945 // 73508.896, 0.000 // 73536.032, 0.000
73537.032, 0.923 // 73538.227, 0.000 // 73565.182, 0.000 // 73566.182, 0.909 // 73567.378, 0.000
73594.295, 0.000 // 73595.295, 0.987 // 73596.481, 0.000 // 73623.390, 0.000 // 73624.390, 0.911
73625.539, 0.000 // 73652.362, 0.000 // 73653.362, 0.892 // 73654.552, 0.000 // 73681.366, 0.000
73682.366, 0.881 // 73683.546, 0.000 // 73710.499, 0.000 // 73711.499, 0.000 // 73712.597, 0.000
73739.353, 0.000 // 73740.353, 0.884 // 73741.542, 0.000 // 73768.280, 0.000 // 73769.280, 0.899
73770.475, 0.000 // 73797.332, 0.000 // 73798.332, 0.870 // 73799.527, 0.000 // 73826.381, 0.000
73827.381, 0.902 // 73828.542, 0.000 // 73855.391, 0.000 // 73856.391, 0.867 // 73857.590, 0.000
73884.636, 0.000 // 73885.636, 0.873 // 73886.824, 0.000 // 73913.779, 0.000 // 73914.779, 0.881
73916.026, 0.000 // 73942.896, 0.000 // 73943.896, 0.854 // 73945.084, 0.000 // 73971.994, 0.000

73972.994, 0.899 // 73974.195, 0.000 // 74001.073, 0.000 // 74002.073, 0.879 // 74003.271, 0.000
74030.179, 0.000 // 74031.179, 0.869 // 74032.344, 0.000 // 74059.340, 0.000 // 74060.340, 0.877
74061.572, 0.000 // 74088.453, 0.000 // 74089.453, 0.873 // 74090.650, 0.000 // 74117.513, 0.000
74118.513, 0.949 // 74119.668, 0.000 // 74146.562, 0.000 // 74147.562, 0.903 // 74148.780, 0.000
74175.626, 0.000 // 74176.626, 0.882 // 74177.922, 0.000 // 74204.758, 0.000 // 74205.758, 0.903
74206.955, 0.000 // 74234.053, 0.000 // 74235.053, 0.888 // 74236.266, 0.000 // 74263.216, 0.000
74264.216, 0.887 // 74265.388, 0.000 // 74292.216, 0.000 // 74293.216, 0.872 // 74294.419, 0.000
74321.469, 0.000 // 74322.469, 0.882 // 74323.683, 0.000 // 74350.590, 0.000 // 74351.590, 0.876
74352.795, 0.000 // 74379.650, 0.000 // 74380.650, 0.854 // 74381.810, 0.000 // 74408.762, 0.000
74409.762, 0.881 // 74410.951, 0.000 // 74437.850, 0.000 // 74438.850, 0.846 // 74440.064, 0.000
74466.968, 0.000 // 74467.968, 0.943 // 74469.155, 0.000 // 74496.002, 0.000 // 74497.002, 0.844
74498.171, 0.000 // 74525.034, 0.000 // 74526.034, 0.878 // 74527.219, 0.000 // 74554.274, 0.000
74555.274, 0.856 // 74556.520, 0.000 // 74583.597, 0.000 // 74584.597, 0.904 // 74585.785, 0.000
74612.606, 0.000 // 74613.606, 0.905 // 74614.781, 0.000 // 74641.702, 0.000 // 74642.702, 0.860
74643.920, 0.000 // 74670.825, 0.000 // 74671.825, 0.874 // 74672.996, 0.000 // 74699.864, 0.000
74700.864, 0.872 // 74702.072, 0.000 // 74729.155, 0.000 // 74730.155, 0.889 // 74731.384, 0.000
74758.198, 0.000 // 74759.198, 0.859 // 74760.437, 0.000 // 74787.564, 0.000 // 74788.564, 0.929
74789.777, 0.000 // 74816.756, 0.000 // 74817.756, 0.907 // 74819.146, 0.000 // 74845.974, 0.000
74846.974, 0.837 // 74848.162, 0.000 // 74875.016, 0.000 // 74876.016, 0.869 // 74877.288, 0.000
74904.210, 0.000 // 74905.210, 0.892 // 74906.462, 0.000 // 74933.552, 0.000 // 74934.552, 0.850
74935.744, 0.000 // 74962.541, 0.000 // 74963.541, 0.777 // 74965.439, 0.000 // 74992.388, 0.000
74993.388, 0.854 // 74994.614, 0.000 // 75021.620, 0.000 // 75022.620, 0.861 // 75023.789, 0.000
75050.616, 0.000 // 75051.616, 0.879 // 75052.811, 0.000 // 75079.756, 0.000 // 75080.756, 0.858
75081.931, 0.000 // 75108.804, 0.000 // 75109.804, 0.857 // 75111.027, 0.000 // 75137.877, 0.000
75138.877, 0.890 // 75140.103, 0.000 // 75166.944, 0.000 // 75167.944, 0.837 // 75169.117, 0.000
75195.934, 0.000 // 75196.934, 0.847 // 75198.135, 0.000 // 75225.069, 0.000 // 75226.069, 0.830
75227.244, 0.000 // 75254.037, 0.000 // 75255.037, 0.864 // 75256.258, 0.000 // 75283.069, 0.000
75284.069, 0.834 // 75285.230, 0.000 // 75312.226, 0.000 // 75313.226, 0.883 // 75314.431, 0.000
75341.467, 0.000 // 75342.467, 0.826 // 75343.721, 0.000 // 75370.598, 0.000 // 75371.598, 0.837
75372.809, 0.000 // 75399.715, 0.000 // 75400.715, 0.842 // 75401.912, 0.000 // 75428.854, 0.000
75429.854, 0.034 // 75430.926, 0.000 // 75457.978, 0.000 // 75458.978, 0.898 // 75460.226, 0.000
75487.058, 0.000 // 75488.058, 0.887 // 75489.445, 0.000 // 75516.343, 0.000 // 75517.343, 0.884
75518.531, 0.000 // 75545.501, 0.000 // 75546.501, 0.914 // 75547.714, 0.000 // 75574.703, 0.000
75575.703, 0.934 // 75576.936, 0.000 // 75604.072, 0.000 // 75605.072, 0.902 // 75606.327, 0.000
75633.165, 0.000 // 75634.165, 0.302 // 75635.386, 0.000 // 75662.350, 0.000 // 75663.350, 0.899
75664.560, 0.000 // 75691.457, 0.000 // 75692.457, 0.890 // 75693.625, 0.000 // 75720.584, 0.000
75721.584, 0.895 // 75722.782, 0.000 // 75749.664, 0.000 // 75750.664, 0.717 // 75752.171, 0.000
75779.068, 0.000 // 75780.068, 0.940 // 75781.247, 0.000 // 75808.147, 0.000 // 75809.147, 0.897
75810.341, 0.000 // 75837.303, 0.000 // 75838.303, 0.882 // 75839.471, 0.000 // 75866.325, 0.000
75867.325, 0.902 // 75868.595, 0.000 // 75895.593, 0.000 // 75896.593, 0.916 // 75897.779, 0.000
75924.648, 0.000 // 75925.648, 0.924 // 75926.819, 0.000 // 75953.779, 0.000 // 75954.779, 0.925
75955.959, 0.000 // 75982.866, 0.000 // 75983.866, 0.898 // 75985.089, 0.000 // 76012.038, 0.000
76013.038, 0.916 // 76014.219, 0.000 // 76041.403, 0.000 // 76042.403, 0.915 // 76043.639, 0.000
76070.514, 0.000 // 76071.514, 0.899 // 76072.692, 0.000 // 76099.692, 0.000 // 76100.692, 0.878
76101.884, 0.000 // 76128.704, 0.000 // 76129.704, 0.937 // 76130.934, 0.000 // 76157.965, 0.000
76158.965, 0.915 // 76160.173, 0.000 // 76187.192, 0.000 // 76188.192, 0.912 // 76189.443, 0.000
76216.512, 0.000 // 76217.512, 0.909 // 76218.714, 0.000 // 76245.688, 0.000 // 76246.688, 0.907
76247.879, 0.000 // 76274.824, 0.000 // 76275.824, 0.934 // 76277.104, 0.000 // 76304.084, 0.000
76305.084, 0.922 // 76306.270, 0.000 // 76333.213, 0.000 // 76334.213, 0.918 // 76335.426, 0.000
76362.640, 0.000 // 76363.640, 0.959 // 76364.878, 0.000 // 76391.843, 0.000 // 76392.843, 0.909
76394.008, 0.000 // 76420.881, 0.000 // 76421.881, 0.901 // 76423.084, 0.000 // 76450.044, 0.000
76451.044, 0.913 // 76452.285, 0.000 // 76479.145, 0.000 // 76480.145, 0.903 // 76481.344, 0.000
76508.208, 0.000 // 76509.208, 0.929 // 76510.384, 0.000 // 76537.134, 0.000 // 76538.134, 0.915
76539.481, 0.000 // 76566.347, 0.000 // 76567.347, 0.928 // 76568.512, 0.000 // 76595.543, 0.000
76596.543, 0.909 // 76597.790, 0.000 // 76624.809, 0.000 // 76625.809, 0.879 // 76627.045, 0.000
76654.174, 0.000 // 76655.174, 0.889 // 76656.354, 0.000 // 76683.488, 0.000 // 76684.488, 0.879
76685.680, 0.000 // 76712.585, 0.000 // 76713.585, 0.953 // 76714.783, 0.000 // 76741.842, 0.000
76742.842, 0.920 // 76744.189, 0.000 // 76771.030, 0.000 // 76772.030, 0.909 // 76773.203, 0.000
76800.179, 0.000 // 76801.179, 0.889 // 76802.368, 0.000 // 76829.275, 0.000 // 76830.275, 0.970
76831.466, 0.000 // 76858.474, 0.000 // 76859.474, 0.898 // 76860.650, 0.000 // 76887.533, 0.000
76888.533, 0.892 // 76889.708, 0.000 // 76916.635, 0.000 // 76917.635, 0.935 // 76918.802, 0.000
76945.707, 0.000 // 76946.707, 0.935 // 76947.905, 0.000 // 76974.958, 0.000 // 76975.958, 0.900
76977.200, 0.000 // 77004.205, 0.000 // 77005.205, 0.936 // 77006.428, 0.000 // 77033.613, 0.000

77034.613, 0.883 // 77035.808, 0.000 // 77062.932, 0.000 // 77063.932, 0.870 // 77065.121, 0.000
77091.979, 0.000 // 77092.979, 0.861 // 77094.162, 0.000 // 77121.175, 0.000 // 77122.175, 0.883
77123.342, 0.000 // 77150.420, 0.000 // 77151.420, 0.910 // 77152.559, 0.000 // 77179.665, 0.000
77180.665, 0.913 // 77181.926, 0.000 // 77208.947, 0.000 // 77209.947, 0.902 // 77211.154, 0.000
77238.308, 0.000 // 77239.308, 0.027 // 77240.463, 0.000 // 77267.411, 0.000 // 77268.411, 0.897
77269.633, 0.000 // 77296.540, 0.000 // 77297.540, 0.873 // 77298.718, 0.000 // 77325.663, 0.000
77326.663, 0.899 // 77327.901, 0.000 // 77354.763, 0.000 // 77355.763, 0.938 // 77356.999, 0.000
77383.915, 0.000 // 77384.915, 0.911 // 77386.076, 0.000 // 77412.950, 0.000 // 77413.950, 0.931
77415.180, 0.000 // 77442.085, 0.000 // 77443.085, 0.877 // 77444.252, 0.000 // 77471.088, 0.000
77472.088, 0.904 // 77473.257, 0.000 // 77500.354, 0.000 // 77501.354, 0.868 // 77502.543, 0.000
77529.427, 0.000 // 77530.427, 0.913 // 77531.629, 0.000 // 77558.487, 0.000 // 77559.487, 0.878
77560.700, 0.000 // 77587.784, 0.000 // 77588.784, 0.896 // 77589.973, 0.000 // 77616.885, 0.000
77617.885, 0.885 // 77619.084, 0.000 // 77646.061, 0.000 // 77647.061, 0.892 // 77648.250, 0.000
77675.257, 0.000 // 77676.257, 0.894 // 77677.544, 0.000 // 77704.547, 0.000 // 77705.547, 0.886
77706.842, 0.000 // 77733.885, 0.000 // 77734.885, 0.913 // 77736.104, 0.000 // 77763.077, 0.000
77764.077, 0.887 // 77765.346, 0.000 // 77792.388, 0.000 // 77793.388, 0.920 // 77794.701, 0.000
77821.607, 0.000 // 77822.607, 0.877 // 77823.812, 0.000 // 77850.833, 0.000 // 77851.833, 0.928
77853.023, 0.000 // 77879.959, 0.000 // 77880.959, 0.943 // 77882.149, 0.000 // 77909.119, 0.000
77910.119, 0.901 // 77911.288, 0.000 // 77938.191, 0.000 // 77939.191, 0.889 // 77940.387, 0.000
77967.274, 0.000 // 77968.274, 0.914 // 77969.446, 0.000 // 77996.551, 0.000 // 77997.551, 0.902
77998.728, 0.000 // 78025.630, 0.000 // 78026.630, 0.911 // 78027.813, 0.000 // 78054.704, 0.000
78055.704, 0.891 // 78056.961, 0.000 // 78083.873, 0.000 // 78084.873, 0.918 // 78086.028, 0.000
78113.132, 0.000 // 78114.132, 0.911 // 78115.362, 0.000 // 78142.512, 0.000 // 78143.512, 0.937
78144.738, 0.000 // 78171.720, 0.000 // 78172.720, 0.878 // 78174.011, 0.000 // 78201.046, 0.000
78202.046, 0.885 // 78203.204, 0.000 // 78230.438, 0.000 // 78231.438, 0.923 // 78232.653, 0.000
78259.608, 0.000 // 78260.608, 0.880 // 78261.861, 0.000 // 78288.976, 0.000 // 78289.976, 0.890
78291.163, 0.000 // 78318.048, 0.000 // 78319.048, 0.903 // 78320.300, 0.000 // 78347.396, 0.000
78348.396, 0.923 // 78349.627, 0.000 // 78376.549, 0.000 // 78377.549, 0.956 // 78378.918, 0.000
78406.129, 0.000 // 78407.129, 0.849 // 78408.356, 0.000 // 78435.256, 0.000 // 78436.256, 0.892
78437.414, 0.000 // 78464.433, 0.000 // 78465.433, 0.882 // 78466.661, 0.000 // 78493.708, 0.000
78494.708, 0.685 // 78496.417, 0.000 // 78523.310, 0.000 // 78524.310, 0.943 // 78525.565, 0.000
78552.603, 0.000 // 78553.603, 0.897 // 78554.868, 0.000 // 78581.743, 0.000 // 78582.743, 0.866
78583.926, 0.000 // 78610.850, 0.000 // 78611.850, 0.885 // 78613.074, 0.000 // 78640.010, 0.000
78641.010, 0.893 // 78642.302, 0.000 // 78669.460, 0.000 // 78670.460, 0.902 // 78671.665, 0.000
78698.626, 0.000 // 78699.626, 0.891 // 78700.826, 0.000 // 78727.670, 0.000 // 78728.670, 0.916
78729.858, 0.000 // 78756.722, 0.000 // 78757.722, 0.914 // 78758.966, 0.000 // 78786.010, 0.000
78787.010, 0.949 // 78788.199, 0.000 // 78815.073, 0.000 // 78816.073, 0.932 // 78817.247, 0.000
78844.097, 0.000 // 78845.097, 0.944 // 78846.288, 0.000 // 78873.161, 0.000 // 78874.161, 0.908
78875.408, 0.000 // 78902.451, 0.000 // 78903.451, 0.948 // 78904.636, 0.000 // 78931.671, 0.000
78932.671, 0.933 // 78933.865, 0.000 // 78960.757, 0.000 // 78961.757, 0.985 // 78962.924, 0.000
78989.706, 0.000 // 78990.706, 0.000 // 78991.984, 0.000 // 79019.047, 0.000 // 79020.047, 0.913
79021.249, 0.000 // 79048.123, 0.000 // 79049.123, 0.923 // 79050.290, 0.000 // 79077.326, 0.000
79078.326, 0.869 // 79079.525, 0.000 // 79106.735, 0.000 // 79107.735, 0.896 // 79109.030, 0.000
79135.994, 0.000 // 79136.994, 0.900 // 79138.232, 0.000 // 79165.309, 0.000 // 79166.309, 0.892
79167.633, 0.000 // 79194.669, 0.000 // 79195.669, 0.899 // 79196.861, 0.000 // 79223.729, 0.000
79224.729, 0.870 // 79225.892, 0.000 // 79252.803, 0.000 // 79253.803, 0.849 // 79255.003, 0.000
79281.980, 0.000 // 79282.980, 0.878 // 79284.126, 0.000 // 79310.933, 0.000 // 79311.933, 0.852
79313.102, 0.000 // 79340.033, 0.000 // 79341.033, 0.961 // 79342.303, 0.000 // 79369.404, 0.000
79370.404, 1.034 // 79371.606, 0.000 // 79398.661, 0.000 // 79399.661, 0.883 // 79400.857, 0.000
79427.706, 0.000 // 79428.706, 0.897 // 79429.916, 0.000 // 79456.871, 0.000 // 79457.871, 0.890
79459.088, 0.000 // 79486.153, 0.000 // 79487.153, 0.878 // 79488.375, 0.000 // 79515.348, 0.000
79516.348, 0.899 // 79517.505, 0.000 // 79544.318, 0.000 // 79545.318, 0.916 // 79546.528, 0.000
79573.487, 0.000 // 79574.487, 0.900 // 79575.693, 0.000 // 79602.662, 0.000 // 79603.662, 0.913
79604.849, 0.000 // 79631.823, 0.000 // 79632.823, 0.893 // 79634.067, 0.000 // 79660.943, 0.000
79661.943, 0.906 // 79663.135, 0.000 // 79690.066, 0.000 // 79691.066, 0.922 // 79692.258, 0.000
79719.197, 0.000 // 79720.197, 0.899 // 79721.424, 0.000 // 79748.502, 0.000 // 79749.502, 0.958
79750.679, 0.000 // 79777.731, 0.000 // 79778.731, 0.880 // 79779.943, 0.000 // 79806.777, 0.000
79807.777, 0.887 // 79809.091, 0.000 // 79836.077, 0.000 // 79837.077, 0.960 // 79838.328, 0.000
79865.339, 0.000 // 79866.339, 0.930 // 79867.590, 0.000 // 79894.350, 0.000 // 79895.350, 0.936
79896.595, 0.000 // 79923.556, 0.000 // 79924.556, 0.944 // 79925.742, 0.000 // 79952.719, 0.000
79953.719, 0.911 // 79954.980, 0.000 // 79981.823, 0.000 // 79982.823, 0.926 // 79984.032, 0.000
80010.990, 0.000 // 80011.990, 0.893 // 80013.144, 0.000 // 80040.091, 0.000 // 80041.091, 0.953
80042.300, 0.000 // 80069.326, 0.000 // 80070.326, 0.925 // 80071.555, 0.000 // 80098.506, 0.000

80099.506, 0.901 // 80100.692, 0.000 // 80127.550, 0.000 // 80128.550, 0.905 // 80129.874, 0.000
80156.906, 0.000 // 80157.906, 0.935 // 80159.138, 0.000 // 80186.187, 0.000 // 80187.187, 0.912
80188.563, 0.000 // 80215.466, 0.000 // 80216.466, 0.919 // 80217.719, 0.000 // 80244.821, 0.000
80245.821, 0.913 // 80247.226, 0.000 // 80274.129, 0.000 // 80275.129, 0.910 // 80276.339, 0.000
80303.254, 0.000 // 80304.254, 0.918 // 80305.401, 0.000 // 80332.405, 0.000 // 80333.405, 0.911
80334.625, 0.000 // 80361.872, 0.000 // 80362.872, 0.910 // 80364.131, 0.000 // 80391.114, 0.000
80392.114, 0.906 // 80393.303, 0.000 // 80420.194, 0.000 // 80421.194, 0.922 // 80422.389, 0.000
80449.460, 0.000 // 80450.460, 0.945 // 80451.691, 0.000 // 80478.594, 0.000 // 80479.594, 0.922
80480.848, 0.000 // 80507.664, 0.000 // 80508.664, 0.901 // 80509.852, 0.000 // 80536.723, 0.000
80537.723, 0.907 // 80538.984, 0.000 // 80566.204, 0.000 // 80567.204, 0.931 // 80568.425, 0.000
80595.397, 0.000 // 80596.397, 0.903 // 80597.609, 0.000 // 80624.638, 0.000 // 80625.638, 0.913
80626.844, 0.000 // 80653.714, 0.000 // 80654.714, 0.973 // 80655.848, 0.000 // 80682.842, 0.000
80683.842, 0.896 // 80685.070, 0.000 // 80712.010, 0.000 // 80713.010, 0.920 // 80714.331, 0.000
80741.290, 0.000 // 80742.290, 0.924 // 80743.488, 0.000 // 80770.332, 0.000 // 80771.332, 0.916
80772.547, 0.000 // 80799.540, 0.000 // 80800.540, 0.886 // 80801.766, 0.000 // 80828.749, 0.000
80829.749, 0.896 // 80830.924, 0.000 // 80857.708, 0.000 // 80858.708, 0.906 // 80859.866, 0.000
80886.910, 0.000 // 80887.910, 0.000 // 80888.977, 0.000 // 80915.990, 0.000 // 80916.990, 0.891
80918.196, 0.000 // 80945.046, 0.000 // 80946.046, 0.872 // 80947.239, 0.000 // 80974.191, 0.000
80975.191, 0.897 // 80976.360, 0.000 // 81003.332, 0.000 // 81004.332, 0.929 // 81005.534, 0.000
81032.452, 0.000 // 81033.452, 0.894 // 81034.649, 0.000 // 81061.668, 0.000 // 81062.668, 0.916
81063.856, 0.000 // 81090.776, 0.000 // 81091.776, 0.937 // 81092.965, 0.000 // 81119.860, 0.000
81120.860, 0.965 // 81122.050, 0.000 // 81148.924, 0.000 // 81149.924, 0.902 // 81151.090, 0.000
81178.060, 0.000 // 81179.060, 0.893 // 81180.247, 0.000 // 81207.046, 0.000 // 81208.046, 0.883
81209.254, 0.000 // 81236.224, 0.000 // 81237.224, 0.904 // 81238.420, 0.000 // 81265.350, 0.000
81266.350, 0.913 // 81267.563, 0.000 // 81294.497, 0.000 // 81295.497, 0.868 // 81296.657, 0.000
81323.778, 0.000 // 81324.778, 0.915 // 81325.964, 0.000 // 81352.752, 0.000 // 81353.752, 0.929
81354.886, 0.000 // 81381.782, 0.000 // 81382.782, 0.898 // 81384.014, 0.000 // 81410.844, 0.000
81411.844, 0.926 // 81413.054, 0.000 // 81439.995, 0.000 // 81440.995, 0.925 // 81442.229, 0.000
81469.247, 0.000 // 81470.247, 0.904 // 81471.440, 0.000 // 81498.386, 0.000 // 81499.386, 0.875
81500.584, 0.000 // 81527.711, 0.000 // 81528.711, 0.909 // 81529.902, 0.000 // 81556.904, 0.000
81557.904, 0.893 // 81559.133, 0.000 // 81586.197, 0.000 // 81587.197, 0.917 // 81588.380, 0.000
81615.317, 0.000 // 81616.317, 0.904 // 81617.505, 0.000 // 81644.644, 0.000 // 81645.644, 0.905
81646.841, 0.000 // 81673.655, 0.000 // 81674.655, 0.888 // 81675.837, 0.000 // 81702.751, 0.000
81703.751, 0.918 // 81704.958, 0.000 // 81731.772, 0.000 // 81732.772, 0.916 // 81734.043, 0.000
81761.034, 0.000 // 81762.034, 0.880 // 81763.227, 0.000 // 81790.122, 0.000 // 81791.122, 0.881
81792.474, 0.000 // 81819.456, 0.000 // 81820.456, 0.953 // 81821.711, 0.000 // 81848.587, 0.000
81849.587, 0.918 // 81850.754, 0.000 // 81877.735, 0.000 // 81878.735, 0.894 // 81880.024, 0.000
81907.090, 0.000 // 81908.090, 0.914 // 81909.284, 0.000 // 81936.107, 0.000 // 81937.107, 0.909
81938.292, 0.000 // 81965.212, 0.000 // 81966.212, 0.937 // 81967.418, 0.000 // 81994.496, 0.000
81995.496, 0.924 // 81996.691, 0.000 // 82023.493, 0.000 // 82024.493, 0.903 // 82025.729, 0.000
82052.631, 0.000 // 82053.631, 0.917 // 82054.814, 0.000 // 82081.661, 0.000 // 82082.661, 0.907
82083.892, 0.000 // 82110.953, 0.000 // 82111.953, 0.885 // 82113.135, 0.000 // 82140.130, 0.000
82141.130, 0.923 // 82142.315, 0.000 // 82169.254, 0.000 // 82170.254, 0.924 // 82171.497, 0.000
82198.501, 0.000 // 82199.501, 0.904 // 82200.760, 0.000 // 82227.876, 0.000 // 82228.876, 0.911
82230.090, 0.000 // 82257.091, 0.000 // 82258.091, 0.872 // 82259.244, 0.000 // 82286.041, 0.000
82287.041, 0.859 // 82288.244, 0.000 // 82315.066, 0.000 // 82316.066, 0.886 // 82317.277, 0.000
82344.077, 0.000 // 82345.077, 0.887 // 82346.298, 0.000 // 82373.274, 0.000 // 82374.274, 0.916
82375.482, 0.000 // 82402.397, 0.000 // 82403.397, 0.918 // 82404.628, 0.000 // 82431.586, 0.000
82432.586, 0.939 // 82433.776, 0.000 // 82460.790, 0.000 // 82461.790, 0.879 // 82463.004, 0.000
82490.018, 0.000 // 82491.018, 0.922 // 82492.221, 0.000 // 82519.229, 0.000 // 82520.229, 0.920
82521.405, 0.000 // 82548.320, 0.000 // 82549.320, 0.939 // 82550.500, 0.000 // 82577.479, 0.000
82578.479, 0.924 // 82579.665, 0.000 // 82606.656, 0.000 // 82607.656, 0.925 // 82608.867, 0.000
82635.702, 0.000 // 82636.702, 0.897 // 82638.031, 0.000 // 82665.027, 0.000 // 82666.027, 0.901
82667.238, 0.000 // 82694.204, 0.000 // 82695.204, 0.892 // 82696.371, 0.000 // 82723.368, 0.000
82724.368, 0.900 // 82725.555, 0.000 // 82752.516, 0.000 // 82753.516, 0.919 // 82754.774, 0.000
82781.601, 0.000 // 82782.601, 0.870 // 82783.787, 0.000 // 82810.921, 0.000 // 82811.921, 0.967
82813.102, 0.000 // 82839.975, 0.000 // 82840.975, 0.850 // 82842.169, 0.000 // 82869.105, 0.000
82870.105, 0.902 // 82871.362, 0.000 // 82898.280, 0.000 // 82899.280, 0.855 // 82900.617, 0.000
82927.554, 0.000 // 82928.554, 0.872 // 82929.756, 0.000 // 82956.706, 0.000 // 82957.706, 0.899
82958.922, 0.000 // 82986.041, 0.000 // 82987.041, 0.856 // 82988.284, 0.000 // 83015.495, 0.000
83016.495, 0.000 // 83017.515, 0.000 // 83044.454, 0.000 // 83045.454, 0.867 // 83046.677, 0.000
83073.594, 0.000 // 83074.594, 0.884 // 83075.786, 0.000 // 83102.689, 0.000 // 83103.689, 0.887
83104.872, 0.000 // 83131.819, 0.000 // 83132.819, 0.905 // 83134.093, 0.000 // 83161.171, 0.000

```
83162.171, 0.930 // 83163.375, 0.000 // 83190.323, 0.000 // 83191.323, 0.921 // 83192.530, 0.000
83219.557, 0.000 // 83220.557, 0.947 // 83221.773, 0.000 // 83248.740, 0.000 // 83249.740, 0.918
83251.002, 0.000 // 83278.171, 0.000 // 83279.171, 0.869 // 83280.571, 0.000 // 83307.615, 0.000
83308.615, 0.000 // 83309.752, 0.000 // 83336.798, 0.000 // 83337.798, 0.000 // 83339.069, 0.000
83366.124, 0.000 // 83367.124, 0.026 // 83368.200, 0.000 // 83395.286, 0.000 // 83396.286, 0.000
83397.362, 0.000 // 83424.505, 0.000 // 83425.505, 0.000 // 83426.580, 0.000 // 83453.608, 0.000
83454.608, 0.000 // 83455.742, 0.000 // 83482.675, 0.000 // 83483.675, 0.034 // 83484.762, 0.000
83511.949, 0.000 // 83512.949, 0.000 // 83514.061, 0.000 // 83541.063, 0.000 // 83542.063, 0.000
83543.111, 0.000 // 83570.156, 0.000 // 83571.156, 0.872 // 83572.383, 0.000 // 83599.257, 0.000
83600.257, 0.881 // 83601.585, 0.000 // 83628.530, 0.000 // 83629.530, 0.891 // 83630.716, 0.000
83657.744, 0.000 // 83658.744, 0.867 // 83659.933, 0.000 // 83686.829, 0.000 // 83687.829, 0.874
83689.053, 0.000 // 83716.204, 0.000 // 83717.204, 0.864 // 83718.411, 0.000 // 83745.230, 0.000
83746.230, 0.877 // 83747.427, 0.000 // 83774.336, 0.000 // 83775.336, 0.885 // 83776.556, 0.000
83803.548, 0.000 // 83804.548, 0.875 // 83805.811, 0.000 // 83832.903, 0.000 // 83833.903, 0.863
83835.143, 0.000 // 83862.074, 0.000 // 83863.074, 0.874 // 83864.299, 0.000 // 83891.148, 0.000
83892.148, 0.904 // 83893.335, 0.000 // 83920.251, 0.000 // 83921.251, 0.844 // 83922.472, 0.000
83949.328, 0.000 // 83950.328, 0.878 // 83951.532, 0.000 // 83978.479, 0.000 // 83979.479, 0.878
83980.715, 0.000 // 84007.704, 0.000 // 84008.704, 0.927 // 84009.909, 0.000 // 84037.064, 0.000
84038.064, 0.850 // 84039.372, 0.000 // 84066.334, 0.000 // 84067.334, 0.892 // 84068.555, 0.000
84095.649, 0.000 // 84096.649, 0.863 // 84097.852, 0.000 // 84124.795, 0.000 // 84125.795, 0.896
84126.987, 0.000 // 84154.004, 0.000 // 84155.004, 0.898 // 84156.227, 0.000 // 84183.322, 0.000
84184.322, 0.879 // 84185.509, 0.000 // 84212.581, 0.000 // 84213.581, 0.873 // 84214.792, 0.000
84241.737, 0.000 // 84242.737, 0.848 // 84243.985, 0.000 // 84271.062, 0.000 // 84272.062, 0.859
84273.302, 0.000 // 84300.396, 0.000 // 84301.396, 0.900 // 84302.584, 0.000 // 84329.665, 0.000
84330.665, 0.873 // 84331.881, 0.000 // 84358.982, 0.000 // 84359.982, 0.850 // 84361.200, 0.000
84388.097, 0.000 // 84389.097, 0.878 // 84390.393, 0.000 // 84417.283, 0.000 // 84418.283, 0.855
84419.505, 0.000 // 84446.666, 0.000 // 84447.666, 0.898 // 84448.856, 0.000 // 84475.801, 0.000
84476.801, 0.831 // 84478.046, 0.000 // 84505.015, 0.000 // 84506.015, 0.845 // 84507.223, 0.000
84534.160, 0.000 // 84535.160, 0.881 // 84536.347, 0.000 // 84563.324, 0.000 // 84564.324, 0.832
84565.512, 0.000 // 84592.670, 0.000 // 84593.670, 0.849 // 84594.908, 0.000 // 84621.955, 0.000
84622.955, 0.864 // 84624.180, 0.000 // 84651.179, 0.000 // 84652.179, 0.854 // 84653.373, 0.000
84680.558, 0.000 // 84681.558, 0.866 // 84682.791, 0.000 // 84709.820, 0.000 // 84710.820, 0.854
84712.048, 0.000 // 84739.129, 0.000 // 84740.129, 0.836 // 84741.429, 0.000 // 84768.409, 0.000
84769.409, 0.834 // 84770.666, 0.000 // 84797.651, 0.000 // 84798.651, 0.838 // 84799.814, 0.000
84826.855, 0.000 // 84827.855, 0.849 // 84829.051, 0.000 // 84855.935, 0.000 // 84856.935, 0.853
84858.164, 0.000 // 84885.375, 0.000 // 84886.375, 0.836 // 84887.591, 0.000 // 84914.603, 0.000
84915.603, 0.837 // 84916.812, 0.000 // 84943.713, 0.000 // 84944.713, 0.838 // 84945.924, 0.000
84972.691, 0.000 // 84973.691, 0.825 // 84974.912, 0.000 // 85001.839, 0.000 // 85002.839, 0.840
85004.042, 0.000 // 85031.035, 0.000 // 85032.035, 0.828 // 85033.271, 0.000 // 85060.247, 0.000
85061.247, 0.807 // 85062.534, 0.000 // 85089.592, 0.000 // 85090.592, 0.821 // 85091.796, 0.000
85118.639, 0.000 // 85119.639, 0.895 // 85120.824, 0.000 // 85147.831, 0.000 // 85148.831, 0.844
85150.044, 0.000 // 85176.980, 0.000 // 85177.980, 0.841 // 85179.165, 0.000 // 85206.195, 0.000
85207.195, 0.831 // 85208.385, 0.000 // 85235.345, 0.000 // 85236.345, 0.000 // 85237.484, 0.000
85264.532, 0.000 // 85265.532, 0.840 // 85266.734, 0.000 // 85293.607, 0.000 // 85294.607, 0.863
85295.778, 0.000 // 85322.664, 0.000 // 85323.664, 0.872 // 85324.855, 0.000 // 85351.722, 0.000
85352.722, 0.883 // 85354.002, 0.000 // 85380.980, 0.000 // 85381.980, 0.853 // 85383.173, 0.000
85410.057, 0.000 // 85411.057, 0.840 // 85412.285, 0.000 // 85439.139, 0.000 // 85440.139, 0.889
85441.745, 0.000 // 85468.668, 0.000 // 85469.668, 0.777 // 85471.001, 0.000 // 85497.942, 0.000
85498.942, 0.872 // 85500.132, 0.000 // 85527.233, 0.000 // 85528.233, 0.827 // 85529.458, 0.000
85556.602, 0.000 // 85557.602, 0.855 // 85558.811, 0.000 // 85585.865, 0.000 // 85586.865, 0.866
85588.111, 0.000 // 85615.251, 0.000 // 85616.251, 0.845 // 85617.411, 0.000 // 85644.317, 0.000
85645.317, 0.839 // 85646.524, 0.000 // 85673.517, 0.000 // 85674.517, 0.849 // 85675.743, 0.000
85702.675, 0.000 // 85703.675, 0.872 // 85704.909, 0.000 // 85731.765, 0.000 // 85732.765, 0.881
85734.052, 0.000 // 85761.110, 0.000 // 85762.110, 0.863 // 85763.325, 0.000 // 85790.299, 0.000
85791.299, 0.882 // 85792.496, 0.000 // 85819.558, 0.000 // 85820.558, 0.897 // 85821.769, 0.000
85848.656, 0.000 // 85849.656, 0.847 // 85850.867, 0.000 // 85877.929, 0.000 // 85878.929, 0.873
85880.090, 0.000 // 85907.020, 0.000 // 85908.020, 0.846 // 85909.207, 0.000 // 85936.207, 0.000
85937.207, 0.857 // 85938.462, 0.000 // 92909.000, 0.000 // 92914.000, 1.240 // 92915.236, 0.000
93042.213, 0.000 // 93047.213, 1.270 // 93048.424, 0.000 // 93175.360, 0.000 // 93180.360, 1.265
93181.541, 0.000 // 93308.498, 0.000 // 93313.498, 1.269 // 93314.677, 0.000 // 93441.548, 0.000
93446.548, 1.270 // 93447.745, 0.000 // 93574.585, 0.000 // 93579.585, 1.274 // 93580.784, 0.000
93707.725, 0.000 // 93712.725, 1.271 // 93713.988, 0.000 // 93841.086, 0.000 // 93846.086, 1.271
93847.335, 0.000 // 93974.316, 0.000 // 93979.316, 1.275 // 93980.516, 0.000 // 94107.529, 0.000
```

94112.529, 1.288 // 94113.769, 0.000 // 94240.796, 0.000 // 94245.796, 1.140 // 94246.988, 0.000
94373.883, 0.000 // 94378.883, 1.132 // 94380.100, 0.000 // 94507.286, 0.000 // 94512.286, 1.234
94513.483, 0.000 // 94640.556, 0.000 // 94645.556, 1.238 // 94646.756, 0.000 // 94773.717, 0.000
94778.717, 1.286 // 94779.954, 0.000 // 94906.938, 0.000 // 94911.938, 1.278 // 94913.107, 0.000
95040.150, 0.000 // 95045.150, 1.281 // 95046.368, 0.000 // 95173.287, 0.000 // 95178.287, 1.267
95179.488, 0.000 // 95306.417, 0.000 // 95311.417, 1.274 // 95312.597, 0.000 // 95439.810, 0.000
95444.810, 1.299 // 95446.054, 0.000 // 95573.118, 0.000 // 95578.118, 1.290 // 95579.327, 0.000
95706.321, 0.000 // 95711.321, 1.283 // 95712.554, 0.000 // 95839.535, 0.000 // 95844.535, 1.283
95845.786, 0.000 // 95972.716, 0.000 // 95977.716, 1.271 // 95978.873, 0.000 // 96106.074, 0.000
96111.074, 1.288 // 96112.307, 0.000 // 96239.489, 0.000 // 96244.489, 1.288 // 96245.684, 0.000
96372.682, 0.000 // 96377.682, 1.238 // 96378.882, 0.000 // 96506.049, 0.000 // 96511.049, 1.288
96512.260, 0.000 // 96639.216, 0.000 // 96644.216, 1.265 // 96645.421, 0.000 // 96772.509, 0.000
96777.509, 1.279 // 96778.738, 0.000 // 96905.810, 0.000 // 96910.810, 1.273 // 96912.063, 0.000
97039.006, 0.000 // 97044.006, 1.264 // 97045.218, 0.000 // 97172.208, 0.000 // 97177.208, 1.251
97178.421, 0.000 // 97305.390, 0.000 // 97310.390, 1.271 // 97311.598, 0.000 // 97438.544, 0.000
97443.544, 1.263 // 97444.695, 0.000 // 97571.767, 0.000 // 97576.767, 1.254 // 97577.956, 0.000
97704.905, 0.000 // 97709.905, 1.265 // 97711.084, 0.000 // 97838.102, 0.000 // 97843.102, 1.260
97844.299, 0.000 // 97971.296, 0.000 // 97976.296, 1.250 // 97977.480, 0.000 // 98104.442, 0.000
98109.442, 1.242 // 98110.625, 0.000 // 98237.598, 0.000 // 98242.598, 1.260 // 98243.791, 0.000
98368.555, 0.000 // 98373.555, 0.000 // 98377.020, 0.000 // 98504.052, 0.000 // 98509.052, 1.262
98510.264, 0.000 // 98637.020, 0.000 // 98642.020, 1.249 // 98643.292, 0.000 // 98770.404, 0.000
98775.404, 1.263 // 98776.604, 0.000 // 98903.558, 0.000 // 98908.558, 1.255 // 98909.765, 0.000
99036.742, 0.000 // 99041.742, 1.267 // 99042.937, 0.000 // 99169.872, 0.000 // 99174.872, 1.255
99176.056, 0.000 // 99302.957, 0.000 // 99307.957, 1.242 // 99309.146, 0.000 // 99436.024, 0.000
99441.024, 1.249 // 99442.258, 0.000 // 99569.282, 0.000 // 99574.282, 1.252 // 99575.420, 0.000
99702.446, 0.000 // 99707.446, 1.252 // 99708.634, 0.000 // 99835.684, 0.000 // 99840.684, 1.246
99841.851, 0.000 // 99968.713, 0.000 // 99973.713, 1.256 // 99974.874, 0.000 // 100101.938, 0.000
100106.938, 1.238 // 100108.138, 0.000 // 100235.133, 0.000 // 100240.133, 1.260 // 100241.314, 0.000
100368.333, 0.000 // 100373.333, 1.257 // 100374.502, 0.000 // 100501.538, 0.000 // 100506.538, 1.260
100507.768, 0.000 // 100634.707, 0.000 // 100639.707, 1.255 // 100640.913, 0.000 // 100767.826, 0.000
100772.826, 1.261 // 100774.031, 0.000 // 100901.028, 0.000 // 100906.028, 1.251 // 100907.221, 0.000
101034.045, 0.000 // 101039.045, 1.252 // 101040.298, 0.000 // 101167.511, 0.000 // 101172.511, 1.260
101173.746, 0.000 // 101300.876, 0.000 // 101305.876, 1.255 // 101307.018, 0.000 // 101434.013, 0.000
101439.013, 1.159 // 101440.854, 0.000 // 101567.869, 0.000 // 101572.869, 1.253 // 101574.107, 0.000
101701.274, 0.000 // 101706.274, 1.250 // 101707.556, 0.000 // 101834.475, 0.000 // 101839.475, 1.248
101840.685, 0.000 // 101967.605, 0.000 // 101972.605, 1.242 // 101973.802, 0.000 // 102100.888, 0.000
102105.888, 1.257 // 102107.109, 0.000 // 102234.341, 0.000 // 102239.341, 1.259 // 102240.519, 0.000
102367.387, 0.000 // 102372.387, 1.242 // 102373.624, 0.000 // 102500.587, 0.000 // 102505.587, 1.238
102506.752, 0.000 // 102631.314, 0.000 // 102636.314, 0.000 // 102639.818, 0.000 // 102766.662, 0.000
102771.662, 1.252 // 102772.856, 0.000 // 102900.022, 0.000 // 102905.022, 1.256 // 102906.309, 0.000
103033.559, 0.000 // 103038.559, 1.255 // 103039.741, 0.000 // 103166.740, 0.000 // 103171.740, 1.249
103173.070, 0.000 // 103299.845, 0.000 // 103304.845, 1.238 // 103306.073, 0.000 // 103433.059, 0.000
103438.059, 1.258 // 103439.237, 0.000 // 103566.128, 0.000 // 103571.128, 1.245 // 103572.344, 0.000
103699.397, 0.000 // 103704.397, 1.251 // 103705.574, 0.000 // 103832.564, 0.000 // 103837.564, 1.262
103838.768, 0.000 // 103965.896, 0.000 // 103970.896, 1.263 // 103972.102, 0.000 // 104099.152, 0.000
104104.152, 1.244 // 104105.355, 0.000 // 104232.257, 0.000 // 104237.257, 1.261 // 104238.440, 0.000
104365.446, 0.000 // 104370.446, 1.238 // 104371.612, 0.000 // 104498.615, 0.000 // 104503.615, 1.251
104504.845, 0.000 // 104631.802, 0.000 // 104636.802, 1.244 // 104638.087, 0.000 // 104765.130, 0.000
104770.130, 1.199 // 104771.329, 0.000 // 104895.979, 0.000 // 104900.979, 0.000 // 104904.429, 0.000
105031.418, 0.000 // 105036.418, 1.220 // 105037.611, 0.000 // 105164.748, 0.000 // 105169.748, 1.251
105170.964, 0.000 // 105297.746, 0.000 // 105302.746, 1.246 // 105303.974, 0.000 // 105430.906, 0.000
105435.906, 1.227 // 105437.097, 0.000 // 105564.401, 0.000 // 105569.401, 1.242 // 105570.632, 0.000
105697.731, 0.000 // 105702.731, 1.227 // 105703.944, 0.000 // 105830.863, 0.000 // 105835.863, 1.229
105837.128, 0.000 // 105964.289, 0.000 // 105969.289, 1.222 // 105970.478, 0.000 // 106097.569, 0.000
106102.569, 1.226 // 106103.780, 0.000 // 106230.662, 0.000 // 106235.662, 1.221 // 106236.843, 0.000
106361.474, 0.000 // 106366.474, 0.000 // 106370.021, 0.000 // 106496.970, 0.000 // 106501.970, 1.214
106503.176, 0.000 // 106630.041, 0.000 // 106635.041, 1.197 // 106636.252, 0.000 // 106763.432, 0.000
106768.432, 1.203 // 106769.606, 0.000 // 106896.666, 0.000 // 106901.666, 1.224 // 106902.851, 0.000
107029.832, 0.000 // 107034.832, 1.214 // 107036.010, 0.000 // 107163.205, 0.000 // 107168.205, 1.234
107169.384, 0.000 // 107296.343, 0.000 // 107301.343, 1.228 // 107302.503, 0.000 // 107429.419, 0.000
107434.419, 1.213 // 107435.634, 0.000 // 107560.522, 0.000 // 107565.522, 0.000 // 107568.887, 0.000
107695.780, 0.000 // 107700.780, 1.218 // 107702.014, 0.000 // 107828.902, 0.000 // 107833.902, 1.205
107835.127, 0.000 // 107962.118, 0.000 // 107967.118, 1.214 // 107968.309, 0.000 // 108095.222, 0.000

108100.222, 1.220 // 108101.435, 0.000 // 108228.585, 0.000 // 108233.585, 1.209 // 108234.804, 0.000
108359.904, 0.000 // 108364.904, 0.000 // 108367.958, 0.000 // 108495.053, 0.000 // 108500.053, 0.138
108501.253, 0.000 // 108628.276, 0.000 // 108633.276, 1.216 // 108634.471, 0.000 // 108761.540, 0.000
108766.540, 1.221 // 108767.736, 0.000 // 108894.627, 0.000 // 108899.627, 1.195 // 108900.851, 0.000
109027.845, 0.000 // 109032.845, 1.223 // 109034.019, 0.000 // 109160.916, 0.000 // 109165.916, 1.219
109167.131, 0.000 // 109294.121, 0.000 // 109299.121, 1.219 // 109300.361, 0.000 // 109427.367, 0.000
109432.367, 1.238 // 109433.622, 0.000 // 109560.866, 0.000 // 109565.866, 1.243 // 109567.018, 0.000
109693.923, 0.000 // 109698.923, 1.213 // 109700.193, 0.000 // 109827.196, 0.000 // 109832.196, 1.207
109833.360, 0.000 // 109960.645, 0.000 // 109965.645, 1.223 // 109966.825, 0.000 // 110093.689, 0.000
110098.689, 1.213 // 110100.028, 0.000 // 110227.027, 0.000 // 110232.027, 1.257 // 110233.965, 0.000
110360.986, 0.000 // 110365.986, 1.224 // 110367.200, 0.000 // 110494.133, 0.000 // 110499.133, 1.215
110500.363, 0.000 // 110627.372, 0.000 // 110632.372, 1.214 // 110633.600, 0.000 // 110760.638, 0.000
110765.638, 1.225 // 110766.836, 0.000 // 110893.859, 0.000 // 110898.859, 1.248 // 110900.116, 0.000
111027.068, 0.000 // 111032.068, 1.218 // 111033.257, 0.000 // 111160.212, 0.000 // 111165.212, 1.216
111166.420, 0.000 // 111293.416, 0.000 // 111298.416, 1.205 // 111299.546, 0.000 // 111426.533, 0.000
111431.533, 1.192 // 111432.743, 0.000 // 111559.918, 0.000 // 111564.918, 1.232 // 111566.159, 0.000
111690.762, 0.000 // 111695.762, 0.000 // 111699.344, 0.000 // 111826.304, 0.000 // 111831.304, 1.238
111832.487, 0.000 // 111959.379, 0.000 // 111964.379, 1.217 // 111965.570, 0.000 // 112092.595, 0.000
112097.595, 1.160 // 112098.780, 0.000 // 112225.689, 0.000 // 112230.689, 1.220 // 112231.852, 0.000
112358.749, 0.000 // 112363.749, 1.206 // 112364.954, 0.000 // 112491.916, 0.000 // 112496.916, 1.208
112498.161, 0.000 // 112625.129, 0.000 // 112630.129, 1.216 // 112631.327, 0.000 // 112758.272, 0.000
112763.272, 1.209 // 112764.497, 0.000 // 112891.368, 0.000 // 112896.368, 1.207 // 112897.564, 0.000
113024.520, 0.000 // 113029.520, 1.204 // 113030.806, 0.000 // 113157.746, 0.000 // 113162.746, 1.216
113163.934, 0.000 // 113291.038, 0.000 // 113296.038, 1.215 // 113297.214, 0.000 // 113424.206, 0.000
113429.206, 1.206 // 113430.433, 0.000 // 113557.562, 0.000 // 113562.562, 1.210 // 113563.766, 0.000
113690.759, 0.000 // 113695.759, 0.497 // 113696.948, 0.000 // 113823.768, 0.000 // 113828.768, 1.189
113829.988, 0.000 // 113956.863, 0.000 // 113961.863, 1.193 // 113963.060, 0.000 // 114090.154, 0.000
114095.154, 1.206 // 114096.386, 0.000 // 114223.385, 0.000 // 114228.385, 1.214 // 114229.559, 0.000
114356.385, 0.000 // 114361.385, 1.190 // 114362.588, 0.000 // 114489.459, 0.000 // 114494.459, 1.191
114495.623, 0.000 // 114622.548, 0.000 // 114627.548, 1.184 // 114629.043, 0.000 // 114756.072, 0.000
114761.072, 1.193 // 114762.289, 0.000 // 114889.173, 0.000 // 114894.173, 1.197 // 114895.348, 0.000
115022.279, 0.000 // 115027.279, 1.182 // 115028.512, 0.000 // 115155.446, 0.000 // 115160.446, 1.217
115161.650, 0.000 // 115288.652, 0.000 // 115293.652, 1.190 // 115294.832, 0.000 // 115421.651, 0.000
115426.651, 1.188 // 115427.866, 0.000 // 115554.739, 0.000 // 115559.739, 1.185 // 115560.984, 0.000
115688.051, 0.000 // 115693.051, 1.187 // 115694.225, 0.000 // 115821.349, 0.000 // 115826.349, 1.180
115827.542, 0.000 // 115954.497, 0.000 // 115959.497, 1.161 // 115960.700, 0.000 // 116087.829, 0.000
116092.829, 1.172 // 116094.005, 0.000 // 116220.918, 0.000 // 116225.918, 1.162 // 116227.119, 0.000
116354.285, 0.000 // 116359.285, 1.165 // 116360.551, 0.000 // 116485.241, 0.000 // 116490.241, 0.000
116493.734, 0.000 // 116620.764, 0.000 // 116625.764, 1.198 // 116626.985, 0.000 // 116753.948, 0.000
116758.948, 1.221 // 116760.133, 0.000 // 116887.308, 0.000 // 116892.308, 1.192 // 116893.497, 0.000
117020.651, 0.000 // 117025.651, 1.186 // 117026.972, 0.000 // 117154.168, 0.000 // 117159.168, 1.187
117160.380, 0.000 // 117287.551, 0.000 // 117292.551, 1.201 // 117293.739, 0.000 // 117420.865, 0.000
117425.865, 1.202 // 117427.059, 0.000 // 117554.094, 0.000 // 117559.094, 1.191 // 117560.339, 0.000
117685.302, 0.000 // 117690.302, 0.000 // 117693.568, 0.000 // 117820.654, 0.000 // 117825.654, 1.198
117826.895, 0.000 // 117953.906, 0.000 // 117958.906, 1.192 // 117960.154, 0.000 // 118087.121, 0.000
118092.121, 1.181 // 118093.338, 0.000 // 118220.402, 0.000 // 118225.402, 1.188 // 118226.613, 0.000
118353.477, 0.000 // 118358.477, 1.190 // 118359.699, 0.000 // 118486.614, 0.000 // 118491.614, 1.209
118492.858, 0.000 // 118619.854, 0.000 // 118624.854, 1.192 // 118626.066, 0.000 // 118753.323, 0.000
118758.323, 0.000 // 118759.523, 0.000 // 118886.431, 0.000 // 118891.431, 1.187 // 118892.685, 0.000
119019.826, 0.000 // 119024.826, 1.207 // 119026.028, 0.000 // 119153.061, 0.000 // 119158.061, 1.181
119159.282, 0.000 // 119286.234, 0.000 // 119291.234, 1.176 // 119292.454, 0.000 // 119419.456, 0.000
119424.456, 1.192 // 119425.695, 0.000 // 119552.829, 0.000 // 119557.829, 1.198 // 119559.003, 0.000
119685.889, 0.000 // 119690.889, 1.178 // 119692.098, 0.000 // 119819.217, 0.000 // 119824.217, 1.181
119825.451, 0.000 // 119952.398, 0.000 // 119957.398, 1.171 // 119958.608, 0.000 // 120085.555, 0.000
120090.555, 1.159 // 120091.718, 0.000 // 120218.603, 0.000 // 120223.603, 1.161 // 120224.795, 0.000
120351.848, 0.000 // 120356.848, 1.146 // 120358.039, 0.000 // 120485.137, 0.000 // 120490.137, 1.151
120491.310, 0.000 // 120618.240, 0.000 // 120623.240, 1.146 // 120624.484, 0.000 // 120751.449, 0.000
120756.449, 1.156 // 120757.692, 0.000 // 120884.764, 0.000 // 120889.764, 1.148 // 120891.006, 0.000
121018.203, 0.000 // 121023.203, 1.157 // 121024.516, 0.000 // 121149.506, 0.000 // 121154.506, 0.000
121158.033, 0.000 // 121285.097, 0.000 // 121290.097, 1.169 // 121291.305, 0.000 // 121418.324, 0.000
121423.324, 1.137 // 121424.710, 0.000 // 121551.928, 0.000 // 121556.928, 1.145 // 121558.113, 0.000
121685.128, 0.000 // 121690.128, 1.138 // 121691.570, 0.000 // 121818.661, 0.000 // 121823.661, 1.147
121824.970, 0.000 // 121952.086, 0.000 // 121957.086, 1.155 // 121958.284, 0.000 // 122085.265, 0.000

122090.265, 1.140 // 122091.408, 0.000 // 122218.557, 0.000 // 122223.557, 1.136 // 122224.734, 0.000
122351.756, 0.000 // 122356.756, 1.145 // 122357.972, 0.000 // 122484.974, 0.000 // 122489.974, 1.135
122491.159, 0.000 // 122618.236, 0.000 // 122623.236, 1.139 // 122624.453, 0.000 // 122751.360, 0.000
122756.360, 1.129 // 122757.572, 0.000 // 122884.597, 0.000 // 122889.597, 0.000 // 122890.797, 0.000
123017.827, 0.000 // 123022.827, 1.144 // 123024.032, 0.000 // 123151.016, 0.000 // 123156.016, 1.129
123157.249, 0.000 // 123284.259, 0.000 // 123289.259, 1.134 // 123290.464, 0.000 // 123417.684, 0.000
123422.684, 1.147 // 123423.870, 0.000 // 123551.027, 0.000 // 123556.027, 1.151 // 123557.234, 0.000
123684.256, 0.000 // 123689.256, 1.133 // 123690.440, 0.000 // 123817.421, 0.000 // 123822.421, 1.135
123823.642, 0.000 // 123950.657, 0.000 // 123955.657, 1.131 // 123956.859, 0.000 // 124083.721, 0.000
124088.721, 1.152 // 124089.854, 0.000 // 124216.925, 0.000 // 124221.925, 1.137 // 124223.126, 0.000
124350.004, 0.000 // 124355.004, 1.146 // 124356.189, 0.000 // 124483.183, 0.000 // 124488.183, 1.143
124489.394, 0.000 // 124616.390, 0.000 // 124621.390, 1.157 // 124622.561, 0.000 // 124747.044, 0.000
124752.044, 0.000 // 124755.627, 0.000 // 124882.641, 0.000 // 124887.641, 1.164 // 124888.855, 0.000
125015.844, 0.000 // 125020.844, 1.157 // 125022.032, 0.000 // 125148.893, 0.000 // 125153.893, 1.151
125155.082, 0.000 // 125282.019, 0.000 // 125287.019, 1.154 // 125288.272, 0.000 // 125415.399, 0.000
125420.399, 1.153 // 125421.659, 0.000 // 125546.621, 0.000 // 125551.621, 0.000 // 125555.002, 0.000
125681.877, 0.000 // 125686.877, 1.146 // 125688.081, 0.000 // 125815.031, 0.000 // 125820.031, 1.142
125821.287, 0.000 // 125948.262, 0.000 // 125953.262, 1.144 // 125954.441, 0.000 // 126079.169, 0.000
126084.169, 0.000 // 126087.579, 0.000 // 126214.686, 0.000 // 126219.686, 1.182 // 126221.849, 0.000
126348.927, 0.000 // 126353.927, 1.164 // 126355.156, 0.000 // 126482.158, 0.000 // 126487.158, 1.138
126488.374, 0.000 // 126615.342, 0.000 // 126620.342, 1.143 // 126621.571, 0.000 // 126748.571, 0.000
126753.571, 1.144 // 126754.763, 0.000 // 126881.850, 0.000 // 126886.850, 1.143 // 126888.194, 0.000
127013.047, 0.000 // 127018.047, 0.000 // 127021.582, 0.000 // 127148.627, 0.000 // 127153.627, 0.000
127154.827, 0.000 // 127280.067, 0.000 // 127285.067, 0.000 // 127288.098, 0.000 // 127415.109, 0.000
127420.109, 0.000 // 127421.309, 0.000 // 127548.257, 0.000 // 127553.257, 1.167 // 127554.491, 0.000
127681.453, 0.000 // 127686.453, 1.169 // 127687.664, 0.000 // 127814.641, 0.000 // 127819.641, 1.166
127820.846, 0.000 // 127948.092, 0.000 // 127953.092, 1.177 // 127954.296, 0.000 // 128081.345, 0.000
128086.345, 1.173 // 128087.587, 0.000 // 128214.695, 0.000 // 128219.695, 1.170 // 128220.844, 0.000
128347.893, 0.000 // 128352.893, 1.174 // 128354.110, 0.000 // 128481.296, 0.000 // 128486.296, 1.176
128487.503, 0.000 // 128614.398, 0.000 // 128619.398, 1.155 // 128620.677, 0.000 // 128747.715, 0.000
128752.715, 1.143 // 128753.919, 0.000 // 128881.169, 0.000 // 128886.169, 1.142 // 128887.339, 0.000
129014.498, 0.000 // 129019.498, 1.126 // 129020.755, 0.000 // 129147.746, 0.000 // 129152.746, 1.155
129154.026, 0.000 // 129281.199, 0.000 // 129286.199, 1.149 // 129287.495, 0.000 // 129414.535, 0.000
129419.535, 1.140 // 129420.757, 0.000 // 129547.867, 0.000 // 129552.867, 1.138 // 129554.073, 0.000
129681.237, 0.000 // 129686.237, 1.154 // 129687.478, 0.000 // 129814.555, 0.000 // 129819.555, 1.146
129820.731, 0.000 // 129947.660, 0.000 // 129952.660, 1.176 // 129953.888, 0.000 // 130080.728, 0.000
130085.728, 1.105 // 130086.940, 0.000 // 130214.083, 0.000 // 130219.083, 1.120 // 130220.309, 0.000
130347.423, 0.000 // 130352.423, 1.128 // 130353.627, 0.000 // 130480.648, 0.000 // 130485.648, 0.923
130486.837, 0.000 // 130613.659, 0.000 // 130618.659, 0.916 // 130619.844, 0.000 // 130746.970, 0.000
130751.970, 0.922 // 130753.199, 0.000 // 130880.398, 0.000 // 130885.398, 0.937 // 130886.575, 0.000
131013.696, 0.000 // 131018.696, 0.940 // 131019.906, 0.000 // 131147.006, 0.000 // 131152.006, 0.890
131153.239, 0.000 // 131280.137, 0.000 // 131285.137, 0.884 // 131286.418, 0.000 // 131413.551, 0.000
131418.551, 0.899 // 131419.760, 0.000 // 131546.831, 0.000 // 131551.831, 0.906 // 131553.083, 0.000
131680.156, 0.000 // 131685.156, 0.895 // 131686.382, 0.000 // 131813.490, 0.000 // 131818.490, 0.927
131819.749, 0.000 // 131946.926, 0.000 // 131951.926, 0.915 // 131953.134, 0.000 // 132080.179, 0.000
132085.179, 0.884 // 132086.366, 0.000 // 132213.287, 0.000 // 132218.287, 0.880 // 132219.482, 0.000
132346.652, 0.000 // 132351.652, 0.904 // 132352.900, 0.000 // 132479.978, 0.000 // 132484.978, 0.913
132486.204, 0.000 // 132611.020, 0.000 // 132616.020, 0.000 // 132619.497, 0.000 // 132746.498, 0.000
132751.498, 0.895 // 132752.757, 0.000 // 132879.836, 0.000 // 132884.836, 0.923 // 132886.020, 0.000
133012.788, 0.000 // 133017.788, 0.854 // 133019.016, 0.000 // 133145.990, 0.000 // 133150.990, 0.867
133152.195, 0.000 // 133278.991, 0.000 // 133283.991, 0.857 // 133285.213, 0.000 // 133412.381, 0.000
133417.381, 0.891 // 133418.609, 0.000 // 133545.560, 0.000 // 133550.560, 0.882 // 133551.793, 0.000
133678.652, 0.000 // 133683.652, 0.911 // 133684.832, 0.000 // 133811.858, 0.000 // 133816.858, 0.895
133818.033, 0.000 // 133945.144, 0.000 // 133950.144, 0.918 // 133951.356, 0.000 // 134078.326, 0.000
134083.326, 0.890 // 134084.538, 0.000 // 134211.638, 0.000 // 134216.638, 0.888 // 134217.850, 0.000
134344.894, 0.000 // 134349.894, 0.891 // 134351.081, 0.000 // 134477.919, 0.000 // 134482.919, 0.889
134484.124, 0.000 // 134611.116, 0.000 // 134616.116, 0.878 // 134617.321, 0.000 // 134744.326, 0.000
134749.326, 0.889 // 134750.599, 0.000 // 134877.715, 0.000 // 134882.715, 0.000 // 134883.915, 0.000
135010.866, 0.000 // 135015.866, 0.849 // 135017.079, 0.000 // 135143.987, 0.000 // 135148.987, 0.847
135150.189, 0.000 // 135277.143, 0.000 // 135282.143, 0.878 // 135283.446, 0.000 // 135410.477, 0.000
135415.477, 0.884 // 135416.678, 0.000 // 135543.613, 0.000 // 135548.613, 0.885 // 135549.787, 0.000
135674.467, 0.000 // 135679.467, 0.000 // 135682.963, 0.000 // 135809.879, 0.000 // 135814.879, 0.000
135816.079, 0.000 // 135940.867, 0.000 // 135945.867, 0.000 // 135949.294, 0.000 // 136076.447, 0.000

136081.447, 0.893 // 136082.647, 0.000 // 136209.791, 0.000 // 136214.791, 0.992 // 136216.033, 0.000
136343.207, 0.000 // 136348.207, 0.972 // 136349.518, 0.000 // 136476.497, 0.000 // 136481.497, 0.934
136482.663, 0.000 // 136609.613, 0.000 // 136614.613, 0.945 // 136616.015, 0.000 // 136743.132, 0.000
136748.132, 0.964 // 136749.483, 0.000 // 136876.489, 0.000 // 136881.489, 0.729 // 136882.689, 0.000
137009.808, 0.000 // 137014.808, 0.928 // 137015.985, 0.000 // 137143.044, 0.000 // 137148.044, 0.924
137149.255, 0.000 // 137276.158, 0.000 // 137281.158, 0.940 // 137282.307, 0.000 // 137409.289, 0.000
137414.289, 0.939 // 137415.469, 0.000 // 137542.594, 0.000 // 137547.594, 0.912 // 137548.800, 0.000
137675.759, 0.000 // 137680.759, 0.930 // 137681.986, 0.000 // 137808.895, 0.000 // 137813.895, 0.887
137815.091, 0.000 // 137942.013, 0.000 // 137947.013, 0.883 // 137948.225, 0.000 // 138075.188, 0.000
138080.188, 0.868 // 138081.438, 0.000 // 138208.295, 0.000 // 138213.295, 0.909 // 138214.467, 0.000
138341.521, 0.000 // 138346.521, 0.908 // 138347.737, 0.000 // 138474.689, 0.000 // 138479.689, 0.885
138480.897, 0.000 // 138607.897, 0.000 // 138612.897, 0.928 // 138614.113, 0.000 // 138741.022, 0.000
138746.022, 0.896 // 138747.193, 0.000 // 138874.539, 0.000 // 138879.539, 0.420 // 138880.739, 0.000
139007.661, 0.000 // 139012.661, 0.874 // 139013.876, 0.000 // 139140.972, 0.000 // 139145.972, 0.959
139147.209, 0.000 // 139274.194, 0.000 // 139279.194, 0.913 // 139280.412, 0.000 // 139407.426, 0.000
139412.426, 0.896 // 139413.649, 0.000 // 139540.638, 0.000 // 139545.638, 0.865 // 139546.919, 0.000
139674.177, 0.000 // 139679.177, 0.877 // 139680.419, 0.000 // 139807.336, 0.000 // 139812.336, 0.901
139813.502, 0.000 // 139940.464, 0.000 // 139945.464, 0.882 // 139946.652, 0.000 // 140073.622, 0.000
140078.622, 0.972 // 140079.859, 0.000 // 140206.899, 0.000 // 140211.899, 0.914 // 140213.063, 0.000
140340.121, 0.000 // 140345.121, 0.903 // 140346.348, 0.000 // 140473.217, 0.000 // 140478.217, 0.865
140479.426, 0.000 // 140606.360, 0.000 // 140611.360, 0.926 // 140612.627, 0.000 // 140739.837, 0.000
140744.837, 0.901 // 140746.051, 0.000 // 140873.016, 0.000 // 140878.016, 0.918 // 140879.307, 0.000
141006.414, 0.000 // 141011.414, 0.924 // 141012.619, 0.000 // 141139.800, 0.000 // 141144.800, 0.901
141146.060, 0.000 // 141273.112, 0.000 // 141278.112, 0.891 // 141279.365, 0.000 // 141406.429, 0.000
141411.429, 0.901 // 141412.635, 0.000 // 141539.536, 0.000 // 141544.536, 0.878 // 141545.762, 0.000
141672.835, 0.000 // 141677.835, 0.941 // 141679.051, 0.000 // 141806.075, 0.000 // 141811.075, 0.941
141812.295, 0.000 // 141939.273, 0.000 // 141944.273, 0.960 // 141945.450, 0.000 // 142072.444, 0.000
142077.444, 0.944 // 142078.628, 0.000 // 142205.600, 0.000 // 142210.600, 0.945 // 142211.800, 0.000
142338.804, 0.000 // 142343.804, 0.915 // 142344.931, 0.000 // 142471.878, 0.000 // 142476.878, 0.997
142478.023, 0.000 // 142605.207, 0.000 // 142610.207, 0.920 // 142611.544, 0.000 // 142738.651, 0.000
142743.651, 0.906 // 142744.865, 0.000 // 142871.839, 0.000 // 142876.839, 0.904 // 142878.025, 0.000
143005.056, 0.000 // 143010.056, 0.883 // 143011.253, 0.000 // 143138.310, 0.000 // 143143.310, 0.000
143144.510, 0.000 // 143271.598, 0.000 // 143276.598, 0.906 // 143277.772, 0.000 // 143404.693, 0.000
143409.693, 0.909 // 143410.917, 0.000 // 143538.154, 0.000 // 143543.154, 0.930 // 143544.423, 0.000
143671.479, 0.000 // 143676.479, 0.932 // 143677.609, 0.000 // 143804.586, 0.000 // 143809.586, 0.877
143810.802, 0.000 // 143938.052, 0.000 // 143943.052, 0.948 // 143944.282, 0.000 // 144071.338, 0.000
144076.338, 0.883 // 144077.512, 0.000 // 144204.328, 0.000 // 144209.328, 0.933 // 144210.508, 0.000
144337.592, 0.000 // 144342.592, 0.949 // 144343.776, 0.000 // 144470.751, 0.000 // 144475.751, 0.946
144476.925, 0.000 // 144604.012, 0.000 // 144609.012, 0.954 // 144610.196, 0.000 // 144737.424, 0.000
144742.424, 0.903 // 144743.555, 0.000 // 144870.495, 0.000 // 144875.495, 0.935 // 144876.773, 0.000
145003.818, 0.000 // 145008.818, 0.922 // 145010.035, 0.000 // 145137.128, 0.000 // 145142.128, 0.920
145143.388, 0.000 // 145270.455, 0.000 // 145275.455, 0.972 // 145276.714, 0.000 // 145403.652, 0.000
145408.652, 0.917 // 145409.895, 0.000 // 145536.974, 0.000 // 145541.974, 0.945 // 145543.220, 0.000
145668.014, 0.000 // 145673.014, 0.000 // 145676.238, 0.000 // 145803.156, 0.000 // 145808.156, 0.918
145809.420, 0.000 // 145936.440, 0.000 // 145941.440, 0.912 // 145942.646, 0.000 // 146069.760, 0.000
146074.760, 0.950 // 146075.962, 0.000 // 146202.937, 0.000 // 146207.937, 0.922 // 146209.150, 0.000
146336.072, 0.000 // 146341.072, 0.889 // 146342.305, 0.000 // 146469.095, 0.000 // 146474.095, 0.906
146475.326, 0.000 // 146602.439, 0.000 // 146607.439, 0.916 // 146608.641, 0.000 // 146735.695, 0.000
146740.695, 0.924 // 146741.887, 0.000 // 146868.977, 0.000 // 146873.977, 0.931 // 146875.185, 0.000
147002.109, 0.000 // 147007.109, 0.944 // 147008.324, 0.000 // 147135.349, 0.000 // 147140.349, 0.912
147141.541, 0.000 // 147268.495, 0.000 // 147273.495, 0.930 // 147275.247, 0.000 // 147402.346, 0.000
147407.346, 0.958 // 147408.578, 0.000 // 147535.706, 0.000 // 147540.706, 0.936 // 147541.947, 0.000
147669.052, 0.000 // 147674.052, 0.915 // 147675.272, 0.000 // 147802.282, 0.000 // 147807.282, 0.963
147808.490, 0.000 // 147935.496, 0.000 // 147940.496, 0.922 // 147941.723, 0.000 // 148066.898, 0.000
148071.898, 0.035 // 148074.783, 0.000 // 148201.869, 0.000 // 148206.869, 1.004 // 148208.034, 0.000
148335.233, 0.000 // 148340.233, 0.927 // 148341.420, 0.000 // 148468.476, 0.000 // 148473.476, 0.890
148474.720, 0.000 // 148601.761, 0.000 // 148606.761, 0.905 // 148607.928, 0.000 // 148735.079, 0.000
148740.079, 1.004 // 148741.307, 0.000 // 148868.305, 0.000 // 148873.305, 1.022 // 148874.549, 0.000
149001.490, 0.000 // 149006.490, 1.007 // 149007.724, 0.000 // 149134.791, 0.000 // 149139.791, 1.021
149141.021, 0.000 // 149268.234, 0.000 // 149273.234, 1.024 // 149274.435, 0.000 // 149401.440, 0.000
149406.440, 0.967 // 149407.619, 0.000 // 149534.566, 0.000 // 149539.566, 1.015 // 149540.774, 0.000
149667.584, 0.000 // 149672.584, 1.015 // 149673.791, 0.000 // 149800.786, 0.000 // 149805.786, 1.020
149806.995, 0.000 // 149933.874, 0.000 // 149938.874, 1.009 // 149940.112, 0.000 // 150067.374, 0.000

150072.374, 1.081 // 150073.580, 0.000 // 150200.664, 0.000 // 150205.664, 1.046 // 150206.870, 0.000
150333.807, 0.000 // 150338.807, 1.032 // 150340.007, 0.000 // 150467.031, 0.000 // 150472.031, 1.016
150473.227, 0.000 // 150600.331, 0.000 // 150605.331, 1.019 // 150606.548, 0.000 // 150733.812, 0.000
150738.812, 1.011 // 150740.016, 0.000 // 150867.038, 0.000 // 150872.038, 1.013 // 150873.234, 0.000
151000.417, 0.000 // 151005.417, 1.028 // 151006.612, 0.000 // 151133.636, 0.000 // 151138.636, 1.009
151139.835, 0.000 // 151266.823, 0.000 // 151271.823, 1.017 // 151272.985, 0.000 // 151400.006, 0.000
151405.006, 1.020 // 151406.204, 0.000 // 151533.091, 0.000 // 151538.091, 1.029 // 151539.332, 0.000
151666.323, 0.000 // 151671.323, 1.013 // 151672.569, 0.000 // 151797.750, 0.000 // 151802.750, 0.000
151805.877, 0.000 // 151932.863, 0.000 // 151937.863, 1.011 // 151939.068, 0.000 // 152066.166, 0.000
152071.166, 1.007 // 152072.387, 0.000 // 152199.466, 0.000 // 152204.466, 0.904 // 152205.676, 0.000
152332.693, 0.000 // 152337.693, 1.028 // 152338.899, 0.000 // 152465.769, 0.000 // 152470.769, 0.995
152471.910, 0.000 // 152598.935, 0.000 // 152603.935, 0.986 // 152605.128, 0.000 // 152732.027, 0.000
152737.027, 0.936 // 152738.240, 0.000 // 152865.218, 0.000 // 152870.218, 1.003 // 152871.386, 0.000
152998.390, 0.000 // 153003.390, 1.029 // 153004.589, 0.000 // 153131.555, 0.000 // 153136.555, 1.011
153137.745, 0.000 // 153264.718, 0.000 // 153269.718, 1.019 // 153270.936, 0.000 // 153395.947, 0.000
153400.947, 0.000 // 153404.095, 0.000 // 153531.136, 0.000 // 153536.136, 1.020 // 153537.298, 0.000
153664.305, 0.000 // 153669.305, 1.025 // 153670.506, 0.000 // 153795.383, 0.000 // 153800.383, 0.000
153803.768, 0.000 // 153930.670, 0.000 // 153935.670, 1.027 // 153936.871, 0.000 // 154063.995, 0.000
154068.995, 1.012 // 154070.205, 0.000 // 154197.363, 0.000 // 154202.363, 1.005 // 154203.569, 0.000
154330.569, 0.000 // 154335.569, 0.997 // 154336.800, 0.000 // 154463.722, 0.000 // 154468.722, 1.025
154469.958, 0.000 // 154596.819, 0.000 // 154601.819, 0.993 // 154603.034, 0.000 // 154730.072, 0.000
154735.072, 0.989 // 154736.327, 0.000 // 154863.341, 0.000 // 154868.341, 0.993 // 154869.518, 0.000
154996.587, 0.000 // 155001.587, 1.010 // 155002.799, 0.000 // 155129.787, 0.000 // 155134.787, 1.016
155135.987, 0.000 // 155263.191, 0.000 // 155268.191, 1.016 // 155269.402, 0.000 // 155396.430, 0.000
155401.430, 1.001 // 155402.687, 0.000 // 155529.613, 0.000 // 155534.613, 1.028 // 155535.862, 0.000
155662.931, 0.000 // 155667.931, 1.020 // 155669.146, 0.000 // 155796.164, 0.000 // 155801.164, 1.014
155802.405, 0.000 // 155929.451, 0.000 // 155934.451, 1.026 // 155935.627, 0.000 // 156062.808, 0.000
156067.808, 1.037 // 156068.987, 0.000 // 156196.024, 0.000 // 156201.024, 1.009 // 156202.245, 0.000
156329.373, 0.000 // 156334.373, 1.027 // 156335.615, 0.000 // 156462.686, 0.000 // 156467.686, 1.013
156468.884, 0.000 // 156595.731, 0.000 // 156600.731, 1.002 // 156601.959, 0.000 // 156729.171, 0.000
156734.171, 1.036 // 156735.374, 0.000 // 156862.571, 0.000 // 156867.571, 1.032 // 156868.762, 0.000
156995.932, 0.000 // 157000.932, 0.984 // 157002.197, 0.000 // 157129.229, 0.000 // 157134.229, 0.995
157135.435, 0.000 // 157262.452, 0.000 // 157267.452, 1.001 // 157268.618, 0.000 // 157395.429, 0.000
157400.429, 0.998 // 157401.627, 0.000 // 157528.659, 0.000 // 157533.659, 0.999 // 157534.846, 0.000
157661.783, 0.000 // 157666.783, 1.006 // 157668.087, 0.000 // 157794.912, 0.000 // 157799.912, 1.018
157801.206, 0.000 // 157928.167, 0.000 // 157933.167, 1.005 // 157934.370, 0.000 // 158061.443, 0.000
158066.443, 1.014 // 158067.689, 0.000 // 158194.793, 0.000 // 158199.793, 1.013 // 158200.958, 0.000
158327.867, 0.000 // 158332.867, 1.009 // 158334.182, 0.000 // 158461.290, 0.000 // 158466.290, 1.016
158467.534, 0.000 // 158594.574, 0.000 // 158599.574, 1.015 // 158600.869, 0.000 // 158727.845, 0.000
158732.845, 1.022 // 158734.064, 0.000 // 158860.949, 0.000 // 158865.949, 1.010 // 158867.157, 0.000
158994.177, 0.000 // 158999.177, 1.024 // 159000.382, 0.000 // 159127.296, 0.000 // 159132.296, 1.036
159133.508, 0.000 // 159260.441, 0.000 // 159265.441, 1.020 // 159266.642, 0.000 // 159393.671, 0.000
159398.671, 1.031 // 159399.908, 0.000 // 159526.920, 0.000 // 159531.920, 1.055 // 159533.240, 0.000
159660.373, 0.000 // 159665.373, 1.032 // 159666.591, 0.000 // 159793.719, 0.000 // 159798.719, 1.018
159799.924, 0.000 // 159926.879, 0.000 // 159931.879, 1.012 // 159933.046, 0.000 // 160060.149, 0.000
160065.149, 0.997 // 160066.393, 0.000 // 160193.326, 0.000 // 160198.326, 1.018 // 160199.571, 0.000
160326.599, 0.000 // 160331.599, 1.015 // 160332.830, 0.000 // 160459.836, 0.000 // 160464.836, 1.030
160465.949, 0.000 // 160592.930, 0.000 // 160597.930, 1.032 // 160599.183, 0.000 // 160726.059, 0.000
160731.059, 1.022 // 160732.292, 0.000 // 160859.283, 0.000 // 160864.283, 1.017 // 160865.541, 0.000
160992.572, 0.000 // 160997.572, 1.022 // 160998.809, 0.000 // 161125.891, 0.000 // 161130.891, 1.005
161132.108, 0.000 // 161259.075, 0.000 // 161264.075, 1.003 // 161265.330, 0.000 // 161392.411, 0.000
161397.411, 1.010 // 161398.524, 0.000 // 161525.785, 0.000 // 161530.785, 1.025 // 161531.889, 0.000
161659.043, 0.000 // 161664.043, 0.991 // 161665.233, 0.000 // 161790.617, 0.000 // 161795.617, 0.000
161798.764, 0.000 // 161925.827, 0.000 // 161930.827, 1.008 // 161932.022, 0.000 // 162059.103, 0.000
162064.103, 1.067 // 162065.276, 0.000 // 162192.190, 0.000 // 162197.190, 1.032 // 162198.405, 0.000
162325.443, 0.000 // 162330.443, 1.005 // 162331.606, 0.000 // 162458.579, 0.000 // 162463.579, 1.048
162464.819, 0.000 // 162591.993, 0.000 // 162596.993, 1.041 // 162598.242, 0.000 // 162725.186, 0.000
162730.186, 1.011 // 162731.396, 0.000 // 162858.324, 0.000 // 162863.324, 1.001 // 162864.575, 0.000
162991.674, 0.000 // 162996.674, 0.990 // 162997.936, 0.000 // 163124.892, 0.000 // 163129.892, 1.027
163131.820, 0.000 // 163259.135, 0.000 // 163264.135, 1.028 // 163265.369, 0.000 // 163392.718, 0.000
163397.718, 1.027 // 163398.977, 0.000 // 163526.044, 0.000 // 163531.044, 1.028 // 163532.319, 0.000
163659.372, 0.000 // 163664.372, 1.046 // 163665.559, 0.000 // 163792.587, 0.000 // 163797.587, 1.018
163798.786, 0.000 // 163925.845, 0.000 // 163930.845, 1.009 // 163932.071, 0.000 // 164059.156, 0.000

164064.156, 1.001 // 164065.360, 0.000 // 164192.483, 0.000 // 164197.483, 1.005 // 164198.780, 0.000
164325.901, 0.000 // 164330.901, 1.002 // 164332.017, 0.000 // 164459.131, 0.000 // 164464.131, 0.977
164465.382, 0.000 // 164592.449, 0.000 // 164597.449, 1.007 // 164598.684, 0.000 // 164725.715, 0.000
164730.715, 1.018 // 164731.909, 0.000 // 164859.089, 0.000 // 164864.089, 1.005 // 164865.315, 0.000
164992.271, 0.000 // 164997.271, 0.985 // 164998.481, 0.000 // 165125.589, 0.000 // 165130.589, 1.002
165131.816, 0.000 // 165258.780, 0.000 // 165263.780, 1.014 // 165265.018, 0.000 // 165392.131, 0.000
165397.131, 0.994 // 165398.325, 0.000 // 165525.346, 0.000 // 165530.346, 0.979 // 165531.662, 0.000
165658.699, 0.000 // 165663.699, 0.996 // 165664.878, 0.000 // 165791.906, 0.000 // 165796.906, 0.990
165798.093, 0.000 // 165925.248, 0.000 // 165930.248, 0.995 // 165931.360, 0.000 // 166058.474, 0.000
166063.474, 0.995 // 166064.765, 0.000 // 166191.660, 0.000 // 166196.660, 0.967 // 166197.830, 0.000
166324.849, 0.000 // 166329.849, 1.002 // 166331.070, 0.000 // 166458.013, 0.000 // 166463.013, 0.967
166464.195, 0.000 // 166591.127, 0.000 // 166596.127, 0.975 // 166597.354, 0.000 // 166724.333, 0.000
166729.333, 0.995 // 166730.537, 0.000 // 166857.447, 0.000 // 166862.447, 0.971 // 166863.704, 0.000
166990.825, 0.000 // 166995.825, 0.982 // 166997.091, 0.000 // 167124.039, 0.000 // 167129.039, 0.959
167130.221, 0.000 // 167257.373, 0.000 // 167262.373, 0.972 // 167263.645, 0.000 // 167390.629, 0.000
167395.629, 0.953 // 167397.103, 0.000 // 167524.189, 0.000 // 167529.189, 0.970 // 167530.358, 0.000
167657.377, 0.000 // 167662.377, 0.957 // 167663.613, 0.000 // 167790.812, 0.000 // 167795.812, 0.995
167797.000, 0.000 // 167924.042, 0.000 // 167929.042, 0.963 // 167930.227, 0.000 // 168057.112, 0.000
168062.112, 0.989 // 168063.324, 0.000 // 168190.492, 0.000 // 168195.492, 0.971 // 168196.670, 0.000
168323.736, 0.000 // 168328.736, 0.974 // 168329.938, 0.000 // 168456.926, 0.000 // 168461.926, 0.995
168463.175, 0.000 // 168590.307, 0.000 // 168595.307, 0.999 // 168596.537, 0.000 // 168723.588, 0.000
168728.588, 0.964 // 168729.824, 0.000 // 168857.079, 0.000 // 168862.079, 0.962 // 168863.377, 0.000
168990.473, 0.000 // 168995.473, 0.979 // 168996.667, 0.000 // 169123.632, 0.000 // 169128.632, 0.959
169129.834, 0.000 // 169256.791, 0.000 // 169261.791, 0.985 // 169262.963, 0.000 // 169389.975, 0.000
169394.975, 0.954 // 169396.205, 0.000 // 169523.118, 0.000 // 169528.118, 0.981 // 169529.274, 0.000
169656.476, 0.000 // 169661.476, 0.977 // 169662.689, 0.000 // 169789.860, 0.000 // 169794.860, 0.971
169796.054, 0.000 // 169922.984, 0.000 // 169927.984, 1.002 // 169929.193, 0.000 // 170056.201, 0.000
170061.201, 0.981 // 170062.386, 0.000 // 170189.376, 0.000 // 170194.376, 0.970 // 170195.619, 0.000
170322.521, 0.000 // 170327.521, 1.006 // 170328.784, 0.000 // 170455.696, 0.000 // 170460.696, 0.994
170461.934, 0.000 // 170588.893, 0.000 // 170593.893, 0.983 // 170595.135, 0.000 // 170722.253, 0.000
170727.253, 0.963 // 170728.505, 0.000 // 170855.499, 0.000 // 170860.499, 0.961 // 170861.785, 0.000
170988.755, 0.000 // 170993.755, 0.956 // 170994.977, 0.000 // 171122.145, 0.000 // 171127.145, 0.939
171128.357, 0.000 // 171255.311, 0.000 // 171260.311, 0.982 // 171261.506, 0.000 // 171388.749, 0.000
171393.749, 0.952 // 171394.965, 0.000 // 171520.392, 0.000 // 171525.392, 0.055 // 171528.262, 0.000
171655.319, 0.000 // 171660.319, 0.969 // 171661.517, 0.000 // 171788.551, 0.000 // 171793.551, 0.962
171794.816, 0.000 // 171921.719, 0.000 // 171926.719, 0.952 // 171928.034, 0.000 // 172055.056, 0.000
172060.056, 0.974 // 172061.407, 0.000 // 172188.606, 0.000 // 172193.606, 0.971 // 172194.822, 0.000
172321.929, 0.000 // 172326.929, 0.961 // 172328.175, 0.000 // 172455.469, 0.000 // 172460.469, 0.988
172461.673, 0.000 // 172588.759, 0.000 // 172593.759, 0.975 // 172594.960, 0.000 // 172722.068, 0.000
172727.068, 0.954 // 172728.222, 0.000 // 172855.498, 0.000 // 172860.498, 0.937 // 172861.712, 0.000
172988.694, 0.000 // 172993.694, 0.995 // 172994.895, 0.000 // 173121.929, 0.000 // 173126.929, 0.935
173128.087, 0.000 // 173255.163, 0.000 // 173260.163, 0.992 // 173261.395, 0.000 // 173388.409, 0.000
173393.409, 0.932 // 173394.575, 0.000 // 173521.669, 0.000 // 173526.669, 0.960 // 173527.911, 0.000
173655.035, 0.000 // 173660.035, 0.946 // 173661.228, 0.000 // 173788.236, 0.000 // 173793.236, 0.948
173794.432, 0.000 // 173921.330, 0.000 // 173926.330, 0.925 // 173927.534, 0.000 // 174054.422, 0.000
174059.422, 0.947 // 174060.662, 0.000 // 174187.659, 0.000 // 174192.659, 0.958 // 174193.892, 0.000
174321.052, 0.000 // 174326.052, 0.943 // 174327.322, 0.000 // 174454.196, 0.000 // 174459.196, 0.974
174460.459, 0.000 // 174587.546, 0.000 // 174592.546, 0.941 // 174593.764, 0.000 // 174720.876, 0.000
174725.876, 0.933 // 174727.087, 0.000 // 174854.176, 0.000 // 174859.176, 0.941 // 174860.377, 0.000
174987.303, 0.000 // 174992.303, 0.955 // 174993.529, 0.000 // 175120.465, 0.000 // 175125.465, 0.944
175126.679, 0.000 // 175253.561, 0.000 // 175258.561, 0.936 // 175259.727, 0.000 // 175386.645, 0.000
175391.645, 0.920 // 175392.857, 0.000 // 175519.827, 0.000 // 175524.827, 0.949 // 175526.066, 0.000
175653.284, 0.000 // 175658.284, 0.932 // 175659.472, 0.000 // 175786.622, 0.000 // 175791.622, 0.959
175792.834, 0.000 // 175917.697, 0.000 // 175922.697, 0.000 // 175925.981, 0.000 // 176052.956, 0.000
176057.956, 0.966 // 176059.187, 0.000 // 176186.480, 0.000 // 176191.480, 0.941 // 176192.746, 0.000
176319.668, 0.000 // 176324.668, 0.943 // 176325.886, 0.000 // 176452.831, 0.000 // 176457.831, 0.977
176459.068, 0.000 // 176586.074, 0.000 // 176591.074, 0.928 // 176592.335, 0.000 // 176719.304, 0.000
176724.304, 0.925 // 176725.571, 0.000 // 176852.608, 0.000 // 176857.608, 0.951 // 176858.835, 0.000
176985.828, 0.000 // 176990.828, 0.945 // 176992.048, 0.000 // 177119.174, 0.000 // 177124.174, 0.917
177125.365, 0.000 // 177252.402, 0.000 // 177257.402, 0.903 // 177258.709, 0.000 // 177385.877, 0.000
177390.877, 0.923 // 177392.106, 0.000 // 177519.303, 0.000 // 177524.303, 0.915 // 177525.655, 0.000
177652.659, 0.000 // 177657.659, 0.919 // 177658.910, 0.000 // 177785.827, 0.000 // 177790.827, 0.930
177792.028, 0.000 // 177918.988, 0.000 // 177923.988, 0.935 // 177925.181, 0.000 // 178051.997, 0.000

```
178056.997, 0.902 // 178058.313, 0.000 // 178185.345, 0.000 // 178190.345, 0.917 // 178191.603, 0.000
178318.734, 0.000 // 178323.734, 0.913 // 178325.008, 0.000 // 178452.052, 0.000 // 178457.052, 0.884
178458.248, 0.000 // 178585.377, 0.000 // 178590.377, 0.879 // 178591.583, 0.000 // 178718.702, 0.000
178723.702, 0.867 // 178724.891, 0.000 // 178852.026, 0.000 // 178857.026, 0.893 // 178858.345, 0.000
178985.323, 0.000 // 178990.323, 0.942 // 178991.545, 0.000 // 179118.590, 0.000 // 179123.590, 0.944
179124.844, 0.000 // 179251.658, 0.000 // 179256.658, 0.955 // 179257.865, 0.000 // 179384.705, 0.000
179389.705, 0.914 // 179390.895, 0.000 // 179518.046, 0.000 // 179523.046, 0.904 // 179524.327, 0.000
179651.588, 0.000 // 179656.588, 0.925 // 179657.845, 0.000 // 179784.982, 0.000 // 179789.982, 0.912
179791.171, 0.000 // 179918.123, 0.000 // 179923.123, 0.901 // 179924.262, 0.000 // 180051.370, 0.000
180056.370, 0.912 // 180057.628, 0.000 // 180184.580, 0.000 // 180189.580, 0.913 // 180190.785, 0.000
180317.804, 0.000 // 180322.804, 0.916 // 180324.058, 0.000 // 180451.323, 0.000 // 180456.323, 0.920
180457.527, 0.000 // 180584.521, 0.000 // 180589.521, 0.930 // 180590.836, 0.000 // 180717.865, 0.000
180722.865, 0.955 // 180724.008, 0.000 // 180850.987, 0.000 // 180855.987, 0.901 // 180857.164, 0.000
180984.096, 0.000 // 180989.096, 0.929 // 180990.287, 0.000 // 181117.245, 0.000 // 181122.245, 0.924
181123.454, 0.000 // 181250.729, 0.000 // 181255.729, 0.928 // 181256.955, 0.000 // 181383.984, 0.000
181388.984, 0.935 // 181390.227, 0.000 // 181517.156, 0.000 // 181522.156, 0.932 // 181523.374, 0.000
181650.470, 0.000 // 181655.470, 0.939 // 181656.664, 0.000 // 181783.601, 0.000 // 181788.601, 0.923
181789.766, 0.000 // 181916.832, 0.000 // 181921.832, 0.928 // 181923.039, 0.000 // 182050.085, 0.000
182055.085, 0.950 // 182056.392, 0.000 // 182183.495, 0.000 // 182188.495, 0.945 // 182189.712, 0.000
182316.713, 0.000 // 182321.713, 0.927 // 182322.912, 0.000 // 182449.906, 0.000 // 182454.906, 0.927
182456.130, 0.000 // 182583.419, 0.000 // 182588.419, 0.911 // 182589.652, 0.000 // 182716.722, 0.000
182721.722, 0.940 // 182722.953, 0.000 // 182850.000, 0.000 // 182855.000, 0.941 // 182856.203, 0.000
182983.218, 0.000 // 182988.218, 0.993 // 182989.421, 0.000 // 183116.591, 0.000 // 183121.591, 0.940
183122.846, 0.000 // 183249.905, 0.000 // 183254.905, 0.950 // 183256.098, 0.000 // 183383.016, 0.000
183388.016, 0.934 // 183389.204, 0.000 // 183514.245, 0.000 // 183519.245, 0.000 // 183522.575, 0.000
183649.432, 0.000 // 183654.432, 0.969 // 183655.694, 0.000 // 183782.714, 0.000 // 183787.714, 0.947
183788.929, 0.000 // 183916.126, 0.000 // 183921.126, 0.931 // 183922.326, 0.000 // 184049.489, 0.000
184054.489, 0.930 // 184055.713, 0.000 // 184182.857, 0.000 // 184187.857, 0.916 // 184189.075, 0.000
184316.150, 0.000 // 184321.150, 0.925 // 184322.455, 0.000 // 184449.654, 0.000 // 184454.654, 0.941
184455.888, 0.000 // 184583.123, 0.000 // 184588.123, 0.921 // 184589.324, 0.000 // 184716.595, 0.000
184721.595, 0.921 // 184722.881, 0.000 // 184850.066, 0.000 // 184855.066, 0.923 // 184856.313, 0.000
184983.541, 0.000 // 184988.541, 0.943 // 184989.657, 0.000 // 185114.553, 0.000 // 185119.553, 0.000
185122.880, 0.000 // 185249.794, 0.000 // 185254.794, 0.951 // 185256.054, 0.000 // 185383.092, 0.000
185388.092, 0.931 // 185389.299, 0.000 // 185516.322, 0.000 // 185521.322, 0.919 // 185522.532, 0.000
185649.457, 0.000 // 185654.457, 0.932 // 185655.696, 0.000 // 185782.717, 0.000 // 185787.717, 0.945
185789.362, 0.000 // 185914.362, 0.000 //
POPULATIONS
COUNTS
END
```